SPM-2018

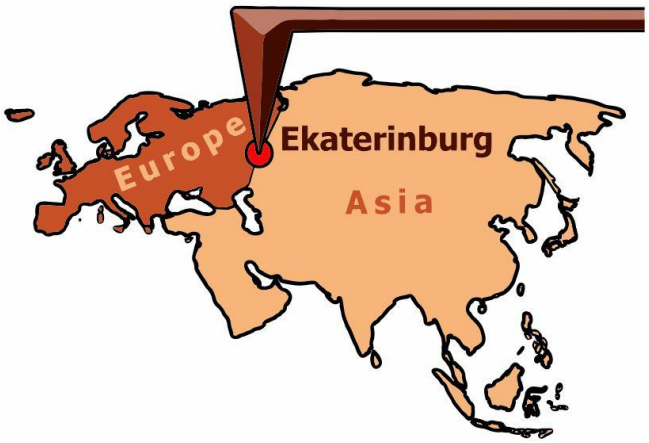

International Conference
SCANNING PROBE MICROSCOPY
International Workshop
MODERN NANOTECHNOLOGIES
International Youth Conference
FUNCTIONAL IMAGING OF NANOMATERIALS

August 26 – 29, 2018

Ural Center for Shared Use "Modern Nanotechnologies"
Institute of Natural Sciences and Mathematics
Ural Federal University

Abstract book

Ural Federal University
named after the first President of Russia B.N.Yeltsin

UrFU
Institute of Natural Sciences and Mathematics

УДК **538.9**
ББК 22.37
С-423

Scanning Probe Microscopy. Abstract Book of International Conference
(Ekaterinburg, August 26-29, 2018) Ekaterinburg, Ural Federal University, 2018- 233 с.
ISBN 978-5-9500624-1-4

Organizers

School of Natural Sciences and Mathematics, Ural Federal University
named after the first President of Russia B.N. Yeltsin (UrFU)
http://www.urfu.ru

Ural Center for Shared Use "Modern Nanotechnology" UrFU
http://nanocenter.urfu.ru

Labfer Ltd.
http://www.labfer.com

Ferroelectric Laboratory, INSM UrFU
http://labfer.ins.urfu.ru

Laboratory for Nanoscale Ferroelectric Materials, INSM UrFU

Conference chairmen

Prof. Vladimir Shur	Ekaterinburg, Russia
Prof. Viktor Mironov	Nizhny Novgorod, Russia

Program committee

Prof. A.V. Ankudinov	Saint-Petersburg, Russia
Prof. A.A. Bukharaev	Kazan, Russia
Prof. V.A. Bykov	Zelenograd, Russia
Prof. S.A. Chizhik	Minsk, Belarus
Prof. A.L. Gruverman	Lincoln, USA
Prof. O.V. Kolosov	Lancaster, UK
Prof. A.L. Kholkin	Aveiro, Portugal
Prof. A.V. Latyshev	Novosibirsk, Russia
Prof. V.L. Mironov	Nizhny Novgorod, Russia
Prof. G.M. Mikhailov	Chernogolovka, Russia
Prof. A.A. Saranin	Vladivostok, Russia
Prof. V.Ya. Shur	Ekaterinburg, Russia
Dr. V.V. Shvartsman	Essen, Germany
Dr. A.P. Volodin	Leuven, Belgium
Prof. I.V. Yaminsky	Moscow, Russia

Local organizing committee

Prof. Vladimir Shur	Ekaterinburg, Russia
Mrs. Elena Pelegova	Ekaterinburg, Russia
Dr. Dmitry Pelegov	Ekaterinburg, Russia
Mrs. Alevtina Shur	Ekaterinburg, Russia
Mrs. Ekaterina Shishkina	Ekaterinburg, Russia
Ms. Victoria Pryakhina	Ekaterinburg, Russia
Ms. Olga Dyachuk	Ekaterinburg, Russia

ISBN 978-5-9500624-1-4

ББК 22.37

Ural Federal University
named after the first President
of Russia B.N. Yeltsin

SPM-2018 sponsors

Taylor and Francis Group
http://www.tailorandfrancis.com

Russian Foundation for Basic Research
http://www.rfbr.ru/

NT-MDT Spectrum Instruments
http://www.ntmdt-si.com

INTERTECH Corporation
http://www.intertech-corp.ru/

Promenergolab
http://www.czl.ru

Ostec ArtTool
http://www.arttool.ru

OPTEC
http://www.optecgroup.com/

IMC Group
http://imc-systems.ru/

MERCK
http://www.merckgroup.com

LECTURES

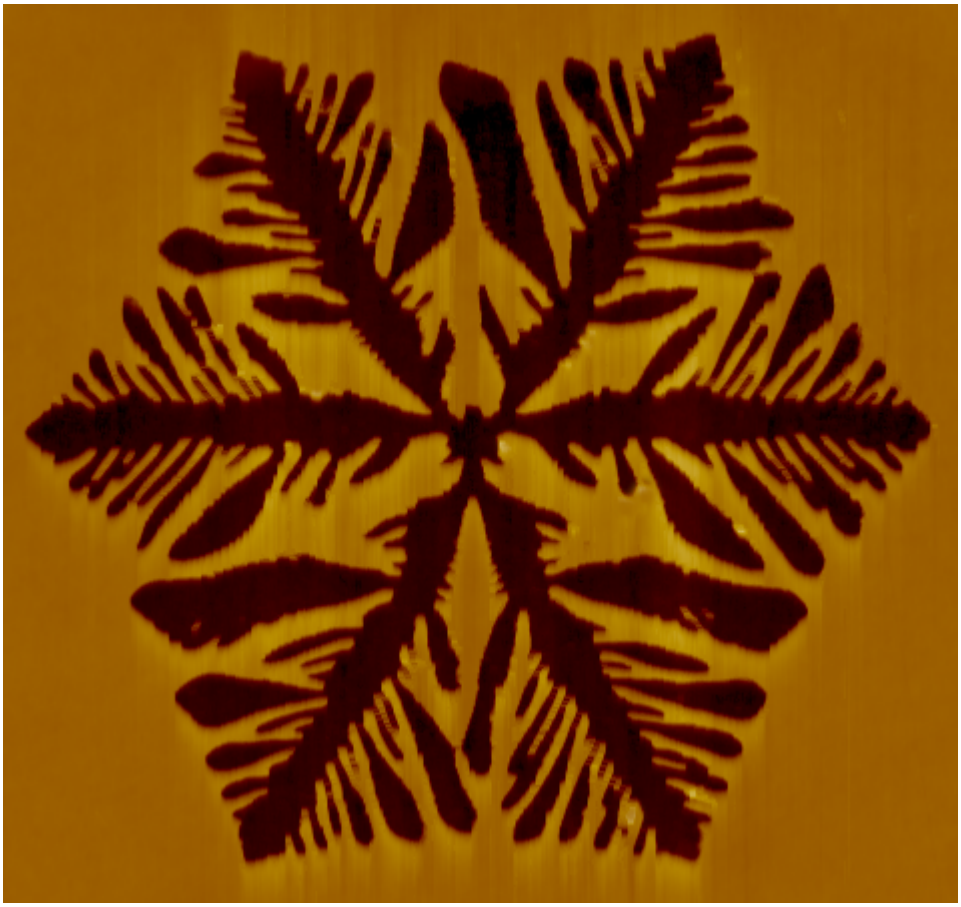

L-01

Scanning probe methods for studying surface structures - history of development and recent possibilities

V.A. Bykov[1,2,3]

[1]*Group of companies NT-MDT Spectrum Instruments, Moscow, Zelenograd, 124460*

[2]*Chair of microelectronics FPKE MIPT, Moscow, Zelenograd, 124460*

[3]*Nanotechnological Society of Russia, Moscow, Zelenograd, 1246832*
e-mail: vbykov@ntmdt-si.ru

The idea of using solid-state probes for recording and reproducing information was born at the end of the 19th century by the invention of a gramophone. In 1929 the German engineer Schmalz G. made the first probe microscope Stylus Profiler with which it was possible to obtain a surface image of 11x18 mm with an increase of 1000 times. The image was recorded on a photographic plate. These developments were developed in the direction of creating co-ordinate profilometers with profile registration by piezoelectric cantilevers. Profilometers of similar type are used in industry today.

High-resolution probe technology for visualization of surface structures began to be developed since 1966. At the Institute of Standards in the US Russell Young group made a device Topographer which was able to see atomic steps. Personal computers were still in their infancy and had a small memory, so the mapping of topography was carried out using a two-coordinate recorder. The first exceptionally important, key innovation proposed by the Russell Young group was the use of piezoelectric ceramics for movement of the tip and sample.

The historical period in the development of scanning probe microscopy began in 1971 in the group of Heinrich Rohrer and Helmut Binnig in the IBM Tsurikh branch from the target installation for obtaining atomic resolution (the Nobel Prize in 1986).

G. Binnig and G. Rohrer showed that using an instrument called a scanning tunnel microscope, whose schematic diagram is similar to the Young topographer, allows one to obtain images of individual atoms. Personal computers were used to control the device and to process the results. Progress in the capabilities of devices is determined by the power of the used computers. In 1986, the same group proposed the use of a tubular piezoceramic scanner. To record the surface relief, it was suggested to use flexible beams with a sharp needle on the loose end - cantilevers, and instruments for recording the relief were called atomic-force microscopes (AFM). In the AFM of Binnig, Kwait and Gerber, a tunnel sensor was used to record the normal displacement of the cantilever, which is extremely inconvenient. A powerful innovation that made AFM a reality was Ammer and Maier's invention of an opto-positional scheme for recording the change in the angles of cantilever inclination, when a four-section photodiode is used as a recording element, it is possible to record both normal and lateral interaction forces probe and the test surface of the sample.

Innovation to prevent the effect of the capillary was born in 1986. It was proposed by Binnig, his real possibilities are shown by Ducker, Cook and Clarke is integrated into the first industrial atomic force microscopes by Vergil Eling called "tipping" or semi-contact mode.

In 1987, a group of researchers were asked to make cantilevers using the silicon technology, where the selective etching both "grooves" and tips with an angle at the apex determined by the properties of the crystal were already developed. The beams thickness could be set either by the coating thickness or by the depth of alloying with boron or phosphorus. The ability to manufacture cantilevers using the methods of microelectronic technologies made them an affordable consumable and ensured the possibility of wide distribution of the method.

In the late eighties and early nineties, the possibility of recording a number of surface physical properties in various conditions, from ultrahigh vacuum to liquid, and methods for modifying the surface (SPM lithography) was realized, which are now integrated into all scanning probe microscopes (SPM) under several different names.

In the late 1980s, the work on the creation of SPM was also launched in the USSR. A corporation MDT started to create SPMs with the capabilities of lithographers, where it would be possible to carry out both research and modification of the properties of molecular structures. By 1995, AFMs were created, and by 1997 - multi-mode instruments for complex studies of surface structures without destroying in the process of investigation.

To date, scanning probe microscopy has become part of the classical methods of studying nanostructures and is widely used for qualitative assessment of physical and chemical properties and geometrical parameters of the surfaces.

In addition to topography, SPMs can measure a distribution of many physical properties: surface electric potential; surface conductivity; electrical capacity of the probe-surface system; magnetic forces in a system of probe and given magnetic surface; piezoelectric properties; thermal conductivity; mechanical properties (Young's modulus, hardness); adhesion properties. Measurements can be made in air, in a gaseous atmosphere, in a liquid and in a vacuum in wide temperature range from superlow to several hundred degrees Celsius. The modern possibilities of computer technology and digital technologies allow to reduce significantly the requirements for the user's qualification.

The training of specialists is an exceptionally important task for development of modern technology which must begin at a school bench. The ability to see and actively influence molecular structures changes dramatically and intensifies the depth of understanding of physics, chemistry, and biology. Fig. 1 shows the last version of the NANOEDUCATOR device, which currently equips dozens of educational classes in Russia and abroad. This device was among the best world products according to the version of Research & Developments magazine in 2011.

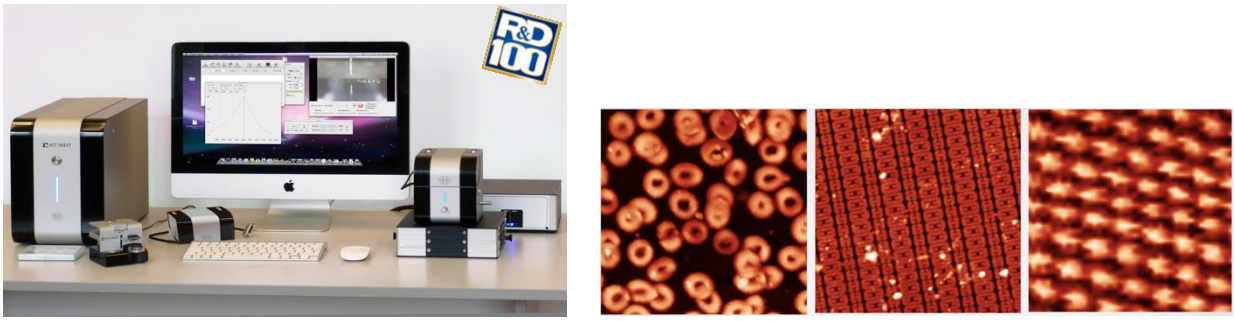

Figure 1. The education device NANOEDUCATOR-II and the obtained images of erythrocytes (image area 50x50 μm), section of microcircuit (30x30 μm), atomic structure of highly oriented pyrolitic graphite (2x2 nm).

It should be noted that SPMs are devices that are very sensitive to acoustic disturbances, changes of temperature and humidity. To minimize these factors, it is necessary to operate inside acoustically protected boxes equipped with an active or passive vibro-protection system, a system for maintaining temperature and humidity of high accuracy. The provision of all these conditions has been solved for the entire range of NT-MDT SPMs, providing a drift of less than 10 nm/h, which allows to obtain atomic resolution at relatively low scanning frequencies.

A powerful development was obtained by combines of SPMs and spectrometers, combining methods of high-resolution measurements of topography and various physical properties of surface structures. Instruments allow to obtain information both on the physical properties of surface structures and on the qualitative composition from luminescence spectroscopy, Raman spectroscopy and high-resolution IR spectroscopy.

The consistent innovative development of SPMs allowed re-positioning these devices, significantly reducing the requirements for users from the entourage of the method, to specialists in probe microscopy, and at present the devices of the latest developments of the NT-MDT Spectrum Instruments group can be successfully used by laboratory technicians and engineers to monitor the technological parameters of processes, and materialists, whose goal is to obtain well-interpreted information on physical and physicochemical properties of different structures.

L-02

Principles and applications of Piezoresponse Force Microscopy

A.L. Kholkin[1,2]

[1]*Department of Physics & CICECO-Aveiro Institute of Materials, University of Aveiro, 3810-193 Aveiro, Portugal*

[2]*School of Natural Sciences and Mathematics, Ural Federal University, 620000 Ekaterinburg, Russia*
e-mail: kholkin@urfu.ru

Over the last several years the field of ferroelectric and multiferroic oxides has been experiencing a significant revival. A clear manifestation of this trend is the publication of the new developments in this field in the Science and Nature magazines, as well as in numerous reviews. This is partly due to recent experimental achievements allowing synthesis of complex oxides and composites with atomic scale precision. As the quality of ferroelectric and multiferroic structures has proven to be essential to their functionality, a necessity to characterize their properties down to the nano- and even atomic scale lead to the wide application of electron and scanning probe microscopy (SPM) methods in this field. Specifically, Piezoresponse Force Microscopy (PFM) proved to be an indispensable tool for high-resolution characterization of ferroelectrics [1-3]. Versatility of PFM, which allows measurements of electronic behavior along with the nanoscale polarization control, makes it a method of choice for addressing the problems relevant to the scaling behavior of ferroelectrics. The standard implementation of this technique where an electrically biased probe scans the sample surface to modify or visualize the domain structure has been around for almost 20 years. However, recent years witnessed development of advanced modes of PFM such as resonance-enhanced PFM, Band Excittion PFM, switching spectroscopy PFM and so on.

This tutorial will briefly cover the physical, instrumental and interpretation aspects of a conventional PFM technique before focusing on application of advanced PFM modes to investigation of the dynamic switching and electronic properties of ferroelectric and piezoelectric nanostructures.

1. B.J. Rodriguez, S.V. Kalinin, D. Pelegov, et al., *Encyclopedia of Nanotechnology*, Springer, **4**, 2600 (2015).
2. N. Balke, I.K. Bdikin, S.V. Kalinin, et al., *J. Amer. Ceram. Soc.* **92**, 1629 (2009).
3. S.V. Kalinin, N. Setter, A.L. Kholkin, *MRS Bulletin* **34**, 634 (2009).

L-03

Influence of deformation distribution in console-probe-sample system on AFM measurements

A.V. Ankudinov

Ioffe Institute, Saint Petersburg, Russia
e-mail: alexander.ankudinov@mail.ioffe.ru

In [1, 2] some drawbacks of an optical lever method to detect the cantilever deflections in the atomic force microscope (AFM) were analyzed. In this method, only two angles, bending and torsion of the cantilever are measured, while the displacement vector or the interaction force may have three spatial components. The state with the probe clamped at the sample surface moving upward leads to the anomalous buckling of the cantilever console (the deviation angle profile along the console has an extreme), in contrast to the bending (the profile is monotonous) for the state when the probe is sliding. Since the deviation angle is detected only at one point of the console, anomalous buckling may lead to ambiguous, erroneous measurements not only of the amplitude but also of the interaction force sign. This ambiguity was recently partly overcome, after an appearance of the AFM device having both optical lever and interferometric sensor [3].

The lecture discusses calculations of deformations in the console-probe-sample system, that permit to reveal clamped or slipping states in the probe-sample contact. The calculations were performed taking into account the stiffness tensors to describe: console; probe, attached to the console edge; and sample. A general solution is presented for three types of holonomic constraints: clamped contact; probe slides in the selected direction; probe slides in the selected plane. Also, two closely related particular solutions are investigated: 1) rectangular console; probe approximated by a truncated cone with an axis not coinciding with Z direction, "infinitely rigid" sample; 2) rectangular console; "infinitely rigid" probe, mechanically anisotropic sample with finite rigidity.

The calculations are checked in AFM experiments on various test samples: cleaved GaAs (110). TGG1 sample, microdrops of Ga, Hg, polymer glue UV50, polydimethylsiloxane, glycerol. Also, we used the data of AFM studies of native, living cells (PeakForce QNM mode, under conditions as close to physiological as possible): sensory neurons and fibroblasts of chick embryos, rat erythrocytes [4].

The lecture materials may be useful for: intellectual "upgrade" of the optical lever method; developing accurate nanomechanical measurements of solid state objects, polymers, living cells; optimizing cantilever parameters for quantitative piezoresponse force microscopy; creating effective algorithms for nanoparticle manipulation.

1. S. Fujisawa et al., *Rev. Sci. Instr*. **65**, 3, 644 (1994).
2. H. Kawakatsu et al., *Jpn. J. Appl. Phys*. **34**, 3400 (1995).
3. https://www.oxford-instruments.com
4. M.M. Khalisov et al., *IOP Conf. Series: Materials Science and Engineering* **256**, 1, 012010 (2017).

L-04

Nanoscale resolved solid-state electrochemistry: the scanning probe microscopy approach

D.O. Alikin

[1]*School of Natural Science and Mathematics, Ural Federal University, 620002, Ekaterinburg, Russia boris.slautin@urfu.ru*

[2]*Physics Department & CICECO – Aveiro Institute of Materials, University of Aveiro, 3810-193, Aveiro, Portugal*

Progress in secondary batteries and fuel cells is driven by advances in development of more effective materials for mobile ion storage and conduction. The crucial part of this process is a thorough understanding of material functional behavior at the micro- and nanoscale. Variety of structural methods is now available in commercial equipment to resolve and study material transformation due to intercalation-deintercalation process. In the same time there is still a lack of functional methods allowing to probe local potential, ion mobility together with mechanical properties and electronic conductivity.

Tendency to conduct nanoscale resolved studies of battery materials functionality forces rapid development of scanning probe microscopy (SPM) methods. In this contribution we consider recent advantages in this specific area of investigations. Both conventional current-based methods, such as scanning electrochemical microscopy and conductive atomic force microscopy, and strain-based SPM methods as electrochemical strain microscopy and Kelvin probe force microscopy are discussed on the basis of their application and limitations. The particular focus of the talk will be on electrochemical strain microscopy (ESM) as a method with simplest realization possible to de bone in different experimental configurations and possessing high spatial resolution. The realization of the method is based on Vegard displacement of the surface under the action of charge carrier's concentration gradient stimulating by the biased SPM tip. ESM allows to probe quantitatively ionic mobility in the different electrochemical systems [1]. The recent development of ESM experimental approach and supporting theoretical basis will be reported on the basis on our recent publications [1,2].

The work was financially supported by Russian Science Foundation (Grant 17-72-10144). The equipment of Ural Center for Shared Use "Modern Nanotechnology" Ural Federal University was used.

1. D.O. Alikin, K.N. Romanyuk, B.N. Slautin, et al., *Nanoscale* **10**, 2503 (2018).
2. D.O. Alikin, A.V. Ievlev, S.Yu. Luchkin et al. *Appl. Phys. Lett.* **108**, 113106 (2016).

.

L-05

Application of magnetic force microscopy to study the epitaxial ferro- and antiferromagnetic microstructures

L.A. Fomin, G.M. Mikhailov

IMT RAS, 142432 Chernogolovka, Russia
e-mail: fomin@iptm.ru

In the last few decades, spintronics has become to one of the promising areas of electronics, in which the electron spin is essentially exploited. Because of the use of ferro- and antiferromagnets in spintronics, the study of their magnetic states that depends on the external magnetic field and the applied spin-polarized current is of great interest. The most common method for such studies is magnetic force microscopy (MFM), having advantages in ease of use and availability. However, the magnetic contrast obtained by this method is not always easy to interpret and unambiguously determine the magnetic structure - the spatial distribution of magnetization. For this interpretation, the simulation within the framework of the Brown's approach, called micromagnetism, is actively used in combination with other experimental methods.

The magnetic states of micro- and nanostructures fabricated from ferro- and antiferromagnetic films depend strongly on the quality of their crystal structure. For the purity of the experiments, it is worth to investigate epitaxial micro - and nanostructures, which guarantees implementation of spatially ordered and regular magnetic states. Examples of studies of such structures by magnetic force microscopy in combination with micromagnetic calculations and other magnetically sensitive methods are presented below.

Studies by the MFM and micromagnetic calculations of iron epitaxial microstructures revealed a dependence of their magnetic states versus both the type of the substrate, microstructure's dimensions and lateral orientation against the substrate. The different types of regular magnetic states were experimentally observed. It was shown that the iron films on the a-plane sapphire substrate possess one easy in-plane magnetization axis, made 35° angle against the base cut of the substrate, while for the r- plane sapphire substrate – there are two easy axes, parallel and perpendicular to the base cut. This corresponds to the epitaxial growth of iron films of (011) and (001) orientations, respectively. Using the same approach, the magnetic states of the epitaxial microstructures of the Heusler alloys Co_2FeAl and Fe_2CoAl that grown on the same substrates were also investigated. New results have been found, which can be explained by the deviation of the lattice symmetry of the grown films from the cubic symmetry.

Carried experiments have been also accomplished by magnetoresistive measurements, the results of which allow finding the coercive fields and the type of the magnetic anisotropy in epitaxial films consisting of ferro- and antiferromagnetic metals and their alloys. These measurements also made it possible to study the interlayer exchange interaction in epitaxial ferromagnetic – antiferromagnetic (FM/AFM) structures, in which the application of annealing in a magnetic field above the Neel temperature forms a unidirectional exchange anisotropy. This anisotropy is manifested in the magnetic structure of the ferromagnetic layer, which can be studied by MFM. Micromagnetic calculations have predicted the influence of the roughness of the FM/AFM interface on this interaction.

INVITED

PRESENTATIONS

I-01

3D visualizations of solid surfaces properties by scanning probe microscopy and spectroscopy technics

V.A. Bykov[1,2], A. Kalinin[1], V. Polyakov[1], A. Shelaev[1]

[1]*Group of companies NT-MDT Spectrum Instruments, Moscow, Zelenograd, 124460*
www.ntmdt-si.com, e-mail: spm@ntmdt-si.ru

[2]*Moscow Institute of Physics and Technology*

The development of scanning probe microscopy (SPM) as itself and in a combination with optical and spectroscopic technics can give a lot of information on the physical properties of nanostructures:

- Electron state density and work function distribution to use Scanning Tunneling microscopy and spectroscopy;
- The profile of surface structures and its dependence on the pressing pressure;
- Inhomogeneity of the frictional force in the probe-surface system;
- Heterogeneity of adhesion forces;
- Distribution of surface potential (Kelvin-mode);
- Distribution of electrical capacity in the cantilever-surface contact;
- Distribution of thermal conductivity;
- Young's modulus distribution;
- Diagnostics of limits of elastic deformation;
- Distribution of undersurfaces magnetic forces;
- Distribution of piezoelectric characteristics of surface structures;
- The distribution of the optical properties of the surface with a resolution significantly exceeding diffraction limits (near-field optical microscopy);
- Possibility of surface modification.

The application field was increased very wide – from one side micro- and nanoelectronics with extra high-level the metrology requirements and up to material science, biology, ecology with requirements to the side of simplification in operation procedures, possibility of the materials and molecules recognitions.

SPM gives an opportunity to carry out studies of spatial, physical and chemical properties of objects with the typical dimensions of less than a few nanometers. Owing to its multifunctionality, availability and simplicity, Atomic Force Microscope (AFM) has become one of the most prevailing “tools for nanotechnology” nowadays. NTEGRA platform has been designed as the special base for the constantly developing options of SPM that combines them with various other modern research methods: confocal and luminescence microscopy, Raman scattering and Infrared Apertureless Nearfield spectroscopy. Owing to the effect of giant amplification of Raman scattering (TERS – Tip Enhances Raman Scattering) it allows carrying out spectroscopy studies and obtaining images with 10 nm resolution.

New generation of AFM control electronics now allows a real-time cantilever deflection tracking and analyzing. Based on a fast force-distance measurement we developed a new group of non-resonant AFM methods of scanning probe spectroscopy called Hybrid mode. It is the most proposal AFM mode since it summarizes all advantages of amplitude modulation and contact modes allowing simultaneously: free of share force topography measurement with direct tip-sample interaction control, real-time quantitative nanomechanical measurements, conductivity, piezoresponse and electrostatic imaging with conventional scanning speed. Hybrid mode is also very helpful for liquid measurements as it utilizes the issue with cantilever eigenfrequency detection.

Progress in micromechanics manufacturing resulted in significant increase of the cantilever yield rate (to practically 100%) with repeatability of resonant characteristics at 10% level, thus preconditioning implementation of the concept of multi-probe cartridges for AFM. A cartridge is a multi-probe contour-type sensor with 38 cantilevers. The cantilevers can be either of the same

type or "colored" with predefined coverings and rigidities. Depending on AFM system type the cartridge rotation to select working cantilever can be manual or software-controlled and takes a few seconds. A whole cartridge can be exchanged manually through a simple procedure without the risk to damage cantilevers. The cartridges operate in dedicated measuring heads, which are designed for integration in the latest Company instruments (Titanium, NEXT, SOLVER-NANO, VEGA-SPM).

For fully software-controlled AFMs Titanium and NEXT the cantilever setup procedure was motorized and automated including: precise cartridge rotation to the user-selected cantilever, optical beam deflection (OBD) system adjustment, lock-in amplifier tuning and sample positioning. This approaches us to the concept of ease-of-use AFM where routine system adjustment before scanning is proceeded automatically in a few tens of seconds. Ease-of-use is not the only feature of automated multi-probe cartridge. One of the most demanding applications of modern AFM is routine and repeatable atomic and molecular resolution. This requires extra-low tip-sample thermal drift assumed us lower than 1 Å/min. Development of thermally stabilized cabinet with 0.01°C temperature control accuracy and drift-minimized mechanical design of Titanium AFM helped us to achieve mentioned drift level and repeatable atomic/molecular resolution imaging. But conventional cantilever exchange procedure requires opening the cabinet and manipulating with AFM therefore destabilizing the temperature conditions. So the concept of automated multi-probe cartridge together with active thermal stabilization and drift-minimized mechanical design can be a perfect tool for routine high-resolution AFM imaging.

AFM is a candidate to solve some of “Metrology Difficult Challenges” proposed by The International Technology Roadmap for Semiconductors like: “Structural and elemental analysis at device dimensions and measurements for beyond CMOS”, “Nondestructive, production worthy wafer and mask-level microscopy for critical dimension measurement for 3D structures, overlay, defect detection, and analysis”. A rapid development of polymer and single-molecular electronics also requires AFM to measure and control the topography, nanomechanical, conductivity, temperature and other properties at the nanoscale. To summarize, future electronics development and manufacturing can be a wide field for AFM application, especially for large-sample AFMs. But the biggest drawback of AFM technology to overcome is low throughput.

Throughput of AFM is limited by: system adjustment time before scanning (OBD system and lock-in adjustment, area of interest searching time etc.), scanning parameters adjustment time, scanning speed and amount of data gathered after one scanning session. So to develop the next-generation AFM all these limits should be overcome.

To minimize system adjustment and scanning parameters tuning time we develop and improve new software algorithms allowing fully automated topography imaging. New high-speed control electronics together with Hybrid mode allow more data points and different properties to be recorded per one scanning session. We also develop new AFM-scanner control algorithms to increase a topography imaging speed noticeably. These developments implemented to the fully motorized large-sample AFM is a promising tool for nanotechnology industry. To use AFM-cluster technology in the portable SPM, such as Solver-NANO can open the road for using of this unit right on the Space Stations for material quality control in Space and Space Station conditions.

Development of modes for scanning spectroscopy combined with SPM in the instruments NTEGRA-SPECTRA-II provides new options of confocal laser luminescence spectroscopy and Raman spectroscopy as well as higher reliability of detection for TERS and high-resolution scanning probe-optical microscopy and spectroscopy. Probes with diamond nanocrystals containing N-V defects are capable to detect magnetic states as microscopic as single spins and so they are promising for studies of surface catalytic activity and for detection of free radicals, including applications in biology and medicine.

Apertureless scanning nearfield optical microscope (ASNOM) probe induce lite scattering give the possibility to investigate infrared as chemical nature of surface functional gropes and to measure the doped impurity implantations in microelectronic structures that it impossible to observed in electron microscopy.

I-02

Magnetic resonance force microscopy

V.L. Mironov

Institute for physics of microstructures PAS, 603950, Nizhny Novgorod, GSP-105, Russia
e-mail: mironov@ipmras.ru http://mrfm.ipmras.ru

In recent years a new technique for detecting local microwave properties of materials and nanostructures has been developed, which is called “magnetic resonance force microscopy” (MRFM) and combines the advantages of magnetic force microscopy and resonance microwave diagnostics. The main idea of MRFM is the detection of a local power interaction between the magnetic force microscope probe and a sample under microwave pumping. Upon microwave excitation, the magnetic moments of sample electrons and nuclei are changes, which lead to a change in the force acting on the probe from the side of the sample. This method enables recording of local microwave absorption spectra and studying the spatial distributions of the resonant oscillations for the spins of the electrons and nuclei in the sample. In current work we present the review of different application of MRFM for the diagnostics of ferromagnetic resonance (FMR) [1,2], electron spin resonance (ESR) [3,4] and nuclear resonance (NMR) [5,6] in the solid state structures.

The work in this area is supported by Russian Science Foundation in the frames of project # 16-12-10254.

1. O. Klein, G. De Loubens, V.V. Naletov, et al., *Physical Review B* **78**, 144410 (2008).
2. F. Guo, L.M. Belova, R.D. McMichael, *Physical Review Letters* **110**, 017601 (2013).
3. D. Rugar, R. Budakian, H.J. Mamin, et al., *Nature* **430**, 329 (2004).
4. E.W. Moore, S.G. Lee, S.A. Hickman, et al., *Proceedings of National Academy of Science USA* **106**, 2251 (2009).
5. H.J. Mamin, M. Poggio, C.L. Degen, et al., *Nature nanotechnology* **2**, 301 (2007).
6. S. Won, S.-B. Saun, S. Lee, et al., *Scientific reports* **3**, 3189 (2013).

I-03

Regular and irregular shaped isolated domains in uniaxial ferroelectrics

V.Ya. Shur

School of Natural Sciences and Mathematics, Ural Federal University, 620000 Ekaterinburg, Russia
e-mail: vladimir.shur@urfu.ru

The variety of domains shapes appeared in uniaxial ferroelectrics will be presented, classified and described systematically. The obtained experimental results will be discussed using unified kinetic approach based on the analogy between domain structure evolution and phase growth during first-order phase transformation.

The classical theoretical approach predicted only the regular polygonal shape of isolated domains defined by crystal symmetry [1,2]. Recent systematic experimental study of the domain shapes allowed revealing wide shape variety which can be divided into: (i) circular shapes, (ii) regular polygons, (iii) irregular polygons, (iv) irregular shapes. The kinetic approach to domain growth based on generation of steps (pairs of kinks) and kink motion has been used for explanation of all obtained results [3]. The nucleation probabilities are determined by the local value of the sum of the applied field and residual depolarization field at the domain wall.

The crucial role of the bulk screening retardation in domain growth is demonstrated. The domain shape complication due to screening ineffectiveness was demonstrated experimentally and by computer simulation [3]. Two limiting mechanisms of the step nucleation have been considered: (a) stochastic with equiprobable position of nucleation sites, (b) determined with step generation at fixed points and anisotropic kink motion.

Stochastic nucleation leads to formation of the circular domains, whereas determined one stimulates formation of the polygonal shapes. The convex polygons with walls parallel to the main crystallographic axis appeared for effective screening: (a) hexagons for C_{3v} symmetry (lithium niobate, lithium tantalate and lead germanate), (b) squares for C_4 symmetry, (strontium-barium niobate), (c) rectangles for C_2 symmetry (potassium titanyl phosphate [4]). Obtained domain shape stability effect (fast restoration of the initial concave polygonal shapes after domain merging) was attributed to formation of the short-lived super-mobile walls [5]. It was demonstrated that polygons and stars with concave angles can appear as a result of screening retardation only [6].

The stochastic nucleation at the elevated temperatures leads to lack of the domain shape stability thus opens the way to complicated fractal and dendrite domain shapes [7,8]. The dendrite (snowflakes) domain structures can be created by: (i) discrete switching with subsequent merging, (ii) domain shrinkage under the action of the pyroelectric field or spontaneous backswitching, (iii) domain growth at the elevated temperatures in the plates with artificial dielectric layer [9].

The equipment of the Ural Center for Shared Use “Modern nanotechnology” Ural Federal University was used. The research was made possible by Russian Science Foundation (Grant 14-12-00826).

1. V. Gopalan, V. Dierolf, D.A. Scrymgeour, *Annu. Rev. Mater. Res.* **37**, 449 (2007).
2. L. Tian, D.A. Scrymgeour, V. Gopalan, *J. Appl. Phys.* **97**, 114111 (2005).
3. V.Ya. Shur. *J. Mater. Sci*. **41**, 199 (2006).
4. V.Ya. Shur, E.M. Vaskina, E.V. Pelegova, M.A. Chuvakova, A.R. Akhmatkhanov, O. Kizko, M. Ivanov, A.L. Kholkin, *Appl. Phys. Lett*. **109**, 132901 (2016).
5. V.Ya. Shur, A.I. Lobov, A.G. Shur, E. Rumyantsev, K. Gallo, *Ferroelectrics* **360**, 111 (2007).
6. A.I. Lobov, V.Ya. Shur, I.S. Baturin, E.I. Shishkin, D.K. Kuznetsov, A.G. Shur, M.A. Dolbilov, K. Gallo, *Ferroelectrics* **341**, 109 (2006).
7. V.Ya. Shur, D.S. Chezganov, M.S. Nebogatikov, et al., *J. Appl. Phys*. **112**, 104113 (2012).
8. V.Ya. Shur, M.S. Kosobokov, E.A. Mingaliev, D. Kuznetsov, P. Zelenovskiy, *J. Appl. Phys*. **119**, 144101 (2016).
9. V.Ya. Shur, A.R. Akhmatkhanov, *Phil. Trans. R. Soc. A* **376**, 20170204 (2018).

I-04

Magnetic force microscopy of epitaxial Fe_2CoAl and Co_2FeAl Heusler alloy films and microstructures

G.M. Mikhailov, L.A. Fomin, V.A. Berezin, I.V. Malikov

Institute of Microelectronics Technology and High Purity Materials RAS, 142432, Chernogolovka, Russia
e-mail: mikhailo@iptm.ru

The Heusler alloys have many unique properties. Among them, it is a high level of spin polarization achieving 100% [1]. In work [2], by means of ab initio calculations it was shown that some of these alloys, in particular Co_2FeAl possess the large constant of anisotropy which more than by an order exceeds that for iron. This makes it possible to use Heusler alloys as materials for permanent magnets that do not have rare earth elements in their composition, as fixed layers in spin valves and also as an effective spin injector. In the same work, it was shown that the electronic structure of these alloys varies greatly with the change of lattice type from cubic to tetragonal. In the process of epitaxial growth due to the mismatch between the growing film and the substrate crystal structure, such a transition can occur, leading to a change in the spin polarization of the alloy and its magnetic anisotropy.

The films of Heusler alloys Fe_2CoAl and Co_2FeAl were grown epitaxially by pulsed laser deposition in ultrahigh vacuum on the R - and A - planes of sapphire with a 20 nm thick W(001) or Mo (001) seed layer that was preliminary grown at 450 °C on the substrate. From the grown films, by application of subtractive microstructurization the microstructures of different sizes and shapes – circles, quadrates, rectangles and crosses, were fabricated.

Magnetic force microscopy (MFM) supported by micromagnetic calculations using OOMMF [3] was applied to study their magnetic structure. MFM measurements and micromagnetic calculations have shown that the microstructures of Fe_2CoAl have an in-plane uniaxial anisotropy with an easy magnetization axis directed at an angle close to 45° to the base cutoff of the R-plane sapphire substrate. After annealing these microstructures at a temperature of 600 °C, the in-plane anisotropy of the films becomes biaxial (Fig. 1).

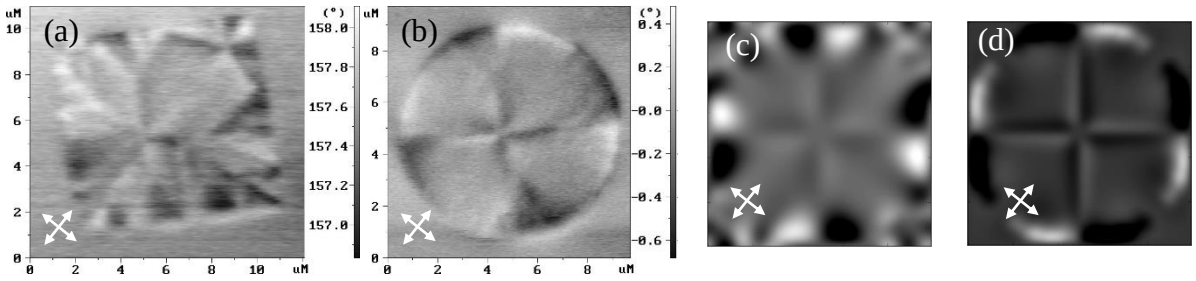

Figure 1. MFM images (a), (b) and their simulation (c), (d) for a quadrate and circle of Fe_2CoAl after annealing. The arrows indicate the easy axes of magnetization.

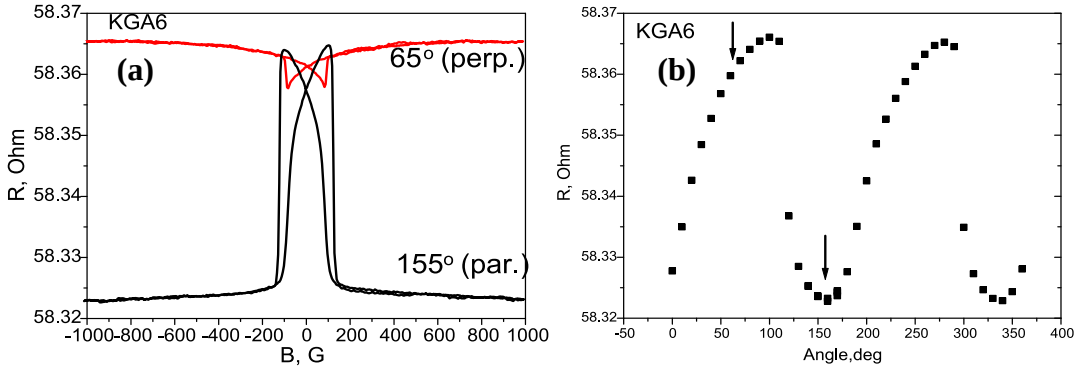

Figure 2. In-plane magnetoresistance of the bridge of Co_2FeAl for magnetic field directed parallel or perpendicular to the bridge (a) and the angular dependence of the resistance in a magnetic field with induction of 400 G, directed at different azimuthal angles (b). Arrows show field direction at which magnetoresistances were measured (numbers in (a) indicate the azimuthal angles).

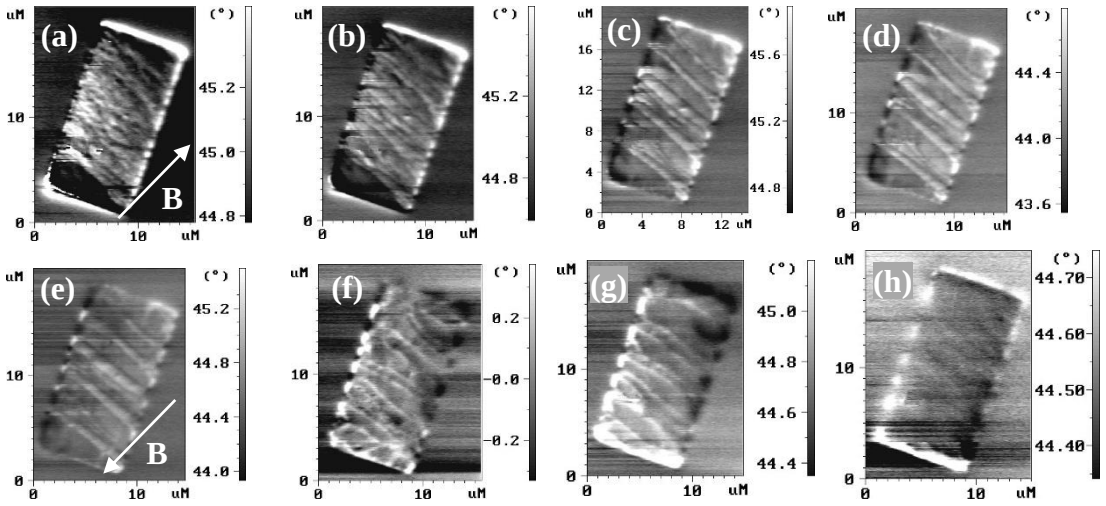

Figure 3. MFM images of rectangular Co2FeAl microstructure in an external magnetic field with induction of -600 (a), -300 (b), -130 (c), -57 (d), 12 (e), 150 (f), 272 (g) and 511 G (h). The field direction is depicted by the arrows (the inserts (a) and (e)).

The Co_2FeAl films grown on the A-plane sapphire showed unusual both field dependent and azimuthal-angle dependent magnetoresistances (Fig. 2). The field dependent magnetoresistance (Fig. 2a) exhibits an increase in the case when the current is parallel to the field and a decrease when it is perpendicular to the field. Usual behavior of anisotropic magnetoresistance should be vise versa. The angular dependence of magnetoresistance (Fig. 2b) has a form other than the sine wave.

To explain found dependences, the magnetic states of microstructures fabricated from grown epitaxial films were studied by MFM with application of external magnetic field (Fig. 3). MFM measurements showed that for the fields ranged from -800 G to -600 G the magnetic contrast is virtually unchanged and is typical to that shown in the Fig. 3a. At lower fields, the domain structure appears (Fig. 3b), which under further decrease of the field evolves to a state with residual magnetization (Fig. 3c). With a gradual increase of the field into the opposite to initial direction, significant changes in the magnetic structure occur under the field of about 150 G (Fig. 3f). It practically unchanges till the fields of 500 G (Fig. 3h), and the magnetic contrast is smeared at higher fields. The magnetic structure can be interpreted as a strip domain structure with the strips directed along the axis of easy magnetization that forms an angle against the base cutoff of the substrate. This can explain the results of measurements of magnetoresistance.

Research supported by RFBR grant 17-57-45024 IND-a.

1. M. Oogane, S. Mizukami, *Phil. Trans. R. Soc.* A **369**, 3037 (2011)
2. Y-I. Matsushita, G. Madjarova, J. K. Dewhurst et al., *J. Phys. D: Appl. Phys.* **50**, 095002 (2017)
3. http://math.nist.gov/oommf

I-05

Magnetoelectric effect in composite structures based on piezoelectric single crystals

A.L. Kholkin[1,2], A.V. Turutin[3,4], J.V. Vidal[1], I.V. Kubasov[4], A.M. Kislyuk[4], S.P. Kobeleva[4], M.D. Malinkovich[4], N.A. Sobolev[3,4]

[1]*Department of Physics & CICECO-Aveiro Institute of Materials, University of Aveiro, 3810-193 Aveiro, Portugal.*

[2]*School of Natural Sciences and Mathematics, Ural Federal University, 620000 Ekaterinburg, Russia. e-mail: kholkin@urfu.ru*

[3]*Department of Physics and I3N, University of Aveiro, 3810-193 Aveiro, Portugal*

[4]*National University of Science and Technology MISiS, 119049 Moscow, Russia*

The magnetoelectric (ME) effect is defined as coupling between polarization and magnetic fields (direct effect) and conversely between magnetization and electric fields (converse effect) in a matter. This effect has been of immense interest in the scientific community over the past few years. Unlike the ME single-phase multiferroics, numerous ME composites, combining elastically coupled piezoelectric (PE) and magnetostrictive (MS) phases, have been shown to yield very strong ME effects even at room temperature [1–3]. These structures also offer a great flexibility in the sense that a large number of parameters may be tuned independently including the material properties of the constituent phases as well as the connectivity between them. Consequently, nowadays these materials are already very close to some promising applications which include: DC and AC magnetic vector field sensors and electric current sensors, magneto-electro-elastic energy harvesters, multiple-state memory devices, micro-sensors in read heads, transformers, spinners, diodes, spin-wave generators and electrically tunable microwave devices.

In this work we have studied a variety of different magnetoelectric laminates by bonding magnetostrictive metglas foils onto single-crystalline substrates of $LiNbO_3$ (LNO), $GaPO_4$ (GPO) and PMN-PT. The measurements have been performed as a function of the crystal cut, magnitude and orientation of the magnetic bias field and the frequency of the modulation field [4]. Despite much weaker PE coefficients of LNO and GPO, direct ME effects have been found to have comparative magnitudes as compared to PMN-PT. Greatly enhanced ME coefficients in certain resonance modes are explored and their relations to the material properties of the crystals and the geometry of the composites are investigated. We demonstrate that control of the PE crystal's orientation can be used in order to obtain almost any desired quasi-static and resonant anisotropic ME properties for some given application. The anisotropic quasistatic ME coupling was generally found to be two times larger in the bidomain LNO samples stronger to their monodomain counterparts [5]. Large ME effects were obtained in low-frequency electromechanical resonance modes of the piezoelectric crystals. Of note is the fact that the contour modes were suppressed in the bidomain systems, whereas the bending modes were greatly enhanced. At a bending resonance frequency of 6862 Hz, we found a giant $|\alpha_{E31}|$ value up to 1704 $V\cdot(cm\cdot Oe)^{-1}$ in laminate composite metglas / bidomain *y*+140°-cut lithium niobate. Furthermore, the equivalent magnetic noise spectral density of the investigated composite material was only 92 $fT/Hz^{1/2}$, a record value for such a low operation frequency [6]. Thus, we have shown that such systems may be used in simple and sensitive low-frequency magnetic and current sensors.

1. C.-W. Nan, M.I. Bichurin, S. Dong, et al., *J. Appl. Phys.* **103**, 031101 (2008).
2. J. Ma, J. Hu, Z. Li, et al., *Adv. Mater.* **23**, 1062 (2011).
3. Y. Wang, J. Hu, Y. Lin, et al., *NPG Asia Mater.* **2**, 61 (2010).
4. J.A. Vidal, A. A. Timofeev, A. L. Kholkin, et al., in Nanostructures and Thin Films for Multifunctional Applications in Nanostructures and Thin Films for Multifunctional Applications, (Springer Intl. Publishing, Switzerland), 227 (2016).
5. J.V. Vidal, A.V. Turutin, I.V. Kubasov et al, *IEEE Trans. Ultrasonics, Ferroelectrics and Frequency Control* **64**, 1102 (2017).
6. A.V. Turutin, J.V. Vidal, I.V. Kubasov et al, *Appl. Phys. Lett.* **112**, 262906 (2018).

I-06

Stick and slip states in the probe-sample force interaction and informative nanomechanical measurements using AFM

A.V. Ankudinov[1,2]

[1]*Ioffe Institute, 194021, Saint Petersburg, Russia*
[2]*ITMO University, 197101, Saint Petersburg, Russia*
e-mail: alexander.ankudinov@ioffe.mail.ru

Most modern atomic force microscopes (AFM) use an optical lever deflection system [1], which may monitor two angles of deflection (bending, torsion) of the console carrying the probe. Alternative methods, as a rule, control one parameter. In the interference and capacitive methods [2] the vertical Z-displacement is measured, the piezoresistive method [3] is the most sensitive to the force F_Z producing the maximum moment. Using any of the mentioned methods is not sufficient to determine the three components of the displacement of the probe or the interaction force [2,4,5]. To completely describe the ideal case without friction, when the probe slides over the surface, it is sufficient to know just one component of the force F_Z or of the displacement Z. In a real situation, the probe may stick or slip at the sample surface, which creates prerequisites for the appearance of ambiguities in the AFM measurements.

In contact and hybrid AFM modes, this leads to the scanning instabilities and to the measurements errors of relief height, interaction forces, contact stiffness, Young's modulus, piezoresponse signals, and also creates limitations for nanomanipulations and nanolithography. In resonance AFM modes, the problem is partly eliminated, but, simultaneously, the possibilities of contact regimes also disappear.

We analyze our recent AFM studies of native, living cells in the hybrid mode (PeakForce QNM): erythrocytes [6], fibroblasts [7], neurons [8,9]. For the comparison, the AFM studies of the artificial objects, partially simulating the living cells, are also presented: micro- and nanoscopic drops of glycerol, Hg and Ga; solid and polymeric test structures with well defined relief. The important features of the PeakForce QNM mode are high speed measurements of indentation force curves and subsequent automatic processing of the detected data array. Due to this, not only the surface relief is studied, but also a whole spectrum of sample's local characteristics: contact stiffness, deformation, probe adhesion to the sample, energy dissipation in the loading-unloading cycle.

The measurement data are analyzed and compared with analytical calculations of the deformations in the console-probe-sample system, taking into account stiffness tensors of the subsystems: cantilever console; a pyramidal probe attached to the edge of the console; sample. (The stiffness tensor describes linear relation between the concentrated force vector and the deformation vector). A general solution is presented for three types of holonomic constraints: the probe sticks to the sample, the probe slides along the selected direction, the probe slides in the selected plane. A particular solution is considered in detail for the case: a rectangular console; "infinitely rigid" probe; a flat sample with finite, anisotropic stiffness, the plane of the sample is deviated from the horizontal by an arbitrary angle.

In particular, the comparison carried out showed the following. With respect to the silicon AFM probe, native fibroblasts behave as slippery (and erythrocytes as sticky) objects, which is manifested by increasing (decreasing) apparent deformation on strongly inclined regions of these cells. The native neurons are sticky with respect to the silicon and nitride silicon material of the probe. This is attributed to the observed decrease in the average apparent Young's modulus with an increase in the ratio of the height of the probe to the length of the console. On flat, horizontal regions of the erythrocytes and neurons, contact stiffness and, as a consequence, the apparent Young's modulus are underestimated. Contact stiffness on flat, horizontal areas of the fibroblasts is measured correctly.

In conclusion, we discuss possible uses of cantilever sensitivity calculations to the displacements of a sample in contact with the probe: improvement of the optical lever deflection

system; accurate AFM measurements accounting for stick-slip effects; optimization of cantilever parameters for effective piezoresponse force microscopy and atomic force acoustic microscopy.

The work was supported by FTP № 14.604.21.0200 (RFMEFI60417X0200).

1. G. Meyer, N. M. Amer, *Appl. Phys. Lett*. **53**, 12, 1045 (1988).
2. B. Bhushan (Ed.), *Nanotribology and Nanomechanics* (Springer), 1148 (2005).
3. M. Tortonese, R. C. Barrett, and C. F. Quate, *Appl. Phys. Lett*. **62**, 834 (1993).
4. S. Fujisawa, M. Ohta, T. Konishi, et al., *Rev. Sci. Instr.* **65**, 3, 644 (1994).
5. H. Kawakatsu, H. Bleuler, T. Saito, et al., *Jpn. J. Appl. Phys.* **34**, 6B, 3400 (1995).
6. M.M. Khalisov, K.I. Timoshchuk, A.V. Ankudinov, et al., *Tech. Phys.* **62**, 2, 310 (2017).
7. M.M. Khalisov, A.V. Ankudinov, V.A. Penniyaynen, et al., *Tech. Phys. Lett.* **43**, 2, 209 (2017).
8. M.M. Khalisov, V.A. Penniyaynen, N.A. Esikova, et al., *Tech. Phys. Lett.* **43**, 1, 85 (2017).
9. M.M. Khalisov, A.V. Ankudinov, V.A. Penniyaynen, et al., *IOP Conf. Ser. Mater. Sci. Eng.* **256**, 1, 012010 (2017).

I-07

Electrical properties and polarization switching in polycrystalline $BiFeO_3$ thin films

E.B. Araujo[1], D.O. Alikin[2], S.P. Reis[1], V.Ya. Shur[2], A.L. Kholkin[2,3]

[1]*Department of Physics and Chemistry, São Paulo State University, 15385-000 Ilha Solteira, Brazil*
e-mail: eudes@dfq.feis.unesp.br

[2]*School of Natural Sciences and Mathematics, Ural Federal University, 620000 Ekaterinburg, Russia*

[3]*Department of Physics & CICECO, University of Aveiro, 3810-193 Aveiro, Portugal*

The multiferroic bismuth ferrite ($BiFeO_3$) has been considered as a potential material for the development of the next generation of technological devices due to its high Curie temperature and superior ferroelectric properties with a giant remanent polarization. However, the practical applications of the $BiFeO_3$ thin films are still limited due to their large leakage current at room temperature. Studies on the physical properties at nanoscale and the search for alternatives that allow the development of new technological devices based on this system have motivated recent research. In the present work, we report studies on the electrical properties and polarization switching in polycrystalline $BiFeO_3$ thin films prepared by chemical solution route and crystallized in air and O_2 atmosphere under pressure at 600°C for 30 min. The piezoresponse force microscopy technique was used to study the polarization switching in $BiFeO_3$ thin films under different voltages. The observed domain sizes were smaller than 200 nm and showed a significant anisotropy of the spontaneous polarization orientation in the grains. Smooth movement of domain walls is observed for weak electric fields, while jumping motion is observed for larger fields. These results will be discussed in terms of pinning of the domain walls and possible macroscopic defects. Electrical properties were studied in terms of *ac* conductivity and complex electric modulus characterized through real (ε') and imaginary (ε'') dielectric permittivity measurements. The frequency (100 Hz to 1 MHz) and electric field effects (0 to 84 kV/cm) on the dielectric relaxation and electric conductivity were reported in the temperature range $300 \leq T \leq 480\,K$. The dependence of the *ac* and *dc* electric field shows a dielectric relaxation like observed as a function of temperature, but fundamentally different from the thermally activated process. Intrinsic defects and interfacial polarization are probable responsible by dielectric relaxation and conduction mechanisms in the studied films.

I-08

Quasi-two-dimensional electron gas at the interface of two dielectrics: ferroelectric/antiferromagnet

R.F. Mamin

Zavoisky Physical-Technical Institute, FRC KazanSC of RAS, 420029, Kazan, Russian Federation
e-mail: rf_mamin@yahoo.com

A high-mobility electron gas was first observed in 2004 [1] at the interface of $LaAlO_3$ (LAO) and $SrTiO_3$ (STO). After that, such heterointerfaces involving two insulating nonmagnetic oxides were comprehensively studied. In particular, it was found that the metallic phase (quasi-two-dimensional electron gas, q2DEG) is formed in the STO layers at the LAO/STO interface when the number of LAO layers is larger than three [2,3]. Such a system undergoes a transition to a superconducting state below 300 mK [4]. It has been shown that analogous to the ionic polar discontinuity, the quasi two dimensional electron gas (q2DEG [1]) may be created at an interface due to electric polarization discontinuity [2,3]. The creation of quasi-two-dimensional superconducting states at the interface and the ability to control such states by magnetic and electric fields is impossible without the use of new materials and without the development of new design interfaces. Unique properties of functional materials are achieved due to the effects associated with the complex composition of the interface structure. Such new materials include oxide heterointerfaces between two nonconducting oxides in which, owing to strong electronic correlations, unique transport properties are observed. We check the idea, that antiferromagnetic $LaMnO_3$ might be transferred to ferromagnetic state by increasing the concentration of free carriers by injection. This means that increasing the free change carriers might lead to the local ferromagnetic state and magneto-resistivity in a system with 2DEG. Therefore, there is an opportunity to switch both conductivity by an electric field (trigger effect), and the magnetic order (magnetoelectric effect) in the heterostructures similar to BTO/LMO.

We investigate the optical properties of q2DEG at the interface between ferroelectric oxide and insulating oxide in heterostructures, isostructural to $BaTiO_3/LaMnO_3$. The numerical simulations of the structural and electronic characteristics of the $BaTiO_3/LaMnO_3$ ferroelectric-antiferromagnet heterostructure have been performed. The temperature dependence of the electrical resistance has been studied for heterostructures formed by antiferromagnetic $LaMnO_3$ single crystals of different orientations with epitaxial films of ferroelectric $Ba_{0.8}Sr_{0.2}TiO_3$ (BSTO) deposited onto them. The measured electrical resistance is compared to that exhibited by $LaMnO_3$ (LMO) single crystals without the films. It is found that, in the samples with the film, for which the axis of polarization in the ferroelectric is directed along the perpendicular to the surface of the single crystal, the electrical resistance decreases significantly with temperature, exhibiting metallic behavior below 160 K [5]. The transition to the state with q2DEG at the interface is demonstrated. The effect of a magnetic field on heterostructure BSTO/LMO haves been investigated. It is sown that magnetic field change the resistivity properties of the interface BSTO/LMO very strong. The properties of the interfaces and the transfer to superconducting state are presented for the heterostrocture of ferroelectric/antiferromagnet with other compound.

The reported study was funded by Russian Scientific Foundation, research project No. 18-12-00260.

1. A. Ohtomo, H. Hwang, *Nature* **427**, 6973 (2004).
2. M.K. Niranjan, Y. Wang, S.S. Jaswal, et al., *Phys.Rev.L.* **103**, 016804 (2009).
3. S. Thiel, et al., *Science* **313**, 1942 (2006).
4. N. Reyren, S. Thiel, A. Caviglia, et al., *Science* **317**, 5842 (2007).
5. D.P. Pavlov, et al., *JETP Letters* 106, 440 (2017)

I-09

Magnetic phase transitions in solid solutions of Fe-containing perovskite multiferoics

I.P. Raevski[1], S.P. Kubrin[1], A.V. Pushkarev[2], N.M. Olekhnovich[2], Y.V. Radyush[2], E.A. Bikyashev[3], S.I. Raevskaya[1],V.V. Titov[1], M.A. Malitskaya[1]

[1]*Research Institute of Physics and Faculty of Physics, Southern Federal University, 344090, Rostov-on-Don, Russia*
e-mail: igorraevsky@gmail.com

[2]*Scientific-Practical Materials Research Centre of NAS of Belarus, 220072, Minsk, Belarus*

[3]*Faculty of Chemistry, Southern Federal University, 344090, Rostov-on-Don, Russia*

One of the promising ways of designing new single-phase multiferroic materials is adjusting the temperatures of both ferroelectric and magnetic phase transitions by ion substitutions in the host compound to obtain the maximal magnetoelectric coupling. This presentation summarizes the results of the studies of the effect of ion substitutions in both A and B sublattices of the ABO_3 perovskite structure for several Fe-containing perovskite multiferroics: $BiFeO_3$, $PbFe_{0.5}Nb_{0.5}O_3$ (PFN) and $PbFe_{0.5}Sb_{0.5}O_3$ (PFS) on the temperatures of their magnetic phase transitions. All these perovskites exhibit antiferromagnetic ordering, however in both $BiFeO_3$ and PFN it is of G-type, while in PFS it is of I-type. Some solid solutions were synthesized in the perovskite structure for the first time using the high-pressure synthesis. Magnetic phase transition temperature T_M was determined by studying the Mössbauer spectra at different temperatures.

It is generally believed that in all perovskite ABO_3 multiferroics magnetic and ferroelectric subsystems are independent. Magnetic properties are provided by B-site (e.g. $Mn^{3+}$and Fe^{3+}) cations while ferroelectric properties are provided by the A-site cations having the so-called dangling bonds (Bi^{3+} and Pb^{2+}). In contrast to this assumption not only B-site but also A-site ion substitutions have been found to effect greatly the T_N value of PFN. In $BiFeO_3$- based solid solutions similar effects were also observed but only at high enough degree of the dilution of the Fe-sublattice. These results are explained using the models of magnetic superexchange involving the p-orbitals of Pb^{2+} or Bi^{3+} cations.

In the case of B-site substitutions theT_M values usually decrease with the concentration x of the substituting ion due to dilution of the magnetically active Fe-sublattice. At first T_M decreases rapidly as x grows (i.e. the Fe^{3+} concentration decreases), but then it saturates at $T_M \approx$ 40-50 K. This sharp change in the slope of $T_M(x)$ dependence roughly corresponds to the percolative phase transition from a long-range antiferromagnetic order to a short-range spin-glass one. Interestingly the Fe content at which the crossover between long-range and short-range magnetic ordering is approximately the same for all the substitutions studied, including magnetic and Mn^{3+} or Cr^{3+} ions. The results obtained imply that there is no magnetic exchange between Fe^{3+} and Cr^{3+} or Mn^{3+} ions. The reason of such behavior seems to be a difference in electronic configuration of Cr^{3+} (Mn^{3+}) and Fe^{3+} ions. Both Mn^{3+} and Cr^{3+} have a $t^3_{2g}e^1_g$ electronic configuration, while Fe^{3+} ion has a $t^3_{2g}e^2_g$ one. Thus, the value of transfer integral for 180° cation-anion-cation superexchange between octahedron-site $t^3_{2g}e^1_g$ and $t^3_{2g}e^2_g$ cations is close or equal to zero. The only difference between $T_M(x)$ dependences for nonmagnetic and magnetic substitutions for Fe^{3+} is that in the latter case the blocking temperature of the spin glass phase appears to be somewhat higher.

One more possibility to change the T_M values is to vary the ordering degree of B-cations in ternary $PbFe_{0.5}B^{5+}_{0.5}O_3$ perovskites, because such ordering changes dramatically the number of the magnetic neighbors around each Fe^{3+} ion. Such effects have been observed for some PFS-based solid solutions.

This study was supported by RFBR (project 18-52-00029_a) and by the Ministry of Education and Science of the Russian Federation (project 3.1649.2017/4.6).

I-10

Domain control and the enhanced electro-optical properties in relaxor single crystal PMN-PT

W. Zhao, X. Fu, Q. Hu, F. Qiu, X. Wei, Z. Xu

Electronic Materials Research Laboratory, Key Laboratory of the Ministry of Education & International Center for Dielectric Research, Xi'an Jiaotong University, 28 West Xianning Road, Xi'an, China
e-mail: Wdy@xjtu.edu.cn

Lead magnesium niobate-lead titanate $Pb\left(Mg_{1/3}Nb_{2/3}\right)O_3 - PbTiO_3\,(PMN-PT)$, is one of the most excellent piezoelectric and electro-optic crystals. The efficient EO coefficient $\gamma_c$and EO coefficients along different axis (γ_{31} and γ_{33}) were investigated, using a single beam electric-optic measurement system and a typical Mach-Zehnder interferometer. At the same time, small voltage signals with different frequencies were used to measure the frequency dependence of EO coefficient. The relationship between piezoelectric and electro-optic were studied in order to study the composition, anisotropy, and domain structure dependence of the EO coefficient. The deeper understanding of electro-optic effect will assist us to make reliable and stable optical instruments.

1. X. Wan, H. Luo, X. Zhao, et al., *Applied Physics Letters* **85**, 5233 (2004).

I-11

Self-assembled quasi-1D and 2D nanostructures of fullerenes on silicon

A.V. Zotov[1,2], D.A. Olyanich[1], V.V. Mararov[1], T.V. Utas[1], A.N. Mihalyuk[1,2], A.A. Saranin[1,2]

[1]*Institute of Automation and Control Processes FEB RAS, 690041 Vladivostok, Russia*

[2]*School of Natural Sciences, Far Eastern Federal University, 690950 Vladivostok, Russia*
zotov@iacp.dvo.ru

When C_{60} fullerenes adsorb onto a solid crystal surface, their self-assembly is known to follow one of a few typical scenarios which choice is controlled by the competition between the C_{60}-substrate and C_{60}-C_{60} interactions. When C_{60} fullerenes are strongly bonded to a substrate, in the most cases fullerenes adsorb randomly at the surface (in particular, due to abundance of various adsorption sites with close binding energies) and the growing C_{60} layers are typically lacking a well-defined ordering. When the C_{60}-C_{60} interaction prevails, adsorbed fullerenes self-assemble into the close-packed hexagonal C_{60} arrays with C_{60}-C_{60} separation of ~10 Å, close to that in a bulk fullerite.

Using metal-silicon surface reconstructions (i.e., silicon surfaces covered with monoatomic and submonoatomic layers of metals) as a template for the overgrowth of C_{60} layers, one can have growth modes which do not follow the above scenarios. As a result, unusual ordered C_{60} nanostructures can be fabricated. The C_{60} layers grown on Tl-adsorbed Si(111)5×2-Au and Si(111) surfaces, covered by monolayers of metals, Tl or Pb, as well as their Tl-Pb compound, present such examples.

Si(111)5×2-Au surface comprises a quasi-one-dimensional surface reconstruction consisting of Au stripes mediated by honeycomb Si chains. One could expect that this surface might be a suitable template for growing quasi-one-dimensional C_{60} nanostructures. However intact Si(111)5×2-Au surface has been found to produce a poor template effect on the overgrown C_{60} layers which have a close-packed-like structure without distinct ordering. In contrast, the C_{60} layers grown on the Tl-adsorbed Si(111)5×2-Au surface, where Tl atoms occupy various adsorption sites on the honeycomb Si chains, have a well-ordered quasi-one-dimensional structure consisting of straight C_{60} chains. The C_{60}-C_{60} spacing within the chains of ~12 Å that is ~3.2 a_0 (where, a_0 is the lattice constant of Si(111) surface) reflects the peculiarity of the C_{60}-C_{60} intermolecular interaction on the Tl-adsorbed Si(111)5×2-Au surface.

In the C_{60}/Tl/Si(111), C_{60}/Tl/Ge(111), C_{60}/Pb/Si(111) and C_{60}/(Tl, Pb)/Si(111) systems, a family of the exotic 2D C_{60}-metal nanostructures has been discovered. We named these nanostructures the `trilliumenes' since their common basic building block is the four- $C_{60}$ cluster (`trilliumon') which shape is reminiscent of the three-petal flower called `white trillium'. Various stacking of trilliumons produces various 2D ordered nanostructures, the `trilliumenes'. The periodicity of the trilliumene structure is $\sqrt{57}\times\sqrt{57}$-R±6.5° for the C_{60}/Tl/Si(111) system, $\sqrt{37}\times\sqrt{37}$-R±25.2° for the C_{60}/Tl/Ge(111) system and $\sqrt{21}\times\sqrt{21}$-R±10.9° for the C_{60}/Pb/Si(111) and C_{60}/(Tl, Pb)/Si(111) systems. Remarkably that all metal media triggering formation of the trilliumenes on Si(111) surface, i.e. double-atomic Tl layer and single-atomic Pb layer and Tl-Pb compound, have recently been proved to be 2D superconductors. In this respect, the trilliumenes show promise to be 2D nanostructured superconductors, which properties are awaiting their exploration.

The work was supported by Russian Foundation for Basic Researches (Grant No. 17-02-00577).

I-12

Advance nanostructured materials for photocatalytic water purification

M. Khanuja

Centre for Nanoscience and Nanotechnology, Jamia Millia Islamia, New Delhi- 110025, India
e-mail:manikakhanuja@gmail.com

This water scarcity catches the eye of many researchers in field of water remediation. Since only 1% of fresh water is accessible to living beings out of 2.5% of total fresh water, perhaps the need for its purification is a major issue to our health. Various organisations are spending a ton of principle in its purification, also investing in research to find a best low cost way to cleanse the water bodies to make it available for human use and avoid various water borne diseases. Organic dye(s) is one of the major impurities found in water and is big threat to health of living beings. Numerous existing metal oxides sheets e.g. TiO_2, ZnO, SnO_2 and WO_3 usage as photocatalyst is restricted due to (i) under-utilization of sunlight for photogeneration of charge carriers due to their wide band gap, (ii) poor charge transport due to low mobility, (iii) high recombination rate of the photogenerated electron-hole pairs, thus limiting its catalytic activity, (iv) agglomeration of nanomaterials leading to poor dispersion.

In the present work, two dimensional (2D) metal dichalcogenides, MX2 (M = Mo, W; X = S, Se) are used for photocatalytic activity owing to their unique physicochemical properties such as porous structures, high specific surface areas, good crystallinity, better charge carrier separation, and abundant surface active sites. Despite all these advantages, the key drawback of employing MX_2 as a photocatalytic material is its poor electronic conductivity and agglomeration. The weak interlayer bonding and large interlayer spacing causes stacking of MX_2 nanosheets. In the present work, various approaches have been attempted to address this issue to improve conductivity and stacking including stacking with conducting polymers, graphene, coating and mixing with carbon nanotubes etc. The rationally designed two dimensional hybrid nanostructures have the potential to overcome the aforementioned challenges prevalent in existing photocatalytic material.

1. A. Baral, M. Khanuja, S.S. Islam, et al., *Journal of Luminescence* **183**, 383 (2017).
2. S. Singh, R. Pendurthi, M. Khanuja, et al., *Applied Physics A* **123**, 184 (2017).
3. R. Sharma, M. Khanuja, S.S Islam, et al., *Research on Chemical Intermediates* **43**, 5345 (2017).
4. R. Sharma, Uma, S. Singh, et al., *Journal of photochemistry and photobiology* **162**, 266 (2016).
5. T. Bhuyan, M. Khanuja, R. Sharma, et al., *Journal of Nanoparticle Research* **17**, 288 (2015).

I-13

Advances of scanning probe microscopy in biomedical applications

I.V. Yaminsky[1,2]

[1]*Lomonosov Moscow State University, 119991, Moscow, Russian Federation*

[2]*Advanced Technologies Center, 119311, Moscow, Russian Federation*
e-mail: yaminsky@nanoscopy.ru

Scanning probe microscopy has proved to be an efficient tool for the visualization of biomacromolecules, bacteria, living cells and tissue in ambient conditions with unprecedented space resolution. Informative scanning probe microscopy atlases of bacterial cells and virus particles are in the stage of permanent successful additions. Scanning probe microscopy is making successful steps in the development of molecular diagnostics methods for personalized medicine - early detection of biological agents and markers of various diseases. Scanning probe microscopy techniques has recently demonstrated the detection of individual bacterium, virus [1], protein and even one atom [2]. An efficient way for the rapid detection of bacterial resistance to antibiotics has been developed and demonstrated in [3]. High-sensitive detection of viral particles at low concentration in liquid solutions is shown in [4].

Modern scanning capillary microscopy plays a crucial role in a variety of biomedical applications. A capillary probe or nanopipette of scanning capillary microscope can act as a drug delivery device, an electrochemical sensor, a pH biosensor, a test system for detecting metal ions, and many others. Capillaries with two or more channels also allow directed mass transfer of substances, biomacromolecules (peptides, proteins, nucleic acids, etc.) to the surface of bioobjects or inside their volume. In our research we use a device built onto an inverted microscope, so that optical and probe microscopy data can be obtained and analyzed simultaneously [5]. In [6], for example, red blood cells were observed with the help of scanning capillary microscope, and analysis of the results has showed that the roughness of their surface was in the range of 20 nm. In the present report we use the term "capillary microscopy", because it unites much more functions and methods of application in comparison with "scanning ion conductance microscopy (SICM)" which was more widely used previosly. Scanning capillary microscopy successfully is developing due to the effective application of multichannel capillaries for directional surface modification and 3D printing. It is possible to predict the further widespread use of scanning capillary (ion conductance) microscopy in biomedical applications, testing of drugs using only one cell, rather than their cultures and stereolithography.

The present and future of scanning capillary microscopy for 3D printing and stereolithography is discussed in the report. The artistic printing using fluorescent proteins was initially demonstrated in [7]. This work opens new exciting opportunities for the use of multichannel capillaries for a variety of technological and biomedical applications.

The author is grateful for the financial support of Russian Foundation for Basic Research (project N 17-52-560001).

1. Gupta, D. Akin, R. Bashir, *Appl. Phys. Lett.* **84**, 11, 1976 (2004).
2. K. Jensen, Kwanpyo Kim, A. Zettl, *Nature Nanotechnology* **3**, 533 (2008).
3. G. Longo, L. Alonso-Sarduy, L. Marques Rio, et al., *Nature Nanotechnology* **8**, 522 (2013).
4. P.V. Gorelkin, A.S. Erofeev, G.A. Kiselev, et al., *Analyst* **140**, 6131 (2015).
5. I. Yaminsky, A. Akhmetova, G. Meshkov, et al., *Nanoindustry* **1**, 44 (2018).
6. E. Makarova, D. Bagrov, P. Gorelkin, et al., *Nanoindustry* **2**, 42 (2015).
7. K.T. Rodolfa, A. Bruckbauer, D. Zhou, et al., *Angew. Chem. Int. Ed Engl*. **44**, 6854 (2005).

I-14

Biological pyroelectrics for energy harvesting and infrared detection

S.A.M. Tofail[1,2], E.U. Haq[1,2], A. Stapleton[1,2], A. Mani[1,2], D. Chovan[1,2], C. Silien[1,2], J. Bauer[3]

[1]*Department of Physics, University of Limerick, Limerick, V94 T9PX, Ireland*

[2]*Bernal Institute, University of Limerick, Limerick, V94 T9PX, Ireland*
e-mail: Tofail.Syed@ul.ie

[3]*Department of Biomedical Engineering, Wroclaw University of Technology, Wybrzeze Wyspianskiego 27, 50–370 Wroclaw, Poland*

Pyroelectricity is the ability of certain non-centrosymmetric materials to generate a current when they experience a change in temperature over time; the pyroelectric current is proportional to the rate of heating or cooling. All pyroelectric materials also demonstrate piezoelectricity, the ability to generate a charge around their surface when subjected to stress (the direct effect) or conversely, to develop a mechanical strain in response to an electric field (the converse effect). A small subset of pyroelectric materials show switchable polarization, making them belonging to ferroelectric materials.

Pyroelectric detectors are thermal detectors where temperature fluctuations produce a change on the surface charge of pyroelectric crystals. The change in surface charge gives rise to a corresponding electrical signal that can be amplified, and used for temperature measurements, spectroscopy and IR thermography. This temperature gradient can be created by the absorption of light. Of the different pyroelectric materials available, triglycine sulfate, lithium tantalate and lead-zirconia titanate are the most commonly used pyroelectric detectors.

The limitations of these detector materials in relation to advanced applications [1] drive us to explore new materials of biological origin for potential performance improvement and sustainability. Pyroelectricity in biological materials are relatively less studied [2]. Notable exceptions are quantitative studies in bone and tendon [3], poled [4] and un-poled hydroxyapatite [5], γ-Glycine [6] and tear-enzyme lysozyme [7], and qualitative studies in plant leaves [8] and the thorax of live insects [9]. The coefficients of pyroelectricity in biological materials often far exceed that of conventional pyroelectric materials. This suggests that we must now evaluate the opportunity and challenges in using the newly found biological pyroelectrics for technical applications such as pyroelectric energy harvesting and infrared detection.

1. S.A.M. Tofail, A. Mani, J. Bauer et al., *Adv. Eng. Mater., in press* (2018).
2. S.A.M Tofail, *Ferroelectrics* **472**, 11 (2014).
3. S.B. Lang, *Nature* **212**, 704 (1966).
4. S. Tofail, C. Baldisserri, D. Haverty, et al., *J. Appl. Phys.* **106**, 106104 (2009).
5. S. Lang, S. Tofail, A. Gandhi, et al., *Appl. Phys. Lett.* **98**, 123703 (2011).
6. V. Lemanov, *Ferroelectrics* **238**, 211 (2000).
7. A. Stapleton, M.R. Noor, E.U. Haq, et al., *J. Appl. Phys.* **123**, 124701 (2018).
8. S.B. Lang, H. Athenstaedt, *Ferroelectrics* **17**, 511 (1977).
9. H. Athenstaedt and H. Claussen, *Biophys. Jour.* **35**, 365 (1981)

I-15

Silver modified nanomaterials for enhanced photodynamic therapy

K. Wysocka-Król, H. Podbielska, J. Bauer

Department of Biomedical Engineering, Faculty of Fundamental Problems of Science, WroclawUniversity of Science and Technology, Wyb. Wyspianskiego 27, 50-370 Wroclaw, Poland
e-*mail: joanna.bauer@pwr.edu.pl*

Photodynamic therapy (PDT) is an alternative antimicrobial treatment developed nowadays for combating the pathogenic microorganism like bacteria, fungi or viruses, including the most dangerous strains such as methicillin-resistant Staphylococcus aureus (MRSA), cephalosporin-resistant Escherichia coli, vancomycin-resistant Enterococcus (VRE) or antibiotic-resistant Gonorrhea which cause the severe problems in the healthcare sector [1,2]. PDT has been primarily developed as a treatment for cancerous diseases, however it can be as well successfully applied to different infectious diseases such as wound, skin and burn infections, bacterial cystitis and keratitis, dental and periodontal pathogens, ophthalmological infections, localized tuberculosis, or some fungal and viral infections.

The therapy uses different types of biocompatible photoactive dyes called photosensitizers which can generate the free oxygen atoms and radicals to kill microbial cells during irradiation by ultra violet or visible light [3]. Bacterial strains, as well as other microorganisms, are susceptible to photodynamic therapy and, so far, there no resistance mechanism to this therapy has been reported in the literature [4,5]. At present, PDT is considered as more beneficial in comparison to the classic antibiotic therapy mainly due to targeted uptake of the photosensitizers by cells, direct exposure of a cured region to the illumination, and its safety. This is caused by low toxicity outward the illuminated area as the non-irradiated photosensitizers' molecules stay inactivated [6]. Moreover, the therapy outcome can be observed almost directly, while pharmacological therapy requires longer time [7].

In this study we investigated silver modified nanomaterials with antibacterial activity that may find applications in disinfection and photodisinfection. We found that the photodynamic therapy' effectiveness can be enhanced by materials which contain both, silver nanoparticles and photoactive photosensitizers. This combination leads to the reduction of the photosensitizers' concentration which may be caused by the fact that silver nanoparticles interact with cells' walls and organells and thus inhibit microbial growth [8,9].

For the purpose of this research the silica- and titania-based nanopowders were prepared. Next, both types of materials were used as the support for immobilization of silver nanoparticles by use of modified Tollen's method. The morphological parameters of materials were studied by use of TEM. Moreover, the examination of optical properties of nanopowders doped with silver nanoparticles and photolon was conducted. Various concentrations of photolon solutions and nanomaterials were investigated in order to find the maximum absorption peak. Furthermore, the microbiological study was carried out to check the efficacy of antibacterial activity against chosen pathological strains. It was found that the photosensitizer solutions absorption is dependent on the concentration of silver nanoparticles. Antibacterial study showed moreover, that silver doped silica- and titania-based materials reveal antibacterial activity which can be enhanced by the presence of photolon.

Concluding, decribed here tailored antimicrobial nanomaterials can be applied to support the photodynamic therapy and thus give the opportunity to create a new way of managing the hospital acquired infections, especially combat the growing number of antibiotic resistant bacteria. Altogether, the nano-silver-silica-photolon and nano-silver-titania-photolon present powerful combination of both, antibacterial activity and photoactivity.

1. T. Hiltunen, M. Virta, A-L. Laine, *Philosophical Transactions of the Royal Society of London Series B, Biological Sciences* **372**, 20160039 (2017).
2. T. Maisch, *Lasers in Medical Sciences* **22**, 83 (2007).
3. M.R. Hamblin, *Current Opinion in Microbiology* **33**, 67 (2016).

4. T. Maisch, *Mini-Reviews in Medical Chemistry* **9**, 974 (2009).
5. Tavares, C.M.B. Carvalho, M.A. Faustino, et al., *Marine Drugs* **8**, 91(2010).
6. Y. Liu, R. Qin, S.A.J. Zaat, et al., *Journal of Clinical and Translational Research* **1**, 140 (2015).
7. S.A.M. Tofail, J. Bauer (Eds.), *Electrically Active Materials for Medical Devices* (Imperial College Press), 209 (2016).
8. J. Li, Z. Li-Fang, Z. Kai-Feng, et al., *Materials Research Bulletin* **43**, 2810 (2008).
9. F. Martinez-Gutierrez, P.L. Olive, A. Banuelos, et al., *Nanomedicine: Nanotechnology, Biology, and Medicine* **6**, 681 (2010).

I-16

Magnetic resonance force microscopy of individual domain wall

A. Volodin[1], C. Van Haesendonck[1], E.V. Skorokhodov[2], R.V. Gorev[2], V.L. Mironov[2]

[1]*KU Leuven, AfdelingVaste-stoffysica en Magnetisme, BE-3001, Leuven, Belgium*
e-mail: alexander.volodin@kuleuven.be

[2]*Institute for Physics of Microstructures RAS, GSP-105, 603950, Nizhny Novgorod, Russia*

We report on resonance force microscopy (MRFM) [1] investigations of the ferromagnetic resonance (FMR) of single domain wall (DW) in V-shaped planar permalloy nanowire (NW).

The magnetic permalloy 60°-bent V-shaped NWs (with shoulders of 3000 nm long and 600 nm width) were fabricated on 100 μm thick glass substrates. The samples were defined by e-beam lithography, metallization, and lift-off of 30 nm $Ni_{80}Fe_{20}$ layer deposited using a dc-magnetron sputtering technique. Scanning electron micrograph (SEM) of a V-shaped NW is shown in Figure 1a. In these NWs DWs can be easily created by external magnetic field applied along x-axis (Fig. 1b).

In our MRFM, a nearly spherical Co probe with diameter of ~9 μm attached to the end of a cantilever is used to localize region in which FMR is excited by the microwave strip-line inductor. In this region, the sum of the internal magnetic field and the *x*-component of the probe magnetic field corresponds to the resonance condition of DW. The field gradient produced by the probe couples the modulated high frequency component of magnetization to the cantilever that serves as a resonant (on the modulation frequency) micromechanical force detector. The high-quality factor (~10^4 in vacuum) of the mechanical resonator provides its unique sensitivity.

The example of the MRFM spectrum of DW is presented in Figure 1c. The corresponding MRFM image of the sample area at resonant frequency is presented in Figure 1e which shows that the resonance excitations are strongly localized in the DW region of NV. The resonance spectra and spatial distributions of the resonant oscillation amplitude were calculated by numerical solution of Landau-Lifshitz equation [2]. The measured MRFM spectrum and spatial distribution of resonant mode signal agree with micromagnetic modeling (Fig. 1c,d).

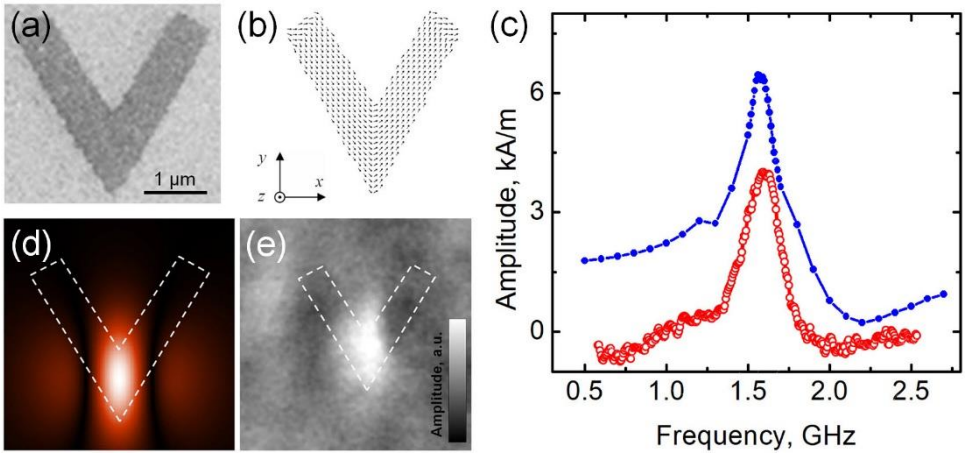

Figure 1. (a) SEM image of the Ni80Fe20 V-shaped NW. (b) Simulated distribution of magnetization in NW after magnetizing in x-direction. (c) MRFM spectra measured (lower curve) and modeled (upper curve) at H = 50 Oe aligned along the film plane perpendicular to DW. (d) Spatial distribution of the simulated amplitudes of the MRFM signal. (e) The MRFM image acquired at a DW resonant microwave frequency of 1.6 GHz.

The sample preparation and micromagnetic simulations were supported by Russian Science Foundation (project # 16-12-10254).

1. Z. Zhang, P. Hamel, P. Wigen, *Appl. Phys. Lett.* **68**, 2005 (1996).
2. R. Gorev, E. Skorokhodov, V. Mironov, *Phys. Solid State* **58**, 2212 (2016).

I-17

MFM investigations of particles with configurational anisotropy fabricated by scanning probe and microsphere lithography

A.A. Bukharaev, D.A. Biziyaev, N.I. Nurgazizov, T.F. Khanipov

Zavoisky Physical-Technical Institute, FRC Kazan Scientific Center of RAS , 420029 Kazan, Russia
e-mail: a_bukharaev@mail.ru

Patterned magnetic nanostructures, such as two-dimensional dot arrays, have attracted a great deal of interest due to their potential applications in many technologically important fields, such as magnetic information storage [1] or nonvolatile magnetic random access memory (MRAM) [2]. Recently the scientists have intensively studied the usage of the Villari effect (the change of magnetic properties of a solid under mechanical strain) for magnetic reversal processes of micro- and nanostructures. It is caused by the possibility to significantly reduce the energy for rewriting of a bit of magnetic information by the simultaneous usage of the magnetic field and mechanical tension and to create the magnetoelectric random access memory (MeRAM). Usually, the uniformly magnetized elliptical particles having two stable states with the opposite magnetization are used for the fabrication of memory cells (MeRAM) [3]. The particles with configurational anisotropy (for example, triangular and square ones) can have several stable states with quasiuniform («near-uniform») magnetization and in principle, they can be used for fabricating MeRAM [4].

In our work, the magnetization in triangular Py (Ni79%, Fe16%, Mo4%) particles of the micron and submicron size fabricated by scanning probe lithography [5] and microsphere lithography [6] were studied by magnetic force microscopy (MFM). Using the scanning probe lithography method, triangular submicron Py particles with different concave wall degrees (from the isosceles triangle to the particles with a shape close to the letter Y) were fabricated. In microsphere lithography Py was deposited in ultrahigh vacuum over the mask made of the two-dimensional array of close-packed 5 μm SiO_2 spheres. The triangular patterned Py particles with concave walls were fabricated on the Si substrate after removing SiO_2 spheres at the last stage.

The experimental MFM images were compared with the results of the computer simulation of its magnetic structure to detect the magnetization distribution in the particles with different sizes and shapes. These calculations were carried out by OOMMF [7]. This magnetization distribution was used for the simulation of the MFM images, which then were compared with the experimental results. The coincidence of the model image with the experimental one made it possible to conclude about the correct calculation of the magnetization distribution. The change of the magnetization distribution in the triangular submicron Py particles induced by the external magnetic field, mechanical compression or tension was also investigated.

These results may be useful for the fabrication of a new type of a straintronic cell (MeRAM) in the form of a heterostructure consisting of two planar particles with configurational anisotropy separated by a tunnel-transparent gap and placed on the piezoelectric substrate. The magnetization of the first particle was fixed and that of the second particle was relatively free.

1. D. Terris, T. Thomson, *J. Phys. D: Appl. Phys.* **38**, R199 (2005).
2. Y. Guoa, P. Wang, M.-M. Chen et al, *J. Appl. Phys*. **97**, 10P506 (2005).
3. J. Atulasimha, S. Bandyopadhyay, *Nanomagnetic and Spintronic Devices for Energy-Efficient Memory and Computing*, (Wiley), 259 (2016).
4. M. Salehi-Fashami, N. D'Souza, *JMMM* **438**, 76 (2017).
5. D.A. Bizyaev, A.A. Bukharaev, S. Ziganshina et al, *Russian Microelectronics* **44**, 389 (2015).
6. H. Zhong, G. Tarrach, P. Wu et al, *Nanotechnology* **19**, 095703 (2008).
7. M.J. Donahue, D.G. Porter OOMMF http://math.nist.gov/oommf.

I-18

Ferroelectric nanocomposites based on polymer ferroelectrics and graphene/oxide graphene: Computer modeling and SPFM experiments

V.S. Bystrov[1,2], X.J. Meng[3], I.K. Bdikin[2,4], M.V. Silibin[2], D.V. Karpinsky[2,5], B.B. Tian[3] , J.L. Wang[3], A.V. Bystrova[1], E.V. Paramonova[1]

[1]*Institute of Mathematical Problems of Biology, Keldysh Institute of Appl. Math., RAS, Pushchino, Russia e-mail: vsbys@mail.ru*

[2]*National Research University «MIET», Moscow, Russia*

[3]*National Laboratory for Infrared Physics, Shanghai Institute of Technical Physics, Shanghai, China*

[4]*Department of Mechanical Eng. & TEMA, University of Aveiro, Aveiro, Portugal*

[5]*Scientific-Practical Materials Research Centre of NAS of Belarus, Minsk, Belarus*

The experimental and computer modeling studies of composite nanomaterials based on polymer ferroelectrics polyvinylidene fluoride (PVDF)/poly(vinylidene fluoride-trifluoroethylene) (P(VDF-TrFE)) and graphene/oxide graphene (G/OG) are presented in this work. The main results of computer molecular modeling of the various nanostructures, piezoelectric properties of such combined nanocomposites of PVDF/(P(VDF-TrFE) thin films and G/GO layers were analysed in comparison with experimental data of the atomic force and scanning piezo-response force microscopy (AFM/SPFM). The computer simulation of the polymer-based nanocomposites of G/GO and PVDF was studied by the different methods using the HyperChem software package: molecular mechanics (MM), quantum mechanics (QM) using the semi-empirical PM3 and molecular dynamics (MD) runs. The piezoelectric response, the dielectric constant and the mechanical properties of the films were studied experimentally and found that they depend on the presence of the G/GO components concentration. The experimental results correlate qualitatively with the results obtained in these calculations. In particular, the calculated data of the piezoelectric coefficients d_{33} ~ 12 - 30 pm/C for PVDF-G/GO models corresponding to their observed experimental behavior, when the concentration of GO components are changed.

Then, using MD methods run with the quantum-chemical semi-empirical PM3 method, calculations of the change in the polarization with increasing temperature were carried out and a P(T) dependence was obtained. Data obtained was in agreement with the thermodynamic dependence of the polarization P(T), provided by Landau-Ginzburg-Devonshire theory for the ferroelectrics with a first-order phase transition (FP1). On the basis of this obtained relationship, the pyro-electric coefficients were calculated, which were in good agreement with the known values for the pure PVDF (~ 40 μC/(m^2*K)). For new nanocomposite models with graphene it turned out that in the case of a single-layer graphene model the pyroelectric coefficients increased by 3-4 times, and for the case of a two-layer model (sandwich model) it were decreased by 2-3 times in comparison with the pure polymeric ferroelectrics model. The experimental measurements of the pyroelectric coefficients values in these nanocomposites are in the work. The obtained results give important information about our understanding of the mechanisms of piezoelectricity and pyroelectricity in such nanocomposites, open new perspectives for the further creation, development and application of these new nanocomposites as multifunctional nanomaterials.

The authors are thankful to the Russian Science Foundation (RSF grant # 16-19-10112) and to the Russian Foundation for Basic Researches (RFBR grants # 16-51-53917) for support. Prof. Xiang-Jian Meng expresses his gratitude to the National Natural Science Foundation of China (NNSFC) for support of the project: "The study on the new type of infrared detector based on ferroelectric tunnel junction".

ORAL

PRESENTATIONS

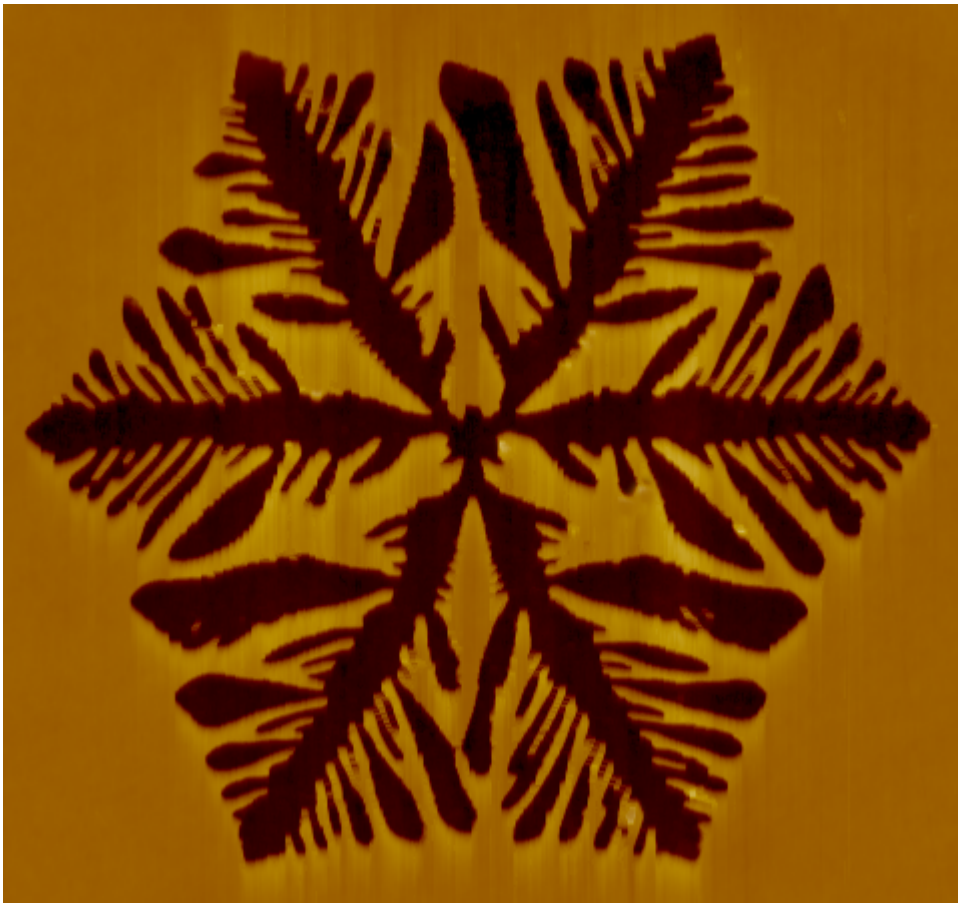

O-01

Bulk microstructure of nanocomposites studied by the impulse acoustic microscopy technique

S. Bellucci[1], V.M. Levin[2], E.S. Morokov[2], Yu.S. Petronyuk[2], A. Shubin[3]

[1]*INFN-Laboratori Nazionali di Frascati, Frascati, Rome, Italy*

[2]*Acoustic Microscopy Lab., N.M. Emanuel Institute of Biochemical Physique RAS, Moscow, Russia*

[3]*Ostec, Moscow, Russia*
e-mail: d2dnano@gmail.com

The idea of nanocomposites implies that substantial changes in composite properties are realized at minimal content of nanofiller. The changes stem from formation of extensive bulk networks of contacting nanoparticles and great value of contact interface of nanoparticles with polymer matrix. Highly dense distribution of contact interfaces results in restructuring polymer matrix and altering properties of the composite material. Therefore, nanoforms with big aspect ratios – nanotubes, nanoplatelets, nanoflakes; are used as filler to provide ramified interparticle contacts. topology of nanofiller distribution is of great importance for nanocomposite properties. Uniform distribution of nanoparticles is needed to provide optimum conditions for forming the continuous clusters of nanoparticles, and for maximal influence of nanofiller on composite properties.

In the paper the bulk mesostructure and local mechanical properties of epoxy nanocomposites with diverse carbon nanoforms – particles of exfoliated graphite (EG), graphite nanoplatelets (GNP), carbon nanoflakes (CNF), multiwall carbon nanotubes (MWCNT); have been studied by methods of the impulse acoustic microscopy (AM). The impulse AM is one of the key techniques that provide direct data on bulk microstructure and local bulk properties of a composite matter. The technique. In comparison with the alternative technique - X-ray microtomography; the impulse acoustic microscopy is characterized by combination of high efficiency, technical primality and availability.

The impulse AM has been applied for studies of 3D microstructure and micron resolution measuring local values of sonic velocities and elastic modules in carbon nanocomposites prepared by conventional technologies as well as with using vacuum mixing. The technique has shown.

Technique of pulse AM has been shown the micronon-uniform distribution of a carbon nanofiller over the nanocomposite bulk. The basic tendency of carbon nanoparticles to local clusterization and to formation of fractal micron-sized clusters containing entrapped air is shown. Nanoparticle aggregates with air content are well visible on layer-by-layer acoustic images of bulk microstructure for all types of nanocarbon composites at arbitrary depth inside their bulk. Results of the executed local elastic measurements demonstrate uniformity of bulk elastic properties and their weak dependence on type and content of carbon nanofiller. Comparison of the images of bulk microstructure produced by techniques of the impulse acoustic microscopy and x-ray microtomography certifies high informational content of acoustic images.

O-02

Novel developments in SPM instrumentation: Interferometer displacement sensor and high-resolution video-rate AFM

V.S. Neudachina

Intertech Corporation, 3 bldg. 2 Krymsky Val, 119049 Moscow, Russia
e-mail: vsn@intertech-corp.ru

Asylum Research, a division of Oxford Instruments and a manufacturer of the quietest AFM in the market, Cypher^{TM}, has recently presented a novel development for high-resolution AFM, an interferometer displacement sensor (IDS). It adds an independent, quantitative measurement of true cantilever displacement, complementing the standard optical beam deflection (OBD) cantilever tracking scheme. The IDS system adds an external laser Doppler vibrometer (LDV) to the existing optical system and therefore can be used as a secondary channel of information during regular AFM imaging with OBD for the tapping mode or can replace the existing OBD detection system for any contact modes.

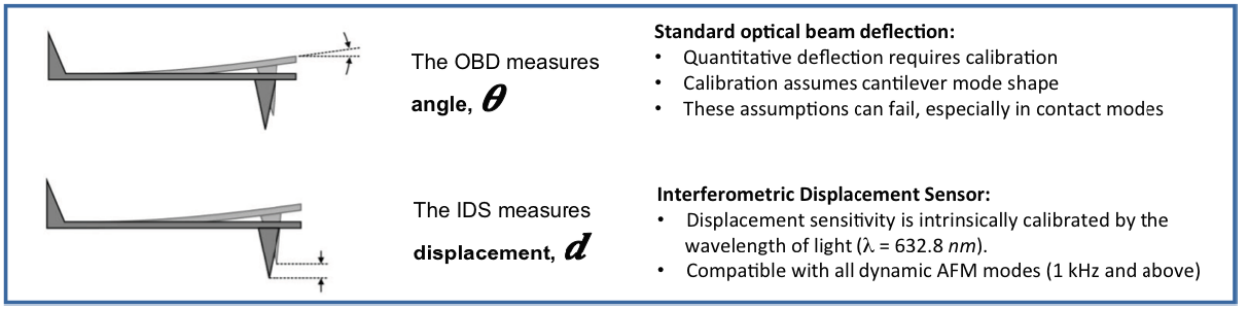

Figure 1. An illustration to the measurement mechanism for OBD and IDS

All research AFMs rely on the OBD for their cantilever deflection signal; it is relatively easy to implement and impressively quiet across a wide dynamic range. However, it is fundamentally a measurement of the changes in angle of the cantilever, and only indirectly related to tip displacement. Interpreting cantilever displacement therefore relies on models of the cantilever mode shape; when the model fails, the measurement is susceptible to errors. Although OBD works remarkably well for certain AFM imaging modes, it is also known to contribute to errors in others. For example, the first research area that was addressed with the IDS option was electromechanics. The result was a remarkable elucidation of the causes of artifacts in quantitative PFM when using OBD (refer to [1] for further detail).

The IDS calibration is based on the wavelength of light (λ=632.8 nm). It can therefore be used to obtain accurate measurements of the true tip displacement across its full measurement bandwidth (1 kHz-2.5 MHz). Furthermore, with a focused spot less than three microns in diameter, the cantilever mode shape can be mapped accurately, enabling quantitative interpretation of AFM experiments with unprecedented precision and accuracy.

The report will also focus on the recent developments in HR video-AFM using Cypher VRS, which was introduced in 2017 and combines video-imaging at up to 625 lines per second with an exceptional ease of use. Various examples from the area of biology and material science will be considered.

1. Labuda, R. Proksch, *Appl. Phys. Lett.* **106**, 253103 (2015).

O-03

Scanning probe microscopy under ultra high vacuum: Technologies and advantages from Scienta Omicron

M.A. Trusov, M.G. Minin

IMC Group Ltd., Moscow, Russia
e-mail: trusov@imc-systems.ru

The goal of the talk is to introduce the Fermi DryCool^{TM} SPM combining a cryogen-Free cooling system with a state-of-the art SPM head for high resolution STM and QPlus imaging, and spectroscopy in UHV for extended operations at low (<10K) temperatures.

The Fermi DryCool™ SPM combines a cryogen-Free cooling system with a state-of-the art SPM head for high resolution STM and QPlus imaging and spectroscopy in UHV for extended operations at low (<10K) and variable temperatures.

The unique DryCool™ technology integrates a closed-cycle, cryo-free cooling element to the SPM, while simultaneously decoupling the mechanical and acoustic impact. The result is a scanned probe system that performs measurements with extremely low drift and picometer stability, providing an excellent platform for long-term experiments such as scanning tunneling spectroscopy (STS), inelastic tunneling spectroscopy (IETS), and atomic manipulations.

A special design enables operation anywhere in the temperature range from below 10K up to 400K, with the unique feature of independent temperature control of the tip and the sample. This approach paves the way for scientists to continuously perform low and variable temperature STM, STS and Q-plus nc-AFM experiments.

The low thermal, mechanical and acoustic noise of the DryCool™ technology results in a stability level comparable to SPM's using conventional cooling techniques. The superior drift performance in XYZ dimensions (<0.2 Å/h) provides an ideal platform for long-term spectroscopy experiments (Fig. 1).

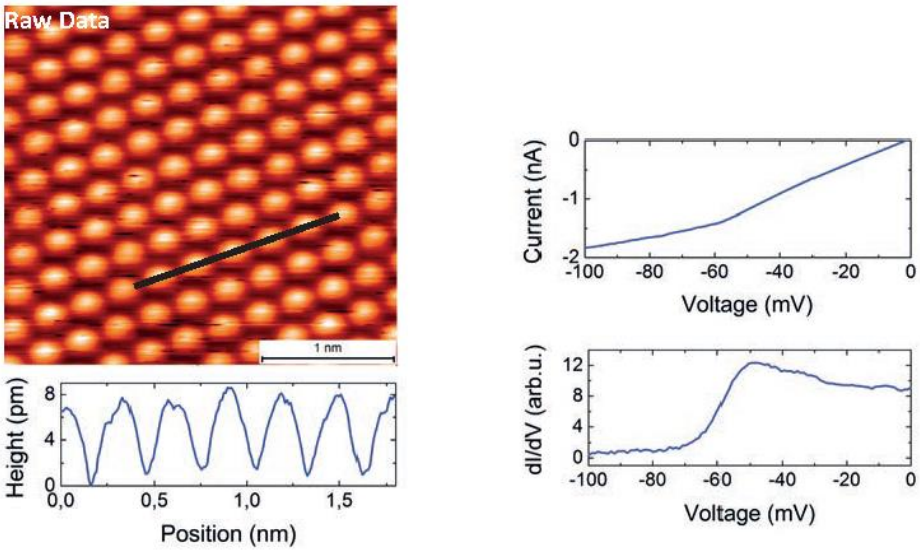

Figure 1. Atomic STM measurement with corresponding line profile along the black line-section, and high resolution scanning tunneling spectroscopy on Ag(111) at T=9.8K with running cooler.

O-04

Atomic force microscopy integrated with laser spectroscopy

V.V. Polyakov, A.V. Shelaev, V.A. Bykov

NT-MDT Co, 124460, Moscow, Zelenograd, Russia
e-mail: polyakov@ntmdt-si.com

Integration of atomic force microscopy (AFM) and laser spectroscopy traditionally makes it possible to obtain more complex information about the object under investigation: whether it is a living cell, a polymer composite, or nanotubes. In the report are given an examples of combined AFM and Raman microscope NTGERA Spectra (NT-MDT Co) application to study both physical properties of the surface (topography, surface potential, magnetic or piezoelectric properties, conductivity, local stiffness) and structural properties measured by Raman spectroscopy. Usually Si cantilevers of top-visual shape are used for optical access to the tip from above by high-res objective (100x, 0.7 NA). It is also possible to use metal needles in the tunneling current microscopy or tuning fork based feed-back. It is possible to carry out combined measurements in a controlled gas or liquid environment, which may be important to maintain the properties of the sample or to eliminate the background low-wavenumbers Raman peaks from the N_2 and O_2 molecules present in the air. The design of the spectrometer makes it possible to use either edge filters or notch filters to suppress laser radiation and provide both Stokes and anti-Stokes scattering, including the THz range down to 10 cm^{-1} from Rayleigh scattering.

Figure 1. NTEGRA Spectra II for combined AFM and Raman.

The most intriguing possibility that appears when integrating atomic force microscopy and Raman spectroscopy is to overcome the diffraction limit due to local amplification of the field near the tip apex [1]. To achieve strong enhancement of the Raman scattering in the Tip Enhanced Raman Scattering (TERS), it is necessary to keep the tip at the surface of the sample as closely as possible. The mode of nonresonant intermittent-contact microscopy, also known as Hybrid mode [2] allows the probe to be held in contact with the surface up to 70% of the time, while eliminating lateral forces during scanning and minimizing the pressing force. In addition, this method is also applicable to keep feedback in the liquid and when the sample is heated, when significant drift of the cantilever tilt is observed.

1. T. Deckert-Gaudig, A. Taguchi, S. Kawata, and V. Deckert, *Chem. Soc. Rev.* **46**, 13, 4077 (2017).
2. Patent US 9,110,092 B1.

O-05

Park Systems atomic force microscopes

S.V. Butiaikin

«Promenergolab» LLC, 107392, Moscow, Russia,
e-mail: svb@czl.ru

Park Systems is a global nanometrology equipment company focused on the development, production and sale of the atomic force microscopy systems. This equipment has incorporated the most advanced technology and more than 20 years' experience in this field.

Park Systems offers a wide number of AFMs that can be used for different jobs: research grade AFMs and industrial grade AFMs.

In both types of systems the same production technology and element base are used. The most popular and widespread are the research grade microscopes of the NX series. The flagships of this series are NX10 and NX20 AFMs (for analysis of small (up to 50 mm) and large (up to 200 mm) samples, respectively).

NX series AFM has unmatched accuracy, scanning speed and long service life of cantilevers which is especially important for modern tasks. These microscopes combine power, versatility and ease of use that is ideal for defects analysis and examining various samples.

The main distinguishing features of our AFM are:

- Crosstalk Elimination that removes background curvature and provides flat scan imaging in all size and conditions. So there is no need for post-processing
- True Non-Contact Mode that frees user from sample damage, minimizes costly tip degradation and prolongs high-resolution imaging
- True sample topography that allows record accurate heights of sample surface and frees from edge overshoot or piezo creep errors

Also high performance is ensured by combining a large number of high-precision elements in a single system:

- The conventional AFM use a piezotube - the bending motion of a piezotube introduces background curvature because you are moving in Z as you move in XY. Software flattening is required to correct the background curvature to a limited success. Park AFM utilizes two independent flexure scanners for sample and probe. XY scanner scans only sample and Z scanner scans only probe. The flexure scanners are Park's own design and make. They are developed and engineered for AFM scan
- The XY scanner comes with dual servo system. They are two pairs of symmetric, low-noise position sensors incorporated on each axis of the XY scanner. One pair of sensors corrects and compensates the non-linear and non-planar positional errors caused by the other pair of sensors. Dual servo is very much needed in order to retain a high orthogonality as the scan size and sample size become larger
- Minimized thermal drift - low thermal drift requires a careful mechanical design to reduce the undesired motion of the tip, relative to the sample. Designed to be thermally stable, the AFM body of Park NX10 and Park NX20 is optimized with thermally matched components and materials. A typical thermal drift rate is less than 0.15 nm/min for the lateral and 0.3 nm/min for the vertical
- High power optics consisting of objective lens with ultra-long working distance allows sample observation with unprecedented vision clarity. The long working distance of the objective lens is essential in enabling the direct on-axis view, the intuitive direct sample view from the top

Despite the complexity of the construction of these AFMs they are surprisingly easy to use even for an untrained user who does not have any knowledge in the field of AFM:

- Flexible and intuitive software has animated presentations that helps you prepare an AFM for measurement in just four clicks

- The system automatically approaches cantilever to the surface of a sample for the required distance – an operator should not be afraid that he can damage a sample or cantilever
- The unique head design of the crosstalk elimination allows a wide open side access for each sample and tip exchange. Hence, probe tip and sample exchange are just an easy snap by hand. Also the AFM head is easily inserted or removed by sliding along a dovetail rail. This locks the AFM head into its pre-aligned position with a positioning repeatability of a few microns, and automatically connects it to the control electronics
- Easy laser alignment - With our advanced pre-aligned cantilever holder, the laser beam is focused on the cantilever upon replacement. The natural on-axis top-down view allows the user to easily find the laser spot. Since the laser beam falls vertically on a cantilever, the laser spot moves intuitively and linearly along X and Y by rotating two positioning knobs. Hence, the laser is easy to position on PSPD

Park Systems has the most extensive range of advanced modes and options in the industry that allows you to equip the AFM in such a way that you can measure any properties that are necessary.

The most popular fields of research with the help of described AFMs are:

- Surface roughness measurement
- Conductive AFM - measures the conductivity across the sample regions
- Scanning capacitance microscopy

Technical support by highly qualified personnel on the user's side as well as online support ensures that you can always solve any emerging problem.

O-06

Probe microscopy of epitaxial structures made of metals: electron transport and exchange bias versus surface morphology

L.A. Fomin, A.V. Chernykh, G.M. Mikhailov

Institute of Microelectronics Technology and High Purity Materials RAS, 142432, Chernogolovka, Russia
e-mail: fomin@iptm.ru

The applications of scanning probe microscopy in various branches of research are widely known. Their multiplicity confirms the uniqueness of the method, as well as the possibility of its use in many seemingly unrelated fields of knowledge. The present report provides examples of the use of probe microscopy at the quantitative level to study the epitaxial structures of metallic films - the influence of surface morphology on electron transport and exchange bias. Such studies are motivated by application of nanosized conductors in electronics, especially taking into account the size of the elements continue to reduce.

It is well known that the electrical conductor with translational symmetry will not resist the current. However, such symmetry can be disturbed by thermal phonons, as well as by static defects, which are point, linear or planar defects, that violate the crystal structure. Although such phenomena are well known, the question remains with regard to what size of the metallic conductor there is no need to take into account the properties inherent to its bulk conductivity, but it demands to study its rough surface, which form the main channel of current dissipation? For these phenomena, specific transverse dimensions of the conductor at room temperature can be estimated as lower than 10 nm. In such circumstances, the conductors of small size have to be considered as a rough waveguide for electron waves, in which the morphology of the boundaries determines how well nanosized structures may conduct charge and spin current [1].

The use of probe microscopy provides direct information on the surface morphology of film structures in the form of a surface profile $z(x, y)$, which is a function of the coordinates along the surface. Using these numerical data, one can determine the spectral density of roughness fluctuations as a modular square of the Fourier transform $z(x, y)$. The spectral density is proportional to the probability of finding Z-harmonics in the measured profile with a certain wave vector directed along the surface. The analysis of this function allows finding statistical characteristics of a surface, in particular, to what type the investigated surfaces belong - Gaussian, fractal or mixed type [2]. Examples of the numerical use of such data for surface characteristics and description of charge and spin wave transport in small-sized metal conductors applying Schrödinger or Pauli equation are given, when the main current dissipation channel belongs to rough surfaces.

Another example of the influence of roughness - as the roughness of the ferromagnetic - antiferromagnetic interface reduces the effect of exchange anisotropy, manifesting itself in the effect of exchange bias of the hysteresis loop [3]. To study this effect, micromagnetic calculations were carried out using the OOMMF [4] software of a rectangular microstructure Fe/FeMn with a size of 1×2 μm^2 that possesses a rough interface.

A schematic representation of this structure is shown in Figure 1. The morphology of rough boundary was calculated from the data of atomic force microscopy collected from the profile of

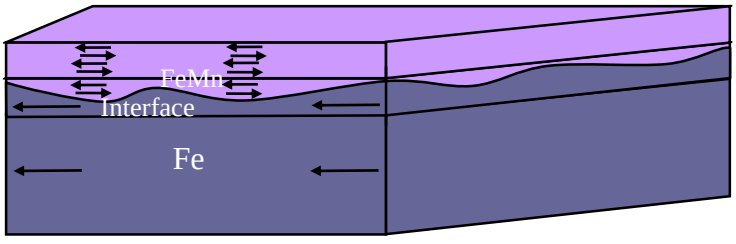

Figure 1. Schematic representation of the simulated structure. The arrows indicate the magnetic moments in the account cells.

real samples. For magnetic state simulation, the initial conditions of the Fe layer were the "diamond" type magnetic structure, and in the FeMn layer and its interface layer, their spins were oriented along the short side of the rectangle. The direction of the spins in FeMn layer was the same in each plane parallel to the plane of the rectangle and opposite between adjacent planes. Figure 2 shows the result of the micromagnetic calculations and the atomic force microscopy image of the rough interface.

The effective field of exchange anisotropy at the interface causes an increase in the area of the central domain, because its magnetization is directed along this field. An external magnetic field compensating for this effective field (exchange bias) can be found when this area becomes equal to 1/4 of the area of the entire rectangle. In the case of a smooth interface, the approximation gives an exchange shift of 128 G, and in the case of rough interface - 30 G.

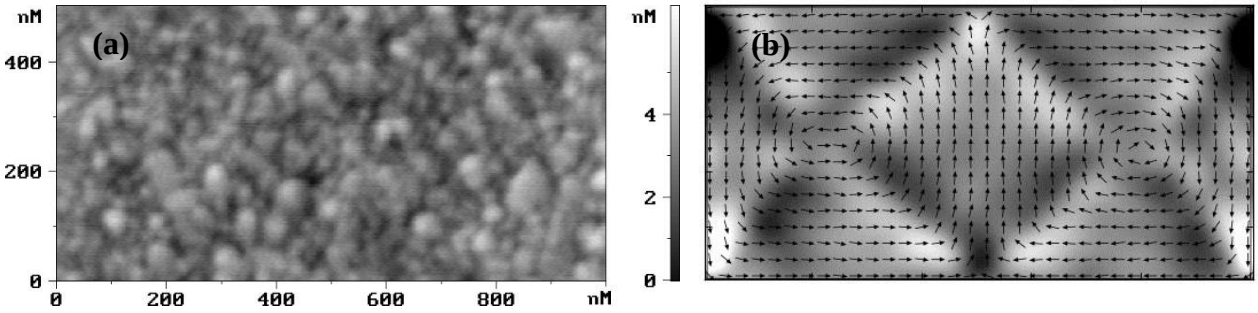

Figure 2. Atomic force microscopy image of epitaxial ferromagnetic film (a) and calculated magnetic force microscopy image of a ferromagnetic - antiferromagnetic layered structure with rough interface (b).

Thus, the value of the exchange bias taking into account the roughness of the interface is close, as it has been calculated, to the experimentally measured value found from the data of magnetic force microscopy and magnetoresistance measurements.

1. G.M. Mikhailov, *Phys. of Low-Dimens. Struct.* **1**, 1-2, (2002).
2. L.A. Fomin, I.V. Malikov, V.Yu. Vinnichenko et al., *J. Surf. Investig.* **2**, 104 (2008).
3. G.M. Mikhailov, L.A. Fomin, A.V. Chernykh, *Materials* **10**, 1156 (2017).
4. http://math.nist.gov/oommf/

O-07

The study of supramolecular structure of asphaltenes by atomic force microscopy

T.I. Sharipov, G.D. Akbutin, R.Z. Bakhtizin

Bashkir State University, 450076, Ufa, Russia
e-mail: sha-t@yandex.ru

Recently, much attention has been paid to works in which organic materials are used as materials for electronics. This is due to the unique properties of the elements of organic electronics which demonstrate semiconductor and even metallic properties and the sizes of these elements can be comparable with the sizes of an organic molecule [1-3]. Asphaltenes are the prospective structural materials in molecular electronic. It is known that asphaltenes in oil dispersed systems are in the form of supramolecular structures with the size of 1 to 1000 nm, which allows us to consider asphaltenes as the perspective object of nanotechnology. At present, the properties of asphaltenes at the supramolecular level are studied by various physical, physicochemical methods and methods of mathematical modeling [4,5].

Asphaltenes are the high-molecular non-hydrocarbon component of oil, consisting of 90-95% of the hydrocarbon. Asphaltene also includes sulfur in addition to carbon, hydrogen, oxygen and nitrogen. [6]. Large number of experiments were conducted to determine the structure and properties of asphaltenes. In 1961, T. Yen proposed the so-called chain-packed model of the structure of "plate to plate" type asphaltene [7]. Asphaltenes have an increased tendency to associate and form liquid crystal or supramolecular structures. Therefore, the important issue is to determine the degree of molecule association in solution.

Aasphaltenes isolated from the rest of the thermal cracking were used as the objects of the study. The mica was chosen as the substrate because it has an atomically smooth surface. The initial task was to find the optimal concentration of asphaltenes in toluene –the working solution for the next preparation of samples suitable for AFM studies. The working solutions with a concentration of 0.1 g/l were prepared by calculating the mass ratio of asphaltene in the toluene volume. Langmuir-Blodgett technique was used to obtain a monomolecular film of asphaltenes. After trying each of the four standard Langmuir-Blodgett techniques, we used up-draw process of the mica substrate through the film, whereby we obtained the highest quality AFM images. The supported asphaltenes thin film was dried in the Petri dish for 60 minutes at the temperature of 24°C. The resulting sample was studied in tapping mode of an atomic force microscopy by Ntegra-Aura probe nanolaboratory (NT-MDT Company, Russia).

The AFM image (Fig. 1a) shows the topography of the monomolecular layer of asphaltenes. Individual disc-shaped objects are observed on it.

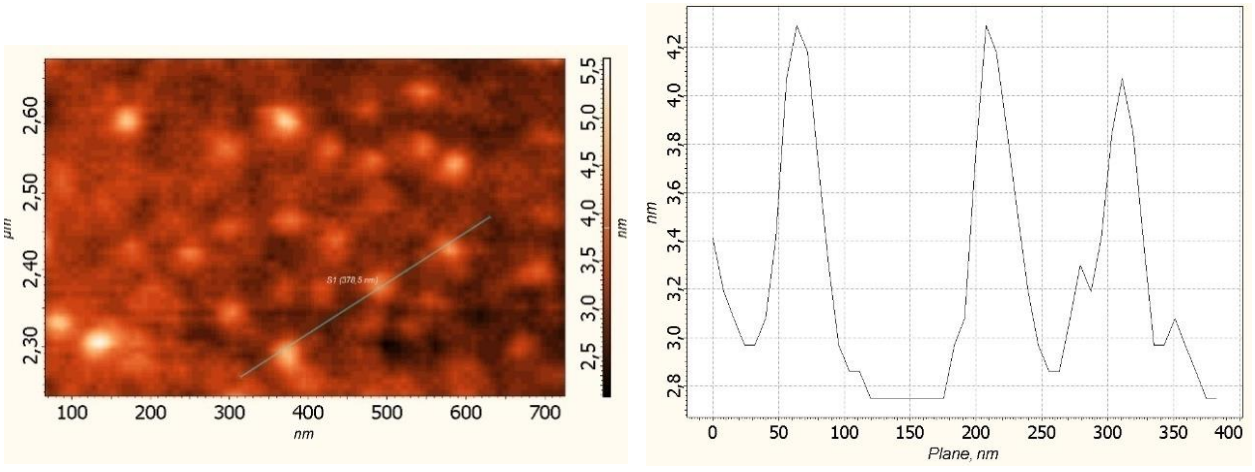

(a) (b)

Figure 1. (a) AFM image of asphaltenes film, (b) cross-section profile along the line marked at (a).

For detailed analysis, a cross-section has been carried out along the line shown in Figure 1a. The cross-section covers 3 separate objects. According to the cross-section profile (Fig. 1b), it can be calculated that the first object has height of 1.3 nm and width of 30 nm. The height of the second object is 1.35 nm and width 30 nm. The third object has height of 1.2 nm and width of 30 nm. Thus, the results of AFM studies show disc-shaped structures constructed from associates of asphaltene molecules. Considering that the size of one molecule does not exceed 3 nm, it can be assumed that the disk-shaped structure consists of about 15-20 molecules. When comparing our experiments results with the results of studies and modeling by Ese et al. [8] and Korzhova et al. [9], it can be assumed that the investigated aggregates have a disk-shaped structure and these structures are similar to discotic liquid crystals.

This work was supported by Russian Foundation for Basic Research under grant No. 17-42-020616.

1. M.A. Ratner, *Nature Nanotechnology* **8**, 378 (2013).
2. Рамбиди Н.Г. *Нанотехнологии и молекулярные компьютеры (*ФИЗМАТЛИТ), 256 (2007)
3. T I Sharipov and R Z Bakhtizin, *IOP Conf. Ser.: Mater. Sci. Eng.* **256,** 012009 (2017).
4. Ганеева Ю.М., Юсупова Т.Н., Романов Г.В, *Успехи химии* **80**, 1034 (2011).
5. Т.И. Шарипов, М.Ю. Доломатов, Р.З. Бахтизин, *«Наноэлектроника, нанофотоника и нелинейная физика»: тез. докл. XII Всерос. конф. молодых ученых* (Саратов: Изд-во «Техно-Декор»), 316 (2017).
6. Сергиенко С.Р., Таимова Б.А., Талалаев Е.И. *Высокомолекулярные неуглеводородные соединения нефти. Смолы и асфальтены (*М.: Наука), 269 (1979).
7. T.F. Yen, J.G. Erdman, S.S. Pollack, *Analytical Chemistry* **33**, 1587 (1961).
8. M.-H. Ese, J. Sjoblom, J. Djuve, et al, *Colloid Polym Sci* **278**, 532 (2000).
9. Коржов Ю.В., Орлов С.А., *Известия Томского политехнического университета. Инжиниринг георесурсов* **327**, 62 (2016).

O-08

Electrical properties of irradiated individual multi-walled carbon nanotubes at gases adsorption

D.V. Sokolov, N.A. Davletkildeev, V.V. Bolotov, I.A. Lobov

Omsk Scientific Center SB RAS, 644024, Omsk, Russia
e-mail: classicsub-zero@mail.ru

Carbon nanotubes (CNTs) present excellent properties when used as sensing materials, supercapacitors, and others [1]. The contribution of nitrogen doping for carbon nanotubes enhances electrical conductivity and nitrogen-containing defects serve as anchoring sites for specific gas molecules. For improve electrical properties of nitrogen-doped CNTs is a need to functionalize them, for example, by electron or ion irradiations [2].

Individual CNTs are ideal materials for nanodevices manufacturing but electrical measurements of a single nanotube are extremely difficult. Scanning probe microscopies techniques allows to get information about electrical properties individual nanoobjects with high resolution.

In present work electrostatic force microscopy (EFM) and conductive atomic force microscopy (C-AFM) successfully have been used for determining the free carrier concentration and the electrical conductivity in individual CNTs (irradiated by electrons, protons and argon ions) during adsorption of oxidative and reductive gases.

Samples preparation, measurements and calculations the electrophysical parameters were described in [3]. The change the electrical properties of CNTs during ammonia and nitrogen dioxide adsorption at a concentration of 1000 ppm were studied.

Figure 1 presents typical values the conductivity of as-grown and irradiated CNTs in dry nitrogen and after ammonia and nitrogen dioxide adsorption.

Figure 2 shows the free carrier concentration of as-grown and irradiated CNTs in dry nitrogen and upon exposure to ammonia and nitrogen dioxide.

Ammonia molecules (reductive gas) adsorbed on CNTs act as electron donors to the nanotubes, which led to increase of conductivity and electron concentration. With adsorption of acceptor molecules (nitrogen dioxide) conductivity and electrons concentration of doped CNTs decreases.

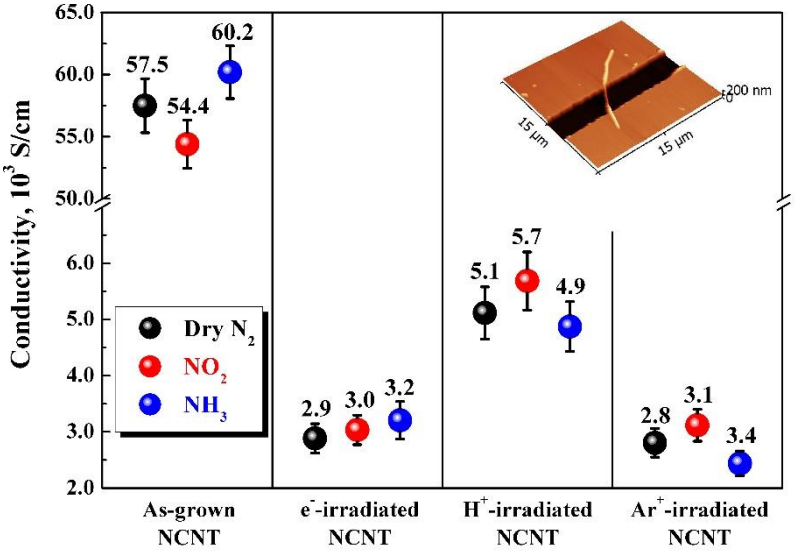

Figure 1. Mean values and range of electrical conductivity of individual nitrogen-doped CNTs (as-grown and irradiated by electrons, protons and argon ions) during adsorption of ammonia and nitrogen dioxide molecules. Inset: 3D AFM image of individual CNT on gold electrodes.

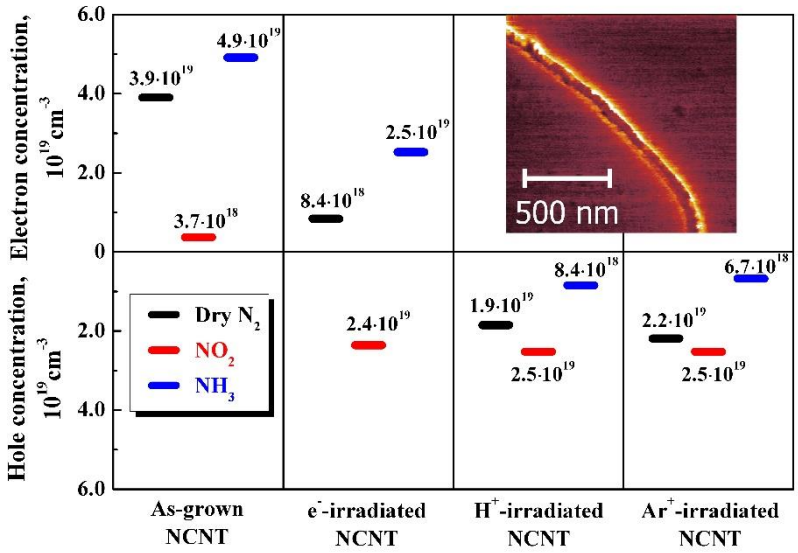

Figure 2. Mean values and range of free carrier concentration in individual doped CNTs (as-grown and irradiated by electrons, protons and argon ions) during adsorption of ammonia and nitrogen dioxide molecules. Inset: EFM image of individual CNT at tip bias +5V.

The type of irradiation particles effects on conductivity and carrier concentration in individual CNTs. Irradiated CNTs have various majority charge carriers due to the kind and concentration of irradiation-induced defects in CNT walls.

A change in conductivity of irradiated CNTs correlates with a change in charge carrier concentration in CNTs under adsorption of ammonia and nitrogen dioxide molecules.

Exposure to nitrogen dioxide increases the hole concentration in CNTs irradiated by protons and argon ions, because the extracted electrons by oxidizing gas molecules result in the generation holes in the valence band. Conductivity of these CNTs increases because the majority charge carriers are holes. The conductivity of the p-type CNTs under exposure to reducing gas (ammonia) decreases because generated electrons recombine with holes.

In CNTs, irradiated by electrons, the majority charge carriers are electrons. Adsorption of nitrogen dioxide leads to a change of the majority charge carriers. As a result, holes concentration more than the electron concentration in the CNTs before to nitrogen dioxide adsorption, so the conductivity increases. Exposure to reductive gas (ammonia) increases the electrons concentration in CNTs irradiated by electrons, and therefore the conductivity increases. Since the Fermi level shift during adsorption of the oxidative and reductive gases is slightly change, the concentrations of the majority charge carriers are practically equal, but they are opposite in sign. Therefore, C-AFM results show that the electrical conductivity of CNTs irradiated by electrons increases during adsorption in both gases.

The electrical parameters of individual nitrogen-doped carbon nanotubes (irradiated by electrons, protons and argon ions) were determined during the ammonia and nitrogen dioxide exposure using the methods of scanning force microscopy.

1. T.S. Williams, N.D. Orloff, J.S. Baker et al., *ACS Appl. Mater. Interfaces* **8**, 9327 (2016).
2. J.-J. Adjizian, R. Leghrib, A.A. Koos et al., *Carbon* **66**, 662 (2014).
3. D.V. Sokolov, N.A. Davletkildeev, V.V. Bolotov et al., *IOP Conf. Series: Materials Science and Engineering* **256**, 012018 (2017).

O-09

Growth and domain structure control of PIN-PMN-PT single crystals

Z. Li, K. Song, H. Guo, M. Ma, S. Fan, Z. Xu

Electronic Materials Research Laboratory and Key Laboratory of Education Ministry and International Center for Dielectric Research, Xi'an Jiaotong University, Xi'an 710049, People Republic of China
e-mail: zhrli@mail.xjtu.edu.cn

Relaxor based ferroelectric single crystals $Pb(In_{1/2}Nb_{1/2})O_3$-$Pb(Mg_{1/3}Nb_{2/3})O_3$-$PbTiO_3$ (PIN-PMN-PT) with composition near morphotropic phase boundary exhibit extraordinary piezoelectric properties. In this talk, we will show recent development of PIN-PMN-PT single crystal researches in Xi'an Jiaotong University. (1) Large size single crystal boule with 108mm in diameter and 170mm in length was successfully grown by modified Bridgeman method. The excellent properties (d_{33}-2774pC/N, k_{33}-0.94, E_C-4kV/cm, T_C-180°C, T_{RT}-100°C) were found near the morphotropic phase boundary composition. (2) The uniformity of dielectric and piezoelectric properties of the crystal boules with 4" diameter by 100mm long were clearly modified and improved along the crystal growth direction by the Bridgman method. For 70% length of the boule, T_{RT} and Tc were around 100°C and 160-180°C along the growth direction， respectively. The variety of piezoelectric constant d_{33} is about 1500-1800pC/N in the same range of the boule. So that PIN-PMN-PT crystals will be more cost-effective and beneficial for ultrasonic applications in higher temperature region. (3) The domain size was controlled by field-cooling method in PIN-PMN-PT single crystals. The domain size was decreased to sub-micrometer (W_d=0.4μm) in [111]-oriented tetragonal rod PIN-PMN-PT crystal using field-cooling method, and the piezoelectric response tremendous increased (d_{33}=1630 pC/N). For the single domain [001]-oriented tetragonal rod PMN-PT crystal, the mechanical factor Q value is 2250. It was found that the piezoelectric property increase with domain size decrease and the mechanical factor increase with domain size increase. The function of relationship between domain size and piezoelectric property was obtained.

O-10

(Tl, Au)/Si(111) and (Tl, Au)/Si(100) 2D compounds: Atomic and electronic structure and transport properties

A.N. Mihalyuk[1,2], C.R. Hsing[3], C.M. Wei[3], S.V. Eremeev[4,5], A.V. Matetskiy[1], N.V. Denisov[1], L.V. Bondarenko[1], A.Y. Tupchaya[1], D.V. Gruznev[1], A.V. Zotov[1,2,6], A.A. Saranin[1,2]

[1]*Institute of Automation and Control Processes FEB RAS, 5 Radio Street, 690041 Vladivostok, Russia*

[2]*School of Natural Sciences, Far Eastern Federal University, 690950 Vladivostok, Russia*
e-mail: saranin@iacp.dvo.ru

[3]*Institute of Atomic and Molecular Sciences, Academia Sinica, P.O. Box 23-166 Taipei, Taiwan*

[4]*Institute of Strength Physics and Materials Science SB RAS, 634021 Tomsk, Russia*

[5]*Tomsk State University, 634050 Tomsk, Russia*

[6]*Department of Electronics, Vladivostok State University of Economics and Service, 690600 Vladivostok, Russia*

Discovery of graphene has stimulated the current interest to atomically thin, two-dimensional (2D) materials which might exhibit unique properties not observed in the bulk materials. Metal-induced surface reconstructions on silicon and germanium (i.e., metal films of a monolayer or submonolayer thickness on silicon or germanium) are vivid examples. Most of the studies in this field have been restricted to reconstructions built of a single atomic species. Natural expansion of the research area is the exploration of the 2D multi-component systems.

Formation of the highly-ordered $\sqrt{7}\times\sqrt{7}$-periodicity 2D compound has been detected in the (Tl, Au)/Si(111) system as a result of Au deposition onto the Tl/Si(111) surface and its composition, structure and electronic properties have been characterized using scanning tunneling microscopy (STM), angle-resolved photoelectron spectroscopy (ARPES) observations and density-functional-theory (DFT) calculations. On the basis of these data, the structural model of the Tl-Au compound has been proposed, which adopts 12 Tl atoms and 10 Au atoms (in total, 22 atoms) per $\sqrt{7}\times\sqrt{7}$ unit cell, i.e. ~1.71 ML of Tl and ~1.43 ML of Au (in total, ~3.14 ML). Qualitatively, the model can be visualized as consisting of truncated-pyramid-like Au clusters with a Tl atom on top, while the other Tl atoms form a double layer around the Au clusters.

On the Si(100) formation of the highly-ordered $\sqrt{2}\times\sqrt{2}$-periodicity 2D compound has been detected and its composition, structure and electronic properties have been characterized using STM, ARPES spectroscopy observations and DFT calculations. The structural model of this Tl-Au compound on the Si(100) surface is much simply than that on the Si(111) one. It adopts 2 Tl atoms and 2 Au atoms per $\sqrt{2}\times\sqrt{2}$ unit cell, i.e. 1.0 ML of Tl and 1.0 ML of Au (in total, 2.0 ML).

Both (Tl, Au)/Si(111)$\sqrt{7}\times\sqrt{7}$ and (Tl, Au)/Si(100)$\sqrt{2}\times\sqrt{2}$ compound has been found to exhibit pronounced metallic properties at least down to the temperatures as low as ~2 K. Low-temperature magnetotransport properties will be discussed in the talk.

O-11

Tunnel electron-vibrational spectroscopy of adsorbed complexes on the surface of ultra-small metal nanoparticles

F.I. Dalidchik, E.M. Balashov, S.A. Kovalevskii

Semenov Institute of Chemical Physics, Russian Academy of Sciences,119991, Moscow, Russia
e-mail: domfdal@mail.ru

Ultra-small nanoparticles (USNP) with sizes less than 10 nm have unique physical, chemical, and biochemical properties and presently attract an increased general interest.

These nanoobjects are intensively studied by many methods, including probe ones with the use of a scanning tunnel microscopy (STM.) In the STM experiments, the structural and dynamical information on the nanoparticles (NPs) is contained in the tunneling spectra, specifically in the V-dependences of dnJ/dVn for n = 0 or 1, where J is current, V is the nanojunction voltage, and z=const is the distance between the tip and NP. For the properly choosen measurement conditions, these dependences show characteristic features, e.g. steps, bends, and maxima, which contain information on the energy E_n of electronic levels, vibrational quanta, electron-vibration interaction constant, etc. [1,2].

In the tunneling spectra of the USNP, the one-electron tunneling effects (Coulomb blockade and Coulomb staircases (oscillations)) can be observed even at room temperatures [3]. In the tunneling spectra of atomic particles adsorbed on the surface of USNPs, which are intensively studied with the object of solving nanocatalysis problems (see e.g. [4]), the resonance and Coulomb features often coexist. In those cases, the known concepts of resonance electron-vibrational tunnel spectroscopy may be insufficient on explaining this fact. The physical nature of the tunnel- current oscillations that can be associated both with vibrational transitions of adatoms and changes in the USNP charge state cannot be recognized. It should be keep in mind that, due to the fact that the ranges of characteristic vibrational energies of adatoms (0.1-0.6 eV) and the charging energies of nanoparticles with sizes from 2 to 10 nm coinside, the equidistant series of resonance singularities, e.g., Coulomb staircases (oscillations) and vibrational spectra, are indistinguishable in the absence of an additional information.

The model of tunnel resonant electronic transitions occurring in a nanojunction, with the A-USNP complex (A-adsorbed particle) situated under the STM tip, provides a simple explanation for the principal experimentally established features and dependencies of the tunneling spectra of metallic nanoparticles (Au, Pt, Ni, Cu) deposited on pyrolytic graphite. As a consequence, this model makes it possible to formulate simple algorithms for recognizing the Coulomb and vibrational oscillations that occur in the tunneling spectra by the biresonance (in the case of a metallic NP) or three-resonance mechanism (for a semiconductor NP). As follows from the model developed by us, the spectra in both cases have the form of equidistant bipolar series of negative differential resistances.

This work was supported by the Russian Foundation for Basic Research (the project no. 18-03-00453) and into frameworks of the state task for ICP RAS 0082-2018-0003 (the state registration number AAAA-A18-118012390045-2).

1. F.I. Dalidchik, B.A. Budanov, N.N. Kolchenko, et al., *J. Exp.Theor. Phys.* **115**, 1068 (2012).
2. F.I. Dalidchik, S.A. Kovalevskii, and E.M. Balashov, *J. Chem. Phys.* **146**, 194308 (2017).
3. D.V. Averin, K.K. Likharev, *J. Low Temp. Phys.* **62**, 345 (1986).
4. Л.И. Трахтенберг, М.Я. Мельников, *Синтез, строение и свойства металл/полупроводник содержащих наноструктурированных композитов*. (Техносфера), 109 (2016).

O-12

Atomic and electronic structure of nanostructured few-layer graphene with self-aligned boundaries synthesized on SiC/Si(001) wafers

A.N. Chaika[1], H.-C. Wu[2,3], O.V. Molodtsova[4], M.-C. Hsu[5], T.-W. Huang[5], C.-R. Chang[5], B. Walls[3], I.V. Shvets[3], V.Yu. Aristov[1,4]

[1]*Institute of Solid State Physics RAS, 142432 Chernogolovka, Russia*
e-mail: chaika@issp.ac.ru

[2]*School of Physics, Beijing Institute of Technology, Beijing, 100081, People's Republic of China*

[3]*CRANN and School of Physics, Trinity College, Dublin 2, Dublin, Ireland*

[4]*Deutsches Elektronen-Synchrotron DESY, D-22607, Hamburg, Germany*

[5]*Department of Physics, National Taiwan University, Taipei 10617, Taiwan*

Few-layer graphene exhibits exceptional properties that are of interest both for fundamental research and technological applications. The abilities to open energy gap and to make graphene magnetic are principal challenges in the fields of graphene-based electronic and spintronic applications. Nanostructured graphene with uniformly aligned nanodomain boundaries and ripples is one of the promising materials because the domain edges can reflect electrons over a large range of energies [1] and host spin-polarized electronic states [2,3]. Additionally, transport gap opening and spin–orbit coupling can be induced by ripples at the graphene domain edges.

In this report we discuss the atomic structure and electronic properties of nanostructured few-layer graphene synthesized on SiC/Si(001) wafers [4-6]. Atomically resolved scanning tunneling microscopy studies revealed that few-layer graphene nanoribbons with self-aligned boundaries can be synthesized in ultra-high vacuum using these technologically relevant substrates [5,6]. The electron transport measurements demonstrated that fabrication of such nanodomain system can produce a charge transport gap about 1 eV at temperatures below 100 K [6]. Magnetic transport measurements of graphene/SiC/Si(001) revealed an unprecedented large positive magnetoresistance in parallel magnetic field with a strong temperature dependence [7]. According to the theoretical calculations performed for different domain edge structures, the transport and magnetic properties of graphene/SiC(001) are most probably related to the localized states at the nanodomain boundaries and linear ripples along them. Our recent scanning tunneling spectroscopy studies performed at low temperatures revealed substantially lower density of the occupied electron states and existence of the energy gap at the nanodomain boundaries and ripples in few-layer graphene/SiC(001). The results show the feasibility of creating new electronic nanostructures using graphene on SiC/Si(001) wafers.

This work was partially supported by the Russian Academy of Sciences, Russian Foundation for Basic Research (grant № 17-02-01139, 17-02-01291), Beijing Institute of Technology Research Fund Program for Young Scholars, and Science Foundation Ireland.

1. O.V. Yazev, S.G. Louie, *Nat. Mater.* **9**, 806 (2010).
2. P. Ruffieux et al., *Nature* **531**, 489 (2016).
3. K. Nakada et al., *Phys. Rev. B* **54**, 17954 (1996).
4. A.N. Chaika et al., *Nano Res.* **6**, 562 (2013).
5. A.N. Chaika et al., *Nanotechnology* **25**, 135605 (2014).
6. H.-C. Wu et al., *ACS Nano* **9**, 8967 (2015).
7. H.-C. Wu et al., *Nat. Commun.* **8**, 14453 (2017).

O-13

Benefits of imaging flow cytometry for the analysis of nanoparticles in the biological environment.

D. Urusov

Merck LLC., 115093, Russia, Moscow
e-mail: russia@merckgroup.com

Exosomes are natural nanoparticles secreted by different cells and capable of carrying protein markers and genetic information, thus participating in intercellular communication. There are serious reasons to believe that the quantitative and qualitative characteristics of microparticles produced by cells of various tissues in normal and pathological ways can provide significant diagnostic and prognostic information and serve as a biomarker for various diseases, including oncological diseases.

Only recently has the importance of extracellular vesicles as key mediators of intercellular communication been appreciated. Extracellular vesicles are membrane derived structures that include exosomes, microvesicles and apoptotic bodies. Exosomes have been shown to transfer molecules between cells and have the potential to transfer signals between cells. Exosomes are released under normal physiological conditions; however, exosomes are also believed to serve as mediators in the pathogenesis of neurological, vascular, hematological and autoimmune diseases as well as cancer. Quantifying and characterizing exosomes in a reproducible and reliable manner has been difficult due to their small size (50 – 100 nm in diameter). Exosomes analysis can be done using high-magnification microscopy; however, this technique has a very low throughput. Attempts to analyze exosomes using traditional flow cytometers has been hampered by the limit of detection of such small particles and low refractive index. To overcome these limitations we have employed multispectral imaging flow cytometry that has the advantage of combining high throughput flow cytometry with higher sensitivity to small particles and the added benefit of imaging that can provide visual confirmation of particle integrity and characterization. In this study we use multispectral imaging flow cytometry to investigate the interaction of exosomes with white blood cells. Exosomes derived from Jurkat cells will be investigated for their preferential interactions with blood cell subsets by combining immunophenotyping with morphological parameters to measure their binding and internalization.

Exosomes derived from Jurkat cells were labeled with anti-human CD63-AF647 and added to human white blood cells. The cells labeled for immunophenotyping, fixed, and then labeled with anti-human CD63-PE to identify external exosomes. By plotting Internalization vs Bright Detail Similarity we were able to identify 3 populations: Internal Exosomes, External/Internal Exosomes, and Co-localized External Exosomes. Neutrophils, monocytes, and lymphocytes were identified by immunophenotyping; we investigated what % of each blood cell subset was associated with the CD63-AF647 labeled exosomes and whether the exosomes were internalized or external. The monocytes had the highest % of cell associated with CD63-AF647 labeled exosomes at 67%. And in all of the cell types the majority of the cells associated with CD63-AF647 labeled exosomes were either internalized or partially internalized (External/Internal Exosomes population).

The ImageStreamX MkII imaging flow cytometry platform has the quantitative power of large sample sizes common to flow cytometry with the information content of microscopy. This study showed a method to determine if exosomes have been internalized by the different blood cell subsets in an objective, quantitative, and statistically robust manner

O-14

Main results obtained in a series of animal experiments for the assessment of the organism's responses to metallic nanoparticles (self-review).

L.I. Privalova[1], B.A. Katsnelson[1], M.P. Sutunkova[1], I.A. Minigalieva[1], V.B. Gurvich[1], O.H. Makeyev[2], I.V. Valamina[2], S.V. Klinova[1], S.N. Solovjeva[1], V.Ya. Shur[3], E.V. Shishkina[3], I.V. Zubarev[3]

[1]*The Medical Research Center for Prophylaxis and Health Protection in Industrial Workers, 620014, Ekaterinburg, Russia*
e-mail: privalova@ymrc.ru

[2]*The Central Research Laboratory of the Ural Medical University, 620028, Ekaterinburg, Russia*

[3]*School of Natural Sciences and Mathematics, Ural Federal University, 620000 Ekaterinburg, Russia*

Nanoparticles (NPs) of Fe_3O_4 were produced by a chemical technique and nanoparticles of Ag, Au, CuO, NiO, Mn_3O_4, PbO, ZnO, TiO_2, SiO_2, Al_2O_3 - by laser ablation. In some experiments, we compared particles of a given chemical composition having different diameters, while in others – equidimensional NPs of different metals or metal oxides (Me-NPs).

We used two experimental models: (a) a single intra-tracheal instillation of Me-NPs 24 h before the bronchoalveolar lavage to obtain a fluid for cytological and biochemical assessment; (b) repeated intra-peritoneal injections during 6-7 weeks in non-lethal doses to assess the thus induced subchronic intoxication by a lot of functional, biochemical and morphological indices. Besides, we carried out long-term inhalation experiments with NPs of Fe_2O_3, SiO_2 and NiO.

We demonstrated that NPs are much more noxious as compared with their fine micrometric or even submicron counterparts and are usually the more toxic the smaller their dimensions *within* the nano-scale range. However, for the RES-rich organs this dependence is not so unique due to intricate and contra-directional influences of the Me-NP's size on toxicodynamics and toxicokinetics. We found also that toxicity of Me-NPs strongly depends on their chemical nature, solubility and specific mechanisms of action characteristic of a given metal in any chemical form. Solubilization of Me-NPs in biological milieus plays an important part in their toxicokinetics which can prevail over that of the physiological mechanisms controlling their distribution, retention and elimination.

On the other hand, thanks to the high activity of these mechanisms, the organism is not defenseless against the impact of Me-NPs. As the protective measure, the toxicity and even genotoxicity of Me-NPs can be significantly attenuated by adequately composed combinations of some bioactive agents in innocuous doses.

O-15

Polymorphic phase transitions and ferroelectric properties in β-glycine single crystals and micro islands

D.S. Vasileva[1], S.G. Vasilev[1], P.S. Zelenovskiy[1], A.S. Nuraeva[1], E. Seyedhosseini[2], D. Isakov[3], K. Romanyuk[1,2], V.Ya. Shur[1], A.L. Kholkin[1,2]

[1]*School of Natural Sciences and Mathematics, Ural Federal University,620000 Ekaterinburg, Russia e-mail: daria.s.vasileva@gmail.com*

[2]*Physics Department & CICECO – Aveiro Institute of Materials, University of Aveiro, 3810-193, Aveiro, Portugal*

[3]*WMG, University of Warwick, Coventry CV4 7AL, UK*

Crystalline structures based on vital biological molecules (amino acids, peptides, DNA) demonstrate nonlinear optical, piezoelectric, and ferroelectric properties similar to their inorganic counterparts [1-4]. Recently observed room-temperature ferroelectricity [5] and high shear piezoelectricity [6] in β-glycine opens up new perspectives of using this material in biocompatible non-volatile memories, optical switches, transistor gates, nonlinear optical and piezoelectric devices. At ambient conditions glycine crystallizes in three polymorphic phases: α, β and γ [7], only β-phase possesses both piezoelectric and ferroelectric properties. Metastable β-phase can irreversibly transform into the γ or α-phases under the presence of moisture [7]. The microscopic mechanism of such transformation still requires detailed investigations. With the continuing demand for miniaturization of ferroelectrics it is becoming extremely important to scale down their dimensions and to form arrays of self-organized micro- and nanocrystals.

In the present work we demonstrate the β→γ polymorphic transformation in glycine single crystal in situ visualized by piezoresponse force microscopy (PFM). Transformation into γ-phase was visualized during gradual decreasing of relative humidity from 30 down to 25%. It was shown that the transformation occurs for relative humidity above 25%. Analysis of the time dependence of ratio β to γ phase area obtained from PFM images allowed to reveal the averaged velocity of the phase boundary motion. Raman analysis of the phase boundary allowed to provide a microscopic model of the process.

The faceted crystals with in-plane polar axis were grown from aqueous solution via drop drying on Pt/SiO/Si substrate in air with controlled relative humidity. The detail experimental study of the neutral and charged domain walls in β-glycine microcrystals using atomic force (AFM) and PFM was performed using scanning probe microscopes Ntegra Aura (NT-MDT, Russia) and Asylum MFP 3D SA (Asylum Research, USA).

Three types of as-grown domain structure were found: (1) striped domains with flat charged domain walls (Fig. 1a), (2) quasiperiodic ensembles of submicron width needle domains (Fig. 1b) and (3) large area domains with irregular shaped domain walls (Fig. 1c). The formation of as-grown domain structure with flat charged domain walls and a smooth change in orientation near the crystal edges can be attributed to growth layers located perpendicular to the polar axis and representing a periodic change in the composition or concentration of impurities [8,9]. The polarization direction is determined by the gradient sign of the composition or concentration, so the domain walls are localized at the places where the gradient sign changes. The formation of two other types of the as-grown domain structure can be attributed to switching the polarization in the striped domains under the action of the pyroelectric field E_{pyr}, which appears when the temperature of the crystal changes [9].

The shallow wells of 0.2-1 nm-depth and about 150 nm-width were revealed along the charged walls. The formation of these features was attributed to selective etching by water layer appeared at the surface in humid air. In contrast the pits appeared at neutral domain walls are due to deformation of the crystal lattice in the vicinity of the wall.

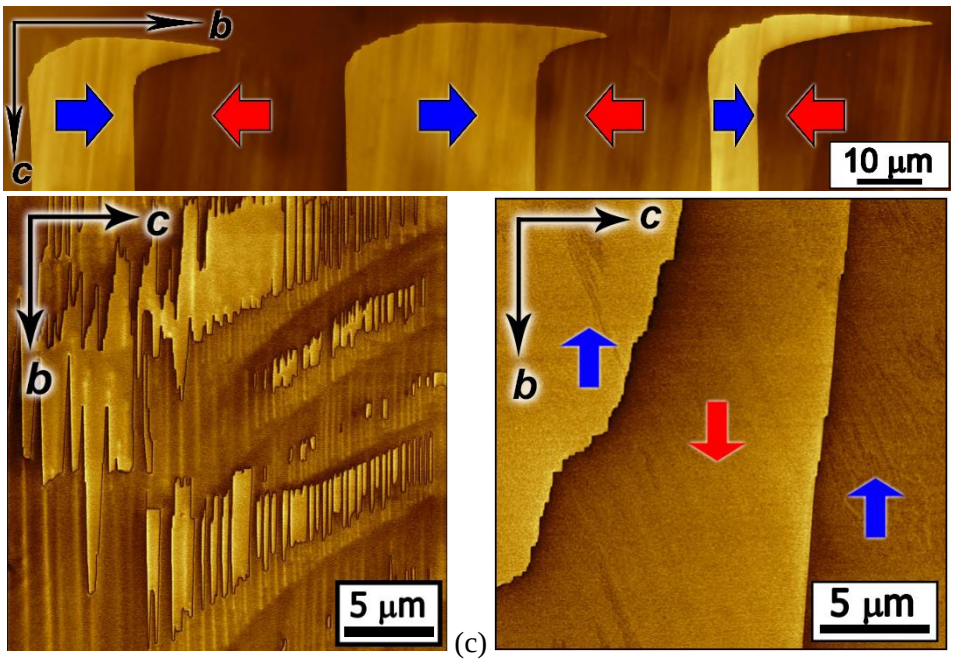

Figure 1. Lateral PFM images of the as-grown domain structure types: (a) striped domains with flat charged domain walls, (b) quasiperiodic ensembles of submicron width needle domains, (c) large area domains with irregular shaped domain walls.

In this work spin-coating formation of self-organized β-glycine films is also presented. The morphology of the obtained films varied from feather-like structures to quasi-regular arrays of individual micro- and nanoislands and nanowires. Micro- and nanoislands are oriented in a radial direction from the center of "grains" formed during evaporative dewetting. The kinetics of the dewetting follows the $t^{-1/2}$ law, which is responsible for the observed polygon shape of the grain boundaries [10]. It was confirmed by confocal Raman microscopy that all the structures belonged to ferroelectric β-phase and possess high stability.

Piezoelectric properties and domain structure of the films were studied by PFM. It was shown that ferroelectric polarization in β-glycine islands is parallel to the substrate and switchable under a relatively small bias applied by the conducting tip of piezoresponse force microscope.

The research was carried out using equipment of Ural Center for Shared Use "Modern Nanotechnologies" Ural Federal University with the financial support by the Government of the Russian Federation (Resolution 211, Contract 02.A03.21.0006). The reported study was funded by RFBR according to the research project № 18-32-00390.

1. V.V. Lemanov, et al., *Ferroelectrics* **285**, 207 (2003).
2. V.V. Lemanov, *Phys. Solid State* **54**, 1841 (2012).
3. A.L. Kholkin, et al., *ACS Nano* **4**, 610 (2010).
4. N. Vijayan, et al., *Cryst. Growth. Des.* **6**, 2441 (2006).
5. A. Heredia, et al., *Adv. Funct. Mater.* **22**, 2996 (2012).
6. S. Guerin, et al., *Nature Materials* **17**, 180 (2018).
7. E.V. Boldyreva, et al., *J. Therm. Anal. Calorim.* **73**, 419 (2003).
8. V.Ya. Shur, E.L. Rumyantsev, et al., *Ferroelectrics* **140**, 305 (1993).
9. V.Ya. Shur, E.L. Rumyantsev, *Journal of the Korean Physical Society* **32**, 727 (1998).
10. E. Seyedhosseini, et al., *ACS Appl. Mater. Interfaces* **9**, 20029 (2017).

O-16

The study of organogel formation with cyclo(leucyl-leucine) by the AFM method

A.S. Safiullina[1], M.A. Ziganshin[1], S.A. Ziganshina[2], A.A. Bukharaev[2]

[1]*Butlerov Institute of Chemistry, Kazan Federal University, 420008, Kazan, Russian Federation e-mail: englishfile94@gmail.com*

[2]*Zavoisky Physical-Technical Institute, Kazan Scientific Center, Russian Academy of Sciences Russian Federation, 420029, Kazan, Russian Federation*

Physical organogels, which are self-assembled from simple *cyclo*(dipeptide)s, are a novel biocompatible class of soft material with promising applications in materials engineering fields. The present study is devoted to the efficiently gelation of a wide variety of organic solvents using a representative model of the *cyclo*(dipeptide)s family by example of *cyclo*(leucyl-leucine). We propose that the water as co-solvent, might have a potential implication in controllable molecular self-assembly, due formation of hydrogen bond bridge between molecules of organic solvents and dipeptide.

Atomic force microscopy is an amazing technique for study of the interactions of biological molecules. In the present work, the ability *cyclo*(leucyl-leucine) to formation of gel structures from polar and non-polar solvent was studied using atomic force microscopy. This method was also used for demonstration the change in morphology of the surface dipeptide's films of *cyclo*(leucyl-leucine) obtained from different solutions as a result of interaction with different compounds of binary solvents. A mechanism for organic solvent-water binding to *cyclo*(dipeptide)s is proposed, based on results from this experiment.

The results of present work can be used for further development of techniques for the preparation of nanomaterials based on *cyclo*(dipeptide)s.

This work was supported by the ministry of education and science of russian federation [grant №14.y26.31.0019]

O-17

Mechanical and piezoelectric properties of pure and modified microtubes of diphenylalanine

A.S. Nuraeva[1], V.V. Yuzhakov[1], P.S. Zelenovskiy[1], T.A. Koryukova[1], S.G. Vasilev[1], E.V. Gunina[1], D.S. Chezganov[1], A.L. Kholkin[1,2], V.Ya. Shur[1]

[1]*School of Natural Sciences and Mathematics, Ural Federal University, 620000 Ekaterinburg, Russia e-mail: alla.nuraeva@urfu.ru*

[2]*Physics Department & CICECO – Materials Institute of Aveiro, 3810-193 Aveiro, Portugal*

Self-assembled supramolecular peptide structures are a class of chiral organic piezoelectrics capable for biomedical applications and devices [1], nanoelectronics [2], etc. Functionalization of peptide nanostructures by nanoparticles (NPs) leads to formation of new organo-inorganic composites. Interaction between NPs and biological macromolecules via weak hydrogen bonds and van-der-Waals forces represents fundamental interest, since NPs act on the formation and structural stability of the supramolecular structures [3].

Diphenylalanine (FF) is a model material intrinsically chiral in pure form. Different chirality of structures – L- (left) and D- (right) conformations – can influence on their physical properties as well as embedding the NPs. Although physical properties of D-FF microtubes are well known, the properties of their composites with NPs and microtubes of L-conformation are insufficiently studied.

In this work, we studied the growth kinetics, structure, mechanical and piezoelectric properties of pure FF microtubes with different chirality and composite D-FF microtubes with inclusion of nanoparticles (NPs) of piezoelectric ZnO (diameter 30±11 nm) and nonpiezoelectric SiO_2 (diameter 43±11 nm) and TiO_2 (diameter 26±7 nm). Pure FF microtubes were obtained using conventional method of growth from water solution [4]. The composite FF-NPs microtubes were obtained using modified method: FF powder dissolved in 1,1,1,3,3,3-hexafluoro-2-propanol was mixed with stable NPs water suspensions (concentration 0.5 mg/mL).

The growth kinetics study didn't show noticeably influence of chirality and any type of NPs on growth of FF microtubes. Moreover, FF microtubes of both chiral conformations have similar values of Young's modulus and axial piezoelectric coefficients. In case of embedding of NPs it was shown that voids and cavities appeared in FF microtubes. The effective transverse Young's modulus of the obtained composite FF-NPs microtubes was slightly reduced due to these defects while their axial piezoelectric coefficients decreased almost two times. At the same time, insertion of ZnO NPs provided appearance of noticeable vertical piezoresponse which is absent in pure FF microtubes. The obtained results demonstrate the ability to control the properties of self-assembling composite biomaterials by various NPs.

The research was carried out using equipment of Ural Center for Shared Use "Modern Nanotechnologies" Ural Federal University with the financial support by the grant of the President of the Russian Federation for young scientists (Contract 14.Y30.17.2294-MK) and the Government of the Russian Federation (Resolution 211, Contract 02.A03.21.0006). Part of this work was developed in the scope of project CICECO-Aveiro Institute of Materials (ref FCT UID/CTM/50011/2013), financed by national funds through the FCT/MEC and, when applicable, cofinanced by FEDER under the PT2020 Partnership.

1. E. Gazit, *Chemical Society Reviews* **36**, 1263 (2007).
2. G. Rosenman, P. Beker, I. Koren, et al., *Journal of Peptide Science* **17**, 75 (2011).
3. A.D. Pomogailo, *Russian Chemical Reviews* **69**, 53 (2000).
4. A. Nuraeva, S. Vasilev, D. Vasileva, et al., *Crystal Growth & Design* **16**, 1472 (2016).

O-18

Measurement of the bending of thin inclined nanowires as a method for determining elastic modulus

M.S. Dunaevskiy[1], P.A. Alekseev[1], P. Geydt[2], E. Lahderanta[2], T. Haggren[3], H. Lipsanen[3]

[1]*Ioffe Institute, 194021, Saint-Petersburg, Russia*
e-mail: Mike.Dunaeffsky@mail.ioffe.ru

[2]*Lappeenranta University of Technology, FI-53851, Lappeenranta, Finland*

[3]*Aalto University, P.O. Box 15100, Espoo FI-00076, Finland*

Recently, researchers are interested in semiconductor nanowires, which may have unusual mechanical and electrophysical properties [1]. In a number of studies it was shown that the Young's modulus of thin nanowires (ZnO[2], GaAs[3]) can significantly differ from the tabulated values of the Young's modulus of bulk materials. In this paper, scanning probe microscopy (SPM) method is presented that allows measuring the Young's modulus of thin and flexible nanowires, which consists in measuring the bending profiles of nanowires in the precise force control regime. Using this approach, it was possible to measure the Young's modulus of thin InP tapered nanowires with (i) wurtzite structure and (ii) zinc blende structure.

Samples with thin tapered InP nanowires were studied, differing both in their geometric parameters and in their crystal structure (wurtzite or zinc blende). The samples were grown by chemical vapor deposition method by the vapor-liquid-solid mechanism with catalytic gold droplets on a Si substrate at temperature of T=450°C. The geometric parameters of the nanowires were determined by scanning electron microscopy and then by scanning probe microscopy methods. The type of crystal structure of InP nanowires was determined from electron diffraction data.

For precision bending of nanowires in this work the “PeakForce” regime [4] was applied. This mode was specially created to minimize the SPM-probe force acting on the surface and makes it possible to study "very soft objects" including nanowires with a small bending stiffness. In the experiment, we had the opportunity to reduce the SPM-probe force acting on the surface down to 0.05 nN and maintain it during scanning with a high degree of accuracy. The use of scanning with ultra-small forces made it possible to obtain noiseless images of inclined InP nanowires without their bending. This was an important step, necessary for further accurate measurement of nanowires bending.

In this work we propose the method of measuring the bending profiles w(x) on inclined InP nanowires with different SPM-probe forces F_{peak} acting on the nanowire. With increasing values of the magnitude of the peak force (F_{peak}=0.05nN, 1nN, 2nN, 5nN, 10nN) the deflection of the nanowire will increase, which will lead to a change in the scanning topography of the inclined nanowire. We can assume that the deflection of the nanowire is close to zero when working with an ultra-small force (0.05nN) acting on the nanowire. Therefore, when subtracting from the topographic profile of the inclined nanowire obtained with the force 5 nN ($h(x)_{5nN}$) of the profile obtained with a force of 0.05 nN ($h(x)_{0.05nN}$), we obtain the nanowire bending profile w(x) corresponding to the force 5nN ($w(x)_{5nN}=h(x)_{5nN}-h(x)_{0.05nN}$). During our measurements, we observed a linear increase in the bending profiles with increasing values of the peak force $w \sim F_{peak}$. This means that in the range of applied forces there is a linear bending of the nanowire for which Hooke's law is valid. Once the set of deflection profiles is measured along the nanowire, these profiles are divided by the values of the corresponding forces and profile of inverse stiffness is obtained $1/k(x)=w(x)/F$.

To analyze the inverse stiffness profiles of thin tapered InP nanowires a formula was used that relates the value 1/k(x) of a tapered nanowire and its Young's modulus E. Using this approach, it was possible to measure the Young's modulus of tapered InP nanowires with a wurtzite structure and zinc blende structure. The measured value of Young's modulus of wurtzite InP nanowires was E_{WZ}=130±30 GPa. It should be noted that the experimental measurement of Young's modulus of wurtzite InP was performed for the first time. The theoretical calculations of the Young's modulus

in wurtzite InP (E_{WZ_theory} = 120 GPa) are in good agreement with the obtained experimental results.

1. P. Krogstrup, H.I. Jorgensen, M. Heiss, et al., *Nat. Photonics* **7**, 306, (2013).
2. Q. Chen, Y. Shi, Y.S. Zhang, et al., *Phys. Rev. Lett.* **96**, 075505, (2006).
3. P.A. Alekseev, M.S. Dunaevskii, A.V. Stovpyaga, et al., *Semiconductors* **46**, 641 (2012).
4. T.J. Young, M.A. Monclus, T.L. Burnett, et al., *Meas. Sci. Technol.* **22**, 125703, (2011).

O-19

The effect of the probe magnetic moment orientation of magnetic resonance force microscope on the spectra of spin wave resonances

E.V. Skorokhodov[1], M.V. Sapozhnikov[1], R.V. Gorev[1], A.P. Volodin[2], V.L. Mironov[1]

[1]*Institute for Physics of Microstructures, 603950, Nizhny Novgorod, Russia*
e-mail: evgeny@ipm.sci-nnov.ru

[2]*KU Leuven, Celestijnenlaan 200D, BE-3001 Leuven, Belgium*

Magnetic resonance force microscopy (MRFM) is a powerful method for investigation of local ferromagnetic resonance (FMR) [1,2]. We use MRFM for the study of FMR in the array of permalloy microstripes with a size of 3000×500×30 nm^3 arranged on a rectangular lattice of 3.5×6 μm^2 under the conditions of strong probe-sample interaction. This interaction leads to complex modification of the FMR spectra expressed both in splitting lines and in changes in the shape of spectra. Dependences of the MRFM spectra of the sample on the probe-sample distance and the orientation of the probe magnetic momentum are analyzed.

Magnetic resonance may appear in the spectrum as a peak or a dip. It is determined by sigh of interaction force between probe and sample [3]. Figure 1 shows the MRFM spectra depending on the mutual direction of the magnetic momentum of probe of the microscope and the external magnetic field. It is seen that the change of direction of the external magnetic field relative to the magnetic momentum of the probe leads to replacement of the dips on the peaks and, on the contrary. The interaction force sign between the probe and the sample has a different sign in these experimental configurations.

Figure 2 shows the MRFM spectra for different distances between probe and sample and for different the magnetic momentum of probe orientations: magnetic momentum is directed along the sample surface (Fig. 2a) and perpendicular to sample surface (Fig. 2b). It is seen that orientation of probe magnetic momentum has a big influence on MRFM spectrum.

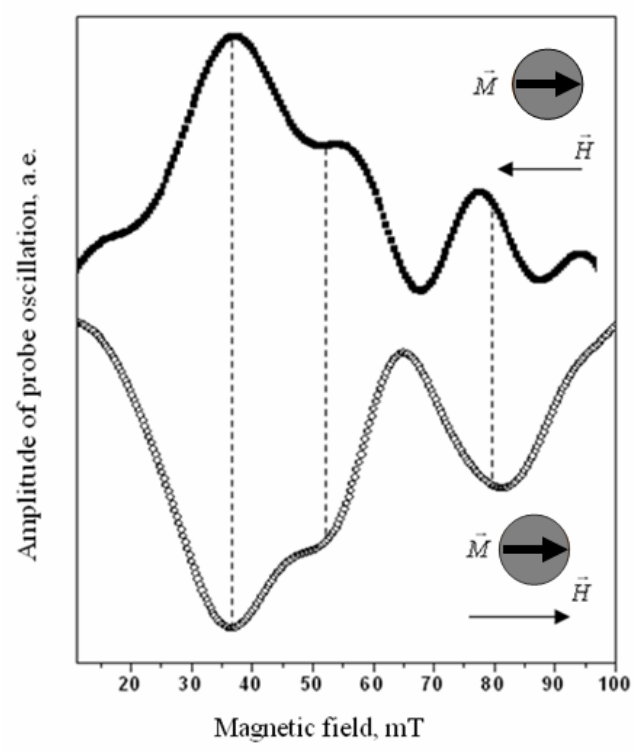

Figure 1. FMR MRFM spectra of permalloy microstripe for the case when the probe is magnetized along the surface of the sample. The external magnetic field is directed as well as the magnetic moment of the probe (light circles) and in the opposite direction (black circles). The distance between the probe and the sample surface is 3 μm.

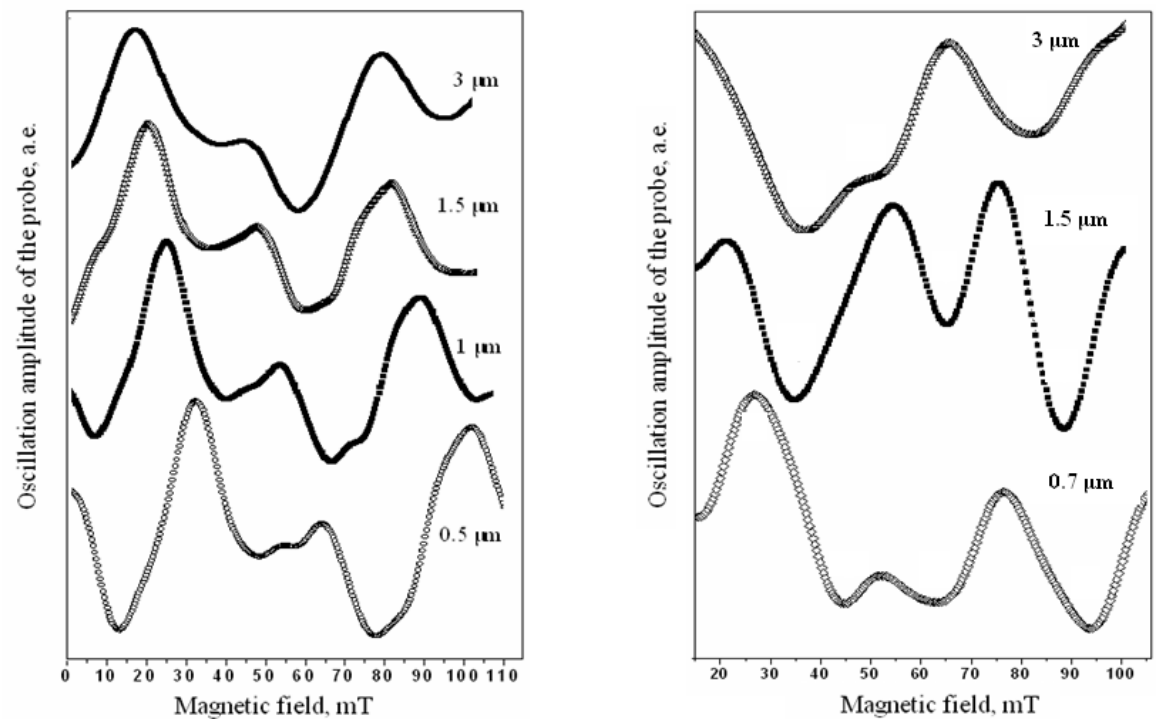

(a) (b)

Figure 2. MRFM spectra of microstripes. The magnetic momentum of probe is directed along the sample surface (a) and perpendicular to sample surface (b).

This work was supported by the Russian Science Foundation (project 16-12-10254).

1. J.A. Sidles. *Applied Physics Letters* **58**, 2854, (1991).
2. D. Rugar, R. Budakian, H.J. Mamin, et al, *Nature* **403**, 329, (2004).
3. F.Guo, L.M. Belova, D. McMichael, *Physical Review Letters* **110**, 017601, (2013).

O-20

Structure of natural impact glasses on AFM data

Ye.A. Golubev, T.G. Shumilova, S.I Isaenko

Institute of Geology of Komi SC of Uralian Branch of RAS, 167982 Syktyvkar, Russia
e-mail: golubev@geo.komisc.ru

Natural glasses were one of the first mineralogical objects to study by SPM. The main types of natural glasses are *impactites* (as a result of explosive and shock processes in rocks), *tektites* (as a result of ablation and transport of the melted substance over significant distances) and *obsidians* (solidified volcanic melts) [1]. AFM observations of the glasses fracture predominantly show small hillocks, a few tens nanometers wide and about one nanometer high [2-6]. It is tempting to assume that the surface of cleavage in glass fracture reveals the structural heterogeneity. Structural differences due to PT-conditions of cooling, concentration and composition of impurities, contribute to the appearance of nanoscale structural heterogeneity of the glasses. This heterogeneity can be caused both by density fluctuations in pure silicon dioxide, and by composition fluctuations in multicomponent glasses [7]. The aim of this study is to attempt to connect structural and chemical data on natural impactite glasses to the results of AFM observations of their surface.

The objects of our study are natural impact glasses: *irgizite* from Zhamanshin Crater (Kazakhstan) and *Libyan Desert glass* (Egypt), from the rocks of the Rice crater (Germany) and the Kara astroblem (Russia); and *moldavite*, related to tektites (Czech Republic).

The chemical and local structure was determined by the methods of infrared and Raman spectroscopy, the local chemical composition was estimated by X-ray energy-dispersive spectral analysis. Nanoscale topography was detected by the atomic force microscopy.

The surface morphology of the samples has been characterized by AFM measurement in tapping mode using an Integra Prima (NT-MDT, Russia) with super sharp silicon cantilevers of model SSS-NCH (Nanosensors). In the majority of works, the surface roughness is used to quantify objects on AFM images, which is estimated from a standard histogram. In this work we proposed to evaluate the nanoheterogeneity of glasses by the diameter of hillocks.

The dependence of the degree of saturation of the structure of natural glasses with cation-modifiers (Al, Na, Ca, Mg) on the dimensions of inhomogeneities on their surface is revealed. These results allow relating IR spectroscopic and EDS analysis data with nanostructural features of the glasses. This suggests that the factor, mainly determining the nanoheterogeneity of the glasses at the AFM images, is chemical. Cations of modifiers are located in free cavities of the structural lattice, compensating excessive negative charge of the complex anion. The strength of the modifier-oxygen bond is much lower than the strength of the glass-to-oxygen bond, so the modifiers do not form strong coordination groups, and when the glass breaks, the bonds break along the clusters of modifier elements. The presence of impurities, partially framing the nanoscale regions of the glass-forming matrix, promotes the cleavage of the material along the impurity-containing regions and the formation of a rough cleavage surface.

This work was supported by the RSF (project No. 17-17-01080).

1. G.S. Henderson, *Canadian Mineralogist* **43**, 1921 (2005).
2. A. Hervé, A. Daniel, *Ceramics-Silikáty* **44**, 121 (2000).
3. J.-F. Poggemann, et al., *J of Non-Crystal Solids* **281**, 221 (2001).
4. E. Radlein, G.H. Frischat, *J of Non-Crystal Solids* **222**, 69 (1997).
5. G. Heide et al., *J of Non-Crystal Solids* **323**, 68 (2003).
6. G.H. Frischat et al., *J of Non-Crystal Solids* **345**, 197 (2004).
7. P.H. Gaskell, *J of Non-Crystal Solids* **222**, 1 (1997).

O-21

AFM-based approach to establish structure/property type correlations for polymeric functional materials

T.S. Sazanova, K.V. Otvagina, T.A. Shestoperova, I.V. Vorotyntsev

Nizhny Novgorod State Technical University n.a. R.E. Alekseev, 603950, Nizhny Novgorod, Russia
e-mail: yarymova.tatyana@yandex.ru

The development of polymer-based functional materials with controlled structure and properties is closely associated with different physical, chemical and material science problems. Fundamental research of polymers structure and their functional properties is needed for the solution of those problems.

Now there are a variety of methods for studying polymeric materials [1-3]. Each of the methods with a range of advantages and drawbacks has a specific application. Since it is known that mechanical and physical properties of polymer-based materials not only depend on their chemical nature but also strongly correlate with their surface structure, the study of this effect is an important task.

For example, in the case of gas separation processes, a non-porous polymeric membrane surface has significant contribution to not only mechanical, but also gas transmission properties. It is due to the fact that first stages in gas separation are deposition of permeating gases on a membrane surface and their absorption. The rougher a membrane surface, the larger will be its actual area, and with the growth of this area, the separation speed also increases, that is, permeable properties are improved.

A polymeric surface can be assessed by atomic force microscopy (AFM). This method is suitable for such study, not only because of high lateral and vertical resolutions, but also its ability of gaining quantitative three-dimensional information about topography without destruction of a soft polymer surface. However, AFM imaging results alone are not sufficient to assess the impact of polymeric morphological features on their properties. For example, to establish the correlation of polymer surface features with its wettable and mechanical properties, it is necessary to use the approach based on AFM combined with wettability measurements and mechanical testing.

In this work, this approach was used to study a range of polymeric films based on polysulfone (PSU), cellulose triacetate (CTA) and polyvinyl alcohol (PVA).

PSU, CTA and PVA flat shits were obtained by corresponding polymer solution casting using automatic coating machine MemcastPlus (Porometr, Belgium) onto inert support followed by solvent evaporation under equilibrium conditions. Solutions of polymers were prepared in the following proportions: 7.5 % PSU in tetrahydrofuran (THF), 1.5 % CTA in glacial acetic acid, 3 % PVA in water. After the polymer films formation they were easily peeled off the support and desiccated under vacuum for 24 hours. Each of the polymers was cast on three glass substrates.

Borosilicate glass was chosen as an inert support, due to its chemical, thermal and mechanical stability. Before use the glass was chemically treated in order to obtain certain surface roughness. Glass support 1 was exposed in the 5 % hydrofluoric acid solution for 10 min, glass support 2 was exposed in the 15 % hydrofluoric acid solution containing 50 % ammonium fluoride for 5 min and glass support 3 was exposed under etching paste containing 30 % HF, 30 % NH_4F and 15 % $BaSO_4$ for 5 min. After etching glass supports were rinsed thoroughly with distilled water in ultrasound bath for 10 min.

The glass supports surface and their roughness were studied by a scanning probe microscope SPM-9700 (Shimadzu, Japan). AFM scanning was performed using a contact mode by silicon nitride cantilevers OMCL-TR800PSA (Olympus, Japan) with a stiffness coefficient of 0.57 N/m and a typical tip radius of no more than 15 nm (guaranteed - no more than 20 nm), a tip height was 29 microns. The experiments were carried out under ambient conditions. Automatic correction of linear noise was applied during scanning. For checking purposes reproducibility, AFM scanning was carried out on different sites of the studied surfaces. After AFM scanning, an arithmetic average

roughness height (R_a) and a mean roughness depth (R_z) were obtained. A base length was 10 μm (Table 1). Processing of the obtained AFM images and their analysis were performed by a software SPM Manager ver. 4.02 (Shimadzu, Japan).

Table 1. The roughness parameters.

R_a, ± 0.01 nm				R_z, ± 0.02 nm			
Support	PSU	CTA	PVA	Support	PSU	CTA	PVA
6.93	1.46	2.88	5.62	39.51	47.03	54.16	37.23
34.94	54.17	54.95	50.27	126.85	260.53	272.55	205.75
137.59	175.20	170.30	173.33	543.51	688.68	710.37	752.47

The same way, the polymers surface was studied. But since polymeric materials have a loosely-coupled surface structure, AFM scanning was performed using a tapping mode by silicon vibrating cantilevers PointProbe FMR-20 (Nano World Innovative Technologies, USA) with a stiffness coefficient of 1.3 N/m and a typical tip radius of no more than 8 nm (guaranteed - no more than 12 nm), a tip height was 15 microns.

According to the AFM results, the polymers surface roughness increases with the growth of the glass supports roughness which is quite logical (Table 1). But it is noteworthy that the films surface roughness is different in the case of the glass support 1 and close in the case of the glass supports 2 and 3. This can be explained as follows. The rigid-chain properties of the studied polymers decrease in the following order: PSU, CTA, PVA. Hence, the higher intermolecular rotation freedom of a polymer, the more its surface reflects a glass support structure and its roughness. At significant values of glass supports roughness, this effect is brought to nothing.

An advancing contact angle of wetting for PSU, CTA and PVA surfaces oriented to glass supports was determent by wettability tests using diiodomethane as test liquid. An image of the drop applied to the sample surface was processed with the ImageJ software in order to calculate the advancing contact angle. According to the obtained measurements, a decrease of wetting with an increase in the surface roughness of the sample was observed for all polymers. This is explained that surfaces with significant roughness tend to be superhydrophobic and not wetted by most liquids.

Mechanical properties of the polymeric films (namely, values of a tensile strength (σ)) were determined on a universal test machine Zwick Z005 (Zwick Roell, Germany) at a pulling speed of 50 mm/min. With the PSU surface roughness growth, its tensile strength decreased from 56 to 44 MPa. This trend is supposedly associated with an increase in the macromolecules rod-like packing defectiveness of rigid-chain PSU. The opposite tendency was observed in the case of PVA. Its tensile strengths increased from 61 to 85 MPa, which is explained by the probable formation of additional intermolecular hydrogen bonding in the extended near-surface layer of this flexible-chain polymer. In contrast with PSU and PVA, CTA tensile strength didn't change (about 57 MPa), which is due to its rigid-chain properties in combination with the ability to form hydrogen bonding.

Thus, it is shown that, polymers wettable and mechanical properties can be controlled by varying their surface roughness with due regard to their chemical nature. At that, necessary correlations of a structure/property type can be established using the considered AFM-based approach.

This work was supported by the RSF (project No. 18-19-00453) and the RFBR (project No. 18-08-01356 A).

1. T.A. Osswald, G. Menges, *Material science of polymers for engineers* (Hanser Publishers), 595 (2012).
2. T.S. Sazanova, I.V. Vorotyntsev, V.B. Kulikov, et al., *Petroleum Chemistry* **56**, 5 (2016).
3. K.V. Otvagina, A.E. Mochalova, T.S. Sazanova, et al., *Membranes* **6**, 2 (2016).

.

O-22

Filamentary charge carrier injection in heterogeneous oxide systems

N.V. Andreeva, D.A. Chigirev, A.S. Kunitsyn, A.A. Petrov

Saint Petersburg Electrotechnical University "LETI", 197376, Saint-Petersburg, Russia
e-mail: nvandr@gmail.com

Resistive switching effects take place in a variety of heterogeneous oxide systems. Thus a study of mechanisms of electron transport in these systems is important. We assume that electron transport in oxide systems with resistive switching effects is due to space charge limited current observed under charge carrier injection from electrode. We experimentally observed that current through our structures doesn't depend on the electrode surface area, thus we believe that we have a filamentary charge carrier injection. In this work a phenomena of filamentary charge carrier injection in bilayer structures (based on a sequence of TiO_2 and Al_2O_3 layers) is experimentally observed by means of tunnel atomic force microscopy. Obtained patterns of current "pinching" formation are analyzed.

The results of our study of resistive switching in bilayers based on a sequence of TiO_2 and Al_2O_3 thin oxide layers [1] indicate that the resistive-switching mechanism is due to electronic processes and is not related to thermal or thermochemical processes. Measured *I-V* characteristics of these systems are nonlinear and symmetrical (regarding polarity of applied bias). An analysis of *I-V* characteristics shows that they are linearized in a double logarithmic scale with several characteristic parts ($I \sim U^n$), corresponding to linear, square, and power dependences with $n \geq 3$. This is typical for space charge limited current in high resistivity materials with low carrier mobility and long dielectric relaxation time. The fact that current through our structures doesn't depend on the electrode surface suggests that we have a filamentary charge carrier injection [2].

To study the phenomena of filamentary charge carrier injection we measured current distribution over the surface of bilayers by means of tunnel atomic force microscopy (tAFM). We experimentally observed that after scanning the surface of bilayers with voltage applied between the microscope probe and the bottom electrode, areas could be associated with current "pinching" appeared. These areas are visualized in a tunnel atomic force microscopy regime on a current distribution as conductive regions and formed in places of the surface previously scanned with bias application. The value of voltage starting from which current "pinching" could be observed roughly corresponds to the voltage at which switching the resistance takes place according to the *I-V* characteristics measured on a top electrode of the structure. Changing the polarity of applied bias leads to the partial disappearance of the conductive regions previously induced by voltage application and forming conductive regions in another places of the structure. Thus, we experimentally observe reversible formation of conductive areas in metal-oxide thin film bilayers and associate them with filamentary charge carrier injection effect.

Based on the findings of the measured size of current "pinching" regions, we try to explain the main parameters of resistive switching in heterogeneous oxide systems. Among these parameters are a ratio of the resistances in high / low resistive states and the value of switching voltage. In the context of our approach we make an assumption regarding the main limiting factor influencing the size of filamentary charge injection areas.

1. N. Andreeva, A. Ivanov, A. Petrov, *AIP Advances* **8**, 025208 (2018).
2. K.C. Kao, W. Hwang, *Oxford: Pergamon Press* (1981).

.

O-23

Electric field-induced phase transformations in ferroelectric polycrystalline $Hf_{0.5}Zr_{0.5}O_2$ thin films

A. Chouprik[1], S. Zakharchenko[1], M. Spiridonov[1], S. Zarubin[1], A. Chernikova[1], R. Kirtaev[1], P. Buragohain[2], A. Gruverman[2,1], A. Zenkevich[1], D. Negrov[1]

[1]*Moscow Institute of Physics and Technology, 9 Institutskiy lane, Dolgoprudny, 141700, Russia*
e-mail: chouprik@gmail.com

[2]*Department of Physics and Astronomy, University of Nebraska, Lincoln, NE 68588, USA*

Because of their full compatibility with the modern Si based technology, the HfO_2-based ferroelectric (FE) films have recently emerged as viable candidates for application in nonvolatile memory devices [1]. Both theoretical [2] and experimental [3-5] studies ascribe the ferroelectricity in polycrystalline HfO_2-based thin films to the presence of a metastable non-centrosymmetric orthorhombic (o) HfO_2 phase (space group $Pbc2_1$), which crystallizes during the annealing of doped HfO_2 thin films. Although it is well established that in the HfO_2-based FE films ac electric cycling of the FE capacitor (training process, also called "wake-up" effect) leads to the increase in the remnant polarization value [6], the origin of such effect as well as the exact mechanism of the polarization switching in this material are still not fully understood. In this work, we correlate the information on the local piezoresponse (domain maps) of the pristine versus trained $Hf_{0.5}Zr_{0.5}O_2$ (HZO) film with the structural properties revealed by the transmission electron microscopy to explain the origin of the wake-up effect in $Hf_{0.5}Zr_{0.5}O_2$ (HZO) film.

TiN (18 nm)/HZO (10 nm)/TiN (18 nm) capacitors were fully grown by the atomic layer deposition technique. Pulsed switching measurements of FE TiN/HZO/TiN capacitors were performed using PUND (Positive Up Negative Down) technique with triangular voltage sweeps. To wake-up pristine FE capacitors, the voltage was cycled 10^4 times by applying rectangular pulses with ±3 V amplitude and 100 μs duration with the pulse generator. P_r-V curves for trained capacitors derived from PUND data are shown in Figure 1g. The obtained remnant polarization was $2P_r \sim 35$ μC/cm^2.

The structural properties of HZO films in FE capacitors were investigated by high-resolution transmission electron microscopy (HRTEM). The selected-area electron diffraction patterns of pristine vs. trained TiN/HZO/TiN stack cross-sections evidence that the nonpolar monoclinic (m) phase is fully converted into polar o- and/or nonpolar tetragonal (t) phase following the electrical cycling.

Piezoresponse mapping of pristine TiN/HZO/TiN capacitor was performed by the resonance-enhanced mode of PFM. The amplitude map of as prepared polycrystalline $Hf_{0.5}Zr_{0.5}O_2$ reveals the mixture of both the grains of polar o-phase with high vertical projection of polarization vector and regions with low PFM amplitude associated with nonpolar m- and t-phases and misaligned o-phase film (Fig. 1b,c), which is consistent with TEM results.

Domain structure of the trained HZO film and its evolution following the applied switching pulses were visualized by the resonance-enhanced band-excitation (BE) PFM. To eliminate the effect of the top polycrystalline TiN electrode surface morphology (Fig. 1a) on the visible domain structure, piezoresponse maps were normalized by mechanical contact response maps obtained simultaneously by the BE atomic force acoustic microscopy [7]. Normalized BE PFM maps in Figure 1e,f,h,i do not contain any regions without piezoresponse. Local decreases in the piezoresponse signal on the fully polarized HZO film (Fig. 1e,h) can be associated with o-phase seeds with opposite polarization vector direction, horizontally oriented domains, antiferroelectric t-phase grains and passive m-phase grains less than 100 nm in size. When comparing these data with those for pristine structures (Fig. 1b,c), it is evident that during the wake-up process the amount of the non-ferroelectric phase is decreasing dramatically. Taking into account the TEM data, we conclude that during the wake-up of TiN/HZO/TiN capacitors, both m- and t-phases undergo almost complete phase transition to the ferroelectric o-phase.

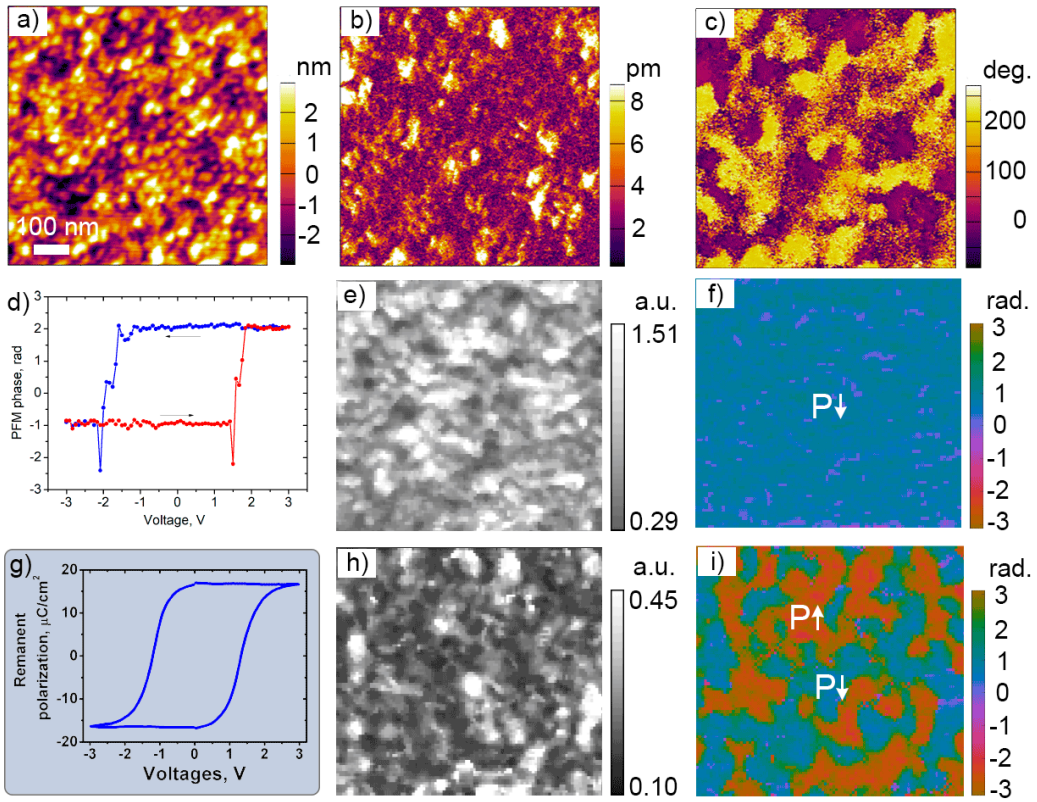

Figure 1. Static domain structure for pristine and trained HZO capacitors:
(a) TiN surface morphology; PFM for pristine film (b) amplitude map,
(c) phase map; (d) BE PFM phase hysteresis loop; BE PFM for trained film at the fully polarized state (-3 V) (e) amplitude map, (f) phase map; (g) P-V hysteresis curves derived from PUND measurements; BE PFM for trained film at the intermediate state (1.4 V) (h) amplitude map, (i) phase map.

Piezoresponse hysteresis loops measured by BE technique within the area subjected to the cycling confirm FE properties of the TiN/HZO/TiN structures (Fig. 1d).

Recently, using DFT calculations, Barabash et al. [8] have shown that the o →t→o phase transition in the HZO films can occur during each switching cycle. We do not see any regions without a relatively strong piezoresponse signal on the BE PFM/AFAM maps of the intermediate domain structures (Fig. 1e,f). Therefore, we consider that the switching process proceeds in a conventional way, i.e. like in other ferroelectrics the polarization reversal in the o-phase grains is due to the nucleation and growth of seeds with the opposite polarization. The o→t→o phase transition in the HZO films during each switching cycle is possible but cannot be detected if the intermediate t-phase is unstable in PFM excitation field.

In conclusion, the PFM results along with TEM analysis for the pristine vs. trained TiN/HZO/TiN FE capacitors indicate the electrically stimulated m→o phase transition during the wake-up process.

1. T.S. Boscke et al., *Appl. Phys. Lett.* **99**, 102903 (2011).
2. S. Clima et al., *Appl. Phys. Lett.* **104**, 092906 (2014).
3. D. Zhou et al., *Appl. Phys. Lett.* **103**, 192904 (2013).
4. M. Pešic et al., *Adv. Funct. Mater.* **26**, 4601 (2016).
5. D. Martin et al., *Adv. Mater.* **26**, 8198 (2014).
6. T. Schenk et al., *ACS Appl. Mater. Interfaces* **6**, 19744 (2014).
7. Chouprik et al. *ACS Appl. Mater. Interfaces* ***10***, 8818 (2018).
8. S.V. Barabash et al., *ECS Meeting Proceedings*, (2016).

O-24

Compositional variation of thin PZT films near morphotropic phase boundary: experiment and simulation

I.P. Pronin[1], E.Yu. Kaptelov[1], S.V. Senkevich[1], D.M. Dolgintsev[2], V.P. Pronin[2], A.V. Volpyas[3], A.B. Kozyrev[3]

[1]*Ioffe Institute, 194021, St. Petersburg,Russia*
e-mail: Petrovich@mail.ioffe.ru

[2]*Herzen State Pedagogical University of Russia, 191186, St. Petersburg, Russia*

[3]*Saint-Petersburg Electrotechnical University "LETI", 197101, St. Petersburg, Russia*

Extreme dielectric and electromechanical properties of PZT as well known can be observed in narrow band of solid solutions with a composition corresponding to the region of morphotropic phase boundary (MPB) (at x ≈ 0.46-0.48), that divides tetragonal and rhombohedral ferroelectric phases. In [1] it is assumed that such properties may be linked to the ferroelectric phase monoclinic modification existing in the region of MPB, which stability depends on element heterogeneity, microstructure and mechanical tensions. The search for compositions with most suitable electromechanical parameters involves accurate composition variation (Zr and Ti proportion) within the region of MPB. One of the ways to vary the multicomponent thin films composition is to control the technological parameters in the process of ion-plasma deposition and create directed flows of some components and diffusion flows of other components in target-substrate drift zone [2].

In this work, the study of coupling between variation of technological parameters of RF magnetron sputtering of ceramic PZT target (with elemental ratio Zr/Ti=54/46) and composition variation of deposited PZT thin layers was held. Two series of the samples were prepared. The first ones were formed under variation of the working gas pressure and the second ones - under variation of the distance between the target and the silicon substrate. To control thin-film compositions SEM EVO-40 (Carl Zeiss) equiped by energy-dispersive detector INCA was used. The films thickness was nearly 1 μm for the first series and nearly 0,5 μm for the second one. The experimental results on composition variation are presented in Figure 1a,b. The data of computer simulations of particles scattering in gas plazma have shown a good agreement with the experimental data.

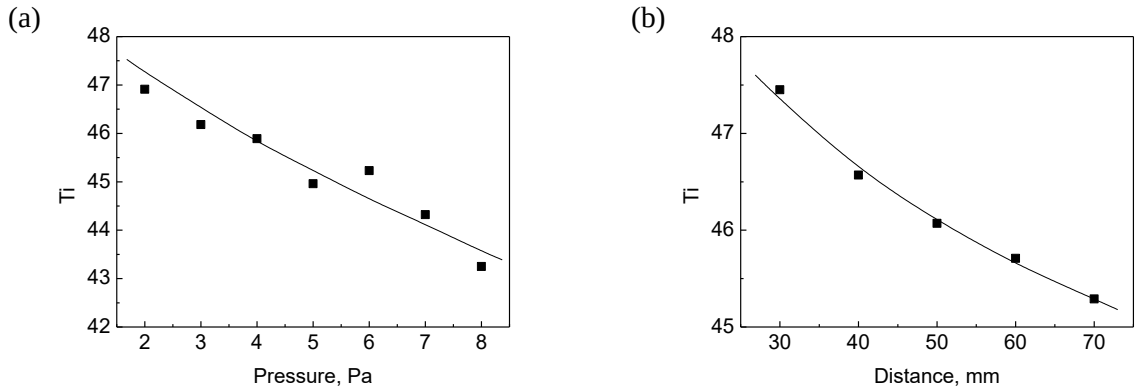

Figure 1. The change of thin PZT films composition versus the pressure of the working $Ar+O_2$ gas (a) and the distance between the target and the substrate (b).

The work was partly supported by the Ministry for Education and Science (Russian Federation) (Grant No 16.2811.2017/4.6) and RFBR (Grant No 16-02-00632).

1. B. Noheda, D.E. Cox, G. Shirane, et al., *Physical. Review B* **63**, 014103 (2001).
2. V.A. Volpyas, A.B. Kozyrev, *J. of Experimental and Theoretical Physics* **113**, 172 (2011).

O-25

Brillouin light scattering and second harmonic generation of strontium barium niobate crystals

A.M. Pugachev[1], I.V. Zaytseva[1], V.K. Malinovsky[1], N.V. Surovtsev[1], L.I. Ivleva[2], P.A. Lykov[2]

[1]*Institute of Automation and Electrometry, Russian Academy of Sciences, Novosibirsk, 630090 Russia*
e-mail: apg@iae.nsk.su

[2]*Prokhorov General Physics Institute, Russian Academy of Sciences, Moscow, 119991 Russia*

Brillouin light scattering and generation of the second optical harmonic (SHG) are investigated in the 115–850 K temperature range in a series of $Sr_xBa_{1-x}Nb_2O_6$ (SBN-x) crystals of various chemical compositions (x = 0.3, 0.5, 0.6, 0.75) which exhibit the properties of both an conventional ferroelectric (x = 0.3, 0.5), and relaxors (x = 0.6, 0.75). The aim of this research is investigation of local noncentrosimmetric inhomogenities in the paraelectric phase in ferroelectric crystals [1].

SHG signal was recorded in TriVista 777 spectrometer with a spectral resolution better than 1 cm^{-1}. It is shown that the integral intensity of the second harmonic signal follows the Arrhenius law with an activation energies of ΔU= 0.09– 0.3 eV. The second harmonic generation is observed in paraelectric phase of the SBN-x crystals, revealing the presence of local asymmetric regions in the volume. The spectral width of the SHG spectrum does not exceed 0.3 cm^{-1} and is temperature independent. Upper limit of the spectral width of the SHG spectrum provides lower limit of the lifetimes of polar regions, which are longer than 15 ps. It suggests that the doubled frequency signal in the paraelectric phase of the SBN-*x* crystals is generated in areas with lifetimes longer than 15 ps. Acoustic properties of the samples were investigated in a Brillouin light scattering experiment in a six-pass Fabry–Perot interferometer with a spectral resolution about 1 GHz. It is shown that local polar regions cannot explain the anomalies of the elastic module near the ferroelectric phase transition in SBN-*x*.

1. G. Burns, B.A. Scott, *Solid State Comm.* **13**, 423 (1973).

O-26

Polarization reversal in KTP single crystals with surface dielectric layer and at elevated temperatures

A.R. Akhmatkhanov[1], E.M. Vaskina[1], M.A. Chuvakova[1], E.V. Pelegova[1], A.A. Esin[1], E. Gachegova[1], D.B. Kolker[2], V.Ya. Shur[1]

[1]*School of Natural Sciences and Mathematics, Ural Federal University, 620000 Ekaterinburg, Russia e-mail: andrey.akhmatkhanov@urfu.ru*

[2]*Research Laboratory of Quantum Optics Technology, Novosibirsk State University, 630090 Novosibirsk, Russia*

Studies of polarization reversal processes in potassium titanyl phosphate ($KTiOPO_4$, KTP) single crystals with surface dielectric layer and at elevated temperatures are important FOR development of bottom-up technology of periodical domain poling for creation of nonlinear-optical elements. It was shown previously that the domain kinetics in ferroelectrics is strongly dependent on the screening retardation which can be controlled by temperature change and deposition of the surface dielectric layer [1]. In this work we present the study of the domain structure evolution and domain wall motion in KTP with artificial dielectric layer and at elevated temperatures.

The crystals under investigation were grown by top-seeded solution method (Novosibirsk, Russia). The studied samples represented 1-mm-thick z-cut plates with optical grade polished both sides and typical sizes 11x16 mm^2. The measured bulk electrical conductivity at room temperature was about $3 \cdot 10^{-9}$ $Ohm^{-1}cm^{-1}$. The photoresist film AZ nlof2020 (AZ Microchemicals) was spin-coated on Z+ polar surface. The polarization reversal with dielectric layer was carried out using liquid electrodes (LiCl aqueous solution) and at elevated temperatures using sputtered ITO electrodes.

It was shown experimentally that the temperature increase leads to essential domain elongation and to rising of the relative input of fast and superfast domain walls [2] during switching process. The analysis of the temperature dependence of the domain wall velocity revealed the activation energies.

Formation and growth of large number of narrow domain rays (streamers) oriented along Y crystallographic direction was observed by *in situ* domain visualization during polarization reversal. The streamer growth was about ten times faster than macroscopic domains. The high resolution study of the static domain structures demonstrated that the streamers are formed by X and Y-oriented domain walls. Qualitative change of the switching current shape has been revealed as compared to polarization reversal without surface dielectric layer.

The switching currents were fitted by Kolmogorov-Avrami approach modified [3] taking into account the abrupt change of growth dimensionality when the streamers reach the opposite electrode edge. It was shown that the strong input of streamers widening to the polarization reversal process decreased with applied field. The obtained results were related to the domain wall shape instability induced by retardation of depolarization field screening in ferroelectric with surface dielectric layer.

The research was made possible in part by Government of the Russian Federation (Act 211, Agreement 02.A03.21.0006) by RFBR (grant 16-02-00724), and by President of Russian Federation grant for young scientists (Contract 14.Y30.17.2837-MK). The equipment of the Ural Center for Shared Use “Modern nanotechnology” Ural Federal University was used.

1. V.Ya. Shur, A.R. Akhmatkhanov, *Philos. Trans. R. Soc. A* **376**, 20170204 (2018).
2. V.Ya. Shur, A.A. Esin, M.A. Alam, A.R. Akhmatkhanov, *Appl. Phys. Lett.* **111**, 152907 (2017).
3. V.Ya. Shur, E.L. Rumyantsev, S.D. Makarov, *J. Appl. Phys.* **84**, 445 (1998).

O-27

Simulation on the relation between ferroelectric and piezoelectric hysteresis loops

T.K. Song[1], M.H. Kim[1], W.-J. Kim[2], T.G. Park[3]

[1]*School of Materials Science and Engineering, Changwon National University, 51140, Changwon, South Korea*
e-mail:tksong@changwon.ac.kr

[2]*Department of Physics, Changwon National University, 51140, Changwon, South Korea*

[3]*Department of Electrical Engineering, Changwon National University, 51140, Changwon, South Korea*

Ferroelectric polarization-electric field hysteresis loops and piezoelectric strain-electric field hysteresis loops of ferroelectric materials are systematically compared especially in the viewpoint of coercive fields. Ferroelectric hysteresis loops were simulated with simple hyperbolic functions by considering linear dielectric responses and non-linear switching responses. And piezoelectric hysteresis loops were simulated with piezoelectric responses of domains. And the simulated hysteresis loops were compared with experimental hysteresis loops of piezoelectric $BiFeO_3$-$BaTiO_3$ ceramics. Based on these results, electric-field dependent piezoelectric constants *d* of samples were calculated.

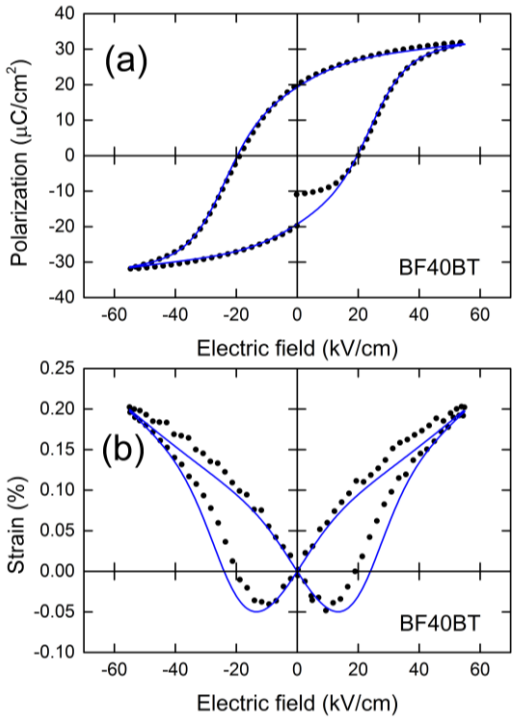

Figure 1. (a) Experimental (symbol) and simulated (line) *P-E* hysteresis loops of $0.6BiFeO_3$-$0.4BaTiO_3$ ceramic and (b) experimental (symbol) and simulated (line) *S-E* hysteresis loops of $0.6BiFeO_3$-$0.4BaTiO_3$ ceramic.

1. T.K. Song, *New Physics: Sae Mulli(Korean)* **67**, 822 (2017).

O-28

Dielectric properties of 1:1 ternary $Pb_2B^{3+}B^{5+}O_6$ perovskite ceramics sintered from mechanochemically synthesized nanopowders

S.I. Raevskaya[1], A.A. Gusev[2], V.P. Isupov[2], I.P. Raevski[1], V.V. Titov[1], M.A. Malitskaya[1], G.R. Li[3], S.P. Kubrin[1], E.I. Sitalo[1]

[1]*Research Institute of Physics and Faculty of Physics, Southern Federal University, 344090, Rostov-on-Don, Russia*
e-mail: sveta.raevskaya@mail.ru

[2]*Institute of Solid State Chemistry and Mechanochemistry SB RAS, 630128, Novosibirsk, Russia*

[3]*Shanghai Institute of Ceramics, Chinese Academy of Sciences, 200050, Shanghai, China*

Ferroelectric 1:1 ternary perovskite oxides of the $Pb_2B^{3+}B^{5+}O_6$ type, are widely used as a basis or components of various functional materials exhibiting giant dielectric, electrostrictive, pyroelectric, and piezoelectric responses. Properties of these oxides depend crucially on the ordering degree of B^{3+} and B^{5+} cations. While in the highly-ordered state a sharp ferroelectric or antiferroelectric phase transition takes place, in the disordered state a relaxor state is observed, characterized by a diffuse and frequency-dependent maximum of the dielectric permittivity.

Recently we have found out that the use of mechanochemical synthesis enables one to modify substantially relaxor properties of ceramics of the disordered perovskites $Pb_2Fe^{3+}Ta^{5+}O_6$ and $Pb_2MgNb_2O_9$ [1,2]. This effect is believed to be caused by the changes of the degree of the short-range ordering. Such explanation is supported by changes in the magnetic phase transition temperature of $Pb_2Fe^{3+}B^{5+}O_6$ powders (B^{5+} - Nb, Ta) obtained by mechanochemical synthesis [3]. In the present study we investigated the effect of the conditions of the mechanochemical synthesis on the structure and dielectric properties of several $Pb_2B^{3+}B^{5+}O_6$ ceramics (B^{3+} - Sc, In, Yb and B^{5+} - Nb, Ta). These ternary perovskite oxides of the 1:1 type are known to possess a high degree of long-range ordering of B^{3+} and B^{5+} ions when synthesized by a usual solid state route. Mechanochemical synthesis was carried out using high-energy planetary-centrifugal mill AGO-2 with steel balls and jars under a ball acceleration of 40g.

It was found out that high-energy mechanical activation during mechanochemical synthesis stimulates disordering of B^{3+} and B^{5+} cations in ceramics of the $Pb_2B^{3+}B^{5+}O_6$ perovskites studied. Using mechanochemical synthesis disordered modifications of $Pb_2B^{3+}B^{5+}O_6$ (B^{3+} - In, Yb and B^{5+} - Nb, Ta) were obtained for the first time without the use of any additives. In some cases it appeared to be possible to vary within a wide range compositional ordering degree of the B^{3+} and B^{5+} cations and correspondingly both the temperature and diffusion of dielectric permittivity maxima in ceramics by changing the regimes of the mechanochemical synthesis and/or using different starting materials (either oxides or preliminary synthesized $B^{3+}B^{5+}O_4$ precursors). The parameters of the dielectric spectra of the samples exhibiting relaxor-like behaviour also depend on the conditions of the mechanochemical synthesis

This study was supported by RFBR (project 17-03-01293_a) and by the Ministry of Education and Science of the Russian Federation (project 3.1649.2017/4.6).

1. A.A. Gusev, S.I. Raevskaya, V.V. Titov, et al., *Ferroelectrics* **475**, 41 (2015).
2. S.I. Raevskaya, A.A. Gusev, V.P. Isupov, et al., *Ferroelectrics* **525**, 37 (2018).
3. A.A. Gusev, S.I. Raevskaya, V.V. Titov, et al., *Ferroelectrics* **496**, 231 (2016).

O-29

Control of charged domain wall parameters in lithium niobate single crystals using various liquid and solid electrodes

A.A. Esin, A.R. Akhmatkhanov, V.Ya. Shur

School of Natural Sciences and Mathematics, Ural Federal University, 620000 Ekaterinburg, Russia
e-mail: alexander.esin@urfu.ru

The domain walls inclined to the polar axis in uniaxial ferroelectrics possess the bound surface charge due to discontinuity of normal component of spontaneous polarization. The charged domain walls (CDW) have attracted great scientific attention during last ten years, due to strong difference of their properties from that of the bulk materials. In particular, it was shown that conductivity of the charged domain walls in lithium niobate (LN) single crystal is 13 orders of magnitude higher than that of the single-domain crystal [1]. The possibilities to create, displace and erase of unit-cell-thick CDW by the external electric field are the appealing prospects for further applications in resistive data storage devices and reconfigurable electronics.

Naturally, the domains in uniaxial ferroelectrics represent themselves right-angle prisms, and the cross-sections of the domains by Z+ and Z- polar surfaces are identical. Domain walls tend to be neutral to reduce electrostatic energy of the system. However, this rule can be violated under certain conditions. Here we show that one of the options to control the domain wall inclination angle is the proper selection of electrode material used for field application during polarization reversal.

We present the experimental study of the CDW formation during polarization reversal in the magnesium oxide doped LN single crystals (MgO:LN). It was shown that material of the electrode at negative polar surface (Z-) is crucial. Conductive charged domain walls could be produced using solid (metal or semiconductor) electrode, whereas liquid electrolyte electrodes lead to growth of neutral walls. The domain walls were visualized in the crystal bulk using scanning Cherenkov SHG microscopy [2]. The time dependence of the conductivity of charged domain walls was measured. Controllable electrodeposition of silver on the conductive domain walls was demonstrated.

The research was funded by RFBR (grant № 18-32-00641). The equipment of the Ural Center for Shared Use “Modern nanotechnology” Ural Federal University was used.

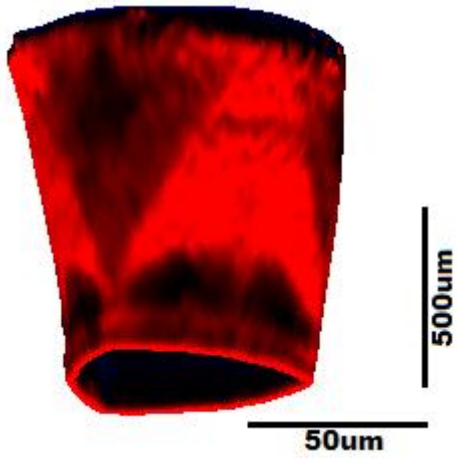

Figure 1. Charged domain wall in MgOLN crystal obtained by 3D reconstruction of Cherenkov SHG microscopy data. Saturation of the red colour is proportional to the wall local inclination from the polar direction.

1. A. Grecov, A. Adonin, N. Protsenko *Ferroelectrics* **13**, 1 (1976).
2. C. Werner, S. Herr, *Scientific Reports* **7**, 1 (2017).
3. Y. Sheng, A. Best, H.-J. Butt, W. Krolikowski, A. Arie, K. Koynov, *Opt. Express* **18**, 16539 (2010).

O-30

Investigation local switching and self-organization effects on non-polar cuts of lithium niobate

A.P. Turygin[1], Yu.M. Alikin[1], D.O. Alikin[1], M.S. Kosobokov[1], A.V. Ievlev[2], V.Ya. Shur[1]

[1]*School of Natural Sciences and Mathematics, Ural Federal University, Ekaterinburg, Russia*
e-mail: anton.turygin@urfu.ru

[2]*The Center for Nanophase Materials Sciences, Oak Ridge National Laboratory, Oak Ridge, TN, USA*

In this work, we studied experimentally domain formation and interaction on non-polar cuts of congruent lithium niobate (LN) and lithium niobate doped by 5% of MgO (MgO:LN) [1]. Self-organized domain structure on nonpolar cuts of CLN was formed during scanning by biased scanning probe microscope (SPM) tip and by grounded SPM tip in the vicinity of the previously formed by pulse application single wedge-like domain. In the last case, charge injected by application of the bias to SPM tip during initial polarization reversal was responsible to further screening of the surface charge to the grounded SPM tip and subsequent realization of local switching by this induced electric field. In both cases, formation of self-organized domain structure was found and attributed to electrostatic interaction of the charged domain apexes of growing domains (charged domain walls). The domain lengths alternating in arrays produced by local switching on nonpolar cut of MgOLN were found to be strongly dependent on the period (spacing between neighboring domains) [1]. Effect of period multiplication of domain array (doubling and quadrupling) and chaotic behavior have been observed (Fig. 1) similar to quasi-periodic domain structures reported earlier to be switched on polar cut of LN [2].

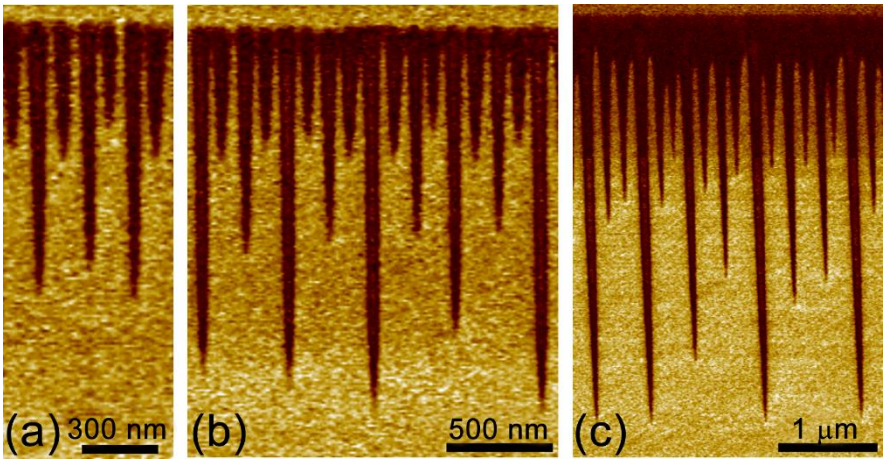

Figure 1. PFM images demonstrating different regimes of polarization switching on X-cut lithium niobate surfaces: (a) doubling, U = 100V, (b) quadrupling, U = 100 V, (c) chaotic behaviour, U = 150 V.

Revealed self-assembled domain growth and interaction of the charged domain walls can provide useful basis for application in nanodomain engineering and development of non-linear optical frequency converters, data storage, and computational devices.

The equipment of the Ural Center for Shared Use “Modern Nanotechnology” Ural Federal University was used. The research was made possible by Russian Science Foundation (Grant 14-12-00826).

1. A.P. Turygin, D.O. Alikin, Y.M. Alikin, V.Ya. Shur, *Materials*, **10**, 1143 (2017).
2. A.V. Ievlev, S. Jesse, A.N. Morozovska, E. Strelcov, E.A. Eliseev, Y.V. Pershin, A. Kumar, V.Ya. Shur, S.V. Kalinin, *Nature Phys.* **10**, 59 (2014).

O-31

Peculiarities of the applications of the two-probe AFM manipulator

A.A. Zhukov[1], V.S. Stolyarov[2]

[1]*Institute of Solid State Physics, Russian Academy of Science, 142432, Chernogolovka, Russia*
e-mail: azhukov@issp.ac.ru

[2]*Moscow Institute of Physics and Technology (MIPT), State University, 141700, Dolgoprudny, Russia*

Experimental investigations of the electronic transport of the nanowires, nanotubes, and biological filaments are the essential point of the interest. The first experiments were done on ropes, but resent ones are performed on a single nano-object with attached metallic contacts and gates defined by e-beam lithography. Beside this, experiments focused on investigations of electronic transport through double wires structure or InAs nanowire junctions show a new physics in this type of devices. In the most cases an additional manipulations of the wires should be done to prepare such kind of structures.

Several approaches to manipulate the nanowires such as Si nano-tweezers, indium soldering technique, standard nano-probe manipulators incorporated in scanning electron microscopes or manipulations by atomic force microscope (AFM) probes are currently in use.

Two-probe AFM helps to make manipulations of the nanowires much more convenient. Besides home built devices, plenty multi-probe microscopes from leading companies are available today. Unfortunately, mentioned above designs are based on the idea of independent probes, in this case each probe is positioned by its own piezo-driver. But for manipulations of the nanowires the design with two semi-independent probes looks to have an essential advantage. In this configuration the main piezo-driver moves both probes and the auxiliary one defines mutual position of probes.

We present a simple two probes AFM manipulator with two individual feedback systems for each semi-independent probe [1]. The design of the AFM probe mounting allows to work with upright microscope with focal distance of 3 mm. Applications of manipulator and advantage of its two semi-independent probe design are presented as well and are in the focus of current report.

Both probes of the manipulator operate in the dynamic full-time contact AFM mode. The main idea of this mode is depicted in Figure 1. The top prong of the tuning fork oscillates in vertical direction as it is shown with two-arrows line. Two positions of the tip, namely, the topmost and the bottommost during the tuning fork oscillation cycle are shown in the picture. The tip end stays on the sample surface during the whole period of the tuning fork oscillation cycle due to the tip flexibility. Thus, this mode is actually a hybrid one, uniting the dynamic tapping and the contact AFM modes. Similar to the tapping mode the amplitude of the oscillations of the tuning fork is used as the feed back signal.

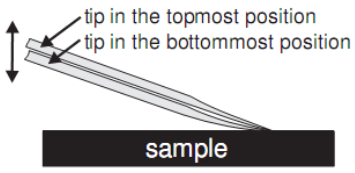

Figure 1. The main idea of the dynamic full-time contact AFM mode. The vertical two-arrows line is depicted the direction oscillations of the tuning fork top prong. Two positions of the tip, the the topmost and the bottommost during the tuning fork oscillation cycle are shown as well. The tip end stays on sample surface permanently due to the flexibility of the tip.

We use the level of the set point in this mode typically equal to 0.90-0.98 of the amplitude of free oscillations. Lower set point level means the higher pressure of the probe on surface and more pronounce bending of the probe. The set point level of 0.95 opens the ability to move the nanowires over substrate surface. The AFM mode used in manipulator is quite similar to standard

contact AFM mode realized with cantilever. It is possible to apply this mode for the measurement of the friction forces of a bunch of InAs wires placed on SiO_2 surface [1]. Measured value of 50pN/nm is approximately 12.5 times larger than the previously reported experimental data [2]. Current measurement is done in ambient conditions and the water film on the sample surface must have influence on the measured friction forces.

Controlled tip-to surface interaction allows to scan nanowires at high set point value (0.98) and the nanowire with 100 nm diameter can be easily allocated [1]. Since the used mode tip constantly stays on the surface, the 100% duty cycle signal can be observe during the conductivity measurements of the metallic pads [2].

The transportation of the nanowire or the bunch of nanowires over substrate surface for dozens microns can be done just with one tip. But for the long-range transportation of big nanowire ($Bi_{1-x}Sb_x$ 400 nm diameter whisker) a more convenient way of the operation is to engage two probes of the manipulator. The advantage of the instrument two-probe design allows to use manipulator as two-prong fork to transfer wires with diameters of several hundreds nanometers (Fig. 2).

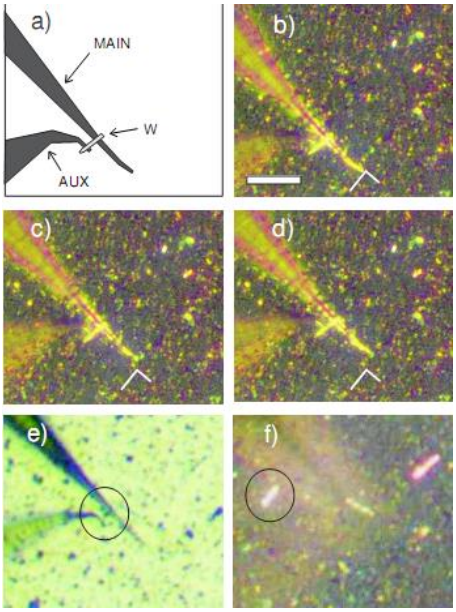

Figure 2. (a) The configuration of MAIN and AUX probes, and the BiSb wire (W) placed on them. (b)-(d) Short-ranged transportation of the wire, both tips stay on substrate surface, white angle points initial position of the MAIN tip end. (e) Both tips and the wire after long-ranged jump to a new position. The wire marked with a circle still lays on the tips. (f) The final position of the transported wire placed on the substrate and marked with a circle. (b)-(d), (f) In crossed polarized light. The horizontal scale bar in (b) corresponds to 10 m. The scale is the same for other four optical images.

So, we present the design of two probes AFM manipulator working together with short focal distance (3 mm) upright optical microscope. AFM of manipulator operates in dynamic full-time contact mode. This mode allows to control probe-to-surface force and to measure as the friction forces, so the conductivity similar to conventional contact AFM mode. Advantage of the instrument semi-independent two-probe design is presented as well.

1. A.A. Zhukov, V.S. Stolyarov, and O.V. Kononenko, *Review of Scientific Instruments* **88**, 063701 (2017).
2. G. Conache, (Lund & Halmstad), *Licentiate Thesis* (2008).

O-32

Formation and study of the RRAM memory elements by local anodic oxidation method

V.I. Avilov, V.A. Smirnov, R.V. Tominov, N.A. Sharapov, N.A. Polupanov

Southern Federal University, Institute of Nanotechnologies, Electronics and Equipment Engineering, 344006 Taganrog, Shevchenko st. 2, Russian Federation
e-mail: AvilovVI@sfedu.ru

One of the current trends in the electronic development is the development and research of resistive memory (RRAM) elements based on memristor structures, which is faster than modern memory, but it is non-volatile, which allows to reduce the power consumption of portable devices and increase the operating time without additional charging.

The analysis of publications has shown that most methods for forming memristor structures for resistive memory contain a complex stage of electroforming oxide nanosized structures (ONS) to give them memristor properties. However, the application of the local anodic oxidation (LAO) method using atomic force microscopy (AFM) techniques makes it possible to form the titanium ONS exhibiting a memristor effect without additional electroforming of structures, which will simplify the technology of manufacturing RRAM memory modules [1-2]. Therefore, the goal of the work is the development of manufacturing technology and the formation of memory elements RRAM based on memristor structures by the method of local anodic oxidation.

In the course of the work, a structure of memory elements RRAM was proposed, which is a cross-bar array of memristor structures containing an insulating SiO_2 substrate, structures of the lower titanium electrodes, and titanium ONS obtained by the LAO method and the structure of the upper electrodes (Fig. 1).

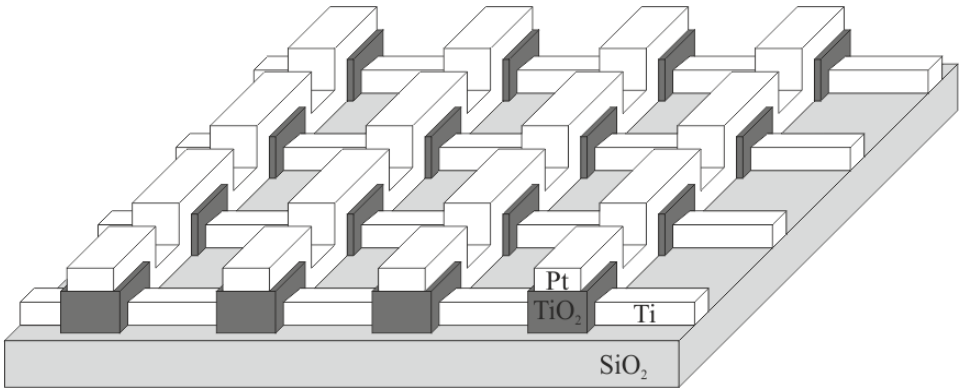

Figure 1. The layout of the memory elements of RRAM based on memristor structures.

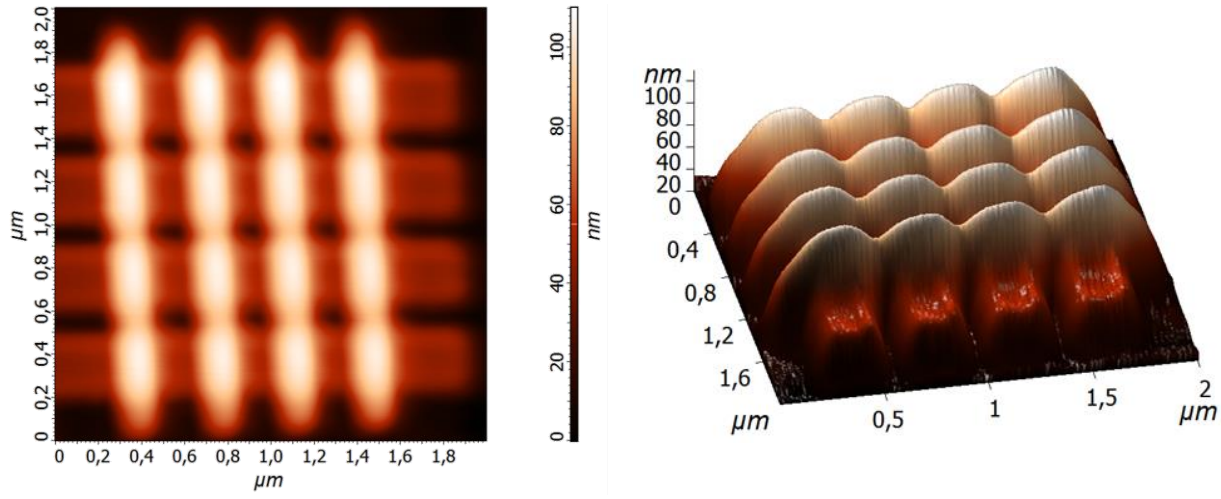

(a) (b)

Figure 2. (a) Topography and (b) 3D-image of the RRAM memory element layout.

On the basis of the proposed structure, a technological route for manufacturing the cross-bar array of the ONS titanium was developed. To do this, a SiO_2substrate is used, by which a thin film of titanium with a thickness of 20 nm was deposited by magnetron sputtering. Then, by the method of focused ion beams, lithography was carried out on the titanium film, resulting in the structures of the lower electrodes. After this, the LAO of the lower electrodes was used to form the memristor ONS of titanium. At the final stage, ion-stimulated deposition of the structures of the upper electrodes based on platinum was carried out. As a result, a model of the memory element RRAM was constructed on the basis of 16 memristor ONS (Fig. 2).

Investigation of the electric characteristics of the array showed that the obtained titanium ONS exhibit a memristor effect and switch between the high and the low resistance state (Fig. 3).

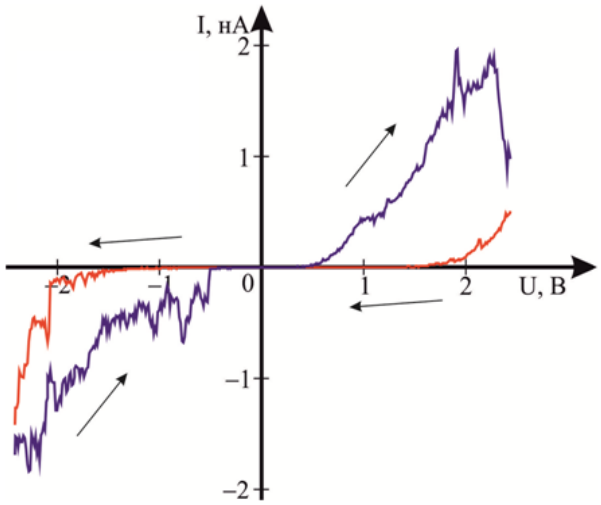

Figure 3. Volt-ampere characteristic of the titanium ONS obtained by the LAO method.

Thus, it was shown that the method of local anodic oxidation can be used in the formation of resistive memory elements. The obtained results can be used in the development of technological processes for manufacturing the elemental base RRAM on the basis of oxide nanosized titanium structures using probe nanotechnology.

This work was supported by RFBR according to the research project № 18-37-00299 and by Grant of the President of the Russian Federation No. MK-2721.2018.8.

1. V.I. Avilov, O.A. Ageev, A.S. Kolomiitsev, et al., *Semiconductors* **48**, 1757 (2014).
2. V.I. Avilov, N.V. Polupanov, V.A. Smirnov, et al., *Materials Science and Engineering* **256**, 5 (2017).

O-33

Domain patterning by focused electron beam in wide temperature range in lithium niobate crystal with surface dielectric layer

D.S. Chezganov[1], E.O. Vlasov[1], L.V. Gimadeeva[1], A.A. Esin[1], M.A. Chuvakova[1], V.Yu. Mikhailovskii[2], P.S. Zelenovskiy[1], V.Ya. Shur[1]

[1]*School of Natural Sciences and Mathematics, Ural Federal University, 620000 Ekaterinburg, Russia Corresponding author e-mail: chezganov.dmitry@urfu.ru*

[2]*Research Park, IRC Nanotechnology, St. Petersburg State University, 198104 St. Petersburg, Russia*

We have studied the domain formation induced by electron beam irradiation in wide temperature range in congruent lithium niobate (CLN) crystals with artificial surface dielectric layer. The results were explained in terms of kinetic approach [1].

The samples represented the 0.5-mm-thick Z-cut CLN plates. The irradiated polar surface was covered by various artificial dielectric layers (e-beam resists, parylene N, SiO_2), while the opposite surface was covered by the solid copper electrode grounded during irradiation. The domain structures have been produced by irradiation of the Z- polar surface using scanning electron microscopes Auriga Crossbeam and Merlin (Carl Zeiss). The irradiation parameters and beam positioning were controlled by electron beam lithography system Elphy Multibeam (Raith). The irradiation at the elevated temperatures (up to 250^{o}C) was carried out using thermal stage C1003 (Gatan Inc.). The static domain structures were visualized by scanning electron microscopy (SEM) after selective chemical etching.

We have measured the dose dependence of the isolated domain shape and size, and the temperature dependence of the threshold dose after dot irradiation. The hexagonal domains appeared at the room temperature, while the temperature increase led to lack of the domain shape stability and to formation of self-assembled domain structures. The obtained effects were explained by discrete switching during switching in highly non-equilibrium conditions caused by artificial dielectric layer and temperature dependence of its dielectric permittivity.

We have distinguished four types of domain structures appeared after stripe irradiation at the room temperature: (1) isolated nanodomains; (2) isolated domain rays oriented along Y+ directions; (3) solid domains with jagged walls (“fish-bone” structure); (4) continuous solid stripe domains. Thee domain patterns have been considered as a subsequent stages of domain structure evolution [2]. The threshold dose necessary for formation of solid stripe domain has been revealed. The influence of the temperature on stripe domain formation was discussed.

The dependences of the domain sizes on dose and accelerating voltage were measured for various dielectric layers. The non-linear increase of domain sizes with dose and accelerating voltage was obtained. The formation of quasi-regular domain fingers (“fingering”) in front of the plane domain wall, mainly oriented along the Y-crystallographic direction has been revealed. The detail study of the domain structure evolution allowed to determine the irradiation parameters for formation of the stripe domains with flat wall. This knowledge will be used for creation of the periodically poled crystals for light frequency conversion [3].

The equipment of the Ural Center for Shared Use “Modern nanotechnology” Ural Federal University was used. The research was made possible by the Russian Science Foundation (grant № 17-72-10152).

1. V.Ya. Shur, *J. Mater. Sci.* **41**, 199 (2006).
2. E. Vlasov, D. Chezganov, M. Chuvakova, V.Ya. Shur, *Scanning* **2018**, 7809826 (2018).
3. V.Ya. Shur, A.R. Akhmatkhanov, I.S. Baturin, *Appl. Phys. Rev.* **2**, 040604 (2015).

O-34

Numerical modelling of two-phase piezocomposites with interface mechanical anisotropic effects

A.V. Nasedkin

Institute of Mathematics, Mechanics and Computer Science, Southern Federal University, 344090, Rostov-on-Don, Russia
e-mail: nasedkin@math.sfedu.ru

Piezocomposite materials and, in particular, two-phase piezoceramic materials with nanosized pores or inclusions are being actively developed in the recent years. The developed in the recent years new nanostructured piezoelectric composite materials have a range of important advantages, such as the possibilities of controllable variation of the functional characteristics within a wide range, the ultra-low mechanical quality factor, etc. Furthermore, the modelling of composite micro- and nanomaterials has the specific features. It is known that some nanomaterials have unconventional physical properties that considerably differ from the characteristics of usual macrosized bodies. Thus, the experimental fact is the increasing of the stiffness with reducing the sizes of nanoobjects. One of the factors that are responsible for this behavior can be surface or interface effects. As research of the recent years shows, for the bodies of submicro- and nanosizes the surface stresses are important and influence the deformation of the bodies. In connection to this, the interesting problem can be an extension of this approach to the nanostructured piezoelectric composite materials.

In present investigation the models of two-phase piezoelectric composite materials developed in the framework of classic continuum approaches of solid mechanics and methods of composite mechanics. These models were used to construct more complicated models of the nanosized piezocomposites that were take into account the surface or interphase mechanical boundary conditions with anisotropic surface properties.

We use an integrated approach to the determination of the effective moduli of nanostructured piezoelecrtric composites with stochastically distributed nanoinclusions. In order to take into account nanoscale level at the borders between two material phases, the Gurtin-Murdoch model of surface stresses are used. ANSYS finite element package was used to simulate representative volumes and to calculate the effective moduli. This approach is based on the theory of effective moduli of composite mechanics, modelling of representative volumes and the finite element method. Here, the contact boundaries between two material phases were covered by the surface membrane elements in order to take the surface stresses into account.

For automated coating of interface boundaries in the cubic representative volume the following algorithm was used. At the beginning, as a result of the formation of the composite structure, the finite element mesh from octanodal cubic elements was created, some of which had the material properties of piezoelectric matrix, and the other part of the elements had the material properties of the inclusions. Further, only the finite elements with material properties of piezoelectric matrix were selected. The resulting elements on the outer boundaries were covered by four nodal target contact elements. Then, the contact elements, which were located on the external surfaces of the full representative volume, were removed, and the remaining contact elements were replaced by the special elastic quasi-shell elements with anisotropic properties inherited by the structure of the main phase. As a result, all the interface facets were coated by elastic quasi-shell shell finite elements.

The next step consisted in solving the static problems for representative volume with the boundary conditions which were conventional for effective moduli method. Further, the averaged stresses and electric fluxes were calculated, both on the volume finite elements and on the surface finite elements for mechanical stresses. Finally, the effective moduli were calculated by using the estimated average characteristics.

This work was supported by the Russian Science Foundation (grant № 15-19-10008-P).

O-35

Adaptive time-frequency analysis of signals in AFM

V. Pukhova

Saint Petersburg Electrotechnical University "LETI", 197376, Saint Petersburg, Russia
e-mail: vmpukhova@etu.ru

The probe-sample interactions during the AFM experiments represent a case of multi-frequency behaviour, since they are characterized by the simultaneous excitation of several modes and/or cantilever harmonics. Analysis of the data obtained as a result of interaction between the probe and the sample is of a particular interest not only from a practical point of view, i.e. obtaining information about the surface of the sample, but also this is an interesting methodological task, since the instantaneous processes resulting from the interaction of the probe with the sample surface carry a huge amount of information. To obtain it, it is necessary to provide an analysis method that is capable of characterizing all the excited cantilever frequencies simultaneously and without averaging, in contrast to the cyclic averaging used in standard methods. In other words, it is necessary to obtain the complete spectral response of the cantilever interacting with the sample, i.e. information about the dynamics of cantilever behaviour in time.

Traditionally, AFM signal analysis is performed by using Fourier transform (FT), which provides high accuracy and analysis speed. However, signal transformation from time to frequency domain by means of FT makes difficult or impossible the process of attribution of the particular parts of the spectrum to their time of appearance. In addition, the Fourier spectrum shows the averaged spectrum corresponding to the state of the system during a certain acquisition time. Thus, the spectral analysis provided by the FT gives a correct interpretation only in cases of stationary signals. The data of AFM experiments contain a lot of non-stationary or transient characteristics, and these characteristics are important parts of the signal. To analyze this type of signals, a method that allows obtaining information about instantaneous changes in rapidly varying signal parameters, as well as performing simultaneous analysis of all cantilever frequencies in the bandwidth of the detection system is required. As such an analysis method, the wavelet transform (WT) method can be used.

Wavelet transform is a powerful and well-developed mathematical tool that combines time and frequency domain. Until now, the most important application of wavelet transform in AFM was its use to reduce noise or extract data from an image of a surface topography. However, the use of WT in AFM as a tip-sample interaction signal analysis technique can give information about the temporal development of the spectral components of the cantilever signal. In other words, the WT gives a representation of the time evolution of the amplitude, frequency, and phase shift of each of the considered modes and/or cantilever harmonics. Such an advantage of the WT can be used to analyze the signals of any AFM experiments, but it is especially important in analyzing the signals of a multifrequency AFM experiments, since the correlation with time of individual spectral components can provide new information on the behaviour of the cantilever, and thus, on the properties of the surface [1-4]. Worth to notice, the basis of WT is called mother wavelet and it is not unified, but should be chosen according to the characteristics of the study signal. There are a number of mother wavelets that can be used for analysis and the choice of the mother wavelet should be done in accordance with the task that needs to be solved in the particular case. The aim of the present work is to show the possibilities of wavelet transform application in analyzing the signals of a multifrequency AFM experiments.

1. V. Pukhova, F. Banfi, G. Ferrini, *Nanotechnology* **24**, 505716 (2013).
2. V. Pukhova, F. Banfi, G. Ferrini, *Nanotechnology* **26**, 175701 (2015).
3. V. Pukhova, F. Banfi, G. Ferrini, *Beilstein J. Nanotechnol.* **5**, 494 (2014).
4. V. Pukhova, G. Ferrini, *IOP Conf. Ser.: Mater. Sci. Eng.* **256**, 012004 (2017).

O-36

On exact solution of the Kardar-Parisi-Zhang equation with determinate spatially-inhomogeneous source

A.E. Rassadin[1], T.S. Sazanova[2], A.V. Stepanov[1,3], L.A. Fomin[1,4]

[1]*Nizhny Novgorod Mathematical Society, 603950, Nizhny Novgorod, Russia*
e-mail: brat_ras@list.ru

[2]*Nizhny Novgorod State Technical University after R.E. Alekseev, 603950, Nizhny Novgorod, Russia*

[3]*Chuvash State Agricultural Academy, 428000, Cheboksary, Russia*

[4]*Institute of Microelectronics Technology and High Purity Materials RAS, 142432, Chernogolovka, Russia*

At present studying of peculiarities for nano- and microstructures is of great importance because information about these features can be used in the design and prediction of physical and physicochemical properties of nano- and micromaterials. Nowadays one of the most popular models for epitaxial growth of surface of solid state is the so-called Kardar-Parisi-Zhang (KPZ) model suggested in article [1]. In the report presented we consider the next kind of this model:

$$\frac{\partial H}{\partial t} = c + \frac{c}{2}\cdot\left(\frac{\partial H}{\partial x}\right)^2 + \nu\cdot\frac{\partial^2 H}{\partial x^2} + Q(x),\ H(x,0) = h_0(x),\ Q(x) \ge 0,\ x \in R, \tag{1}$$

where $H(x,t)$ is the height of growing surface with a cylindrical generatrix, c is the rate of its growth along the local normal to it, ν is the coefficient of surface diffusion and $h_0(x)$ is initial shape of the surface. For instance model (1) is highly adequate for simulation of technological process for manufacturing of X-ray multilayer diffraction gratings and mirrors [2]. But there is a sharp distinction between our model (1) and the ordinary KPZ models namely in our case extra spatially-inhomogeneous source of particles deposition $Q(x)$ is thought to be determinate in contrast to stochastic one in papers [1, 2].

Introducing new unknown function $\varphi(x,t)$ as:

$$H(x,t) = c\cdot t + \frac{2\cdot\nu}{c}\cdot\ln\varphi(x,t), \tag{2}$$

one can reduce nonlinear equation (1) to the Cauchy problem for the linear parabolic equation:

$$\frac{\partial\varphi}{\partial t} = \nu\cdot\frac{\partial^2\varphi}{\partial x^2} + \frac{c\cdot Q(x)}{2\cdot\nu}\cdot\varphi,\quad \varphi(x,0) = \exp\left[\frac{c\cdot h_0(x)}{2\cdot\nu}\right]. \tag{3}$$

Exact solution of equation (3) can be expressed as:

$$\varphi(x,t) = \int_{-\infty}^{+\infty} G(x,\xi;t)\cdot\varphi(\xi,0)\cdot d\xi, \tag{4}$$

where its Green function $G(x,\xi;t)$ is equal to:

$$G(x,\xi;t) = \sum_{n=0}^{N-1}\exp(-E_n\cdot t)\cdot\psi_n(x)\cdot\psi_n^*(\xi) + \int_0^{+\infty}\exp(-E\cdot t)\cdot\psi(x,E)\cdot\psi^*(\xi,E)\cdot dE. \tag{5}$$

Formula (5) contains functions $\psi_n(x)$ ($n = \overline{0,N-1}$) and $\psi(x,E)$ which are solutions of the next stationary Schrödinger equation:

$$-\nu\cdot\frac{d^2\psi}{dx^2} + U(x)\cdot\psi = E\cdot\psi, \tag{6}$$

where role of potential energy is played by function $U(x) \equiv -\frac{c}{2\cdot\nu}\cdot Q(x)$.

Due to nonnegativity of source $Q(x)$ there are both discrete spectrum of negative eigenvalues E_n ($n = \overline{0,N-1}$) and continuous spectrum of positive eigenvalues E. N eigenfunctions of discrete spectrum $\psi_n(x)$ and eigenfunctions $\psi(x,E)$ of continuous spectrum ought to be normalized in accordance with standard rules of quantum mechanics [3, 4]:

$$\int_{-\infty}^{+\infty}\psi_n^*(x)\cdot\psi_m(x)\cdot dx=\delta_{nm}\ ,\quad \int_{-\infty}^{+\infty}\psi^*(x,E)\cdot\psi(x,E')\cdot dx=\delta(E-E')\,. \tag{7}$$

The Green function having been found from expressions (5)-(7), we can return to investigation of the height $H(x,t)$ by means of formulae (4) and (2).

In this report above described method has been applied to the next source:

$$Q(x)=\begin{cases}Q_0, & |x|\le a\\ 0, & |x|>a\end{cases}. \tag{8}$$

This source corresponds to the well-known quantum mechanical problem about rectangular potential well [3]. Physically function (8) can be obtained from homogeneous stream of external particles with help of rectangular aperture.

Furthermore under time tending to infinity for arbitrary initial shapes $h_0(x)$ difference $H(x,t)-c\cdot t$ is sure to tend to some stationary limit $\mathrm{H}(x)$ obeying to the following equation:

$$\frac{c}{2}\cdot\left(\frac{d\mathrm{H}}{dx}\right)^2+\nu\cdot\frac{d^2\mathrm{H}}{dx^2}+Q(x)=0\,. \tag{9}$$

It is easy to see that for function $u(x)=-\dfrac{d\mathrm{H}(x)}{dx}$ equation (9) reduces to the well-known Riccati equation.

In the report for a number of model examples of initial shapes of the surface under investigation for source (8) we consider details of these passages to this limit shape $\mathrm{H}(x)$. Also we describe the case when width $2\cdot a$ of rectangular well (8) tends to zero under constant value of the product $Q_0\cdot a\equiv q_0$ and therefore profile of source (8) tends to delta-function: $Q(x)=2\cdot q_0\cdot\delta(x)$ This situation is reduced to the well-known quantum mechanical problem about delta-functional well [4] and physically can be realized by means of the channeling of slow atomic particles along carbon nanotube [5].

The theory developed in this report may be verified by means of atomic force microscopy.

At last the above described method is of great importance for the situation when extra source $Q(x)$ is considered to be a control. In this case equation (1) ought to be added by requirement of minimization of some functional. For example as this functional one can choose:

$$\int_{-\infty}^{+\infty}[H(x,T)-H_*(x)]^2dx\to\min\,. \tag{10}$$

Conditions (1) and (10) form the problem of optimal control by distributed parameter system [6] namely starting from initial shape $h_0(x)$ by means of control $Q(x)$ it is required to achieve minimal functional difference (10) between height $H(x,T)$ and fixed shape $H_*(x)$ at moment of time $t=T$. In other words it is the problem of nano engineering.

This work was supported by RFBR, grant N 18-08-01356-a.

1. M. Kardar, G. Parisi, Y.C. Zhang, *Phys. Rev. Lett.* **56**, 889 (1986).
2. L.I. Goray, M.N. Lubov, *Journal of Surface Investigation: X-Ray, Synchrotron and Neutron Techniques.* **8**, 444 (2014).
3. S. Flügge, *Practical Quantum Mechanics I* (Springer-Verlag), 62 (1971).
4. V.M. Galitsky, B.M. Karnakov, V.I. Kogan, *Problems on Quantum Mechanics* (Nauka), 237 (1992).
5. A.V. Stepanov, *Journal of Surface Investigation: X-Ray, Synchrotron and Neutron Techniques.* **9**, 789 (2015).
6. A.I. Korotkii, D.O. Mikhailova, *Proceedings of the Steklov Institute of Mathematics (Supplementary issues).* **280**, 98 (2013).

POSTER

PRESENTATIONS

P-01

Local study of the domain wall mobility in ferroelectric ceramics under the action of electric field and mechanical loading

A.S. Abramov[1], D.O. Alikin[1,4], A.P. Turygin[1], M.M. Neradovskiy[1,2], V.S. Kornilova[1], A.V. Nikitin[3], D.V. Karpinsky[3], V.Ya. Shur[1], A.L. Kholkin[1,4]

[1]*School of Natural Sciences and Mathematics, Ural Federal University,620000 Ekaterinburg, Russia e-mail: alexander.abramov@urfu.ru*

[2]*Université Côte d'Azur, CNRS, InPhyNi, 06100 Nice, France*

[3]*Scientific-Practical Materials Research Centre of NAS of Belarus, BY-220072 Minsk, Belarus*

[4]*Department of Physics & CICECO – Aveiro Institute of Materials, University of Aveiro, Portugal*

Domain wall motion in heterogeneous multiaxial materials is quite complicated due to variety of factors necessary to be taken in consideration. Different interfaces such as grain and phase boundaries, domain walls as well as defect structure can impact to the domain growth [1]. It is rather complicated to distinguish the contributions of each mechanism by analysis of the macroscopic studies. Whereas piezoresponse force microscopy allows to realize visualization of the domain structure and determination of the spontaneous polarization orientation.

Here we studied bismuth ferrite (BFO) ceramics, doped by La and Pr, with a composition near the antipolar-to-polar morphotropic phase boundary sintered by conventional solid-phase path. Both electric-field induced polarization reversal by scanning probe microscopy tip and local switching under the mechanical loading action were investigated. Dependences of in-plane and out-of-plane polarization switching on grain orientation were found for non-180-degree domain walls. The mobility of the non-180-degree domain walls was significantly lower than 180-degree walls. Domain wall motion velocity of all domain walls depends linearly on the applied field and the wall displacement demonstrates close-to-logarithmic dependence on voltage pulse duration, which is in line with other homogeneous and heterogeneous systems [2, 3]. The grain boundaries and initial domain structure didn't interact with growing domains through the distortion of electric field, however the switching spectroscopy allowed to reveal existence of frozen polarization component. Polarization reversal via mechanical loading (nano-indentation) resulted in formation of domains in indented area with spatial distribution determined by asymmetry of the stress created with the triangular shaped prism. Electric field and mechanical loading induced local switching was studied in relation to phase content of BFO ceramics and thereby these studies shed further light on understanding of antipolar-to-polar morphotropic phase boundary phenomena.

The equipment of the Ural Center for Shared Use "Modern nanotechnology" was used. The reported study was funded by RFBR (grant No. 17-52-04074) and BRFFR (grant No. F17RM-036). This work was developed within the scope of the project CICECO-Aveiro Institute of Materials, POCI-01-0145-FEDER-007679 (FCT Ref. UID/CTM/50011/2013), financed by national funds through the FCT/MEC and when appropriate co-financed by FEDER under the PT2020 Partnership Agreement. This project has received funding from the European Union's Horizon 2020 research and innovation program under the Marie Skłodowska-Curie grant agreement No 778070.

1. D.M. Marincel, H. Zhang, A. Kumar, et al., *Adv. Funct. Mater.* **24**, 1409 (2014).
2. V.Ya. Shur, A.V. Ievlev, E.V. Nikolaeva, E.I. Shishkin, M.M. Neradovskiy, *J. Appl. Phys.* **110**, 052017 (2011).
3. D.O. Alikin, A.P. Turygin, J. Walker, A. Bencan, B. Malic, T. Rojac, V.Ya. Shur, A. Kholkin, *Acta Mater.* **125**, 265 (2017).

P-02

Investigation of aqueous suspensions of multilayer vesicles of phospholipids by Mandelstam-Brillouin spectroscopy at various temperatures

S.V. Adichtchev, N.V. Surovtsev

Institute of Automation and Electrometry SB RAS, Novosibirsk, 630090, Russia
e-mail: adish2@ngs.ru

Phospholipid vesicles serve as a model of cell membranes that can be used to study various processes taking place in cells. In the study of many questions related to the characterization of the membrane, for example, during the gel-fluid phase transition in the membrane, it becomes necessary to know its elastic properties and the speed of sound. Therefore, the development of non-contact and non-destructive experimental techniques that allow measuring the modulus of elasticity and the speed of sound in systems containing phospholipid membranes is an important task. Until now, a relatively small number of studies have been devoted to the study of the speed of sound in membranes by means of ultrasonic techniques limited to a megahertz range [1]. This range overlaps with the characteristic relaxation response of membranes, which complicates the interpretation of the experimental data. It is desirable to determine the speed of sound in the gigahertz range. An even more significant drawback of ultrasonic methods is the need for direct contact between the generator and the detector with the material being studied. The Mandelstam-Brillouin scattering spectroscopy (MBS), being a method of optical spectroscopy, is free of this shortcoming and allows one to determine the speed of sound in the gigahertz range. Previously, this technique was only used several times for phospholipid membranes. One of the most famous in this area is the work [2], performed on a multilayered sample prepared on a substrate. To date, MBS has not been used to determine the modulus of elasticity in suspensions of phospholipid vesicles

This work is devoted to the development of an experimental technique based on MBS spectroscopy for the study of aqueous suspensions of multilayer vesicles of phospholipids at different temperatures using the example of DPPC phospholipid (1,2-dipalmitoyl-sn-glycero-3-phosphocholine). From the dependence of the MBS spectrum on the sample thickness, the MBS spectrum was reduced to the single-scattering regime. Spectra of MBS suspensions of multilayer vesicles of phospholipids DPPC are obtained, positions MBS lines are determined. The temperature dependence of the position of the line, its change in the transition of the gel-fluid is studied. A comparison of the behavior of MBS lines of polycrystalline ice (T <0°C) and water (T> 0°C) reveals the contribution of phospholipid layers to the MBS spectrum. Analysis of the data made it possible to estimate the value of the elastic modulus and its dependence on temperature.

1. T. Heimburg, *Biochimica et Biophysica Acta*, **1415**, 147 (1998).
2. W. Manglkammer, J.K. Kruger, *J. Phys. IV* **129**, 65 (2005).

P-03

Study of human skin based on scanning probe microscopy

V.O. Ageev

Department of Information Technology Security Southern Federal University, 347900 Taganrog, Russia
e-mail: agee-vlad@yandex.ru

In this paper a method of biometric identification with high reliability based on measuring the elastic properties of the skin of a human finger while scanning his finger prints is presented. This method is shown to allow with a high degree of veracity to distinguish the skin from the inorganic materials used to create the fingerprint. It is found that the elasticity of the skin varies at 15% with increasing interval between the cut and measurement of the skin from 5 to 30 minutes. The elasticity of the skin also depends on the age of the person and is 60,2 ± 4,2 and 42,4 ± 2,6 kPa to 20 and 40 years, respectively. These dependencies can be used for creating additional levels of protection of biological identification method and preventing such methods of its compromетation as the use of moulds and pre-made cuts of skin. The results can be used in the development of biometric identification systems with a high level of protection that verifies either the fingerprint pattern of skin of human finger or its elasticity.

Cuts of epidermis of thumb skin of people aged 20 and 40 were used as experimental samples. The researches of experimental samples' topology were held by the method of SPM in a half-contact regime using probe nanoscale laboratory NtegraVita(NT-MDT,Selenograd). The cantilever NSG-10 of radius 10 nm and of medium rigidity k = 5,5 N/m was used as probe. SPMscan of skin epidermis is shown on (Fig. 1). The research of elastic qualities of experimental samples was held with the help of the method SPM in regime of force spectroscopy, with which on direct and back runs of cantilever the dependence of bend size (DFL signal) is got from the degree of moving-out of z-piestic tube of scanner (signal Height).

Moreover the researches of elastic qualities of medical silicone, plasticine and chewing gum were held for exposure of distinctive peculiarities of dependence DFL (Height) got for skin epidermis cut from dependences DFL (Height) typical for biocompatibleand inorganic materials.

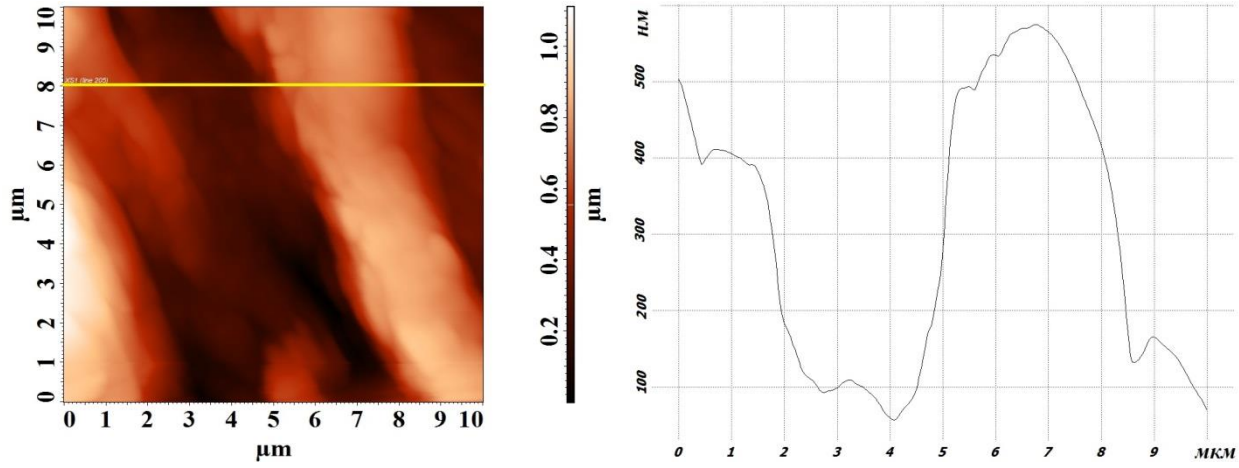

(a) (b)

Figure 1. SPM scan of thumb skin epidermis: (a) topology of the surface; (b) profilogram along cutting plane line.

The measuring of skin elasticity of people aged 20 was held after 5 and 30 minutes after cut in order to exclude the possibility to break the system of biometric identification's protection within usage of the preliminary prepared skin cut.

P-04

Behavior of nonlinear dielectric response and features of elastic properties in a PZT-Based multicomponent system

A.V. Skrylev[1], G.M. Akbaeva[2], A.I. Burkhanov[3], A.V. Sopit[3], E.M. Panchenko[2]

[1]*Institute of High Technologies and Piezotechnics, Southern Federal University, 344090, Rostov-on-Don, Russia*
e-mail: skrylyov@sfedu.ru

[2]*Research Institute of Physics Southern Federal, University, 344090, Rostov-on-Don, Russia*

[3]*Volgograd State Technical University, 400005, Volgograd, Russia*

The nonlinearity of the dielectric response and the velocity of the longitudinal sound wave in a soft piezoceramic material, based on a PZT, in the region of the phase transition, are investigated.

The character of the nonlinearity of the dielectric response in the behavior of the velocity of longitudinal ultrasonic waves in a piezoceramic material based on a PZT ($0.36PbTiO_3$ – $0.33PbZrO_3$ – $0.17Pb(MgZr)_{1/3}Nb_{2/3}O_3$ – $BaTiO_3$ – $SrZrO_3$) was studied. We have found that anomalies in the behavior of the temperature-field dependences of the effective dielectric permittivity $\varepsilon'_{eff}(E,T)$ and the velocity of the longitudinal ultrasonic wave v(T) appear in the temperature range substantially lower than the temperature of the maximum permittivity T_m = 160℃, on 1 kHz (Fig. 1). The character of the manifestation of the anomalies of these parameters indicates the relaxor-like properties of this type of ferroelectric ceramics, where the coexistence of different phase states of the material is possible in a wide temperature range [1-4].

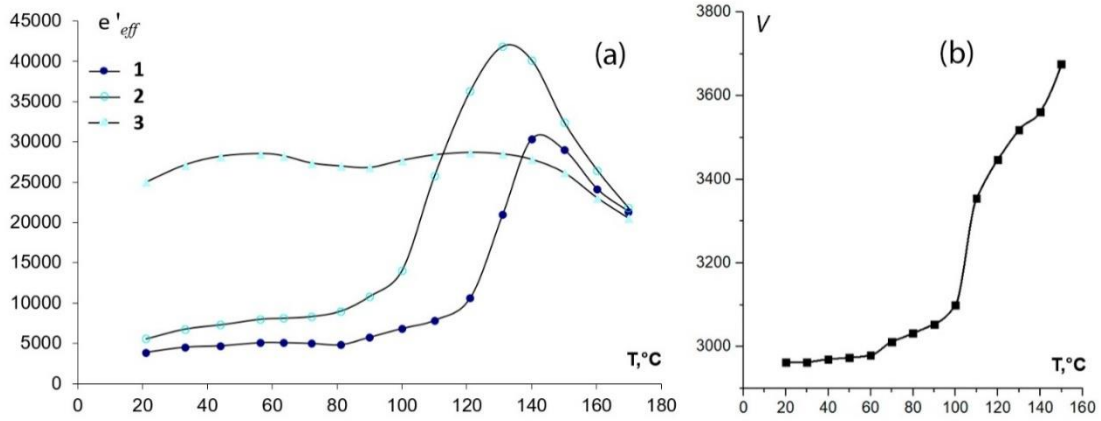

Figure 1. The temperature dependences $\varepsilon'_{eff}(E,T)$ for different values of the amplitude of the measuring field E (curve 1 – 0,95kV/mm, 2 – 3,7kV/mm, 3 – 9,2kV/mm) - (a) and v(T) - (b) in the material under study.

1. G. Burns, B.A. Scott, *Solid State Commun*. **13**, 423 (1973).
2. D. Viehland, S.J. Jang, L.E. Cross, et al., *Phys. Rev. B* **46**, 8003 (1992).
3. S.G. Lushnikov, A.I. Fedoseev, S.N. Gvasaliya, et al., *Phys. Rev. B* **77**, 104 122 (2008).
4. G.A. Smolensky, N.K. Yushin, S.I. Smirnov et al., *Soviet Phys. Solid State* **27**, 801 (1985).

P-05

The surface analysis of the membranes with the different degree of cation-exchanger dispersity by AFM method

E.M. Akberova

FSBEE HE «Voronezh State University», 394018, Voronezh, Russia
e-mail: elmara_09@inbox.ru

At present, one of the directions in improvement of electromembrane methods of substances separation and isolation is the development of new membranes with optimized surface morphology, that allow to increase in the efficiency of electrodialysis in overlimiting current regimes due to the development of electroconvection. The purpose of this work is a comparative analysis of the surface microstructure of the experimental samples of membranes with different ion exchanger dispersity degrees by AFM method.

In the study there was evaluated the geometrical inhomogeneity of experimental samples of heterogeneous cation-exchange Ralex CM Pes membranes (MEGA a.s., Czech Republic) and commercially available MK-40 heterogeneous sulfocation-exchange membrane (LLC "IP Shchekinoazot", Russia). The Ralex membranes were obtained by rolling the homogenised mixture of milled ion-exchanger with varying dispersity degrees with polyethylene. The dispersity degree of sulfocation-exchanger was varied by using of time of its milling from 5 to 80 minutes. The AFM images of dry membrane samples were processed by means of the Nova RC1 software of a Solver P47 Pro microscope.

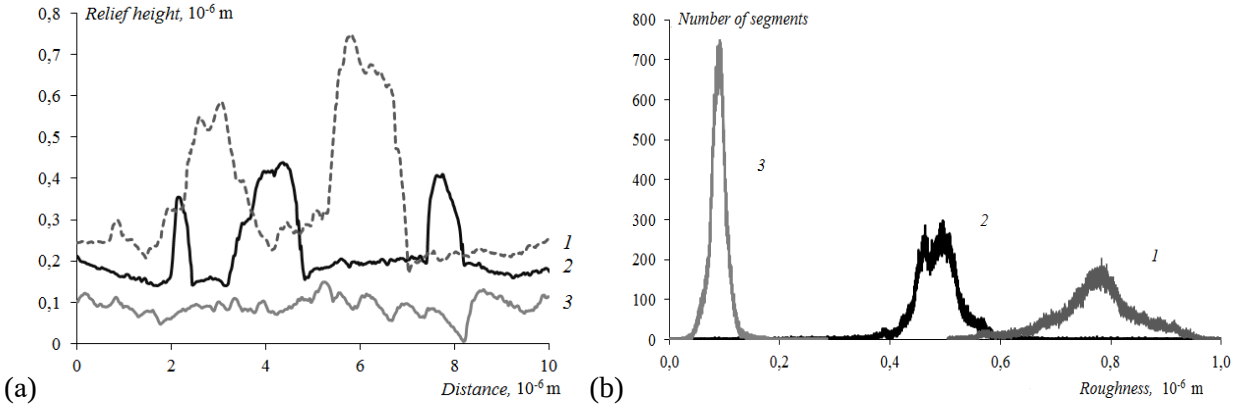

Figure 1. The microprofiles (a) and histograms of the density distribution of the heights for the entire image (b) of the samples of the MK-40 (1) and CM Pes membranes with the ion exchanger milling time of 5 (2) and 80 (3) min. Scanning area of 10 × 10 μm.

A comparison of the surface microrelief and histograms of heights distribution on the surface of the experimental CM Pes and MK-40 heterogeneous cation exchange membranes in the dry state is shown in Fig. 1a. The membrane with a higher degree of ion exchanger dispersity that appropriate milling time 80 min was characterized by a smoother surface on a micrometric scale: the maximum height R_y and the average arithmetic roughness R_a were 286 nm and 12 nm, respectively. Wherein, the maximum density distribution of the heights on the entire surface of the membrane sample was 0.1 μm (Fig. 1b). The microprofile of the membrane containing the ion exchange particles after 5 minutes of milling had the appearance of a more developed chaotic structure with an average roughness scale R_a twice as large. The maximum of density of the height distribution corresponded to a region of 0.4-0.6 μm. For the MK-40 membrane, which characterized by smaller degree of ion exchanger dispersity, the most pronounced surface relief, a significant asymmetry in the distribution of heights and a shift in the distribution toward higher values are revealed.

The work is supported by the grant of the President of Russian Federation MK-925.2018.3.

The author is grateful to the «MEGA» a.s. company (Czech Republic) and its owner Mr. L. Novak for providing experimental samples of the Ralex CM Pes sulfocation-exchange membranes.

AFM-data of the membranes surface were obtained at the CCUSE of VSU.

P-06

The surface electrical heterogeneity of the membranes with the different degree of cation-exchanger dispersity

E.M. Akberova[1], E.Yu. Osipenko[2], E.A. Goleva[1]

[1]*FSBEE HE «Voronezh State University», 394018, Voronezh, Russia*
[2]*SC «VSP-MIKRON» 394033, Voronezh, Russia*
e-mail: elmara_09@inbox.ru

One of the priority tasks of modern membrane electrochemistry and technology is the creation of the ion-exchange membranes with optimized surface for high intensive electrodialysis. The main mechanism for increasing mass transfer in such systems is electroconvection. The purpose of this work is an evaluation of the effect of changing the degree of dispersity of the ion exchanger in the manufacture of the Ralex CM Pes heterogeneous membranes on their surface properties.

In the study there was evaluated the electrical inhomogeneity of experimental samples of heterogeneous cation-exchange Ralex CM Pes membranes (MEGA a.s., Czech Republic) and commercially available MK-40 heterogeneous sulfocation-exchange membrane (LLC "IP Shchekinoazot", Russia). The Ralex membranes were obtained by rolling the homogenised mixture of milled ion-exchanger with varying dispersity degrees with polyethylene. The dispersity degree of sulfocation-exchanger was varied by using of time of its milling from 5 to 80 minutes.

The experimental studies of surface morphology of hydrated and dry membranes were conducted using the method of scanning electron microscopy at JSM-6380 LV microscope (Japan) equipped with regulated pressure, what allows the ion exchange material to be studied under real conditions of its operation (water swollen state). Microphase fractions and sizes were estimated by means of an original software system [1]. The ion-exchange particles dispersity degree *D* was assumed to be the reciprocal of their diameter.

The electrical heterogeneity of the membrane surface is characterized by the proportion and sizes of the conducting regions (ion exchanger particles and pores near them). From the analysis of SEM-images (Fig. 1) of membrane samples, it was found that the proportion of ion exchanger for the heterogeneous sulfocation-exchange membranes is 15-17%.

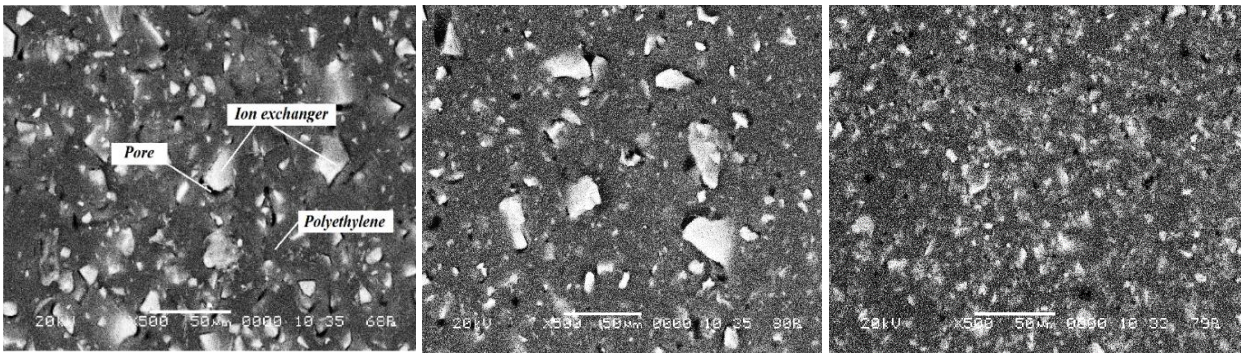

(a) (b) (c)

Figure 1. Micrographs of the surface of MK-40 (a) and Ralex CM Pes (b, c) sulfocation-exchange membranes in swollen state. Time of ion-exchanger milling: (a) 5 min, (b) 80 min.

Analysis of the distribution of ion-exchange regions along the radii shows that, as compared with the MK-40 membrane, the maximum in the distribution curve for the Ralex CM Pes membrane samples shifts towards smaller values and is in the range of 1-2 μm (Fig. 2). With the increase in the time of ion-exchange particles milling, an increase in their total quantity and a significant increase in the fraction of the ion exchanger with a radius of less than 0.7 μm is established. For membrane samples with the milled ion exchanger for 5 and 80 min, the range of the dispersity degree is $(3 – 80)\cdot10^4$ m^{-1} and $(7 – 125)\cdot10^4$ m^{-1} respectively. For the MK-40 membrane, the range of the degree of dispersity of the ion-exchange resin is $(4 – 60)\cdot10^4$ m^{-1}. With an increase in the degree of dispersity of ion-exchange particles on the surface of swollen samples

of CM Pes membranes, the value of their average radius decreases by 20% and amounts to 1.52 ± 0.03 μm for membranes with the maximum ion exchangers grinding time. According to estimates made in [2], the value of the average radius $\overline{R}$ for the Ralex CM Pes sulfocation exchange membrane that is serially produced by the «MEGA a.s.» company is 1.88 μm.

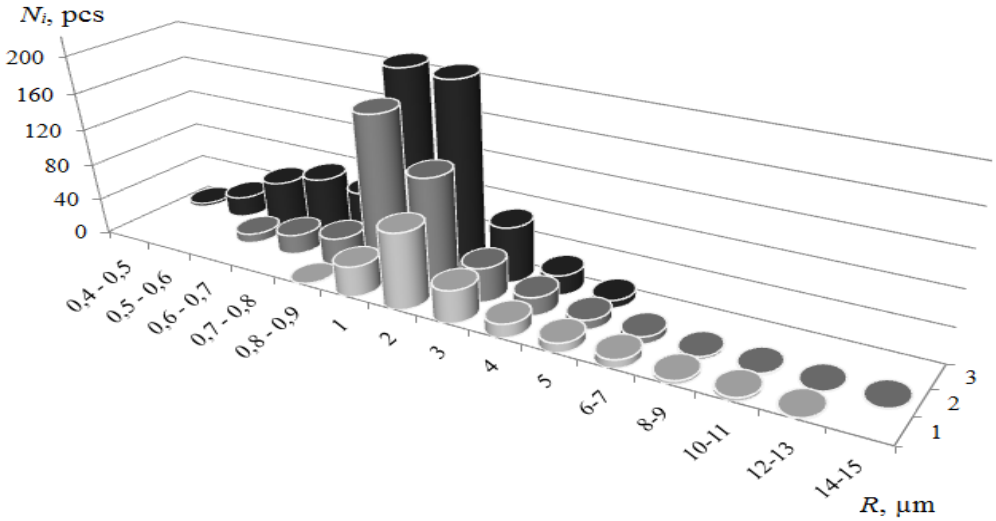

Figure 2. Distribution of ion-exchanger over radii for swollen conditioned samples of MK-40 (1) CM Pes membranes with time of ion-exchanger milling: (2) 5 min, (3) 80 min.

The reduction in the sizes of the ion exchanger regions on the surface of the experimental CM Pes membranes is accompanied by the convergence of the conducting surface zones: the effective distance between the ion exchangers is more than twice and amounts to 9.3 and 5.5 μm for a milling time of 5 and 80 min, respectively.

A significant difference is found between the total surface porosity of CM Pes membranes with the different degree of the ion exchanger dispersity. With increase in time of ion-exchange particles milling from 5 to 80 min, the macroporosity on the surface of the conditioned membranes in the swollen state decreases from 2.5 to 1.8%, wherein the average pore radius values are 1.55 ± 0.03 and 1.27 ± 0.04 μm, respectively.

Thus, the differences in the surface microstructure of the swollen samples of the experimental Ralex CM Pes heterogeneous sulfocation exchange membranes (Czech Republic) with different time of the ion exchanger milling are visualized by the SEM method. The reduction in the size and the convergence of the conducting phase zones, the decrease in the porosity and roughness of the surface of the membranes containing the ion exchanger subjected to a longer milling time are revealed.

The work is supported by the grant of the President of the Russian Federation MK-925.2018.3.

The authors are grateful to the «MEGA» a.s. company (Czech Republic) and its owner Mr. L. Novak for providing experimental samples of the Ralex CM Pes sulfocation-exchange membranes.

Microphotographs of the membranes surface were obtained at the CCUSE of VSU.

1. E. A. Sirota, N. A. Kranina, V. I. Vasil'eva, et al., *Proceedings of Voronezh State University. Series: Chemistry. Biology. Pharmacy* **2**, 53 (2011). (in Russian)
2. V. I.Vasil'eva, A. V. Zhil'tsova, E. M. Akberova, et al., *Condensed Matter and Interphases* **16**, 257 (2014). (in Russian)

P-07

Formation of the charged domain walls in lithium niobate single crystals with various electrode types

A.R. Akhmatkhanov, A.A. Esin, V.Ya. Shur

School of Natural Sciences and Mathematics, Ural Federal University, 620000 Ekaterinburg, Russia
e-mail: andrey.akhmatkhanov@urfu.ru

Magnesium oxide doped lithium niobate single crystals (MgO:LN) are one of the most popular materials for nonlinear-optical applications. It was shown earlier, that during polarization reversal with metal electrodes domains with conductive charged domain walls penetrate through the crystal, leading to decreasing of applied electric field and strongly influencing the periodical poling process [1]. We have shown that this effect is absent for liquid electrolyte electrodes.

We present here the experimental study of the domain structures formed during polarization reversal in MgO:LN single crystals with a various combinations of electrodes at the polar surfaces. Several types of electrodes have been used: the sputtered ITO or Cr thin films with thickness 100-200 nm ("solid electrodes") and saturated water solution of LiCl ("liquid electrodes"). Domain kinetics was visualized *in situ* during polarization reversal with a simultaneous recording of the switching current. The integral conductivity of the obtained domain structures was measured immediately after the polarization reversal. The obtained static domain structures have been investigated by means of Cherenkov Second Harmonic Generation microscopy in the crystal bulk [2], and the complete three-dimensional domain shape was reconstructed.

It was shown that the spike-like domains with charged head-to-head walls appeared for negative polar surface (Z-) covered by solid electrode - metal or semiconductor sputtered film. The charged walls of the created domains possess pronounced conductivity. The domain sideways growth and merging are essentially suppressed in this case. In contrast individual domains merge creating the uniform right-angle prismatic domains with almost vertical low conductive walls at the termination of the switching process for Z- surface covered by liquid electrolyte.

For positive (Z+) polar surface covered by solid electrode the domain backswitching after external field switch-off leads to increase of domain walls inclination angle and higher conductivity along the charged walls due to more pronounced shrinkage at the Z- surface. For Z+ polar surface covered by liquid electrolyte electrode the conductivity along the walls is unipolar and current flow through the wall results in reduction of cations. This effect allowed realizing "domain wall lithography" by direct electrodeposition of metal on the domain walls.

The research was funded by RFBR (grant № 18-32-00641). The equipment of the Ural Center for Shared Use "Modern nanotechnology" Ural Federal University was used.

1. K. Mizuuchi, A. Morikawa, *J. Appl. Phys.* **96**, 11 (2004).
2. Y. Sheng, A. Best, H.-J. Butt, W. Krolikowski, A. Arie, K. Koynov, *Opt. Express* **18**, 16539 (2010).

P-08

The effect of the laser-induced structures' surface morphology on the luminescence of thermostable polybenzimidazoles

A.A. Akovantseva[1,2], B.Ch. Kholhoev[3], G.I. Pudovkina[1], M.M. Suchilova[2], S.L. Kotova[2,4], P.S. Timashev[1,2], A.O. Rybaltovskij[5]

[1]*Institute of Photonic Technologies, Research center "Crystallography and Photonics", RAS, Russia, Moscow*

[2]*Institute for Regenerative Medicine, Sechenov University, Russia, Moscow*
e-mail: akovantseva-a@yandex.ru

[3]*Baikal Institute of Nature Management SB RAS, Russia, Ulan-Ude*

[4]*Semenov institute of chemical physics, RAS, Russia, Moscow*

[5]*Lomonosov Moscow State University, Russia, Moscow*

Here, we present the results of our experiments on the creation of luminescent laser-induced structures in a matrix of thermostable polybenzimidazole under continuous and pulsed irradiation. We used atomic force microscopy to visualize the surface of the structures. The mechanism of the created structures' luminescence was suggested. We have shown that the morphology of the created structures affects the luminescence enhancement in the polymer films.

Creation of stable luminescent structures in solid transparent materials is achieved, as a rule, by introduction of rare earth ions [1] or semiconductor nanoparticles [2] with the subsequent application of certain physico-chemical processes of their deposition. The data have been reported on the creation of laser-induced luminescent structures based on silver and gold nanoclusters in polymer matrices, which may find application in recording information and in the biomedicine [3-4]. However, examples of laser-induced formation of luminescent structures in pure unalloyed luminescent materials have been studied insufficiently so far. Such structures are of interest, first of all, from the viewpoint of studying the mechanisms of luminescent process manifestation in systems with closely positioned emission centers and may be further used for the creation of sensor devices and in the rail defect detection equipment.

This study was aimed at the creation of luminescent structures with different morphology in poly-2,2'-*n*-oxydiphenylene-5,5'-bibenzimidazole (OPBI) films under the action of continuous and pulsed laser irradiation. To create the structures, we used a continuous irradiation laser with the wavelength of 405 nm and a femtosecond laser with the wavelength of 532 nm. Using optical and atomic force microscopy, we visualized the morphology of the created structures. The effect of the laser irradiation type on the luminescence and morphology of the formed structures was demonstrated. The influence of the created structures' roughness increase on the variations of their luminescent properties was evaluated by atomic force microscopy. We have shown that the structures created under continuous irradiation have a stronger luminescence and non-uniform surface, and their sizes vary in the range of 4 to 80 μm, depending on the irradiation parameters. The structures created with the femtosecond laser have a more homogeneous surface, and their sizes vary in the range of 1-2 μm.

This study was performed in the framework of the RFBR grant Mol_a 18-33-00645.

1. N.V. Gaponenko. *Films formed by the sol-gel technique on semiconductors and in mesoporous matrices* (Belaruskaya Navuka), (2003).
2. S. Dirr, S. Wiese, H.-H. Johannes, *Synthetic metals* **91**, 53 (1999).
3. C.-A.J. Lin, C.-H. Lee, J.-T. Hsieh et.al, *J. of Med. and Biolog. Engineering* **29**, 276 (2009).
4. P. Kunwar, J. Hassinen, G.Bautista, et al., *ACS Nano* **8**, 11165 (2014).

P-09

Effect of subphase conditions on the formation of graphene Langmuir monolayer

A.J. Al-Alwani[1,2], A.S. Chumakov[1], N.N. Begletsova[1], O.A. Shinkarenko[1], S.B. Venig[1], E.G. Glukhovskoy[1]

[1]*Department of Nano- and Biomedical Technologies, Saratov State University, 410012, Saratov, Russia*
[2]*Babylon University, Babylon, Iraq*
e-mail: Ammarhamlet2013@yahoo.com

Studying the formation of graphene monolayer by Langmuir-Blodgett technique. The effect of subphase pH and temperature on the graphene Langmuir isotherm are investigated. Also, the influence of subphase conditions on the surface potential of the graphene monolayer was reported, this study. This study helps us to understand the assembly of graphene, showing great promise in efficient sensors and biosensing systems.

Graphene sheet has recently been attracted attention because its electrical properties and this makes graphene sheets a good candidate for the formation of novel materials with a wide potential for applications such as photovoltaic. The graphene sheets properties can be tuned by oxidation and convert the materials from hydrophobic to hydrophilic. The assembly of graphene sheets thin films can be formed by different methods such as spray coating, dip coating and Langmuir Blodgett method. Langmuir Blodgett was used to studying the formation of graphene thin film due to the advantage of this method the possibility of formation of two dimensions monolayer with control limiting monolayer area and control the thickness of thin film, etc [1]. The amphiphilic nature of graphene sheets could form a layer at air–water interface. The changing of subphase parameters leads to changes the properties of the monolayer (such as thickness, interactions between layers and occupied area).

Graphene powder was purchased from (Time-Nano Company in China) and dissolved in chloroform with low concentration of 0.0001g/ml. Graphene solution, 1.5 ml was dropped on the surface of water. After 12 mins, symmetric movable barriers were compressed the monolayer at rate of 12 cm^2/min. Graphene thin film was transferred on solid substrates by the Langmuir-Schaefer (LS). Figure 1 shows the surface morphology of graphene sheets thin film was investigated by scanning electron microscopy (SEM).

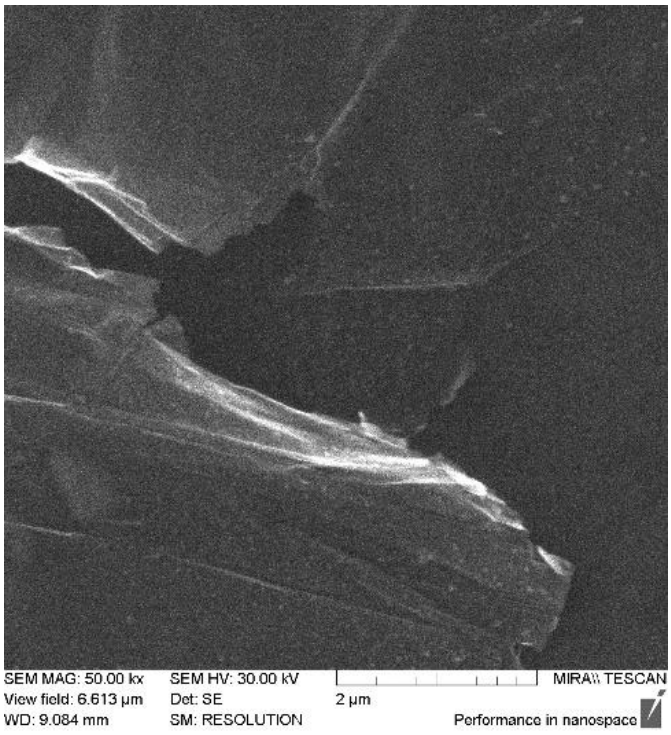

Figure 1. SEM image of grapheme sheets on silicon substrate.

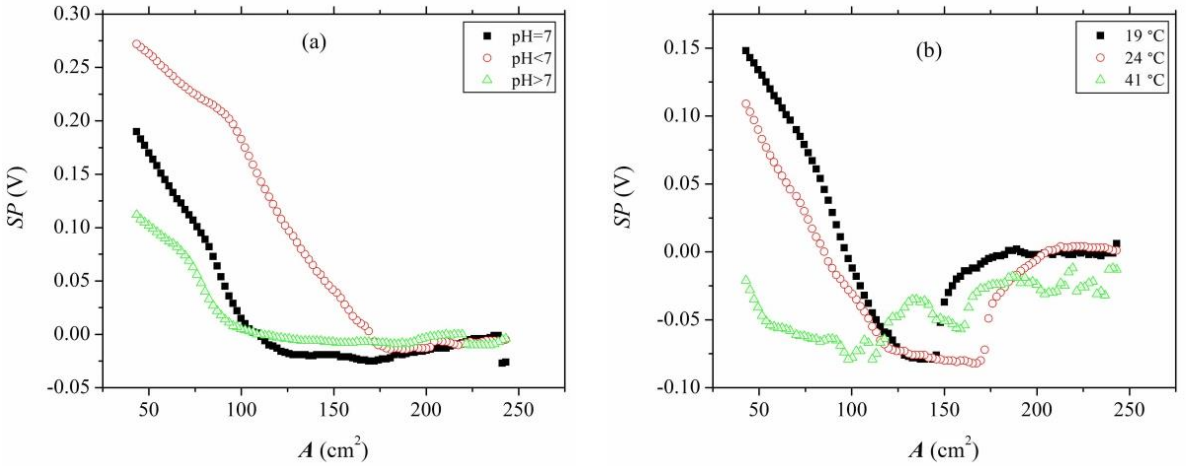

Figure 2. Showing the variation of the surface potential of graphene monolayers at different subphase pH (a) and at different subphase temperature (b).

Figure 2a shows the changing in the surface potential of graphene layer by changing pH of subphase. With increase the acidity of water lead to increase the surface potential and increase the occupied area of graphene layer. However, with increase the basicity leads to decrease the surface potential and decrease in the occupied area of graphene. This can be explained by changing in the charge of graphene surface that cause repulsion and/or attraction between graphene sheets. Figure 2b shows that the surface potential decrease with increase the temperature of subphase lead to decrease the surface potential. In this case, the changing in subphase temperature allows controlling the dissolution rate of monolayer. The result of this work could be used for wide potential in the biological or optoelectronic application, etc.

The graphene layers have been formed successfully by Langmuir method. Was found that the changing in the pH and temperature of water subphase have an influence on the formation of graphene thin film. This can be useful for demonstrating the uniformity of graphene film and thickness.

This work was supported by grant from DAAD 4.9977.2017/5.2.

1. K. Lambert, L. Wittebrood, I. Moreels, et al., *Journal of Colloid and Interface Science* **300**, 597 (2006).
2. A.J. Al-Alwani, A.S. Chumakov, O.A. Shinkarenko, et al., *Applied Surface Science* **424**, 222 (2017).

P-10

Reconstruction of volume structure of carbon based conductive polymer composites

A.M. Alekseev[1], A.E. Efimov[2], J. Loos[3]

[1]*National Research University "MIET", 124498, Moscow, Russia*
e-mail: Alekseev@ntc-nmst.ru

[2]*Shumakov National Medical Research Center for Transplantology and Artificial Organs, 123182, Moscow, Russia*

[3]*DSM Resolve, 6167 RD Geleen, The Netherlands*

Conductive composites based on polymers with different fillers such as graphene, carbon nanotubes, carbon black are promising functional materials for different areas of modern science and technology [1]. One of promising methods of sample preparation of such composites is latex technology [2-5]. In this work several different composites of polystyrene (PS), epoxy resin and graphene (Gr), carbon nanotubes (CNT) and carbon black (CB) were investigated by combination of Atomic Force Microscopy (AFM) and ultramicrotomy [6]. Previously, the volume structure in form of clusters with similar level of conductivity was observed by conductive-AFM (C-AFM) in PS-CNT composite [3]. The 3D reconstruction of single cluster of Gr was carried out in [4]. Here, we report on similar results for PS-Gr and epoxy-CB composites (Fig. 1a). Graphene clusters with different current level were observed on relatively large scale of few micrometers. Similar to PS-CNT results [3], formation of domains with different current level might be explained by connection of neighboring graphene clusters by places with high resistivity. As a result conductivity of whole cluster is determined by such places with high resistance ("bottle neck"). The results of 3D reconstruction of PS-Gr are shown in Figure 1b (9 slices with 180 nm z-step were used). Clusters with different current level are clearly seen in current distribution images. Similar result was observed for epoxy-CB composite. However, highly resistive places between clusters in volume of graphene composite were not detected due to large size of clusters. We found such places in epoxy-CB composite (Fig. 2), where particles and domains are smaller. In Figure 2 transition from one cluster to another one is seen. The obtained results clearly confirm domain organization of conductivity in volume of all measured composites: PS-Gr, PS-CNT, epoxy-CB. All abovementioned volume reconstructions were performed by using C-AFM. However, other AFM techniques can be used for 3D reconstruction of local electrical properties as well. The use of Electrostatic Force Microscopy (EFM) for 3D reconstruction of PS-Gr structure is shown in Figure 3. The EFM contrast is the result of Coulomb interaction between charged Gr flakes and AFM probe. The local I-V curves measured on single particles on surface of all samples show linear and nonlinear behavior, which is the result of coexistence of ohmic and tunneling currents in sample volume.

(a) 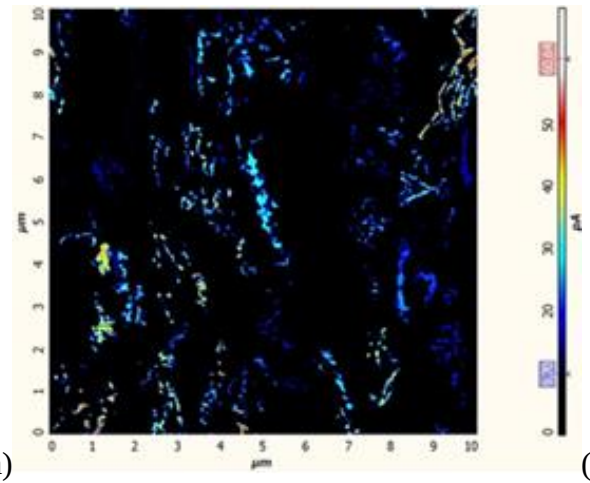 (b) 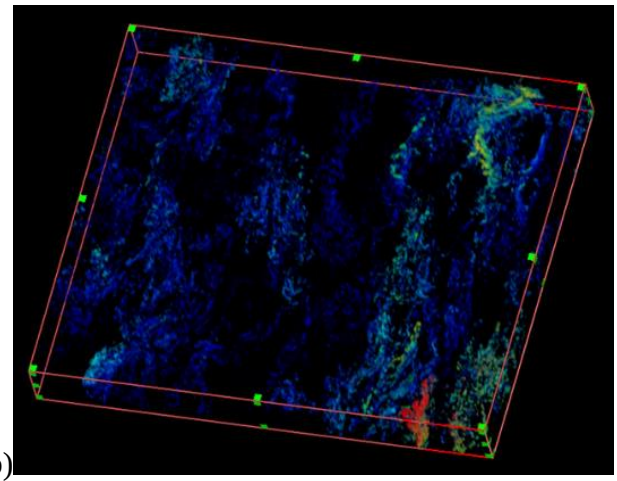

Figure 1. Current distribution images of PS-Gr composite: (a) conductive-AFM image; (b) volume 15.7x13.6x1.4 micrometers, z-step 180 nm, 9 slices.

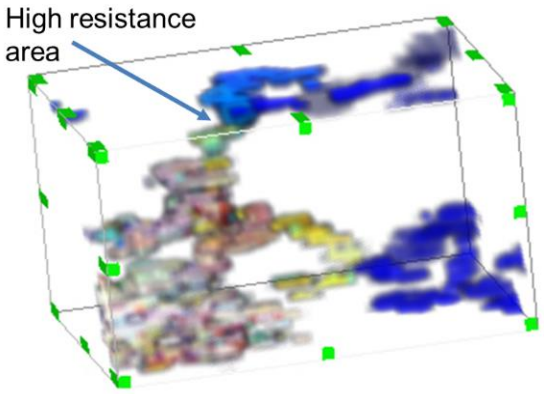

Figure 2. Epoxy-CB composite. The arrow indicates area with high resistance, which determines conductivity of neighboring domain. 28 scans, z-step is 20 nm.

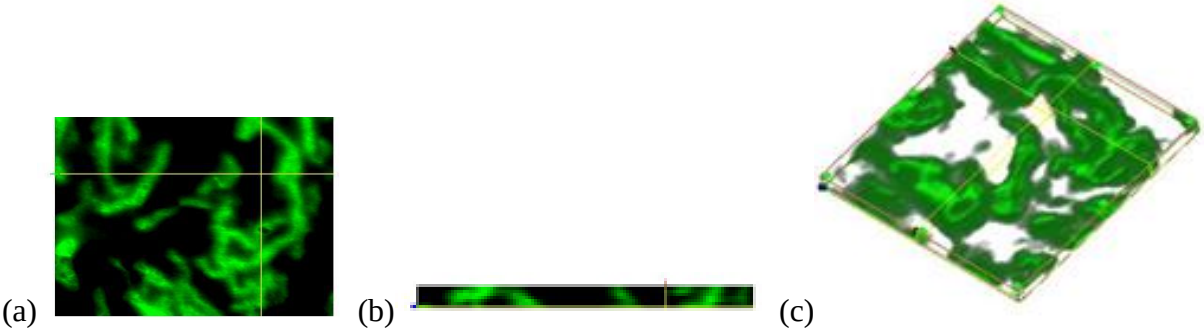

Figure 3. 3D reconstruction of PS-Gr composite by using EFM: (a) EFM image, (b), (c) cross-section and 3D reconstruction of volume structure based on 8 slices.

Authors thank Prof. B. de With, T. Wu, E. Tkalya, M. Ghislandi (Eindhoven University of Technology) for providing the samples. This work was supported by Federal Target Program of MES of Russian Federation (contract 14.575.21.0149, RFMEFI57517X0149).

1. W. Zhang, A.A. Dehghani-Sanij, R.S. Blackburn, *Journal of Materials Science* **42**, 3408 (2007).
2. E. Tkalya, M. Ghislandi, A. Alekseev, et al., *Journal of Materials Chemistry* **20**, 3035 (2010).
3. A. Alekseev, A. Efimov, K. Lu, et al., *Advanced Materials* **21**, 4915 (2009).
4. A. Alekseev, D. Chen, E.E. Tkalya, et al., *Advanced Functional Materials* **22**, 1311 (2012).
5. M. Ghislandi, E. Tkalya, A. Alekseev, et al., *Applied Materials Today* **1**, 88 (2015).
6. A. Alekseev, A. Efimov, J. Loos, et al., *European Polymer Journal* **55**, 245 (2014).

P-11

Modeling of titanium oxide nanostructures formation process by local anodic oxidation

O.G. Karen'kih, V.I. Avilov, V.A. Smirnov, N.A. Sharapov, N.A. Polupanov

Southern Federal University, Institute of Nanotechnologies, Electronics and Equipment Engineering, 344006 Taganrog, Russia
e-mail: AvilovVI@sfedu.ru

The development of components of modern electronics, in particular memristor structures for resistive memory (RRAM) elements, requires the application of new methods for the formation of nanoscale structures that possess precise precision and high reproducibility. One of such methods is the method of local anodic oxidation (LAO) allowing to form titanium oxide nanostructures (ONS) that exhibit a memristor effect without carrying out an additional electroforming operation [1-2]. However, the LAO process is still insufficiently studied, so the actual task is the development of a mathematical model that allows to calculate the geometric dimensions of the titanium ONS on the formation process.

Since the LAO process is associated with the generation and transfer of oxygen ions in the probe-air-oxide-substrate system and subsequent oxidation of the substrate, it is necessary to calculate the oxygen ion flux at each point of the substrate surface, for this it is necessary to solve the system of Poisson and continuity equations:

$$\begin{cases} \nabla(\varepsilon\nabla\varphi) = -\rho(N), \\ \nabla(-\mu N\nabla\varphi + D\nabla N) = R(\varphi). \end{cases} \quad (1)$$

where ε is the dielectric constant, φ and N are the distribution of the electric potential and the concentration of oxygen ions in the system, ρ is the volume density of electrical charges, μ and D are the mobility and diffusion coefficient of oxygen ions, R is the generation rate of oxygen ions in air. As a result of the solution of this system of equations, it is possible to calculate the profile of the titanium ONS at each point of the surface throughout the entire LAO process (Fig. 1).

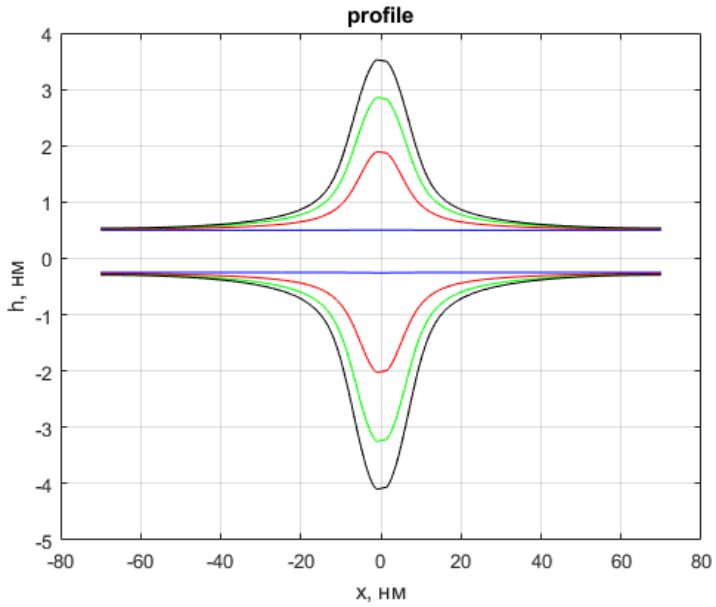

Figure 1. Titanium ONS profile on the various stages of the LAO.

The obtained results can be used in the development of technological processes for the fabrication of the RRAM element base based on titanium oxide nanostructures.

This work was supported by Grant of the President of the Russian Federation No. MK-2721.2018.8. and by RFBR according to the research project № 18-37-00299.

1. V.I. Avilov, O.A. Ageev, A.S. Kolomiitsev, et al., *Semiconductors* **48**, 1757 (2014).
2. V.I. Avilov, V.A. Smirnov, et al., *Materials Science and Engineering* **256**, 5 (2017).

P-12

Properties of KNN ceramics of different phase composition

E.V. Barabanova, O.V. Malyshkina, G. Shishkov, E. Tsamtsurov

Tver State University, 170100, Tver, Russia
e-mail: pechenkin_kat@mail.ru

In this paper we studied the structure and properties of sodium-potassium niobate ceramics (KNN). It was produced using two different technologies. As a result ceramics has a different phase composition.

The raw materials for the synthesis were potassium and sodium carbonates and niobium pentoxide. KNN ceramics were synthesized by the conventional solid state reaction method. In the first case, all three raw components were mixed in specified proportions. In the second case, sodium and potassium niobates were synthesized first. Then KNN ceramics were prepared by mixing $NaNbO_3$ and $KNbO_3$. According to X-ray phase analysis in the first case, the main phase is $K_{0.3}Na_{0.7}NbO_3$, in the second – $K_{0.44}Na_{0.56}NbO_3$.

The ceramics structure was studied by the method of atomic force microscopy (AFM). The ceramics produced by the first method has a grain size larger (2 – 4 μm), than the ceramics produced by the second method (500 nm – 2 μm). Accordingly, the size of domains is also different. The size of domains decreases with decreasing grain size. Despite the fact that the ceramics have a different phase composition, their symmetry (orthorhombic) at room temperature, according to the phase diagram [1], is the same. Thus, the types of the domain structure also coincide (Fig.1). This is a periodic strip domain structure.

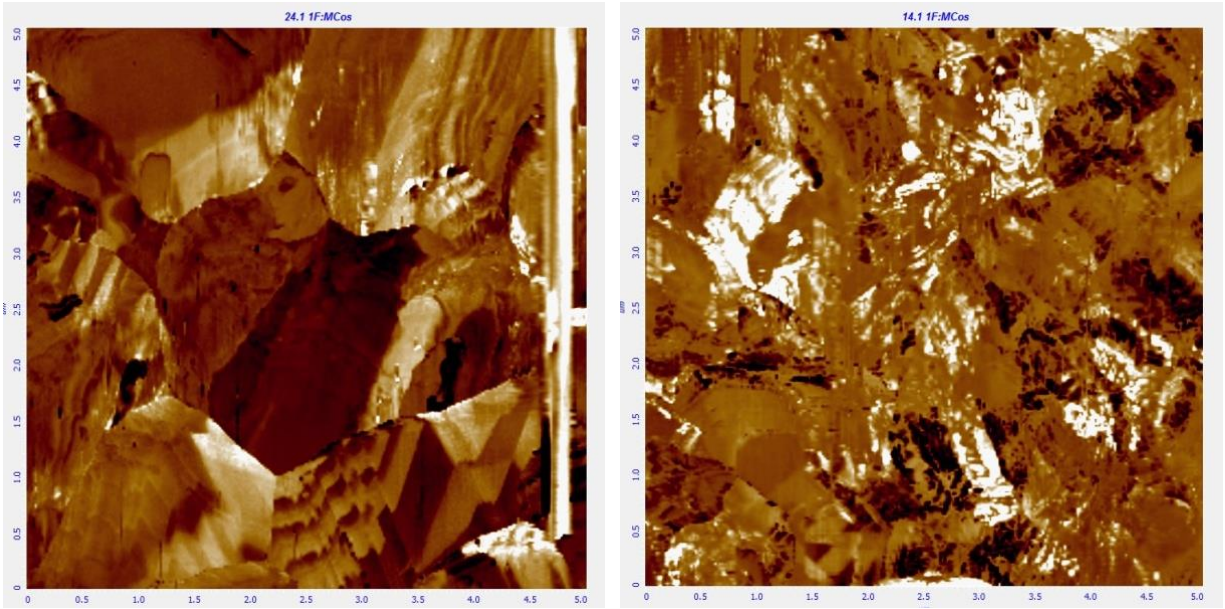

Figure 1. PFM response of ceramics (a) $K_{0.3}Na_{0.7}NbO_3$ and (b) $K_{0.44}Na_{0.56}NbO_3$.

Despite this, the macroscopic properties of these materials, such as the polarization switching, the width of the diffuse phase transition and pyroelectric response, are different. Therefore, the local ferroelectric properties of ceramics were studied using AFM: the properties of domain walls, local polarization switching.

This work was supported by the Ministry of Education and Science of the Russian Federation and performed at the Collective Usage Center of the Tver State University.

1. M. Ahtee, A.M. Glazer, *Acta Cryst. Sec. A: Found.of Cryst*. **32**, 434 (1976).

P-13

Surface topography of the InSb-MnSb thin films

S.M. Baraishuk[1], A.I. Turovets[2], T.M. Tkachenko[1], R.N. Rahimov[3], I.Kh. Mamedov[3], D.G. Arrasly[3], A.A. Khalilova[3]

[1]*Belarus State Agrarian Technical University, 220053, Minsk, Belarus*
e-mail: bear_s@rambler.ru

[2]*Belorussian State Pedagogical University named after Maxim Tank, Minsk, 220050, Minsk, Belarus*

[3]*Institute of Physics of NAS of Azerbaijan, AZ1141, Baku, Azerbaijan*

In that report we observe a semiconductor eutectic composite InSb-MnSb thin films, prepared by the "flash evaporation" method. The atomic force microscopy and the scanning electron microscopy were employed for investigation microstructure and surface relief of the InSb-MnSb thin films.

Eutectic composites based on compounds of groups III-V with 3d-transition metals consisting of a semiconductor matrix and metallic inclusions are of interest because of the preservation of the microstructure at the melting point, the repeatability and stability of the characteristics.Their behavior is similar to inhomogeneous and degenerate semiconductors, and physical properties depend on the electronic configuration of the 3d elements, the geometry of the inclusions and the features of the formation of interphase zones. The presence of ferromagnetic metallic inclusions makes them promising for creating injectors of spin-polarized electrons.

In this paper presented, the results of studying the topography of the surface thin films of InSb-MnSb are presented. The microstructure and physical properties of an eutectic composite based on InSb and GaSb have been previously studied [1-2].

Thin films of the InSb-MnSb eutectic composite were obtained by the method of "flash evaporation", the thickness of which was 0.4-1.0 μm. The films were studied by electronic scanning microskopy (Oxford Instruments) and atomic force microscopy (microtest machines NT-206, tips Mikromasch CSC 38) in contact mode. To evaluate the surface, at least 5 scanning sites were selected from different sections of the surface with a size of 20×20 μm^2 and 5×5 μm^2, which allowed averaging the parameters of the relief. The processing of the obtained data was carried out with the help of the program "SurfaceXplorer" according to the technique described in [3].

AFM studies have shown that the typical surface of thin films of the InSb-MnSb eutectic composite has a complex microrelief. When the size of the scanning regions is 20×20 μm^2 (Fig. 1a), evenly distributed structural formations of a round shape with a diameter of 0.5-2 μm with an average height of 0.8-0.9 μm are observed on the surface, as seen from the section profile (Fig. 1b). Between these formations there are structural objects of a much smaller size.

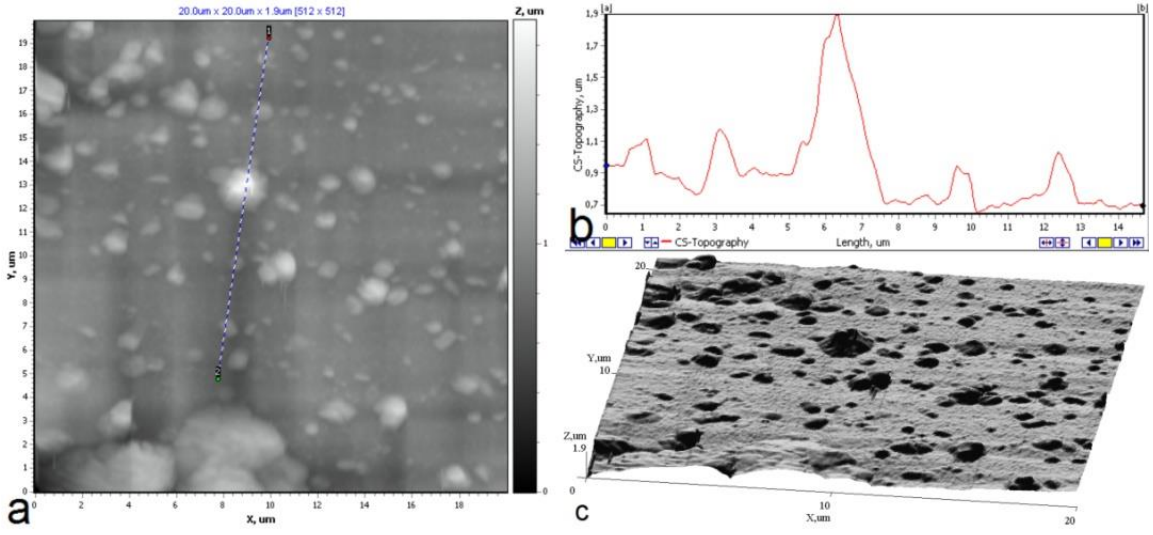

Figure 1. Surface topography (a), section profile along the 1-2 (b) line, 3-dimensional reconstruction of the InSb-MnSb film surface (c).

The average arithmetic roughness of the surface, averaged over 5 values, with this site selection is Ra = 78.3 nm, the rms roughness Rq = 103.3 nm. The ratio of the total surface area to the projective area is 1.14. The distribution of heights for these sites is shown in Figure 1b, and an analysis of the orientation of the surface structures is also given, which allows one to assert that there is no expressed orientation. In addition, in the lower left corner of the presented AFM image, it is possible to notice rounded structures measuring 8-12 μm across, which agrees well with the SEM image.

Based on AFM images, the multifractal dimension of the surface was calculated by the horizontal section method (area perimeter). In calculating the fractal dimension, the systematic deviation characteristic of the method of horizontal cross sections was taken into account [4]. An analysis of the fractality of the investigated sites with 500 sublayers gives an average value of fractal dimension 2.79

In addition, a study was made of the intergrain space at a higher resolution of scanning, as well as areas containing anomalous topographic structures for these surfaces. In particular, when the size of the scanning region is 5×5 μm^2, the AFM images obtained are in good agreement with the SEM data shown in Figure 2. In the regions between the large structures, in both cases a fine-grained structure is clearly visible. In addition to the above features of topography on the surface, the presence of ordered long oblong structures 1.2-1.4 μm in length with a width of ~ 0.1 with a height of 0.15-0.2 μm was observed. The appearance of these structures can be either a feature of the flow of some processes during the application of coatings or a defect in the surface treatment before application.

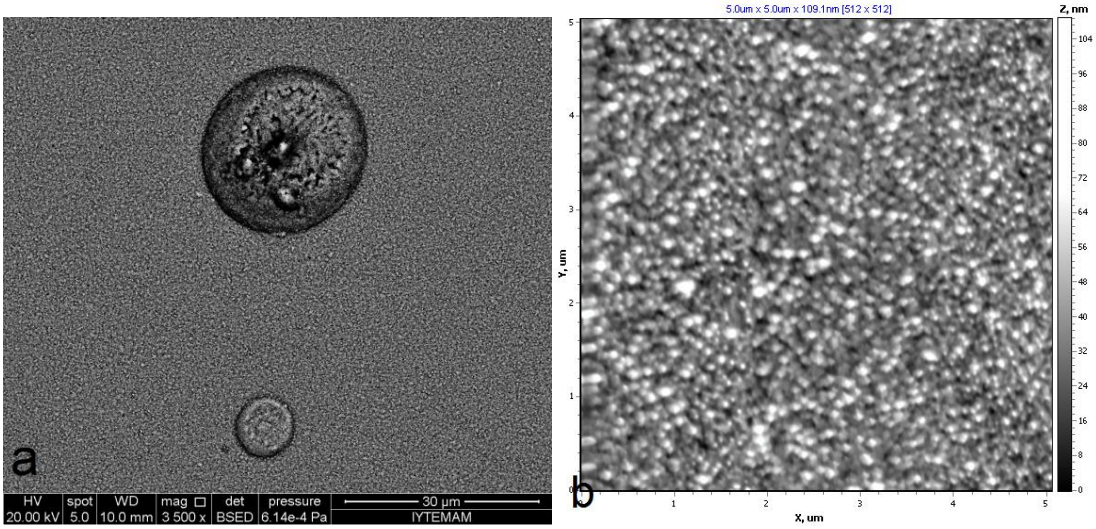

Figure 2. The microstructure of the InSb-MnSb thin film (3500 magnification) and the InSb-MnSb surface topography when scanning on a 5×5 μm^2 site.

These regions are characterized by the absence of any significant structures, but a fine-grained structure with a predominant height of ~ 30 nm is observed. Grains of irregular shape with a size of 40-80 nm in diameter also do not have a pronounced orientation. This leads to a decrease in the mean arithmetic and rms roughness values to Ra = 9.4 nm and Rq = 12.2 nm, respectively. In this case, the average value of the fractal dimension of the sites studied increases somewhat in comparison with the main relief and reaches 2.82, which indicates a developed "bulk" surface. This confirms the high surface quality and sufficiently high uniformity of the coating application.

1. I.Kh. Mamedov, D.G. Arasly, A.A. Khalilova, R.N. Rahimov, *Inorganic Materials* **52**, 423 (2016).
2. M.I. Aliyev, A.A. Khalilova, D.H. Arasly, R.N. Rahimov, M. Tanoglu, L. Ozyuzer, *J. Phys. D: Appl. Phys.* **36**, 2627 (2003).
3. I.S. Tashlykov, S.M. Baraishuk, *Russian Journal of Non-Ferrous Metals* **49**, 303 (2008).
4. W. Zahn, A. Zösch, *Fresenius J. Analen. Chem.* **365**, 168 (1999).

P-14

Surface topography of precursors Cu-Zn-Sn electrochemically deposited on Mo/glass and Mo-foil

A.I. Turavets[1], S.M. Baraishuk[2], T.M. Tkachenka[2], M. Wiertel[3], M. Budzynski[3] A.V. Stanchik[1], V.F. Gremenok[1], S.A. Bashkirov[1]

[1]*State Scientific and Production Association «Scientific-Practical Materials Research Centre of the National Academy of Sciences of Belarus», 220072, Minsk, Belarus*
e-mail: bear_s@rambler.ru

[2]*Belarusian State Agrarian Technical University, 220053, Minsk, Belarus*
[3]*Institute of Physics, University n.a. M. Curie-Sklodowska, 20-031, Lublin, Poland*

The paper discusses the possibility of constructing thin-film solar cells based on non-toxic and abundant $Cu_2ZnSnSe_4$ components (CZTSe) obtained by electrochemical deposition on Ta-foil substrates with subsequent selenization. Foil substrates open up new possibilities for application of flexible thin-film solar cells. Atomic force microscopy and scanning electron microscopy combined with energy dispersive spectrometry of secondary electrons were employed for the investigation of thin films topography.

Introduction: The semiconductor compound $Cu_2ZnSnSe_4$ (CZTSe) is a promising material for thin-film solar cells. Unlike the widely studied materials $CuIn_{1-x}Ga_xSe_2$ (CIGS) and CdTe, all CZTSe components are cheap and do not contain toxic cadmium [1-3]. The maximum achievable photoelectric conversion efficiency of solar cells on their basis is ~ 30% [4]. Studies on increasing the efficiency of photoconverters have shown that the surface of films and the morphology of interfaces characterized by roughness play an important role in improving the absorption of incident light onto the semiconductor layer by reducing reflection losses. A significant increase in the conversion efficiency by introducing the corresponding rough interfaces was reported in several papers [5,6].

Unlike glass substrates, metal foils have a coarser surface, which strongly affects the growth, crystal orientation, and other properties of subsequent layers. The rough surface of the layers in the solar cell directly affects its efficiency [7].

Results and discussion: AFM studies have shown (Fig. 1) that the surface of CZT precursors deposited on metal substrates has a similar microrelief and is different from the Mo/glass observed on the substrate [8,9].

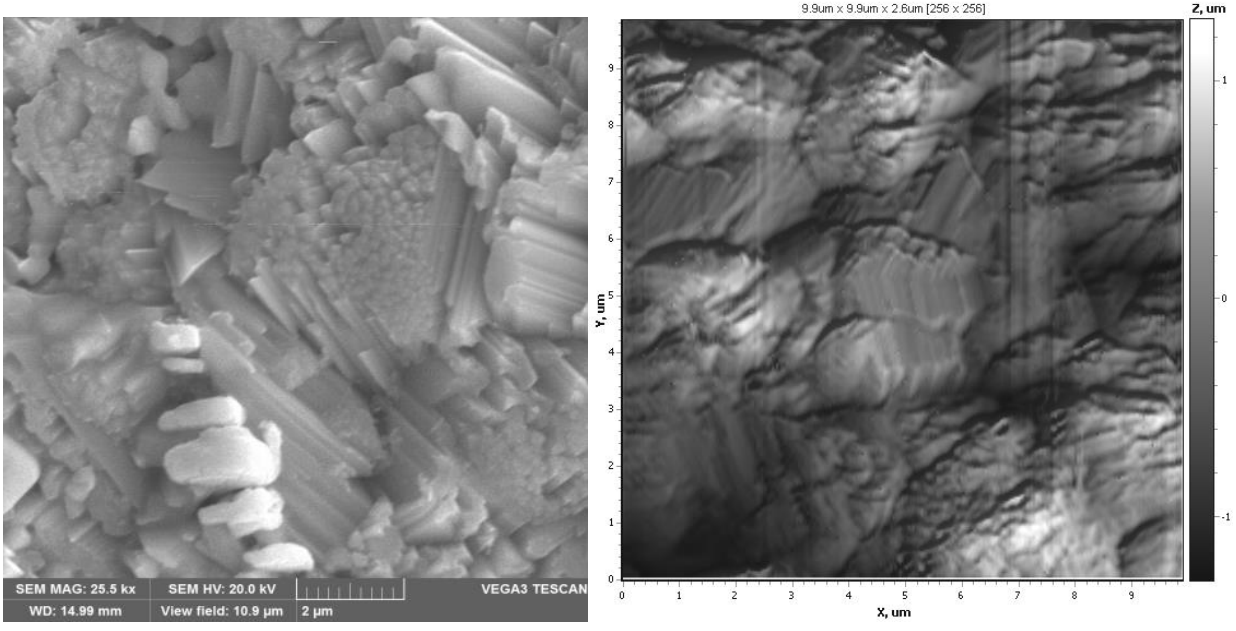

(a) (b)

Figure 1. (a) SEM and (b) AFM images of the surface of Cu-Zn-Sn precursors on Ta-foil substrates.

The presence on the surface of CZTSe-produced coatings of complex micro-dimensional structures deposited on Ta-foils is confirmed by electron microscopy (Fig. 1a).

The surface of CZT precursors deposited on metal substrates is characterized by a complex structure (Fig. 1). When deposited on Ta-foil, a layered structure is observed on the surface, the thickness of the layers is 50-100 nm, the length of clusters formed is 2-4 μm, the transverse dimensions vary from 250 to 1000 nm in diameter, the layers have a common orientation within one cluster. Also, associations of layers in larger structures are observed, with the formation of depressions larger than in the case of previously studied Mo-foil materials. The resulting SEM images also confirm the formation of layered formations on the surface of CZT precursors on foil substrates. (Fig. 1a).

The "illumination" of the surface ends of layered structures on images obtained with the help of electron scanning microscopy may indicate the presence of metallic materials on the surface. In CZTSe films enriched in zinc, according to [10, 11], $Cu_2ZnSnSe_4$ crystals grow large and form a compact layer, leaving an excess of zinc on the surface and, as a result, lead to the formation of fine crystallites of Zinc selenide, which agrees well with the obtained AFM data for films CZTSe. The parameters of the topography of the original samples and samples after coating are presented in Table 1.

Table 1. parameters of the topography of the test samples.

Parameters	R_a, **нм**	R_q, **нм**
Substrate	68.66	88.48
Precipitated precursor CZT	225.48	282.81
Pre-annealed precursor CZT	31.60	40.50
CZTSe film	187.03	244.43

The roughness of the surfaces of precursor films deposited on substrates has a slight difference with a significant difference in the roughness of the substrates. The coating on the foil substrates, in comparison with the glass substrate with a sublayer of molybdenum, contributed to the elimination of defects in the form of scratches. Obviously, the roughness of the metal substrates exerts an insignificant influence on the parameters of the roughness of the coatings obtained, which agrees with the work [12, 13], which makes it possible to use them for thin-film photoconverters.

1. M.P. Paranthaman, W. Wong-Ng, R.N. Bhattacharya, *Springer Internat. Publishing*, 2016.
2. M.A. Green, K. Emery, Y. Hishikawa et al., *Prog. Photovolt: Res. Appl*. **24** (2016).
3. P.D. Moskowitz, V.M. Fthenakis, *Solar Cells* **29** (1990).
4. W. Shockley, H.J. Queisser, *J. Appl. Phys*. **32**, 510 (1961).
5. N. Sahraei, S. Venkataraj, A.G. Aberle, et al., *Energy Procedia* **33**, 166 (2013).
6. J. Krcˇ, M. Zeman, O. Kluth, et al., *Material Research Society Symposium Proceedings* **715**, A13.3.1 (2002).
7. F. Kessler, D. Rudmann, *Solar Energy* **77**, 685 (2004).
8. A.I. Turovets, S.M. Baraishuk, A.V. Stanchik, et al., *SPM-2017. Abstract Book of International Conference* (2017).
9. A.V. Stanchik, S.M. Baraishuk, S.A. Bashkirov, et al., *Proceedings of the NAS of Belarus. Series of physical and mathematical sciences* **4** (2016).
10. R. Kondrotas, A. Juskenas, A. Naujokaitis, et al., *Solar Energy Materials & Solar Cells* **132**, 21 (2015).
11. A. Redinger, K. Hönes, et al., *Appl. Phys. Lett.* **98**, 101907 (2011).
12. I.S. Tashlykov, S.M. Baraishuk, *Russian Journal of Non-Ferrous Metals* **49**, 303 (2008).
13. I. Tashlykov, S. Baraishuk, et al., *Przeglad Elektrotechniczny* **3** (2008).

P-15

Study of the surface microrelief of copper nanoparticles by the method of scanning probe microscopy

N.N. Begletsova[1,2], M.V. Gavrikov[1], A.S. Chumakov[1,2], E.I. Selifonova[2], R.K. Chernova[2,3], V.V. Oliskevich[4], E.G. Glukhovskoy[1,2]

[1]*Department of Nano- and Biomedical Technologies, Saratov State University, 410012, Saratov, Russia*

[2]*Education and Research Institute of Nanostructures and Biosystems, Saratov State University, 410012, Saratov, Russia*
e-mail: nadya-beg98@yandex.ru

[3]*Institute of chemistry, Saratov State University, 410012, Saratov, Russia*

[4]*Scientific Research Institute of Technology of Organic, Inorganic Chemistry and Biotechnology, 410005, Saratov, Russia*

Studies of the microrelief (morphology and surface roughness) of the copper nanoparticles, heat treated glass substrates coated with ITO layer was carried out using scanning probe microscopy mode atomic force microscopy. The investigated samples are characterized by the presence of an uneven surface consisting of spherical copper particles with dimensions in the range from 30 to 110 nm in the organic matrix of the surfactant.

At present, copper nanoparticles (copper NPs) are one of the promising materials for the creation of functional films with high electrical conductivity for devices of micro- and nanoelectronics [1]. Methods of obtaining such particles are given much attention [2,3] as comparison with the study of their surface microrelief. Such a parameter as the surface roughness affects the quality and performance of the various instruments and devices. Therefore, depending on the further functional purpose of the film with copper NPs, it must meet certain requirements. For example, when obtaining high-conductivity films, the conditions for their sputtering or self-assembly must be selected in such a way that the surface roughness is minimal and uniform throughout the sample. This is necessary to reduce the losses associated with the scattering of charge carriers at the inhomogeneities, film defects, etc. When creating coatings of parts operating under conditions of constant friction, the roughness should be of the order of several micrometers.

The morphology and surface roughness of copper NPs on glass substrates with an ITO layer (Indium Tin Oxide) were studied by scanning probe microscopy (AFM) in atomic force microscopy (AFM) modes using the Nanoeducator II (NT-MDT, Russia). AFM images of the surface of copper NPs film (top view) and its profile (Fig.1a and b, respectively) were obtained. The processing of AFM images was carried out using the Gwyddion program. The synthesis of copper NPs was carried out by chemical reduction in an aqueous solution of an anionic type surfactant — sodium dodecyl sulfonate (SDS) ($C_{12}H_{25}SO_4Na$), according to the previously developed procedure [4]. The acidity of the medium was pH = 11.2 at molar ratio of the precursor ($CuCl_2 \cdot 2H_2O$) and the reductant (hydrazine) equal 1:150. Before applying of the solution with copper NPs to solid substrates resulting suspension sample preparation was carried out by centrifugation and decantation of the solution to remove excess surfactant. After the centrifuged solution was taken from the bottom of a micro test-tube eppendorf type and applied to a substrate. Then it was heated for 5 minutes at 100 °C.

The obtained AFM images of the surface microrelief of the sample show the presence on the substrate of glass with ITO layer spherical copper particles. The particles coated with a surfactant have a size in the range from 30 to 110 nm. From Figure 1a it can be seen that the copper particles are uniformly distributed over the surface of the substrate. The change in color contrast of the surface and the extracted profile of the surface of the test sample (Fig. 1b) indicate the presence of defects in the resulting film. They are visualized in the form of depressions and protrusions of various depths, heights and widths. The profile of the surface roughness along lines 1 and 2 extracted along of the investigated sample shows that in regions 1 and 2 the average maximum roughness height is 46 nm and 28 nm. The average maximum depth of the roughness cavity is 51 nm and 22 nm, respectively. A significant difference in the obtained results along lines 1 and 2

may be due to the effect of thermal treatment of the substrate on the distribution of the suspension with copper NPs on its surface and with aggregation of particles.

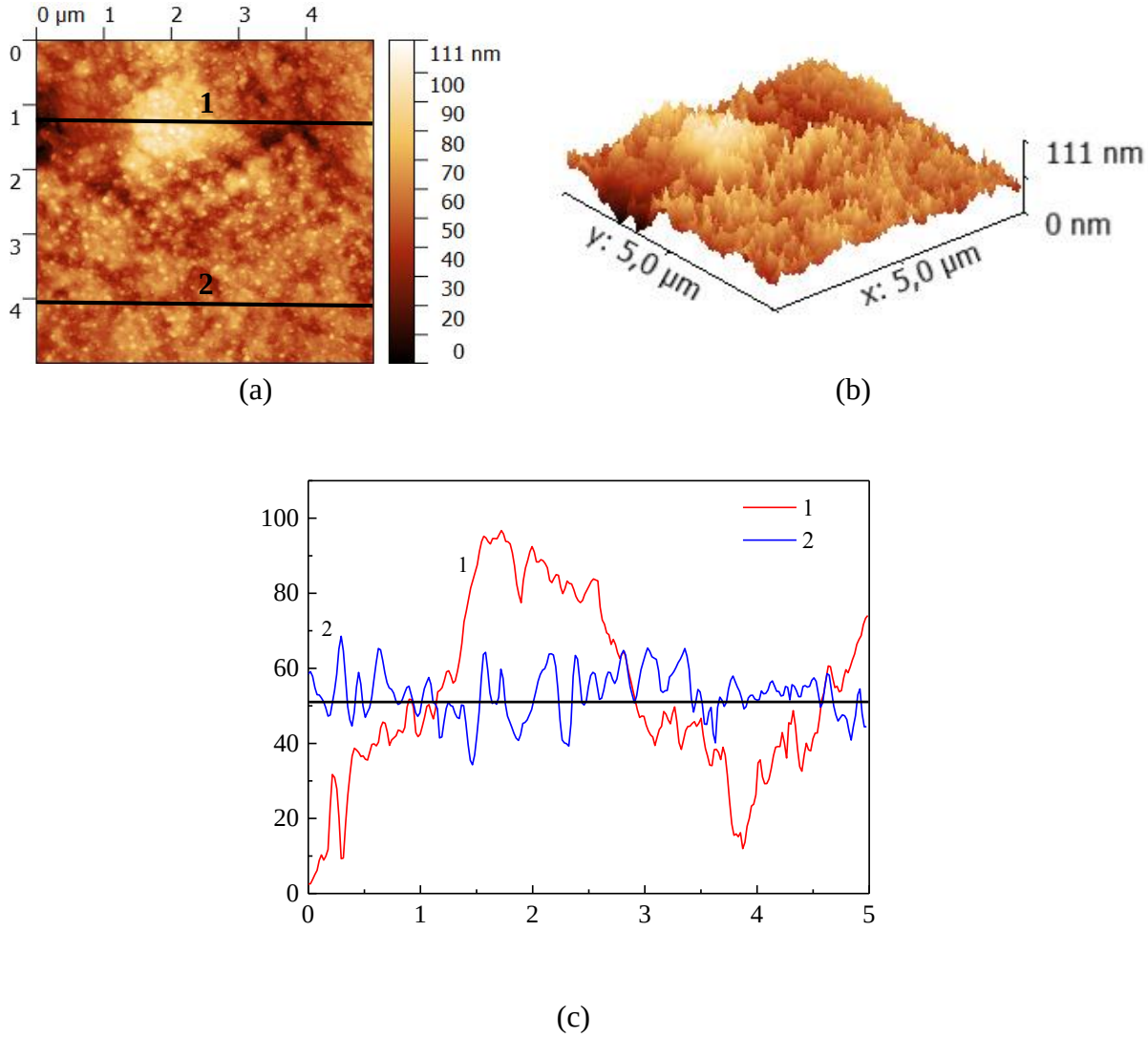

Figure 1. AFM images: (a) morphology (top view) and (b) surface profile (side view), (c) surface roughness of copper nanoparticles on a glass substrate with ITO layer (1, 2 – surface roughness areas of the sample).

Thus, it is shown that when the substrate with copper nanoparticles is thermally treated, an uneven surface microrelief can be formed with differences of the mean maximum height and roughness depth in the ranges from 28 to 46 nm and 22 to 51 nm, respectively.

This work was supported by grants from the RFBR № 17-07-00407-a and № 17-32-50137-mol_nr.

1. A. Yabuki, N. Arriffin, *Thin Solid Films* **518**, 7033 (2010).
2. N.N. Begletsova, O.A. Shinkarenko, A.S. Chumakov, et al., *IOP Conf. Series: Journal of Physics: Conf. Series* **917**, 092014 (2017).
3. N.N. Begletsova, O.A. Shinkarenko, E.I. Selifonova, et al., *Advanced Materials Letters* **8**, 404 (2017).
4. N.N. Begletsova, A.S. Chumakov, O.A. Shinkarenko et al., *4th International School and Conference on Optoelectronics, Photonics, Engineering and Nanostructures «Saint Petersburg OPEN 2017»* (St.Petersburg Academic University), 609 (2017).

P-16

Electron-beam and AFM domain writing in the relaxor ferroelectric SBN

Ya.V. Bodnarchuk[1], T.R. Volk[1], L.S. Kochanchik[2], R.V. Gainutdinov[1], L.I. Ivleva[3]

[1]*Shubnikov Institute of Crystallography of Federal Scientific Research Centre "Crystallography and Photonics" of Russian Academy of Sciences, Moscow 119333, Russia*

e-mail: deuten@mail.ru

[2]*Institute of Microelectronics Technology and High Purity Materials, Russian Academy of Science, Moscow 142432, Russia*

[3]*Prokhorov Institute for General Physics of the Russian Academy of Science, 119991, Moscow, Russia*

The fabrication of ferroelectric domain patterns of a specified configuration belongs to practically important problems of ferroelectricity owing to the potential of these structures for various applications. Writing by electron-beam (EB) irradiation in SEM and by dc-voltages of an AFM-tip provides a possibility to fabricate domain patterns with small spatial periods up to submicron scale. We present the results of domain patterning by these techniques in uniaxial relaxor ferroelectric $Sr_xBa_{1-x}Nb_2O_6$ (SBN). These results provide a deeper insight into the mechanism of domain formation under these conditions, in particular in relaxor ferroelectrics.

Single domains and specified 1D and 2D domain patterns were written on the polar and non-polar crystal surfaces in field-cooled (FC) and zero-field-cooled (ZFC) samples.

The characteristics of domain formation and relaxation were investigated. A specificity of domain writing in SBN is accounted for by the relaxor origin of this material.

Figures 1-3 present the results of domain writing on the nonpolar (X-) crystal surface The formation of counter-propagating (head-to-head or tail-to-tail) domains in ZFC crystals was observed (the inset in Fig. 3) both under electron-beam irradiation and AFM-tip voltages.

An enhanced stability of these patterns as compared with ones written in FC crystals was found. In particular, EB-written domains in ZFC SBN are completely stable (Fig. 3, the upper line) and can be erased only by thermal annealing at T > Tc.

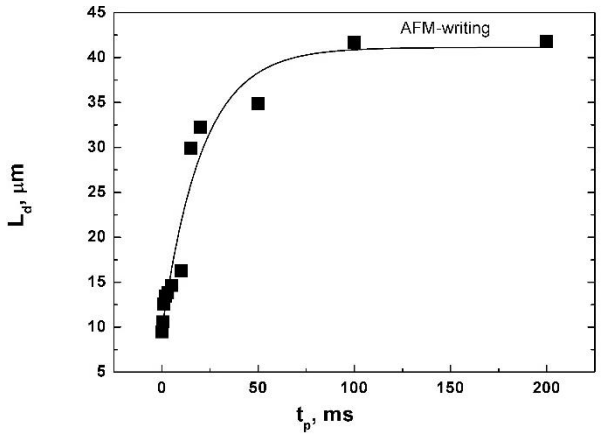

Figure 1. Domain length vs. pulse duration of the AFM-tip voltage (UDC = 40 V).

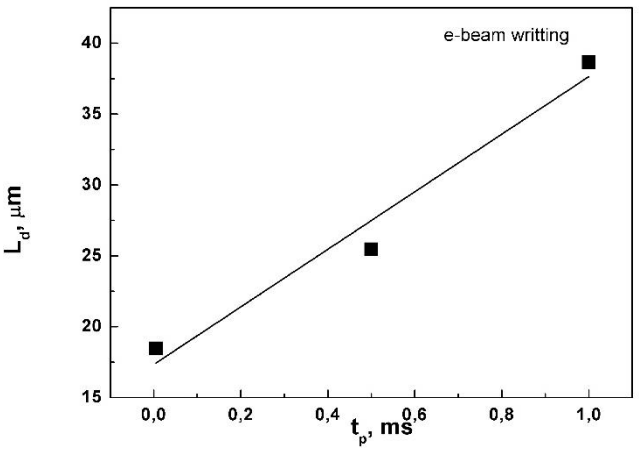

Figure 2. Domain length vs. EB irradiation time (accelerating voltage U = 25 kV, EB current I = 10 nA).

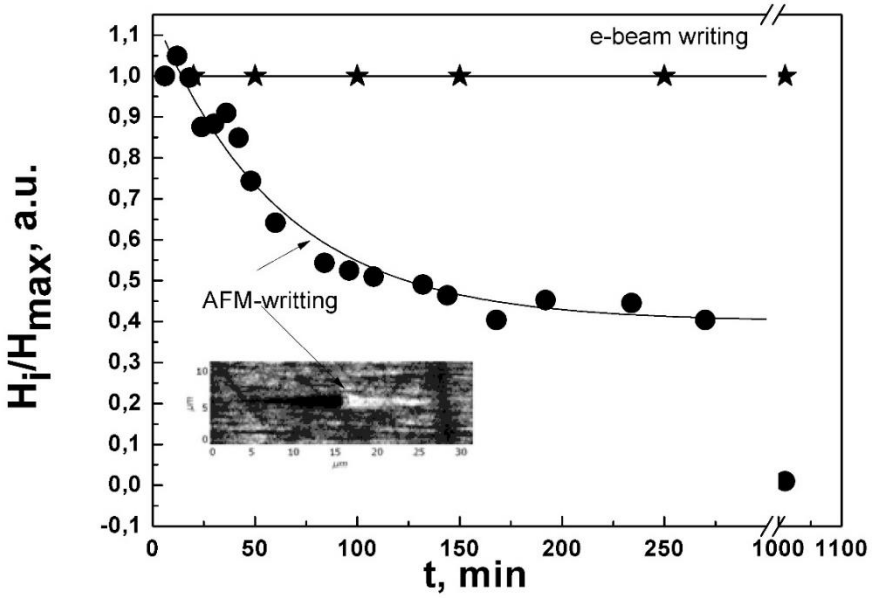

Figure 3. The lower graph presents the relaxation of AFM-written domains; the solid curve shows approximation by y=A*exp(-x/τ)+y0. The upper line demonstrates the stability of EB –written domains.

This work was supported by the Russian Foundation for Basic Researches (projects Nos. 16-29-11777ofi-m and 16-0200439a).

1. N.A. Pertsev, R.V. Gainutdinov, Ya.V. Bodnarchuk, et al., *JAP* **17**, 034101 (2015).
2. T.R. Volk, L.S. Kokhanchik, Ya.V. Bodnarchuk, et al., *JAP*, in press (2018).

P-17

Local anodic oxidation of graphene layers on SiC

B.R. Borodin, M.S. Dunaevskiy, P.A. Alekseev

Ioffe Institute, 194021, St. Petersburg, Russia
e-mail: brborodin@gmail.com

Graphene is a promising material for the creation of electronic and optoelectronic devices of a new generation. To be cost-effective, large-sized layers of high-quality homogeneous graphene are required. High-quality epitaxial graphene can be grown by thermal destruction of a semi-insulating monocrystalline silicon carbide substrate (SiC) [1]. Most lithographic techniques involve the application and removal of resist from the surface of graphene, that reduce the mobility of charge carriers [2]. An alternative method of lithography, excluding the use of resist, is the local anodic oxidation (LAO) [3]. In this method, an electrical voltage between the probe of the atomic force microscope (AFM) and the graphene with water film on the surface leads to the local oxidation of the graphene.

The aim of our work was to perform the LAO of a graphene layers on SiC and to study electronic properties of the graphene and graphene oxide by Kelvin probe microscopy (KPM) and conductive AFM. The experiment was performed with a Ntegra Aura (NT-MDT) microscope using DCP (NT-MDT) and HA_FM / W2C (NT-MDT) conducting probes with a tip diameter of 100 nm and 20 nm, respectively. The sample was a monolayer graphene with a small fraction (~10%) of two-layered islands with submicron dimensions, obtained by thermal destruction in argon of the Si-face of the 6H-SiC substrate (0001) [1]. By the method of local anodic oxidation, graphene oxide regions were obtained. The KPM study showed that oxided region have a 350 mV higher surface potential than the graphene. The I-V curves measured by the C-AFM revealed the semiconducting character of the graphene oxide. In addition, it was studied the LAO regimes for the creation of the graphene nanoribbon and nanoconstriction with the minimal width. The detection of oxidized regions was performed by measuring the frictional force of the probe on the surface. In Figure 1 the maps of the distribution of the frictional force of a surface are presented. Light areas on the image correspond to oxidized graphene, dark areas to not oxidized. Figures show a graphene nanoribbon with a width of 20 nm (Fig. 1a) and a 10 nm wide nanoconstriction (Fig. 1b), which is comparable with the best results obtained on peeled graphene.

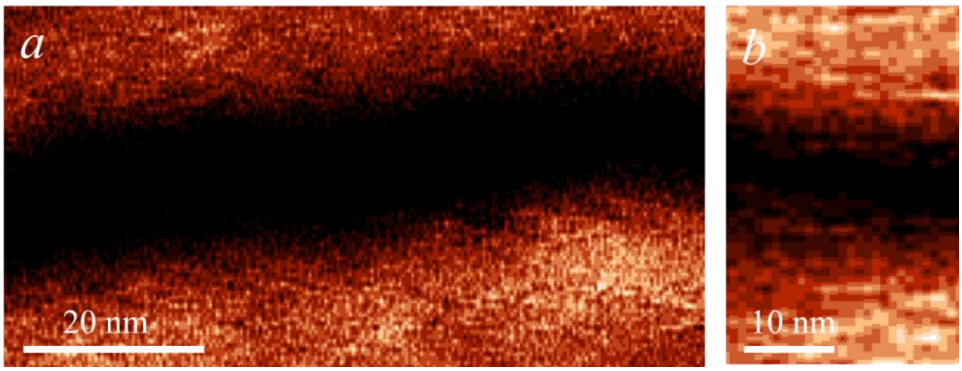

Figure 1. (a) Graphene nanoribbon and (b) graphene nanoconstriction (width ~ 10nm).

To conclude, electrical properties of the graphene oxide layers formed by the LAO were studied. The results of this work allow us to talk about the LAO of graphene on SiC, as a method of nanolithography with a resolution of 10 nm, which can be used to create devices based on thin layers of graphene.

This work is supported by Presidential Grant MK-5852.2018.2.

1. V.Y. Davydov, D.Y. Usachov, S.P. Lebedev, et al., *Semiconductors* **51**, 1072 (2017).
2. H. Song, S. Li, H. Miyazaki, et al., *Sci. Rep.* **2**, 337 (2012).
3. F. Colangelo, V. Piazza, C. Coletti, et al., *Nanotechnology* **28**, 105709 (2017).

P-18

Comparative analysis of Young's modulus measurements of grains of alloys 1013 and B-1461 by the SPM method

K.K. Chaplygin, S.V. Voronin

Samara University, Samara, Russia
e-mail: chapkostya96@mail.ru

The aim of the work was to carry out a comparative analysis of the series of measurements of Young's modulus of individual grains of samples of two alloys. This comparison was carried out to test the feasibility of applying the technique for determining the crystallographic orientation [1] on various aluminum alloys. The technique itself consists in determining the crystallographic orientation by the color of the grain in polarized light. The crystallographic orientation is determined indirectly through the Young's modulus, measured by the SPM method. Further, the relationship between the color of the grain and its Young's modulus is derived. The dependence of the crystallographic orientation on Young's modulus is described in [2].

The color of the grain depends on the thickness of the oxide film, formed after the preparation of the sample surface. On the surface of alloy 1013, blue, orange and yellow grains are observed. Under the same conditions for surface preparation of samples, the same colors as on the surface of alloy 1013 are observed on the surface of alloy B-1461. The images of the surfaces of alloys are shown in Figure 1.

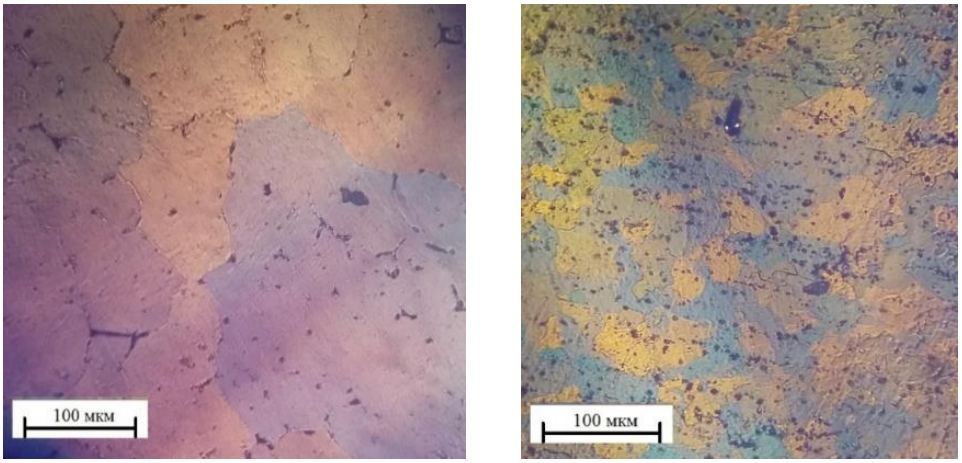

Figure 1. Images of the surfaces of alloys 1013 (left) and B-1461 (right) in polarized light.

When comparing the Young's modulus of the 1013 [1] and B-1461 [3] alloys, carried out with the same calibration of the instrument, it is established that for both alloys the blue grains have a minimum modulus of elasticity, the yellow grains have a maximum modulus of elasticity. Orange grains have intermediate values for both alloys. Also, the data obtained by experimental measurements coincide with the literature data on the Young's modulus, depending on the crystallographic direction for aluminum alloys.

The obtained result allows to draw a conclusion that the previously developed technique for the aluminum alloy 1013 is also applicable to the aluminum-lithium alloy B-1461.

1. Baraev D.I., Chaplygin K.K., sbornik tezisov dokladov Mezhdunarodnoj molodezhnoj nauchnoj konferencii «XLIII Gagarinskie chteniya», Moskva, MAI, 216 (2017)
2. P.G. Miklyaev, YA.B. Fridman, Anizotropiya mekhanicheskih svojstv metallov, M: Metallurgiya, 12 (1986).
3. Voronin S.V., Chaplygin K.K. V-1461, Sbornik materialov XV Vserossijskoj s mezhdunarodnym uchastiem shkoly – seminara po strukturnoj makrokinetike dlya molodyh uchenyh imeni akademika A.G. Merzhanova, 97 (2017)

P-19

Electron beam poling of $[001]_c$-poled PMN-39PT single crystal

D.S. Chezganov[1], E.O. Vlasov[1], L.V. Gimadeeva[1], E.D. Greshnyakov[1], P.S. Zelenovskiy[1], A.D. Ushakov[1], M.S. Nebogatikov[1], Q. Hu[2], X. Wei[2], V.Ya. Shur[1]

[1] *School of Natural Sciences and Mathematics, Ural Federal University, Ekaterinburg 620000, Russia e-mqil: chezganov.dmitry@urfu.ru*

[2] *Electronic Materials Research Laboratory, Key Laboratory of the Ministry of Education & International Center for Dielectric Research, Xi'an Jiaotong University, 710049 Xi'an, China*

The relaxor-based $Pb(Mn_{1/3}Nb_{2/3})O_3$-$PbTiO_3$ (PMN-PT) ferroelectric single crystal is very attractive material as a potential candidate for optical application due to its high values of electrooptic coefficients (r_{33} is 70 pm/V) [1]. The nonlinear-optical applications require methods of precise control of domain walls positions for precise periodical domain structures [2]. The electron beam (e-beam) poling was elaborated for domain patterning in uniaxial crystals such as lithium niobate (LN) and lithium tantalate with simple 180º-domain structure [3] and applied for multiaxial crystals BT [4], $BaMgF_4$ [5], and ceramics [6]. Recently, the modification of the method using surface covering by buffer artificial dielectric layer allow creation of fine periodically poled structure in bulk MgO-doped LN [7] and LN-based waveguides [8]. The second harmonic generation efficiency comparable with commercial elements was demonstrated.

In this work we have used e-beam patterning for creation of the domain structure in PMN-PT crystal covered by surface dielectric layer. The results explained in terms of kinetic approach [9].

The studied tetragonal PMN-PT single crystals were grown by modified Bridgman technique. The studied samples ($5\times8\times1$ mm^3) were cut normal to [001] direction with sides cuts parallel to (010) and (100) planes. The surface was covered by beam resist AZ nLof 2020 (MicroChemicals GmbH, Germany) deposited by Sawatec SM 180 spin coater. The opposite surface was sputtered by100-nm-thick Cu electrode and grounded during irradiation.

The scanning electron microscope (Auriga CrossBeam workstation, Carl Zeiss NTS) with Schottky field emission gun equipped with the e-beam lithography (EBL) system (Elphy Multibeam, Raith GmbH) was used for e-beam domain patterning. The exposure parameters and e-beam positioning were controlled by EBL system. The irradiated patterns were specified by Raith Nanosuite software. The three exposure modes were used: (1) dot exposure, (2) line exposure by single path line-scan and (3) stripe exposure by meander-scan covering of the rectangular area. The domain patterns after chemical removal of resist layer and electrode were visualized by: optical microscopy, piezoresponse force microscopy (PFM), confocal Raman microscopy (CRM) and scanning electron microscopy (SEM).

We revealed that e-beam irradiation led to switching of c-domains. The design of created domain structures corresponded to irradiated ones. The dose dependence of switched domain area for dot irradiation demonstrates the linear behavior up to 50 pC and saturation with large dispersion of domain sizes at higher doses (Fig. 1a). The saturation has been explained by electrostatic interaction of domain walls and by interaction with a-domains. The domain shape changed from circular at low dose to irregular at high doses (Fig. 1b,c).

The line and stripe exposure mode have been used for creating of 1D pattern (Fig. 1d). The appearance of domain fingers at the walls oriented mainly at the angle close to 45º relative to [100] direction was revealed.

We have demonstrated the possibility to write stripe domains along any direction as well as ring shaped domains (Fig. 1e). Since any area element consist of discrete points the circle domain shape upon dot irradiation at low doses is the key point which allows us to produce domain patterns with arbitrary geometry. The width of stripe domains was independent on direction.

The domain visualization in the crystal bulk using CRM modified for PMN-PT crystals allowed to measure the domain depth down to 200 μm.

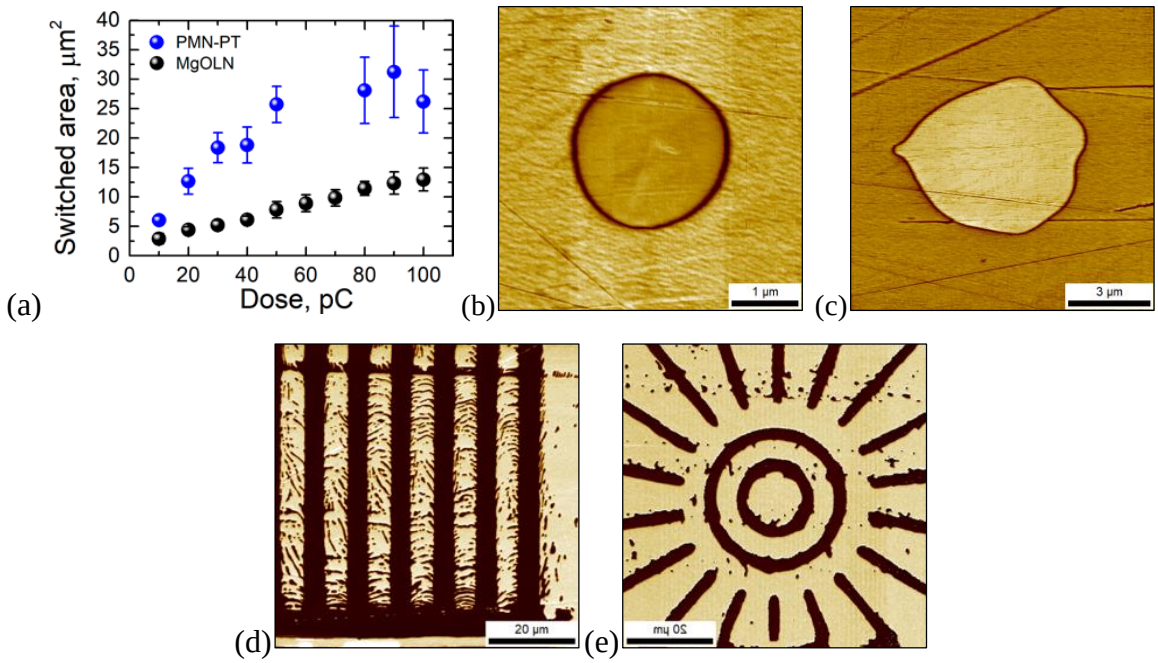

Figure 1. (a) The dose dependence of switched domain area in MgOLN and PMN-PT crystals, (b) – (e) PFM images of c-domains created by e-beam. (b), (c) Dot irradiation with dose: (b) 10 pC, (c) 50 pC. (d), (e) Stripe irradiation along (d) [100] direction, (e) arbitrary direction.

The obtained knowledge can be used for periodical poling in PMN-PT to produce the crystals for light frequency conversion.

The equipment of the Ural Center for Shared Use “Modern Nanotechnology” UrFU has been used. The research was made possible in part by Government of the Russian Federation (Act 211, Agreement 02.180 A03.21.0006) and RFBR (grant 17-52-80116-BRICS_a).

1. X. Wan, H. Xu, T. He, D. Lin, H. Luo, *J. Appl. Phys.* **93**, 4766 (2003).
2. V.Y. Shur, A.R. Akhmatkhanov, I.S. Baturin, *Appl. Phys. Rev.* **2**, 040604 (2015).
3. H. Ito, C. Takyu, H. Inaba, *Electronics Lett.* **27**, 1221 (1991).
4. J.E. Rault, T.O. Mentes, A. Locatelli, N. Barrett, *Scientific Reports* **4**, 6792 (2014).
5. L. Mateos, M.O. Ramírez, I. Carrasco, P. Molina, J.F. Galisteo-López, E.G. Víllora, C. de las Heras, K. Shimamura, C. Lopez, L.E. Bausá, *Adv. Func. Mat.* **24**, 1509 (2014).
6. J.H. Ferris, D.B. Li, S.V. Kalinin, D.A. Bonnell, *Appl. Phys. Lett.* **84**, 774 (2004).
7. V.Y. Shur, D.S. Chezganov, A.R. Akhmatkhanov, D.K. Kuznetsov, *Appl. Phys. Lett.* **106**, 232902 (2015).
8. D.S. Chezganov, E.O. Vlasov, M.M. Neradovskiy, L.V. Gimadeeva, E.A. Neradovskaya, M.A. Chuvakova, H. Tronche, F. Doutre, P. Baldi, M.P. De Micheli, V.Ya. Shur, *Appl. Phys. Lett.* **108**, 192903 (2016).
9. V.Ya. Shur, *J. Mater. Sci.* **41**, 199 (2006).

P-20

Self-organized growth of dendrite domains in lithium niobate and lithium tantalate single crystals

M.A. Chuvakova, A.R. Akhmatkhanov, A.A. Esin, E.D. Saveliev, D.S. Chezganov, D.O. Alikin, M.S. Nebogatikov, A.I. Lobov, V.Ya. Shur

School of Natural Sciences and Mathematics, Ural Federal University, 620000, Ekaterinburg, Russia
e-mail: M.A.Chuvakova@urfu.ru

The various realizations of surface shape instabilities in non-equilibrium systems leading to formation of self-organized non-equilibrium complicated patterns can be used as potential bottom-up technologies for fast and parallel creation of functional nanostructures. Among them the dendrite patterns being one of the most symmetric and organized structures formed by branching mechanism attract growing attention during last decades [1,2]. It should be noted that existence of similar dendrite patterns can be observed in various physical systems indicating that the common underlying formation mechanisms of such structures exist. The examples of the systems are snowflake growth [2] and air displacement of viscous liquid in Hele-Shaw cell [1].

In this work we present the study of formation and growth of dendrite ferroelectric domains in lithium niobate (LN) and lithium tantalate (LT) single crystals in uniform electric field. Two conditions are required: the domain wall shape instability caused by bulk screening retardation and stochastic nucleation [3-5]. We have realized these conditions by polarization reversal at high temperatures in the plates covered by artificial dielectric layer.

The dendrite domain growth was studied by *in situ* optical visualization during polarization reversal at 250°C in the polar-cut plates of congruent LN and LT crystals covered by silicon dioxide film under transparent indium tin oxide electrodes. The main stages of domain structure evolution have been revealed. The increase of the branch diameter before tip splitting and step-like increase of the branch growth velocity after splitting were observed. Analysis of the static domain structures has allowed obtaining the field dependence of the domain envelop shape and filling ratio. The envelop shape changed from triangular to hexagonal and the filling ratio (ratio of domain and its envelop areas) increased with field increase. The visualization of the domain structure in the bulk by second harmonic generation microscopy allowed measuring of the dendrite structure depth – about 10 μm. The qualitative change of domain shape was revealed at the depth about 150 μm from polar surface. In congruent LT the envelop shape of dendrite domains transformed from triangular to strongly rounded hexagonal shape with increase of the external field.

The phase-field simulation was used to verify the analogy between self-organized growth of dendrite domains and dendrite crystals during the first order phase transition taken into account the crystal symmetry C_{3v} [6]. The similarity of simulated and experimentally observed domain shapes was achieved. The phase diagram of growth domain morphology was constructed by computer simulation.

The equipment of the Ural Center for Shared Use “Modern nanotechnology” UrFU was used. The research was made possible by Russian Science Foundation (Project №14-12-00826).

1. E. Ben-Jacob, P. Garik, *Nature* **343**, 523 (1990).
2. K.G. Libbrecht, *Annu. Rev. Mater. Res* **47**, 271 (2017).
3. V.Ya. Shur, A.R. Akhmatkhanov, *Philos. Trans. R. Soc. A Math. Phys. Eng. Sci.* **376**, 2113, (2017).
4. V.Ya. Shur, A.R. Akhmatkhanov, M.A. Chuvakova, M.A. Dolbilov, P.S. Zelenovskiy, A.I. Lobov, *J. Appl. Phys.* **121**, 10 (2017).
5. V.Ya. Shur, D.S. Chezganov, M.S. Nebogatikov, I.S. Baturin, M.M. Neradovskiy, *J. Appl. Phys.* **112**, 10 (2012).
6. A.R. Akhmatkhanov, A.I. Lobov, M.A. Chuvakova, E.D. Saveliev, V.Ya. Shur, *IOP Conf. Ser. Mater. Sci. Eng.* **256**, 1 (2017).

P-21

STEM and HRTEM techniques for investigation of cobalt recovery temperature dependence under ion beam irradiation

M.M. Dementyeva[1], K.E. Prikhodko[1,2], B.A. Gurovich[1], L.V. Kutuzov[1], D.A. Komarov[1]

[1]*National Research Center «Kurchatov Institute», 123182, Moscow, Russia*
e-mail: dementyeva_mm@nrcki.ru

[2]*National Research Nuclear University «MEPhI», 115409, Moscow, Russia*

Currently, there is a great interest in the creation of nanostructures based on ferromagnetic and antiferromagnetic metals. First of all, such interest is associated with the possibility of using it in magnetoelectronics to generate magnetic memory elements. It is known that for production a magnetic medium with a high recording density, it is necessary to form a special medium consisting of individual magnetic granules (single-domain bits) with identical size from 15 to 30 nanometers, shape and orientation (pattern magnetic media) [1]. Moreover, in such structures is important to provide magnetization stability of the individual bits when the external magnetic field is turned off. Creating an antiferromagnetic layer can solve the problem of individual bits stability, for example, CoO - layer along the ferromagnetic Co-bit boundary.

Radiation technology of creating functional nanoelements has been actively developing in the NRC "Kurchatov Institute" during the last ten years. However, it is important to note, that the atomic composition and physical properties controlled modification of selected regions of thin-film materials (ferromagnets, insulators, conductors, superconductors) occurs due to low-energy ions irradiation with various composition (protons, oxygen, nitrogen ions, etc.) at different doses. The problem of determining the irradiation conditions (energy of incident ions, irradiation dose and substrate temperature during irradiation) for functional domains formation with specified composition and properties becomes actual.

In this study, we offer the radiation technology of selective removal of oxygen atoms (SRA) [2] from cobalt oxide Co_3O_4 to create a high-density pattern media. Selection of irradiation conditions and predicting physical properties of modified materials requires structure and chemical composition data after irradiation. Modern analytical transmission electron microscopy makes it possible to obtain quantitative information about chemical composition of samples with a local sensibility up to 1 nm. Analysis of Co_3O_4 films modification degree in depth was carried out using electron energy loss spectroscopy (EELS) in convergent beam mode (STEM mode). Phase analysis of films irradiated at different doses was carried out using high-resolution bright-field images on transmission electron microscope Titan 80 - 300 operated at 200 kV. Preparation of films cross-section was performed at FIB Helios Nanolab 650 facility.

The SRA process was realized by irradiating the initial cobalt oxide films with 1 keV protons at temperature of 20°C and 100°C at doses: $0.94 \cdot 10^{18}$, $1.87 \cdot 10^{18}$ и $3.75 \cdot 10^{18}$ ions/cm^2. An estimate of the chemical composition changes in film depth was carried out after Co_3O_4 thin films proton irradiation at different fluences and substrate temperatures. Results of substrate temperature influence during irradiation are shown in Figure 1. Figure 1 demonstrates elements distribution profiles in depth of irradiated films to a dose of $3.75 \cdot 10^{18}$ ions/cm^2 at substrate temperatures of 20°C and 100°C. As can be seen, the Co_3O_4 film irradiated at 100°C substrate temperature at given dose is restored to pure cobalt at a depth of 17 nm, as compared with irradiation at a temperature of 20°C. This is due to the faster release of knocked out oxygen atoms from the sample during the process of selective removal oxygen atoms from Co_3O_4 under proton irradiation. Furthermore, it was found that at both irradiation temperatures elements depth distribution profiles are non-monotonically, which is due to the nonmonotonic distribution of the damaging dose during irradiation. The direct correspondence of cobalt recovery profile to the dose distribution profile in target depth confirms the radiation nature of selective removal process of atoms.

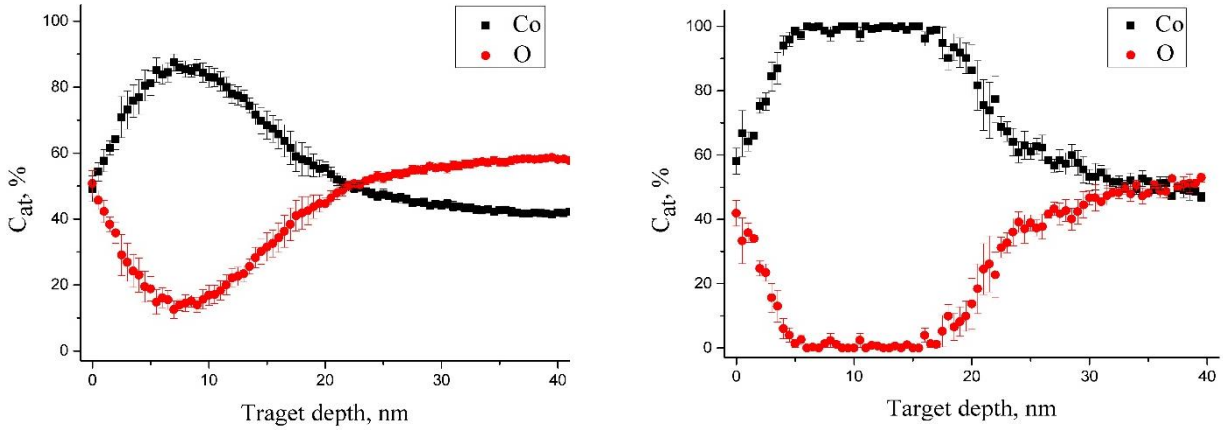

(a) (b)

Figure 1. Elements depth distribution profiles of the Co_3O_4 film irradiated with 1 keV protons (calculated from EELS data) for dose 3.75·1018 ions/cm^2 at different temperatures: (a) 200°C; (b) 1000°C.

Phase identification analysis performed by Fourier - transform of corresponding grains in HRTEM image completely agrees with EELS data. Figure 2 showed that the grain of Co_3O_4 film irradiated at a dose of $3.75 \cdot 10^{18}$ ions/cm^2 at 100^0 C substrate temperature corresponds to the phase of pure Co hexagonal system (P63/mmc) with a lattice parameter a=b=0.2514 nm, c=0.4105 nm.

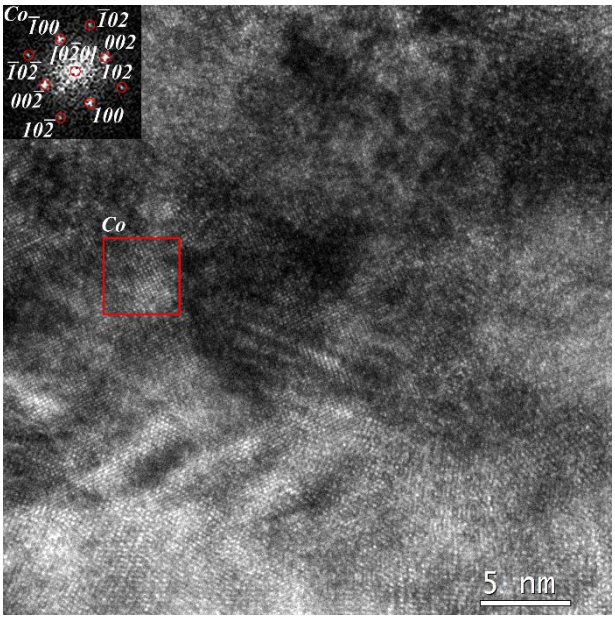

Figure 2. Bright-field HRTEM image of Co_3O_4 film cross section irradiated with 1 keV protons with dose 3.75·1018 ions/cm^2 at 1000°C, diffraction (inset).

1. E.Z. Meilikhov, R.M. Farzetdinova, *FTT* **56**, 2326 (2014).
2. B.A. Gurovich, E.A. Kuleshova, K.E Prikhodko, et al., *Journal of Magnetism and Magnetic Materials* **322**, 3060 (2010).

P-22

Use of EELS STEM technique to estimate the depth profile of tungsten oxide reduction under proton irradiation

M.M. Dementyeva[1], K.E. Prikhodko[1,2], B.A. Gurovich[1], L.V. Kutuzov[1], D.A. Komarov[1]

[1]*National Research Center «Kurchatov Institute», 123182, Moscow, Russia*
e-mail: dementyeva_mm@nrcki.ru

[2]*National Research Nuclear University «MEPhI», 115409, Moscow, Russia*

Binary transition metal oxides system (TMOs), such as NiO, TiO_2, ZrO_2, Cu_xO, TaO_x, WO_x and HfO_2 [1] are attract attention for use in constructing a non-volatile resistive-random access memory (RERAM). TMOs are more promising class of materials for creating switching devices in comparison with $Pr_{0.7}Ca_{0.3}MnO_3$ (PCMO), $La_{0.7}Ca_{0.3}MnO_3$ (LCMO), Cr-doped $SrZrO_3$. It is because of not only TMOs simpler structure and manufacturing but also possibility of compliance with complementary metal oxide (semiconductor (CMOS) [2]. The operation principle of such unipolar memory devices is to change the resistance level from high resistance state (HRS) to low resistance state (LRS) due to the migration of oxygen atoms when an electric field is applied.

In this paper, it is proposed to create a multilayer structure based on W with different oxygen content from tungsten oxide WO_3. Layers depleted by oxygen atoms will be sink for O+ migrating atoms and conversely when the polarity of the applied field is changed Radiation technique of selective removal of oxygen atoms (SRA) under low-energy proton irradiation was used to create such a structure [3,4].

The WO_3 film was fabricated using cathode sputtering technique at room temperature, from metallic W target in oxygen atmosphere on SiO_2/Si substrates. Irradiation of WO_3 thin films with 1 keV protons at doses of $2.8\cdot10^{18}$, $6.75\cdot10^{18}$ and $11.25\cdot10^{18}$ ions/cm^2 were carried out on a special system with a high-frequency source of oxygen plasma and pulse high voltage bias.

Chemical composition of irradiated WO_3 samples were studied using “Titan 80-300ST” electron microscope in STEM mode, equipped with a GIF-2001 energy loss spectrometer. The EEL spectra were obtained with an energy dispersion 0.5 eV/ch, collection angle, as defined by the GIF aperture and camera length was 14.82 mrad, and convergence angle α=10 mrad. A cross sections samples WO_3/SiO2/Si were prepared by FIB “Helios Nanolab 650”.

Quantitative analysis was carried out with equation:

$$\frac{N_A}{N_B} = \frac{I_A(\beta,\Delta)}{I_B(\beta,\Delta)} \cdot \frac{\sigma_B(\beta,\Delta)}{\sigma_A(\beta,\Delta)}, \quad (1)$$

where I_A, I_B - integrated intensities of the peaks after background subtracting, and σ_A and σ_B - ionization cross section [5].

Figure 1 shows elements depth distribution profiles calculated from EELS data of WO_3 film irradiated with low fluence $2.8\cdot10^{18}$ and high fluence $11.25\cdot10^{18}$ ions/cm^2. It can be seen (Fig. 1a) that at small irradiation dose, the process of selective removal of oxygen atoms occurs in the 2.5 nm depth near-surface layer. Remaining volume of the film retains the stoichiometric composition of the original WO_3 film. A significant increase in the irradiation dose (Fig. 1b) leads to oxygen concentration level decrease and composition of the regions at depths from 2 to 8 nm and from 12 to 20 nm corresponds to WO_2 stoichiometric composition. Also from Figure 1b is clearly visible that at about 10 nm depth that corresponding to the maximum damage depth under proton irradiation, a significant tungsten oxide reduction occurs. At the same time, substantially higher doses are required for complete removal of the remaining impurity oxygen, as is known from the results of previous studies [6]. Experimentally obtained tungsten oxide recovery depth distribution under proton irradiation is nonmonotonic and recovery depth-profile corresponds to the distribution of the dose in depth, which confirms the radiation nature of the selective removal of atoms process.

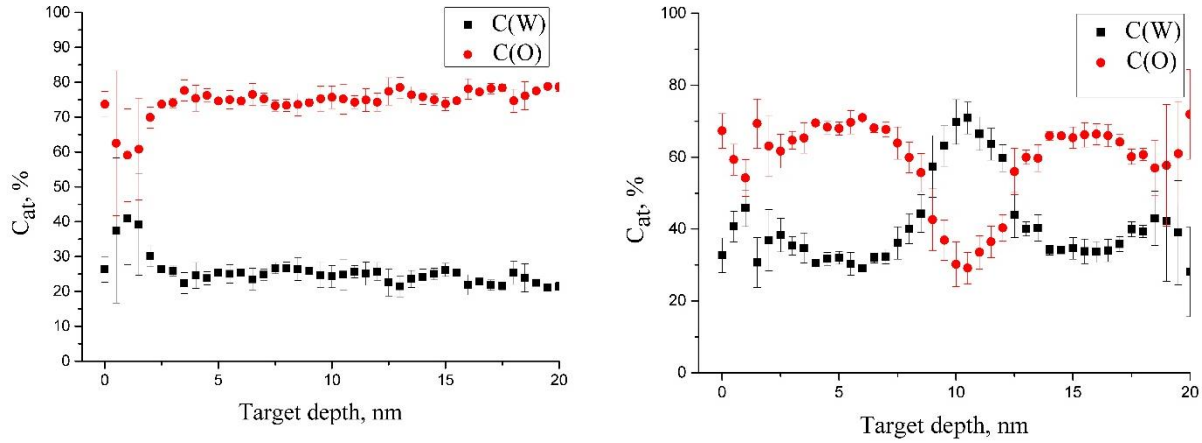

(a) (b)

Figure 1. Elements depth distribution profiles of the WO3 film irradiated with 1 keV protons (calculated from EELS data) for different doses:
(a) $2.8 \cdot 10^{18}$ ions/cm^2; (b) $11.25 \cdot 10^{18}$ ions/cm^2

1. R.G. Elliman, T.-H. Kim et al, *Nuclear Instruments and Methods in Physics Research B* **307**, 98 (2013).
2. M.K. Yang, J.-W. Park et al, *Applied Physics Letters* **95**, 042105 (2009).
3. B.A. Gurovich, A.G. Domantovski et al, *Journal of Surface Investigation: X-ray, Synchrotron and Neutron Techniques* **5**, 25 (2008).
4. B.A. Gurovich, K.E. Prikhodko et al, *Journal of Surface Investigation: X-ray, Synchrotron and Neutron Techniques* **1**, 35 (2011).
5. D. Williams, A. Carter. *Electron microscopy*. (New York: Springer), 760 (2009).
6. B.A. Gurovich, K.E. Prikhodko, *Phys.Usp.* **52**, 165 (2009).

P-23

XPS studies of PMIDA adsorbed on Fe_3O_4 magnetic nanoparticles surfaces

A.A. Esin[1], A.M. Demin[2], V.P. Krasnov[2], V.Ya. Shur[1]

[1]*School of Natural Sciences and Mathematics, Ural Federal University, 620000, Ekaterinburg, Russia*
Corresponding author e-mail: alexander.esin@urfu.ru

[2]*Postovsky Institute of Organic Synthesis of Ural Branch RAS, 620990, Ekaterinburg, Russia*

Magnetic nanoparticles (MNPs) based on Fe_3O_4 are currently the most widely used for biomedicine purposes such as magnetic resonance imaging, hyperthermia, drug delivery and others. Chemical modification of Fe_3O_4 MNPs surface via small organic molecules provides a simple means for their further functionalization with biomolecules. N-Phosphonomethyl iminodiacetic acid (PMIDA) is one of the promising reagents for surface modifications of various oxides including Fe_3O_4 [1]. Recently we assumed that PMIDA molecules are coordinating on the surface due to tridentate binding that involves P-O-Fe bonds [2].

The purpose of this work is comprehensive study of the mechanism of PMIDA binding with Fe_3O_4 nanoparticle surface by X-ray photoelectron spectroscopy (XPS) (K-Alpha+TM XPS system (Thermo Fisher Scientific, USA)).

We investigated the spectrum of initial Fe_3O_4 MNPs, PMIDA and PMIDA-modified nanoparticles (Fig. 1).

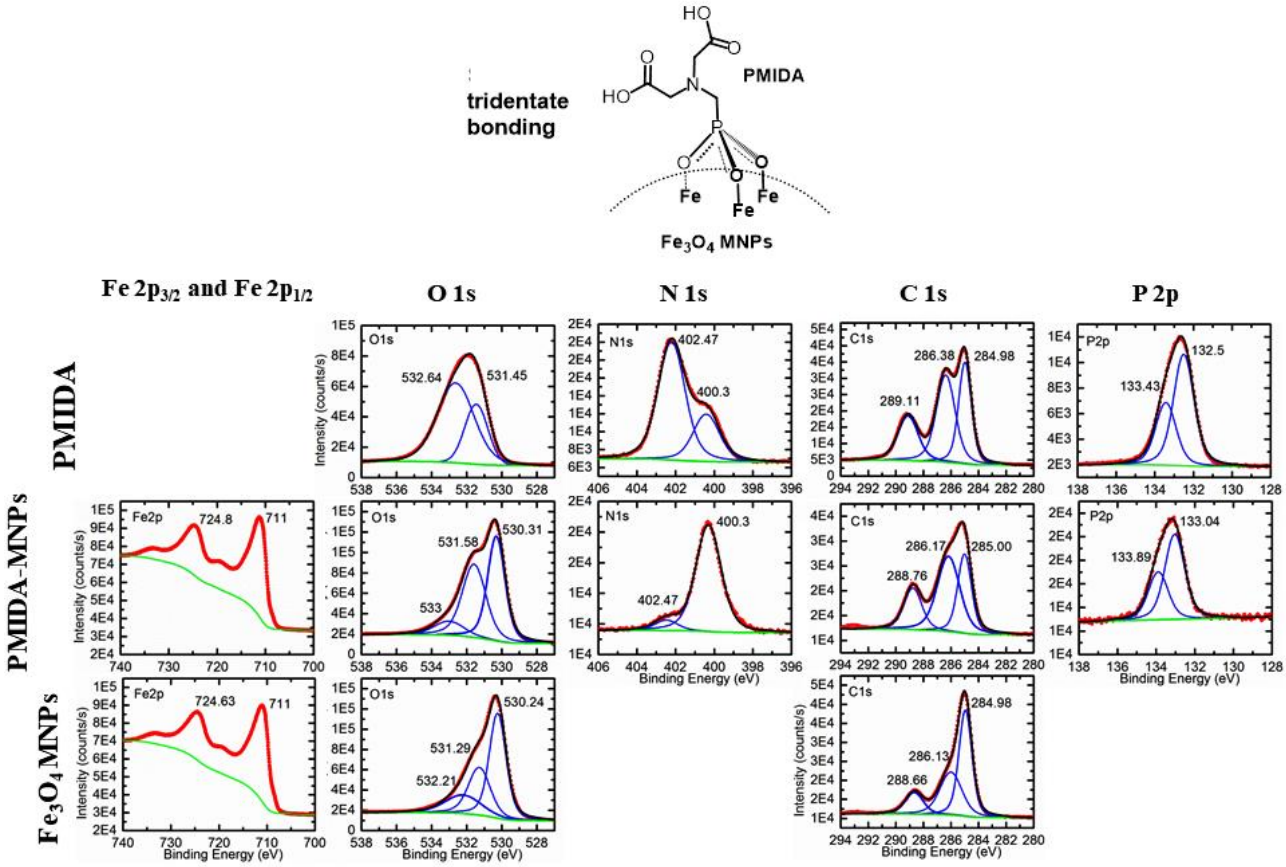

Figure 1. XPS spectra for Fe $2p_{3/2}$ and Fe $2p_{1/2}$, O 1s, N 1s, C 1s and P 2p binding energies of Fe_3O_4 MNPs, PMIDA and PMIDA-modified nanoparticles.

XPS spectrum of bare and modified MNPs shows the Fe2p doublet with same binding energy values), typical for magnetite. In O 1s binding region we observed a little shift of the band at 531.58 eV (compare with 531.45 eV and 531.29 eV corresponding to P-O of PMIDA and Fe_3O_4 MNPs) attributed to P-O-Fe and P=O···Fe bonds. Indirect confirmation of P-O-Fe bonds formation is the redistribution of the intensity of N 1s peaks with binding energy of 402.47 eV (minor) and 400.30 eV (major) for PMIDA-modified MNPs in comparison with spectrum of

PMIDA. In C 1s binding region of PMIDA-MNPs spectrum, the peaks centered at 285.00 eV, 286.17 eV, 288.76 eV can be attributed to C-C; C-N, C–P, C–O; and C=O electrons of phosphonic acids derivative and C-contain contaminants (e.g., CO_2) on the MNP surface, respectively. The P2p spectrum exhibited two peaks at 133.04 eV and 133.89 eV attributed to P $2p_{3/2}$ and P $2p_{1/2}$ and having a shift of about 0.5 eV to high energy in comparison with peaks for PMIDA. Thus, it can be displayed that all P atoms of phosphonic acid participate in to coordinating with Fe atoms on MNP surface.

Thus, the hypothesis about anchoring of PMIDA molecules to magnetic nanoparticle surface through a tridendate bonding involving P-O-Fe bonds was experimentally confirmed. We believe that obtained results will help to provide a better understanding of binding schemes for this phosphonate derivative with MNPs surface.

The equipment of the Ural Center for Shared Use “Modern nanotechnology” Ural Federal University was used. The work was financially supported by the Integrated Program of the Ural Branch of the RAS (no. 18-3-3-20).

1. A.M. Demin, A.G. Pershina, A.S. Minin, A.V. Mekhaev, V.V. Ivanov, S.P. Lezhava, A.A. Zakharova, I.V. Byzov, M.A. Uimin, V.P. Krasnov, L. Ogorodova, *Langmuir* **34**, 3449 (2018).
2. A.M. Demin, A.V. Mekhaev, A.A. Esin, D.K. Kuznetsov, P.S. Zelenovskiy, V.Ya. Shur, V.P. Krasnov, *App. Surf. Sci.* **440**, 1196 (2018).

P-24

Modern methods of atomic force microscopy in the biomedical research

A.A. Frolova[1], A.A. Akovantseva[1], S.L. Kotova[2,3], P.S. Timashev[1,2]

[1]*Institute of Photonic Technologies, Federal Scientific Research center "Crystallography and Photonics", RAS, Troitsk, Moscow, 142190, Russia*
E-mail: NastyFr@yandex.ru

[2]*Institute for Regenerative Medicine, Sechenov University Moscow, 119991, Russia*

[3]*Department of Polymers and Composites, N.N.Semenov Institute of Chemical Physics, Moscow 119991, Russia*

Modern atomic force microscopy (AFM) plays an important role in biomedical research. By selecting different scanning modes and corresponding probes, AFM allows investigation of the structure of both fixed histological sections and living biological objects, as well as very soft adhesive structures, such as natural hydrogels.

Here, we present recently introduced methods in AFM, developed specifically for the biomedical research.

PeakForce Tapping® is a relatively new mode introduced by Bruker. The mode based on the processing of force-distance curves in each point of measurement allows combination of a mild force load on the sample and a high resolution, which is especially important for imaging soft biological samples such as cells.

PeakForce QNM® (Quantitative NanoMechanics, by Bruker) is a scanning mode with the simultaneous measurement of topography and different material properties, such as Young's modulus, adhesion, deformation etc., at the nanoscale. Using PeakForce QNM®, we studied a variety of biological objects using a Multimode 8 atomic force microscope by Bruker. For example, we studied vocal fold tissues of rabbit – normal tissues, scar tissue and the scar tissues after the treatement with autologous mesenchymal stem cells (MSC). We have shown the differences between the normal and scar tissues in the packing of collagen fibrils, their thicknesses and Young's moduli. Besides, we have shown that, after the MSC treatment, both the collagen packing and Young's modulus resemble those of the normal vocal fold tissue that indicates the restoration of the original tissue's elasticity.

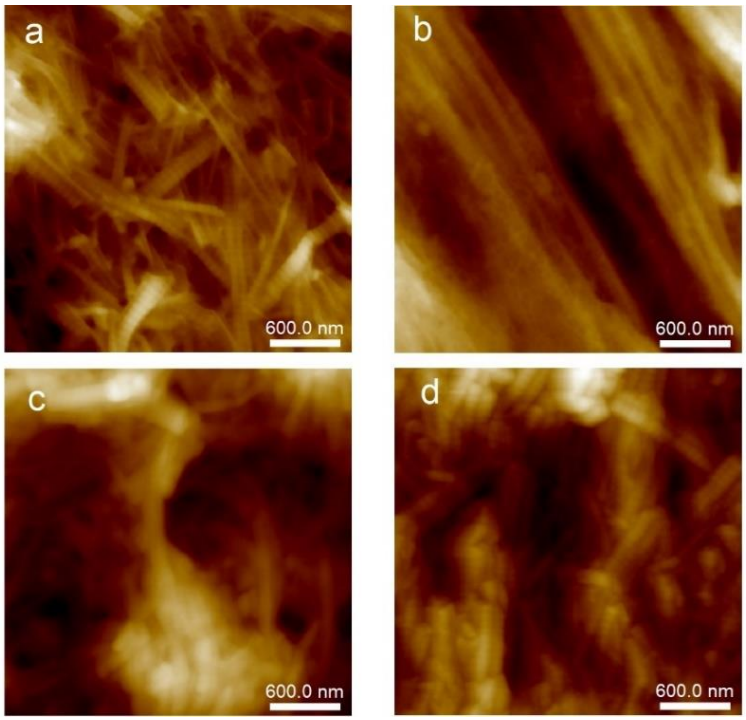

Figure 1. AFM of native matrix and the AT types: (a) native matrix of rib cartilage; (b) "classic" type of AT; (c) "fine-fibred" type of AT; (d) "intertwined" type of AT. All images have a scan size of 3x3 μm^2.

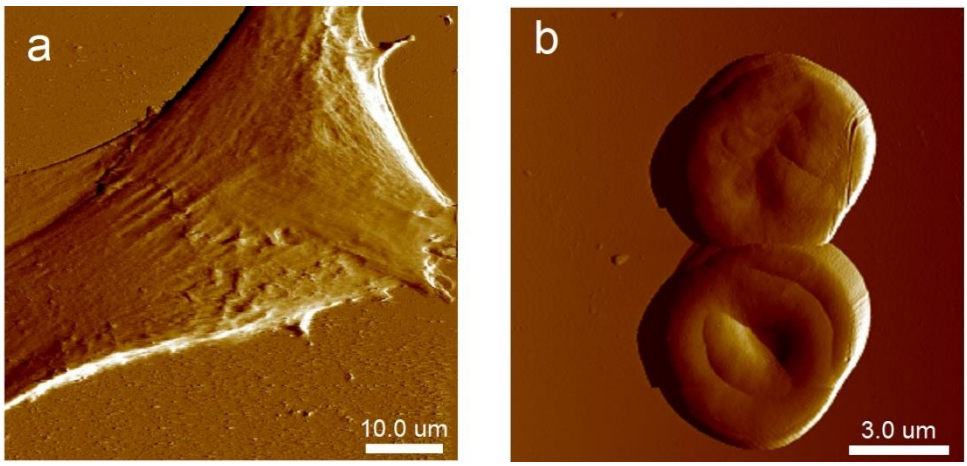

Figure 2. AFM images of live cells in the cell media. (a) human MSC, scan size 60x60 μm^2; (b) Two types of human erythrocytes: spherocyte and discocyte, scan size 14x14 μm^2.

The Fast Force Volume regime allows mapping of Young's modulus and stiffness with the preset number of points on the object's surface. It is convenient for very soft materials, such as hydrogels and certain live cells, where imaging with the Peak Force QNM® regime is not possible.

In Figure 1, we display how PeakForce Tapping® - PeakForce QNM® on air was used to study the pathology of rib cartilage in children aged 8-17 years with congenital deformations of the chest – pectus excavatum (PE) and pectus carinatum (PC). We characterized three new types of amianthoid transformation (AT) of the costal cartilage collagen fibers in children: a "classic", a "fine-fibred" and an "intertwined" type. All the AT types represent different stages of extracellular matrix transformation and have different packing and structure of collagen fibers.

In Figure 2, we demonstrate application of PeakForce Tapping® for imaging live cells in their own cell medium, using a Bioscope Resolve AFM (Bruker).

P-25

Analysis of the conduction mechanism through InSb quantum dot by tunnel CVC method

M.V. Gavrikov, A.I. Mikhailov, V.F. Kabanov, E.G. Glukhovskoy

Saratov State University, Department of Nano and Biomedical Technologies, Saratov, 410012, Russia
e-mail: maks.gavrikov.96@gmail.com

Semiconductor compounds A_3B_5 belong to the most promising and interesting from the practical point of view semiconductor materials for many years. This compounds possess a characteristic features of electrons energy spectrum and extremely low values of conduction electrons effective mass. The last thing provides the de Broglie wavelength of tens of nanometers for the conduction electrons even at room temperature. In this regard, a specific phenomena associated with the size quantization of electrons energy spectrum can manifest themselves in a relatively large structures.

Materials and methods. The properties of obtained film samples with quantum-size objects of indium antimonide were investigated by scanning tunneling microscopy (STM), scanning electron microscopy (SEM), and particle size analyzer (Malvern Mastersizer 2000). To analyze the experimental tunnel CVC, we used the dependence *(dI/dV)/(I/V)* on the voltage *V*.

Results and discussion. To determine the validity of field-emission model use, we made calculations of the CVC for the InSb QD and comparison of the results with the experimental data.

The calculations used data:

InSb: $m^* = 0{,}013m_0$, d = 1nm, As = 4,9 eV, $\theta = 0{,}2$

To estimate the values of the QD spectrum first three levels and, accordingly, the QD size, an analysis of the experimental data was performed by the tunnel CVC method (the dependence *(dI/dV)/(I/V)* on the voltage *V*). The results are shown in Figure 1a. The obtained values of the peaks on the normalized differential CVC were put in correspondence with the calculated energy spectrum levels with an error of up to $2kT$ (the selected area in Fig. 1b).

QD size estimates by comparison of the electronic spectrum calculation with the analysis of the experimental tunnel CVC were in the range 18-22 nm.

Calculated CVC for the field-emission model for the InSb QD with different characteristic sizes a are shown in Figure 2a. For comparison, Figure 2b shows the typical experimental CVC for *InSb* QD.

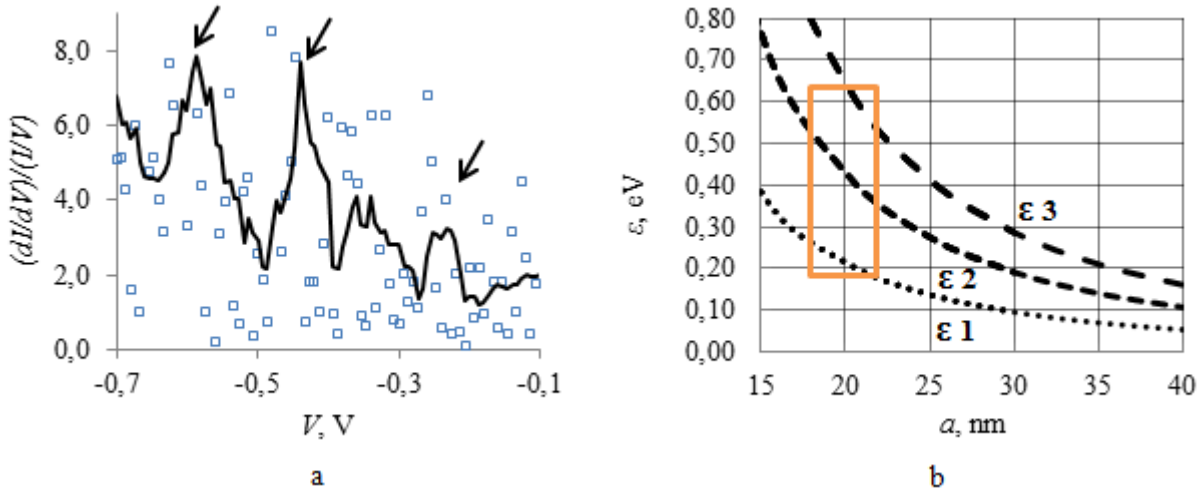

Figure 1. (a) Typical differential tunnel CVC of InSb QD, (b) calculated conduction electron energy values for the first three allowed levels of InSb QD depending on the characteristic size a by the “cubic” QD model.

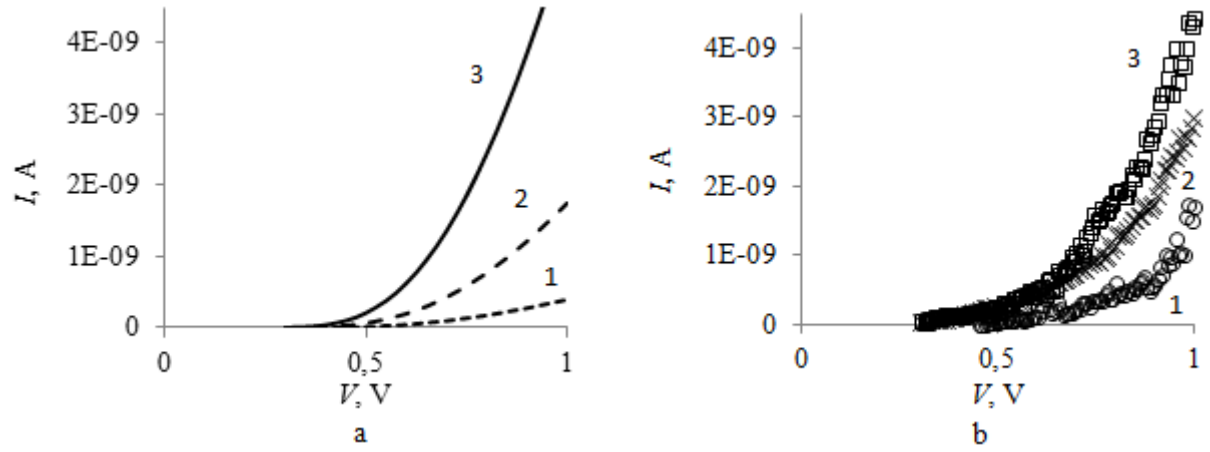

Figure 2. (a) Rated CVC for InSb QD, (b) typical experimental CVC for InSb QD.

Analysis of the experimental results and theoretical calculations showed their qualitative (CVC form) and quantitative (current values in considered voltage range) agreement. QD size estimates by the method of comparing the calculated CVC to the experimental ones (based on the field-emission model) were in the range 20-22 nm.

This work was supported by grants from the Russian Foundation for Basic Research Projects No. 16-07-00093 and No. 16-07-00185.

1. A.I. Mikhailov, V.F. Kabanov, N.D. Zhukov, *Technical Physics Letters* **41**, 1065 (2015).
2. V.L. Mironov, *The textbook for students of the senior courses of higher educational institutions*, Nizhniy Novgorod, 97 (2004).
3. A.I. Mikhailov, V.F. Kabanov, et al., *Nanosystems: physics, chemistry, mathematics* **8**, 596 (2017).

P-26

Domain structure and grain orientation in PLZT ceramics using electron backscatter diffraction and piezoresponse force microscopy

L.V. Gimadeeva[1], D.S. Chezganov[1], A.S. Merzliakova[1], V.V. Yuzhakov[1], B. Malič[2], A.L. Kholkin[1,3], V.Ya. Shur[1]

[1]*School of Natural Sciences and Mathematics, Ural Federal University, 620000, Ekaterinburg, Russia Corresponding author e-mail: lv.gimadeeva@urfu.ru*

[2]*Ceramics Department of Jozef Stefan Institute, Ljubljana, Slovenia*

[3]*Department of Physics & CICECO-Aveiro Institute of Materials, University of Aveiro, Aveiro, Portugal*

The unique properties of relaxor ferroelectrics have raised interest in understanding the micro- and nanodomain structures and their evolution during polarization reversal. The advantages of relaxor ceramic of lanthanum doped lead zirconate-titanate (PLZT) are high optical transparency and electro-optical coefficients. PLZT was successfully used in segment displays, optical closures, coherent modulators, color filters, image storage devices, etc. [1]. The functional properties of ferroelectric ceramic materials are strongly influenced by their nanostructure and crystallographic orientation [2].

We will present the results of crystallographic mapping by electron backscatter diffraction [3] and domain structure visualization by piezoresponse force microscopy [4] in PLZT ceramics.

The studied $Pb_{1-x}La_x(Zn_{0.65}Ti_{0.35})_{1-x/4}O_3$ ceramics (PLZT 8/65/35) were sintered by the hot pressing method at the Ceramics Department of Jozef Stefan Institute, Ljubljana, Slovenia. Samples were polished to the optical quality with a gradual decrease of diamond abrasive down to 0.25 μm and mechanochemical polishing by colloidal silica. Thermal depolarization was carried out during cooling from 200°C to room temperature with cooling rate 5°C/min without electric field. The domain visualization by piezoresponse force microscopy (PFM) by means of scanning probe microscope NTEGRA Aura (NT-MDT SI, Russia) using silicon tips with a diamond-like conductive coating. The grain crystallographic orientations were obtained by electron backscatter diffraction (EBSD) by means of the scanning electron microscope Auriga CrossBeam workstation (Carl Zeiss NTS, Germany). The marking of the investigated area by nano-hardness tester NanoScan-4D (FSBI TISNCM, Russia) allowed to study the same region of the sample surface by both methods.

The analysis of the obtained grain orientation mapping allowed us to reveal the significant texture of the studied ceramics. Moreover, it was demonstrated that the domain patterns depend essentially on the grain orientation. Statistical analysis of the geometrical parameters of domain patterns for the grains with the same orientation has been used for detail characterization of the domain structure.

The realized method will be used for investigation of influence of the grain orientation on the domain structure appeared in ceramics after thermal depolarization, application of uniform electric field and local switching by conductive tip.

The equipment of the Ural Center for Shared Use “Modern nanotechnology” UrFU was used. The research was made possible by Russian Foundation of Basic Research (Grant 16-02-00821-a).

1. A. Sternberg, A. Krumins, *Electro-Optic and Photorefractive Materials* (Springer-Verlag) **18**, 50 (1987).
2. T.L. Burnett, P.M. Weaver, J.F. Blackburn, M. Stewart, M.G. Cain, *J. Appl. Phys.* **108**, 042001 (2010).
3. M. Lowe, T. Hegarty, K. Mingard, J. Li, M Cain, *J. Phys.: Conf. Ser.* **126**, 012011 (2008).
4. P. Gupta, H. Jain, D.B. Williams, S.V. Kalinin, J. Shin, S. Jesse, A.P. Baddorf, *Appl. Phys. Lett.* **87**, 172903 (2005).

Molecular packing, piezo- and pyroelectric properties of *tert*-butyl *N*-(*tert*-butoxycarbonyl)-(*S*)-prolinamide

D.A. Gruzdev[1,2], A.S. Nuraeva[3], S.G. Vasilev[3], A.V. Ushakov[3], V.O. Ustinova[1], P.A. Slepukhin[1,2], V.P. Krasnov[1,2], V.Ya. Shur[3]

[1]*Postovsky Institute of Organic Synthesis, Russian Academy of Sciences (Ural Branch), 620990, Ekaterinburg, Russia*
e-mail: gruzdev-da@ios.uran.ru

[2]*Institute of Chemical Engineering, Ural Federal University, 620002, Ekaterinburg, Russia*

[3]*School of Natural Sciences and Mathematics, Ural Federal University, 620000, Ekaterinburg, Russia*

Chiral organic compounds attract considerable attention as a basis for biocompatible and environmental friendly materials. It is known that natural amino acid derivatives are capable of self-organization in solid state [1] and possess piezoelectric [2] and pyroelectric properties [3].

We studied the properties of crystals of *N*-(*tert*-butoxycarbonyl)-(*S*)-prolinamide **1**. Compound **1** was obtained as a result of coupling between *N*-Boc-(*S*)-proline and *tert*-butylamine by the method of mixed anhydrides. The single crystals of **1** were grown by spontaneous crystallization from a water–methanol mixture and by a vapor diffusion technique.

It has been found that compound **1** forms crystals of two types differing in their morphology. X-Ray diffraction analysis (XDA) has shown that the crystals belong to hexagonal (*hex*-**1**, space group $P6_1$) or triclinic syngony (*tc*-**1**, space group *P*1) (Fig. 1). The general motif of molecular packing of *hex*-**1** is a formation of nanotubes oriented along the main crystal axis.

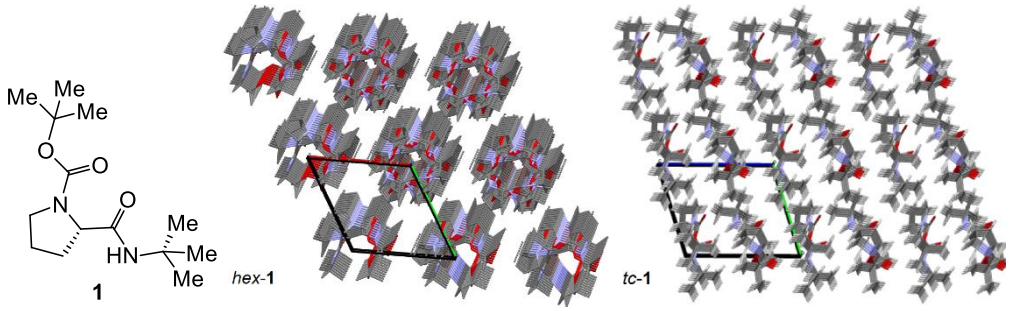

Figure 1. The structural formula and molecular packing of compound **1** according to XDA.

The magnitudes of vertical piezoelectric response of isomorphic crystals *hex*-**1** measured independently by piezoresponse force microscopy and interferometry techniques were in good agreement. The observed piezocoefficients reached 12 pC/N.

The pyroelectric effect of crystals *hex*-**1** was measured.

It has been shown that the phase transition is induced by the IR laser irradiation. The single crystals *hex*-**1** transformed to polymorphic *hex*-**1** / *tc*-**1** conglomerates.

The work was financially supported by the Russian Foundation for Basic Research (grant no. 16-33-60122). The equipment of the Ural Centre for Shared Use “Modern Nanotechnologies” UrFU and Centre for Joint Use “Spectroscopy and Analysis of Organic Compounds” was used.

1. L. Adler-Abramovich, E. Gazit, *Chem. Soc. Rev.* **43**, 6881 (2014).
2. S. Vasilev, P. Zelenovskiy, D. Vasileva, A. Nuraeva, V.Ya. Shur, A.L. Kholkin, *J. Phys. Chem. Solids* **93**, 68 (2016).
3. S. Piperno, E. Mirzadeh, E. Mishuk, D. Ehre, S. Cohen, M. Eisenstein, M. Lahav, I. Lubomirsky, *Angew. Chem. Int. Ed.* **52**, 6513 (2013).

P-28

Current and piezoresponse measurements of repolarized regions of thin $PbZr_{54}Ti_{46}O_3$ films

E.V. Gushchina[1], V.V. Osipov[1,2], B.R. Borodin[1], M.S. Dunaevskiy[1], I.P. Pronin[1]

[1]*Ioffe Institute, 194021, Sankt-Peterburg, Russia*
e-mail: katgushch@yandex.ru

[2]*Herzen University, 191186, Sankt-Peterburg, Russia*

Thin ferroelectric lead zirconate titanate films $Pb(Zr_{1-x}Ti_x)O_3$ (PZT) are promising materials for piezoacoustic, capacitive, electromechanical and sensor devices [1]. PZT films have high dielectric permittivity and large piezoelectric coefficients when x≈0.5 (morphotropic phase boundary). In this work, the processes of local repolarization of these PZT films were studied by scanning probe microscopy (SPM) methods, in particular using the piezoresponse force microscopy (PFM) [2]. Also, the processes of current flow in repolarized regions were studied by conductive atomic force microscopy (CAFM).

Thin films of $PbZr_{54}Ti_{46}O_3$ were grown by high-frequency magnetron sputtering of a ceramic target with the addition of 10% lead oxide (PbO) [3]. The films were deposited at a temperature of 150° C for 40 minutes and 1 hour in an atmosphere of lead vapors. Then they were annealed at a temperature of 600°C. The growth was performed on a $Si/SiO_2/TiO_2/Pt$ substrate. The thickness of $PbZr_{54}Ti_{46}O_3$ films was d = 200 nm and 300 nm [4]. All SPM measurements were performed under room ambient conditions at the «Ntegra-Aura» and «Solver P47» (NTMDT) microscopes. In this work we used DCP01 probes (NTMDT) with a wear-resistant diamond coating.

In the investigated samples, the polarization of the PZT films was performed by applying a voltage to the film. Initially, the samples were not polarized, so it was possible to create polarized regions of different polarity (see Fig. 1). It was found that the repolarization occurs only when the value of the applied voltage U exceeds the value of the coercive voltage U_c for the samples under study. If the voltage U is applied to a small contact area with curvature (R ~ 20 nm), which is less than the thickness of the film under investigation (d> 200 nm), the resulting field in the film will be distributed unevenly. Near the boundary of the film with the substrate, the value of the field strength will be about $E \sim (2R/d^2)U$. The polarization of the region of the film under the probe will occur when the magnitude of this field exceeds the coercive field of the film $U>U_c= (d^2/2R)E_c$. The characteristic values of the coercive fields for thin PZT films are ~ 50-100 kV/cm [5], therefore for these films one can expect characteristic values of coercive voltages U_c ~ 5-10 V.

Figure 1 shows the PFM image and the current map I(x,y) of the surface of 200-nm thick film, which was polarized by voltages U_{dc} = -10V and U_{dc} = +10V (dark and light areas in Fig. 1a, respectively). The corresponding averaged cross-section profiles are also given at the Fig. 1. In the PFM image (Fig. 1a) regions with different polarity of residual polarization (P_r) are clearly seen. It should be noted that these results correlate with the results for a 300-nm thick film annealed at 545°C in [2]. In the «dark» region (Fig. 1a), the residual polarization vector ($-P_r$) is directed from the SPM probe to the substrate. In the «bright» areas (Fig. 1a), the residual polarization vector ($+P_r$) is directed from the substrate to the probe. In addition in Fig.1a (arrows) the boundaries of the «polycrystalline blocks» can be seen.

It should be noted that repolarized regions can also be found in the current map I(x,y) obtained with a small voltage at the probe U = +2V (Fig. 1b). A comparative analysis of the current maps and the distribution of the PFM signal indicate that the current is larger when the field and polarization directions coincide, and less when they are directed oppositely to each other [6]. Also, on the current map (Fig. 1b, arrows) of polarized regions, the boundaries of «polycrystalline blocks» are identified as regions of increased conductivity. It should be noted that in unpolarized films the boundaries of the blocks were not visible. A completely similar situation was observed also for a 300-nm thick film.

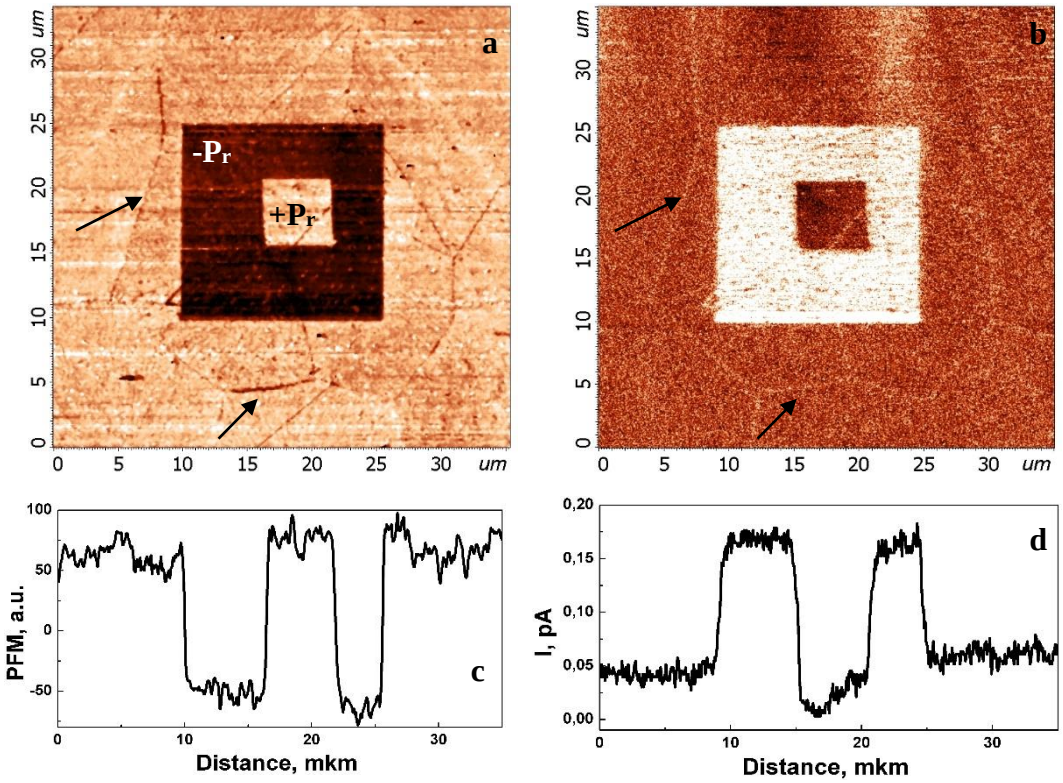

Figure 1. (a) PFM image of domains created when supplied to the probe U_{dc} = ±10V and (c) the corresponding averaged PFM profile; (b) the current map I(x,y) (at voltage +2V) of the same region and (d) the corresponding averaged current profile.

Thus, the technique of creating stable polarized regions (by applying 10V and more voltages) and their visualization in PFM and CAFM signals has been used for the study of piezoelectric and conductive properties of PZT films. The dependence of these signals on the thickness of the films is established. The dependence of the current on the polarization direction is established. It is also found that the polarization of regions allows revealing of the polycrystalline blocks boundaries as areas of increased conductivity.

This work was supported by the RFBR grant N 18-32-00092_mol-a.

1. Scott J.F., *Science* **315,** 954-959 (2007).
2. В.В. Осипов, Д.А. Киселев и др., *ФТТ* **57**, 9, 1748 (2015).
3. И.П. Пронин, Е.Ю. Каптелов и др., *ФТТ* **52**, 124 (2010).
4. В. П. Пронин, А. Г. Канарейкин и др., *Поверхность*, **2** ,1 (2014).
5. J. Pérez de la Cruz, A. L. Kholkin, et.al., *J.Appl.Phys*. **108**, 114106 (2010).
6. Л.А. Делимова, Е.В. Гущина и др. *ФТТ* **56**, 12, 2366 (2014).

P-29

Adhesive coatings based on aligned arrays of carbon nanostructures

O.I. Il'in, M.V. Il'ina, N.N. Rudyk, A.A. Fedotov

Southern Federal University, 347922, Taganrog, Russia
e-mail: oiilin@sfedu.ru

The development of nanotechnologies and the possibility of creating spatially oriented nanoscale structures have generated a wide interest in research in the field of creating artificial bio-like structures [1] in which the reproduction of parameters of biological objects allows solving a number of problems in the field of mechanical contacts of high strength and repair materials with "dry" adhesion working in a vacuum. Among the artificial biomimetic nanostructures, carbon nanostructures based on arrays of vertically aligned carbon nanotubes (VA CNT) possess the best adhesion characteristics, which is associated with an increase in the adhesion force due to an increase in the number of nanostructures contacting the surface [2]. For controlled growth of CNTs with specified characteristics, the most promising method is plasma enhanced chemical vapor deposition (PECVD). However, a large number of parameters of the PECVD method require establishing the relationship between their influence on the growth of carbon nanotubes with controlled parameters.

The purpose of this study is to investigate the influence of patterns of carbon nanotubes growing modes by PECVD on their geometrical dimensions and adhesion properties.

Si/TiN/Ni structure was used for creating experimental samples. Growing VA CNT was performed by PECVD using specialized module cluster complex nanotechnological NANOFAB NTC-9 (NT-MDT, Russia). To provide different CNT parameters during PECVD changed values of the activation time, plasma power, temperature, and growth time. Depending on the type of grown samples, plasma could also be initiated. The initiation of the plasma was carried out using a high-voltage DC source. The samples with 4 types of VA CNT were grown: bundles (Fig. 1a), individual (Fig. 1b), branched (Fig.1c) and disoriented (Fig. 1d).

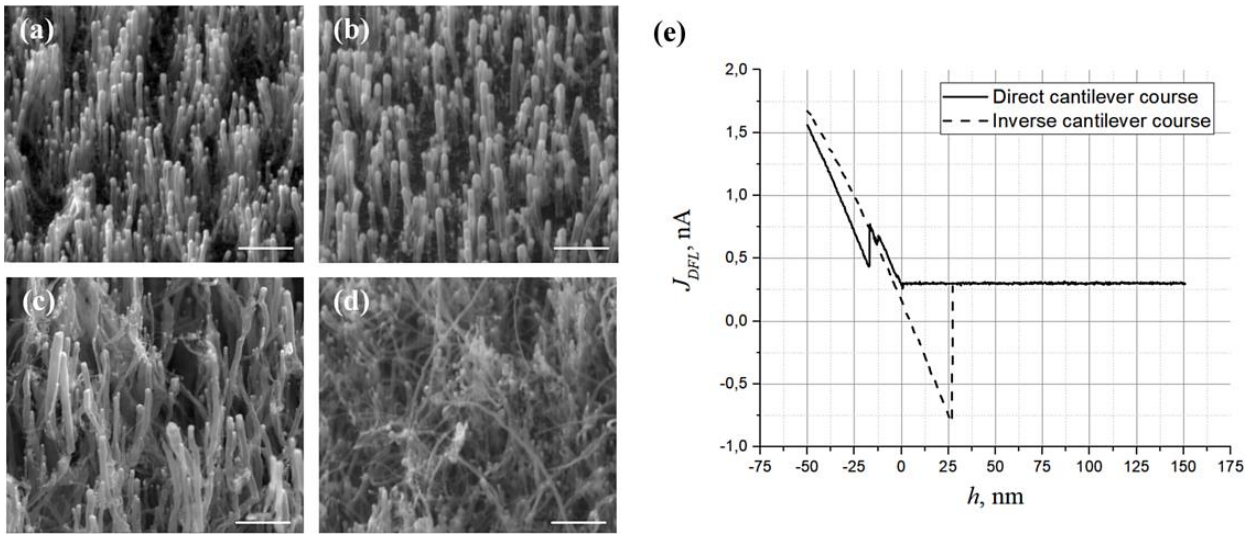

Figure 1. (a) CNTs bundles, (b) individual VA CNTs, (c) branched VA CNTs, (d) disoriented CNTs, (e) experimental dependence ΔJDFL for individual VA CNTs

The estimation of geometrical parameters of CNT arrays was carried out using a scanning electron microscope (SEM) Nova NanoLab 600 (FEI, Netherlands). Investigation of the adhesion strength of the experimental samples was carried out using a probe nanolaboratory Ntegra (NT-MDT, Russia). As a probe of an atomic force microscope (AFM), a colloid probe of the CPC_SiO_2-20/Au series was used with a radius of 20 μm and a stiffness coefficient k = 0,3 N/m. Measurements of the adhesion value were carried out at 10 points of the array of each experimental sample in the AFM force spectroscopy mode. In the process of force spectroscopy was measured the dependence of the cantilever bending value (J_{DFL} signal) on the degree of extension of the z-piezoelectric

element of the scanner (signal *h*) in direct (solid line) and the inreverse (dashed line) cantilever cources. The experimental dependence $\Delta J_{DFL}(h)$ for samples with individual VA CNT is shown in Figure 1e. Using the resulting force spectroscopy AFM dependencies evaluated VA CNT array adhesion force F_a to the surface of AFM probe, by the method described in [1].

The analysis of SEM images of experimental samples with CNT bundles (series A) showed that exposure in an ammonia plasma leads to etching of catalytic centers (CC) Ni and a decrease in their diameter. In this case, the CNT growing regimes with the "activation" time of less than 1 min assist to the formation of CNT bundles. In this case, the measured adhesion strength was 5.03, 8.53 and 11.12 μN for samples A1-A3, respectively.

In the samples with individual VA CNTs (series B), the increase of "activation" time was also accompanied by the processes of combining small CC into larger ones with increasing diameter and decreasing density. At the same time, an increase in the plasma power up to 40 W contributed to the complete removal of small CC and a higher electric field strength, which made it possible to obtain arrays of individual VA CNTs. The measured adhesion strength for samples B1-B3 was 2.3, 0.67 and 1.56 μN, respectively. With a change in the growth temperature from 645 to 675°C on SEM images of samples of branched CNTs (C series), it can be seen that a short "activation" time promotes an increase in the adhesion of the CC to the substrate. As a result, growth occurs both along the "top" and "base" mechanisms with the formation of arrays of branched CNTs. The measured adhesion strength for C1-C3 samples was 3.21, 6.41 and 2.24 μN, respectively. To obtain experimental samples of disoriented CNTs (series D), plasma was not initiated during the growth process. The absence of a vector of electric field strength, which determines the direction of CNT growth, led to the formation of a disoriented array of CNTs. The increase in the growth time from 4 to 12 min allowed the production of CNT arrays with a height of 2.11 to 3.07 μm. The measured adhesion strength for samples D1-D3 was 1.09, 7.38 and 2.71 μN, respectively.

Analysis of the results of measurements showed that the largest average value of the adhesion strength (8.23 microns) had experimental samples of the series A. Individual VA CNTs of experimental samples B series showed the lowest adhesion value among all series of samples (1.51 μN), which may be due to the prevalence of transverse deformation of CNTs and their coalescence during measurement. Analysis of the results of measurements of adhesion in samples with branched (series C) and disoriented (series D) CNT showed that the average adhesion strength was 3.96 and 3.72 μN, respectively.

The results of the research can be used to create adhesive coatings and mechanical contacts of high strength for the space industry and robotics, as well as for the creation of elements of carbon nanoelectronics.

This work was financially supported by Russian Foundation for Basic Research (projects 16-29-14023 and 18-32-00652) and Internal grant of the Southern Federal University (project VnGr-07/2017-26).

1. L. Qu, L. Dai, *Adv. Mater.* **19**, 3844 (2007).
2. M. Rouhrig, M. Thiel, et al., *Small* **8**, 3009 (2012).
3. M.V. Il'ina et al, *J. Phys.: Conf. Ser*. **993**, 012025 (2018).

P-30

Study of the dependence of Young's modulus of vertically aligned carbon nanotubes on their aspect ratio

M.V. Ili'na, A.A. Konshin, O.I. Il'in, N.N. Rudyk, O.A. Ageev

Southern Federal University, "Nanotechnologies" Research and Educational Center, 347922, Taganrog, Russia
e-mail: mailina@sfedu.ru

The rapid development of nanotechnology and the new opportunities in the field of nanoscale structures created a wide interest in the research of carbon nanotubes (CNTs) [1]. For the application of carbon nanotubes as an element base of electronics of new generation their mechanical parameters must be studied in detail. The Young's modulus is one of the main mechanical parameters of a CNT. However this parameter remains poorly understood due to the complexity of the experimental study of carbon nanotubes by using traditional methods (the direct tensile load, the pulse dynamic method, etc.) [2]. The aim of this work is to study the dependence of the Young's modulus of a vertically aligned CNTs on their aspect ratio using previously developed technique based on nanoindentation method.

As the experimental samples were used vertically aligned CNTs arrays grown by plasma enhanced chemical vapour deposition on a silicon wafer with a two-layer Ni/Ti structure on the surface. The arrays have the following values of diameter, height and density in array: No.1 – 43.8 nm, 0.65 μm, 82 μm^{-2}, No.2 – 35.6 nm, 1.21 μm, 72 μm^{-2}, No.3 – 51 nm, 0.69 μm, 69 μm^{-2}, respectively (Fig. 1).

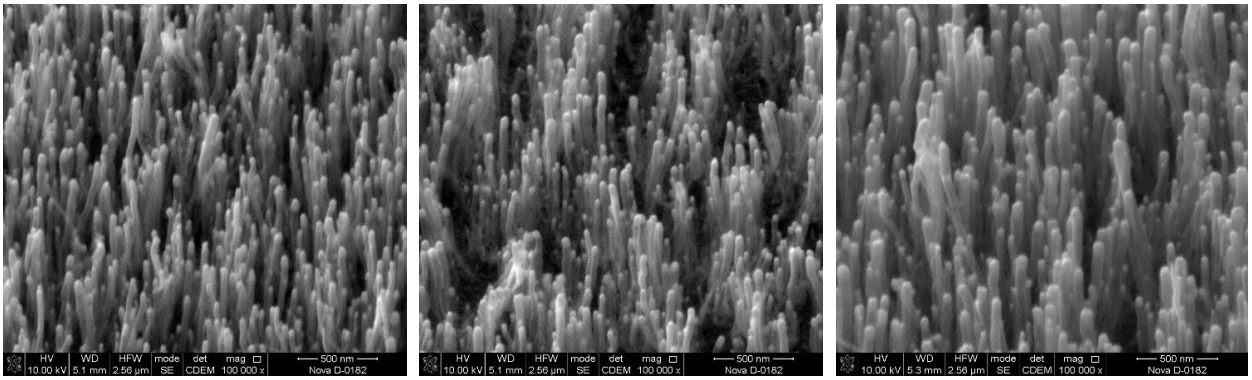

No. 1 No. 2 No. 3

Figure 1. SEM images of experimental samples of vertically aligned CNT arrays.

The studies of the mechanical parameters of the CNT arrays were carried out at the Ntegra probe nanolaboratory using a scanning hardness nanotester integrated in it. The indenter was the diamond tree-sided Berkovich pyramid with the apex angle θ =70º between the edge and height.

The nanoindentation method is as follows: the indentor is pressed into the CNT array at a constant speed to a given depth; the dependence of the load values on the corresponding depth of the indentetion is established [2]. The nanoindentation process was carried out with the application of loads of 100 μN at 20 different points of the CNT array distant about 10 μm from each other. The obtained load curves are shown in Figure 2. The obtained dependence of the penetration depth on the indentation force is nonlinear and has two parts: the regions of elastic and inelastic interactions.

The peculiarity of the nanoindentation method of a vertically aligned CNT array is that nanotubes have the bending strain during the process. Therefore, the calculation of the effective bending stiffness of CNTs is made on the basis of the elastic region of load curves. The elastic region was from 0 to 250 nm for sample No. 1, from 0 to 210 nm for sample No. 2 and from 0 to 250 nm for sample No. 3. Then the Young's modulus is calculated on its basis.

The Young's modulus of carbon nanotubes are calculated by the formula [2]:

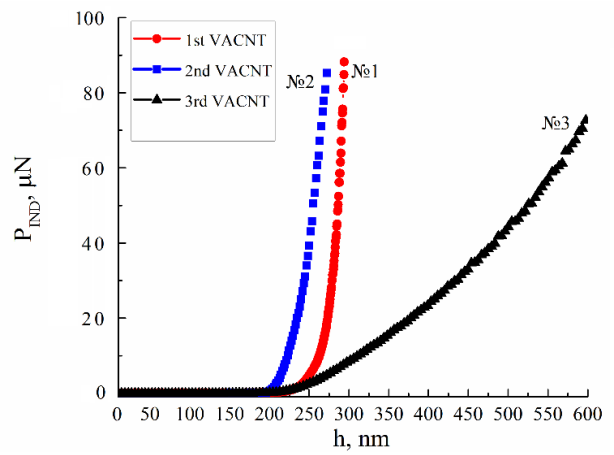

Figure 2. Load curves of vertically aligned carbon nanotubes for each sample.

$$E = \frac{64(P_{IN} - P_i)\cos\theta}{\pi i D^4 k^2},$$

where P_{IN} – indentation force, P_i – indentation force corresponding to the depth of the i-tube touch, i – amount of nanotubes interacting with the indenter at P_{IN}, D – a CNT diameter, $k = (P/(EI)_{eff})^{1/2}$ – the coefficient, $(EI)_{eff}$ – a effective bending stiffness of CNT.

The results of the studies showed that the Young's modulus is 1.15 TPa for sample No. 1 with aspect ratio 14.8, the Young's modulus is 1.29 TPa for sample No. 2 with aspect ratio 34, the Young's modulus is 0.59 TPa for sample No. 3 with aspect ratio 13.5 (Fig. 3). Thus the Young's modulus increases with increasing aspect ratio of CNTs. This is probably due to the fact that the number of defects in the structure of CNTs decreases with increasing their aspect ratio.

Thus, the dependence of Young's modulus of a vertically aligned carbon nanotubes on their aspect ratio is established experimentally. The obtained results are in good agreement with the literature data presented earlier [2,3]. The obtained results can be used to develop and creation of nanoelectronics devices based on vertically aligned CNTs in particular adhesion coatings and nonvolatile memory elements. The results were obtained using the equipment of REC and the Center for collective use "Nanotechnologies" of Southern Federal University.

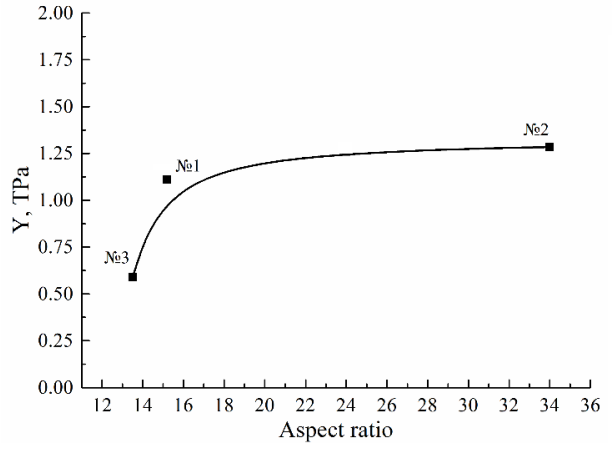

Figure 3. Dependence of the Young's modulus of the CNT on their aspect ratio.

The reported study was funded by RFBR according to the research projects No.16-29-14023 ofi_m, No.18-32-00652 and by grant of the Southern Federal University (project No. VnGr-07/2017-26).

1. Z. Ren, Y. Lan, Y.Wang. *Aligned Carbon Nanotubes, NanoScience and Technology* (Springer-Verlag Berlin Heidelberg) (2013).
2. O.A. Ageev, O.I. Il'in, A.S. Kolomiitsev, et al., *Nanotechnologies in Russia* **7**, 47 (2012).
3. O.A. Ageev, O.I. Ilin, A.S. Kolomiytsev, et al., *Advanced Materials Research* **894**, 355 (2014).

P-31

Influence of AC electric field on the charge generation in albumin solution in a flow-based AFM-fishing system

Yu.D. Ivanov[1], A.F. Kozlov[1], R.A. Galiullin[1], V.Yu. Tatur[2], V.S. Ziborov[3], N.D. Ivanova[4], T.O. Pleshakova[1]

[1]*Institute of Biomedical Chemistry, Moscow 119121, Russia*
e-mail: *yurii.ivanov@rambler.ru*

[2]*Foundation of Perspective Technologies and Novations, Moscow 115682, Russia*

[3]*Joint Institute for High temperatures RAS, 125412, Moscow, Russia*

[4]*Skryabin Moscow State Academy of Veterinary Medicine and Biotechnology, Moscow 109472, Russia*

Previously [1], with the example of albumin detection, we demonstrated that application of AC electric fields to AFM chips can well be used for the enhancement of sensitivity of proteomic AFM-fishing systems. This allowed us to attain 10^{-17} – 10^{-18} M detection sensitivity. As was noted in the same paper, the efficiency of albumin fishing correlated with the generation of charge, which occurred upon inflow of protein solution into the measuring cell.

The present study considers the influence of AC electric field on a charge accumulation in the measuring cell of a flow-based AFM-fishing system for the detection of low-abundant proteins. The charge is generated in a femtomolar (10^{-15} M) albumin solution, which is flowing through the injector of this system. It has been demonstrated that the sinusoidal electric field (100 V, 50 Hz) stimulates the accumulation of charge in the measuring cell upon inflow of protein solution at 38°C temperature. Accounting for this effect is important for the development of novel highly sensitive flow-based proteomic and diagnostic systems for AFM-fishing, as well as for the development of models describing the impact of electric field on hemodynamics and physico-chemical properties of water and aqueous solutions.

The work was supported by the Russian Ministry of Education and Science, Agreement No. 14.613.21.0063, universal identifier RFMEFI61317X0063.

1. T.O. Pleshakova, K.A. Malsagova, A.L. Kaysheva, et al., *FEBS Open Bio* **7**, 1186 (2017).

P-32

Influence of the focused ion beam parameters on the etching of planar nanosized multigraphene/SiC field emitters

I.L. Jityaev, A.M. Svetlichnyi, V.I. Avilov, I.N. Kots, A.S. Kolomiytsev, O.A. Ageev

Southern Federal University, Institute of Nanotechnologies, Electronics, and Electronic Equipment Engineering, 347900, Taganrog, Russia
e-mail: izhityaev@sfedu.ru

Nanoscale field emission structures are a promising element of nanoelectronics. The use of nanocarbon materials in field emission electronics contributes to improving the durability of the cathode, stability of emission and reduction of threshold voltages [1-3]. Multigraphene films obtained by the thermal destruction of silicon carbide in vacuum are considered in the work. This method is technologically efficient and allows one to obtain uniform multigraphene films suitable for electronic application. Semi-insulating silicon carbide was used as a substrate. The two-dimensional structure of the multigraphene film is used in the basis of the field emission nanostructure. The planar design of the field emission structure contributes to the emission of electrons from the end of the multigraphene film when a potential difference is applied. The field emission cathode was performed in the form of a point for increasing the form factor. Focused ion beams (FIB) of gallium were used to form field emission structures with a nanoscale interelectrode distance. The minimum interelectrode distance depended on the width of the ion beam.

The possibility of fabrication of planar field emission nanostructures based on multigraphene films on silicon carbide using FIB-technology is considered in this paper. Nova NanoLab 600 (FEI Company, Netherlands) ion-electron scanning microscope was used for etching experimental samples. Minimum currents (1-10 pA) were used to form the minimum possible interelectrode distance for this technology. An increase in current strength promotes an increase in lateral etching.

The possibility of applying FIB to fabricate planar emission nanostructures based on multigraphene on SiC and determining the effect of FIB-parameters on the etching of the structure were performed using a scanning probe microscope Solver P47 Pro (Nanotechnology MDT, Russia). Scanning of the FIB-processed areas allowed to determine the presence of etched areas and to estimate their depth. It was found that etching of planar field emission nanostructures at a current of 1 pA does not lead to a change in the depth of the treated area. An increase in current up to 10 pA becomes sufficient to initiate the etching process of a multigraphene film on the surface of silicon carbide. The etching depth increases with increasing etching time. The etching depth was considered sufficient when the silicon carbide was etched after the multigraphene film. The fulfillment of this condition is necessary for isolating the cathode from the anode.

Conductive probes were used for local studies of electrical properties of nanoscale structures. The pressure contact was located on the surface of the multigraphene film. The conductive probe was in contact with the investigated region. It was revealed that etched areas do not conduct electric current. This confirms that FIB-treated local sections of the multigraphene film are completely etched to semiinsulating silicon carbide. The contact of the conducting probe with the unetched area of the field emission cathode promoted the appearance of an emission current.

Thus, it is shown that fabrication of field emission structures with a nanoscale interelectrode distance is possible using FIB-technology. The use of a scanning probe microscope made it possible to determine the FIB-parameters for the fabrication of planar field emission structures, to monitor their geometric parameters and to carry out local measurements of electrical parameters.

The equipment of the Collective Usage Center “Nanotechnologies” and the Research and Educational Center "Nanotechnologies" of Southern Federal University was used for this study. This work was funded by Internal grant of Southern Federal University No. VnGr-07/2017-26.

1. R.V. Konakova, O.B. Okhrimenko, A.M. Svetlichnyi, et al., *Semiconductors* **49**, 1242 (2015).
2. I.L. Jityaev, A.M. Svetlichnyi, A.S. Kolomiytsev, et al., *IOP Conference Series: Materials Science and Engineering* **256**, 012021 (2017).
3. A.M. Svetlichnyi, I.L. Jityaev, *JETP Letters* **106**, 613 (2017).

P-33

EDX-analysis for thin films thicknesses determination

A.A. Kamenev[1], A.S. Mankevich[2]

[1]*CJSC SuperOx, Moscow, Russia*
e-mail: a.kamenev@superox.ru

[2]*LLC S-inovation, Moscow Russia*

Recent progress in thin film semiconductor technology requires using of express methods for film analysis, especially for measuring film thickness. From this point of view, energy-dispersive x-ray (EDX) analysis is rather promising. The technique is often based on conventional scanning electron microscope (SEM), which is quick and accessible. However, reliability and accuracy of film thickness measurement from EDX results can be insufficiently high.

The accuracy of the technique can be improved by performing EDX scanning at multiple acceleration voltages (AV). Primary electrons at 5-25 kV penetrate sample by 0.5-2 micrometers respectively, resulting in different EDX spectra. By comparing the spectra, accurate thickness measurements can be carried out. The spectra is usually compared and calculated with special software products like STRATAGEM.

This work is focused on measuring thickness of silicon films on sapphire substrates (SOS). SOS films are fine model samples to calibrate the technique due to their simplicity of preparation and analysis. The films were deposited via chemical vapor deposition (CVD) with thickness ranging from 80 to 800 nm. Microscopy studies were performed at LEO Supra 50 VP SEM (acceleration voltage 5-25 kV, magnification 5000 – 50000). EDX studies were performed at SEM Zeiss EVO 50 with EDX analyzer e2v Sirius SD IXRF. Calculation of film thickness using EDX spectra were performed by STRATAGEM software.

SOS film cross-section SEM images were used for thickness measurements. The same samples were analyzed with EDX technique to deduce correct Si film mass density value used by STRATAGEM software. The density was estimated as 1.9 ± 0.2 g/cm3. The density of Si- thin films is as different as Si-reference value because the real structure of thin films content defects like dislocations, strain etc.

The film thicknesses of another SOS samples were calculated using the calibrated software. The absolute error of thickness measurement is less than 50 nm (for films with thickness ranging from 200 to 1000 nm) while the error of a single acceleration voltage measurement is more than 100 nm.

The work was partly supported by the Ministry of Science and Education of Russian Federation under contract 14.579.21.0141.

P-34

Study of the combined effect of mechanical stress and high temperature on the switching field of submicron particles permilloy

T.F. Khanipov, D.A. Bizyaev, A.A. Bukharaev, N.I. Nurgazizov

Zavoisky Physical-Technical Institute, Federal Research Center "Kazan Scientific Center of RAS", Kazan 420029, Russian Federation
e-mail: timurkhanipov@gmail.com

Nowadays it is known that high density of data magnetic recording is able to be achieved using Heat Assisted Magnetic Recording (HAMR) on a separately located ordered particles. The general idea of this method is decreasing of coercitivity of ferromagnetic particles by heating each particle using pulse laser [1]. So investigation of influence of high temperatures on ferromagnetic particles switching field is in great interest now. On the other hand, rapidly developing scientific direction called "straintronics", that study effects in solid state materials caused by mechanical stress, predicts significant decrease of energy consumption for straintronic devices as compared with nowadays technologies. Considering this, in our work we tried to combine high temperature and mechanical strain influence on permalloy microparticles. The main problem is to find out how the simultaneous effect of heating and mechanical stress on the switching field of permalloy microparticles.

For that reason samples with submicron permalloy particles on silica substrate were prepared using scanning-probe lithography [2]. At first, investigations of only high temperature on switching field were carried out. For this reason sample without induced mechanical strain was manufactured. Another sample was manufactured as it described in paper [3]. Permalloy with negative magnetostriction (Ni 79%, Fe 16%, Mo 4%) was deposited on the surface of bended substrate through the lithography mask. Permalloy film was deposited 50 nm thick. After that substrate was straightened and compression strain was induced in the particles. On the single substrate two arrays of the particles were manufactured for the reason to research arrays with perpendicular direction of the long axises to the direction of compression. Lateral size of the particles was about 1350×350 nm (Fig. 1).

Experiments were carried out on Solver VH (NT-MDT) scanning probe microscope. First of all, all particles in array were magnetized in external magnetic field to the one of the directions along their long axis. After that, in vacuum state particles were heated up to the necessary temperature and cooled down in external magnetic field of the opposite direction. At the next step, using magnetic-force microscopy, we counted the particles that changed the direction of their magnetization. Cycle repeated for the constant temperature, increasing the magnetic field until all particles switched.

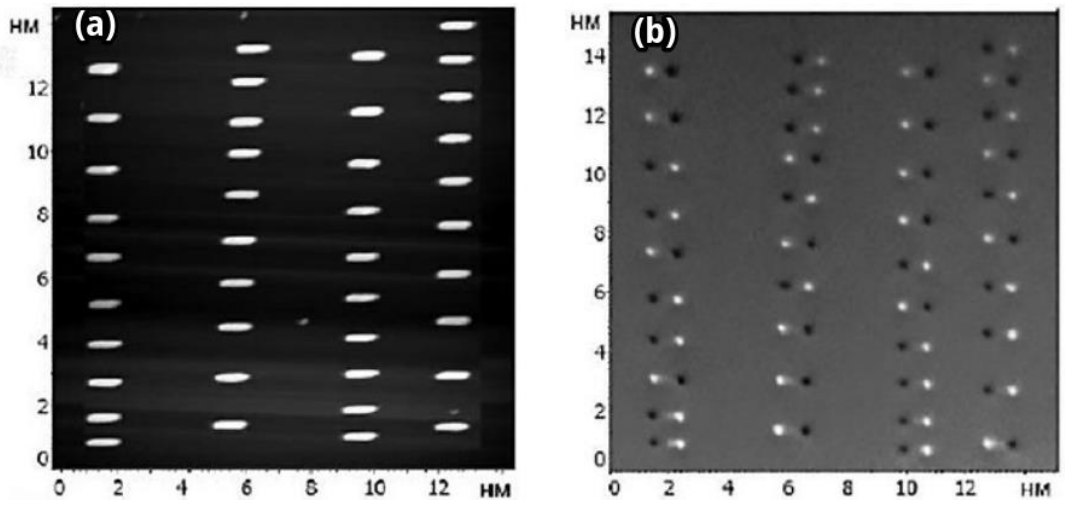

Figure 1. (a) Atomic-force microscopy image of topography of strained permalloy array particles, (b) Magnetic-force microscopy image of the same particles.

During researching the sample without induced strain, temperature dependence of the switching field graphs was built. Temperature range was from 300 K to 800 K. After analysis of the graphs it was shown that field that is necessary to switch the magnetisation of all particles decrease from 700 Oe at 300 K to 180 Oe at 800 K [4].

Stressed sample was studied for both orientations of long particle axises relatively to induced strain direction at a temperature of 100°C (373 K) before heating at 300°C (673 K) and after heating. Previously, it was shown that all kind of strain disappear in permalloy particles of this composition after heating at 300°C.

As a result, of further researches magnetic field dependence of number of switched particles was built at 100 °C before heating and after heating for both of orientations of the particles. So it was shown, that induced mechanical strain changes the switching field of the permalloy particles on about 9 Oe. This change may increase or decrease switching field of the particles depending on direction of the long axises relatively to the direction of strain and magnetostriction sign.

1. Y. Inaba, H. Nakata, D. Inoue, *Fuji Electric Review* **57**, 42 (2011).
2. D.A. Bizyaev, A.A. Bukharaev, S.A. Ziganshina, et al., *Russian Microelectronics* **44**, 389 (2015).
3. D.A. Bizyaev, A.A. Bukhraev, Yu.E. Kandrashkin, et al., *Technical Physics Letters* **42**, 1034 (2016).
4. N.I. Nurgazizov, T.F. Khanipov, D.A. Bizyaev, et al., *Physics of the Solid State* **56**, 1817 (2014).

P-35

Defect mechanism and electrical properties of $BiFeO_3$ based ceramics

J.C. Kim[1], C.-M. Park[1], S.B. Baek[1], T.K. Song[1], W.-J. Kim[2], T.G. Park[3], M.-H. Kim[1]

[1]*School of Materials Science and Engineering, Changwon National University, Changwon,Gyeongnam 51140, South Korea*
e-mail: mhkim@changwon.ac.kr

[2]*Department of Physics, Changwon National University, 51140, Changwon, South Korea*

[3]*Department of Electrical Engineering, Changwon National University, 51140, Changwon, South Korea*

Bismuth ferrite ($BiFeO_3$) is ABO_3 system with multiferroic. *A/B*-site modification in bismuth ferrite is expected to exhibit interesting ferroelectric and conduction properties. In this work, aliovalent cations modifications were carried out in order to improve the structural, dielectric and high-temperature conduction performance of the materials. The polarization response and dielectric properties were improved by the addition of small amount of *A/B*-site cations (Ba^{2+}/Ti^{4+}) and optimal amount of Bi_2O_3 in BFO ceramics. To better understand the effects of defects, the equilibrium electrical conductivity was investigated under various oxygen partial pressures (pO_2) at high temperatures.

P-36

Microstructure and luminescent properties of transparent $MgAl_2O_4$ nanoceramics

A.N. Kiryakov[1], A.F. Zatsepin[1], V.A. Pustovarov[1], T.V. Dyachkova[2]

[1]*Ural Federal University, 620002, Yekaterinburg, Russia*
e-mail: arseny.kiriakov@urfu.ru

[2]*Russian Academy of Sciences Urals Branch Institute of Solid State Chemistry, 620137, Yekaterinburg, Russia*

Transparent ceramics of aluminum-magnesium spinel (AMS) are actively investigated. Optical transparent window from 0.2 to 5 microns, heat resistance, corrosion resistance, radiation resistance allow the use of such ceramics in such fields as laser technology, IR windows of homing missiles, armor, etc [1]. The inherent defectiveness, as well as morphological features of the surface, affect greatly lots of $MgAl_2O_4$ functional properties. The disadvantage of such ceramics is utilizing of LiF additives for transparency obtaining. Thermobaric treatment of AMS nanopowders allows to obtain transparent nanoceramics without LiF. Such ceramics are poorly investigated and of interest for practical applications.

Nanopowder of alumomagnesium spinel was obtained by reverse deposition method using aluminum and magnesium nitrates. Monophasic $MgAl_2O_4$ nanopowder was synthesized by quenching the resulting gel to 1000ºC. The thermobaric treatment was carried out at pressure of 5 GPa and 600°C temperature for 30 min. The powder was annealed preliminarily in vacuum at T = 500°C for 3 hours in order to desorb air.

The surface structure was studied using SIGMA VP scanning electron microscope (Carl Zeiss, Germany) and secondary electron detector (In-lens) in high vacuum at 3 kV accelerating voltage.

The photoluminescence spectra were measured by apparatus equipped with DFR-4 type double prism monochromators using a 400 W deuterium lamp and R-6358-10photomultiplier (Hamamatsu).

Investigated ceramics had a grain size ≤50 nm with spread not more than 20 nm according to SEM data (Fig. 1). Apparently, grain growth was inhibited by plastic deformation processes that were occurring during thermobaric processing [2]. Narrow grain size distribution can also be attributed to similar processes.

The photoluminescence spectra contained two 1.7 and 2.4 eV bands (Fig. 2). The 2.4 eV band was most effectively excited at photon energies of 3.9 eV, and the 1.7 eV band in the 4.85 eV region.

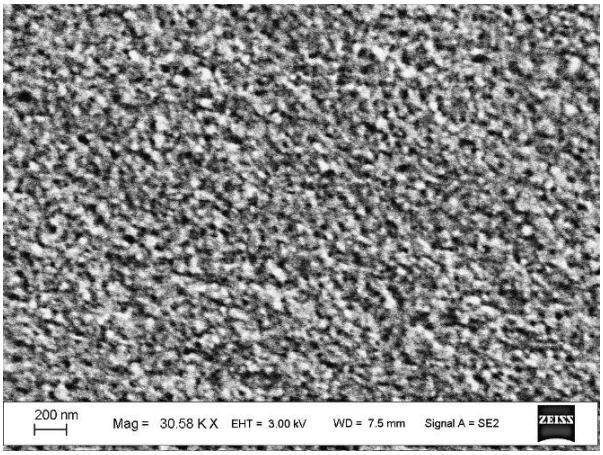

Figure 1. SEM of $MgAl_2O_4$ nanoceramics fragment.

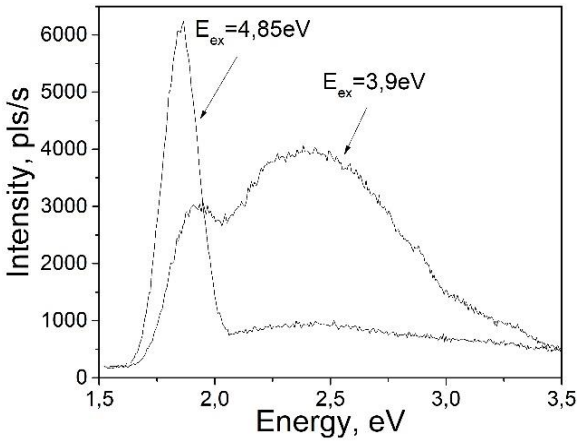

Figure 2. Luminescent spectra of nanoceramics measured at T=295K.

It is known that the Ti^{3+} impurity ions in alumomagnesium spinel contain a narrow band 1.73 eV with maximum excitation of 4.75 eV in PL spectrum [3]. Luminescence at 2.4 eV can be caused by Mn^{2+} ions impurity in tetrahedral position of magnesium [4]. It is interesting that this luminescence band has a half-width more than the one discussed in literature, and excitation energy does not coincide with the values known for single crystals. Additional EPR spectra measurements (not shown in this abstract) allowed us to conclude that there were Mn^{2+} impurity ions in studied ceramic (the presence of hyperfine splitting characteristic of Mn^{2+}).

Observed effect of luminescent bands broadening can be likely associated with grain size decrease [5]. The broadening of spectral lines is usually observed at a grain size of 10 nm or less because of emerging quantum constraints. Broadening was observed at 50 nm in studied samples which may be attributed to the size effect.

1. S.F. Wang et al. *Progress in Solid State Chemistry* **41**, 20 (2013).
2. J. Zhang et al. *Journal of Physics D: Applied Physics* **42**, 052002 (2009).
3. T. Sato et al. *Journal of Luminescence* **114**, 155 (2005).
4. V. Singh et al. *Journal of solid state chemistry* **180**, 2067 (2007).
5. Sch. Hobbutiya et al. *Russian medical journal* **53** (2012).

P-37

Change in the surface density of immobilized enzyme molecules due to photoelectron processes in a silicon substrate

A.V. Kozlowski, E.D. Kiseleva, A.A. Maslennikova, S.V. Stetsyura

Saratov State University, 410012, Saratov, Russia
e-mail: kozlowsky@bk.ru

Atomic force microscopy (AFM) and Kelvin probe force microscopy (KPFM) are an effective methods for monitoring the surface of hybrid and biosensor structures based on silicon substrate and organic components (such as enzyme, DNA, bacteria, etc.).

In our work, AFM and KPFM has been used to study of influence of both the Si illumination during enzyme deposition and salt concentration in enzyme solution on the density of adsorbed enzyme molecules.

The experiments were performed with single-crystal silicon wafers of n-type ($\rho \cong 4\ \Omega$ cm) and p-type ($\rho \cong 8\ \Omega$ cm) with layer of amorphous silicon (a-Si). Initially, the substrates were boiled in a peroxide–ammonia solution and rinsed in deionized water (resistivity 18 MΩ). This treatment leads to "reconstruction" of a native oxide layer while the silicon surface acquires negative charge in deionized water due to activation of OH-groups. Glucose oxidase (GOx) molecules from *Aspergillus niger* was used as enzyme molecules. In a wide pH range of the solution, the GOx molecule have an effective negative charge. The size of the GOx molecule is $6.0\times5.2\times7.7$ nm^3 [1]. A cationic polyelectrolyte polyethylenimine (PEI) with a molecular weight of 25 kDa was used to increase the adsorption of negatively charged GOx onto silicon substrates. The PEI molecules were adsorbed onto silicon substrates from the 1 mg/ml aqueous solution during 10 min followed by rinsing in water during 10 min and drying. The photo-assisted layer-by-layer adsorption technique suggested in [2] was used to adsorb GOx from the 0.5 mg/ml aqueous solution of both with and without NaCl onto bare substrates and covered with PEI silicon substrates. The NaCl concentration was varied from 0.01 M to 0.1 M.

The topography and surface potential of the films were measured using AFM and KPFM by NTGRA Spectra (NT-MDT Spectrum Instruments, Russia). Scanning was performed under ambient conditions at a frequency of 0.5 Hz in taping mode using HA_NC/W_2C cantilevers of ETALON series. The Gwyddion software for statistical analysis of AFM data was used.

Analyzing AFM micrographs of adsorbed GOx molecules on p-Si/a-Si and n-Si/a-Si substrates, we found that adding a small amount of salt to the GOX solution results in a decrease in adsorption. However, further an increase in the salt concentration in the solution leads to an increase in both the number of adsorbed enzyme molecules and the size of the irregularities. Without illumination, the amount of adsorbed particles is larger on the p-Si/a-Si/PEI structure and smaller on the n-Si/a-Si/PEI structure. However, the illumination of the silicon substrate during the adsorption process alters the adsorption significantly: on the p-Si/a-Si/PEI surface, the number of adsorbed particles decreases, while on the p-Si/a-Si/PEI surface, there is a pronounced increase in the amount of adsorbed particles. These data correlate with the KPFM data.

Thus, using the methods of scanning probe microscopy, it has been shown that the adsorption of enzyme molecules is substantially depends on the ionic strength of the solution, the conductivity type of Si substrate as well as on photoelectron processes in semiconductor.

The work was supported by the Russian Foundation for Basic Research, projects no. 16-08-00524.

1. H.J. Hecht, H.M. Kalisz, J. Hendle, et al., *J. Mol. Biol*. **229**, 153 (1993).
2. I.V. Malyar, D.A. Gorin, S. Santer et al., *Langmuir* **29**, 16058 (2013).

.

P-38

In vivo toxicity of Al_2O_3, TiO_2 and SiO_2 nanoparticles acting in different combinations and its alleviation with a complex of bioprotectors

I.A. Minigalieva[1], S.V. Klinova[1], L.I. Privalova[1], V.G. Panov[2], O.H. Makeyev[3], I.E. Valamina[3], E.V. Shishkina[4]

[1]*The Medical Research Center for Prophylaxis and Health Protection in Industrial Workers, 620014, Ekaterinburg, Russia*
e-mail: klinovasv@ymrc.ru

[2]*Institute of Industrial Ecology, the Urals Branch of the Russian Academy of Sciences, 620219, Ekaterinburg, Russia*

[3]*The Central Research Laboratory of the Ural Medical University, 620028, Ekaterinburg, Russia*

[4]*School of Natural Sciences and Mathematics, Ural Federal University, 620002, Ekaterinburg, Russia*

For the animal experiment, stable water suspensions of nanoparticles (NPs) were obtained by laser ablation of 99,99% pure elemental aluminum, titanium or silicon under a layer of deionized water. Male outbred rats with initial body mass 290 g were injected intraperitoneally 3 times a week (up to 18 injections) with suspensions of Al_2O_3-NP, TiO_2-NP or SiO_2-NP in doses 0.25, 0.5 and 0.5 mg per rat, respectively, either separately, or in binary, or in ternary combinations of the same doses, the controls receiving injections of deionized water in the same volume. Toxic effects where estimated with a lot of functional, biochemical and morphometric indices for the organism's status. The results obtained demonstrated that, in many respects, the Al_2O_3-NP was the most toxic as such and the most dangerous component of the studied combinations. Mathematical modeling with the help of the Response Surface Methodology has shown that the organism's response to a simultaneous exposure to any two of the element oxide (ElO) NPs under study is characterized by all possible types of combined toxicity (additivity, subadditivity or superadditivity of unidirectional action and different variants of opposite effects) depending on which outcome this type is estimated for as well as on the levels of the effect and dose. With any third ElO-NP species acting in the background, the type of combined toxicity displayed by the other two ElO-NPs can change significantly. Many adverse effects produced in rats by the combined [Al_2O_3-NP+TiO_2-NP+SiO_2-NP] exposure, including the genotoxic one, were substantially attenuated by per oral administration of a complex of innocuous bioprotective substances during the entire exposure period.

P-39

Flexible anodic alumina nanomembranes

A.N. Kokatev, S.G. Vasiliev, N.M. Yakovleva, M.A. Terletskaya, E.A. Chupachina

Petrozavodsk State University, 185910, Petrozavodsk, Russia
e-mail: nelan-oksid@bk.ru

Traditional technique of alumina membranes production, based on two-step anodizing, was studied. Besides, some disadvantages, such as fragility, time-consuming technique of obtaining membranes and necessity of using a special holder, were also stated. Since their main disadvantage is high fragility, it is necessary, firstly, to create more flexible flat membranes, and, secondly, to form cylindrical nanomembranes, called "tubular".

Samples were made of 50 and 100 μm thick aluminium foil, both flat and in the form of a tube with a diameter of 6-7 mm. Before anodization samples were annealed at 450°C for 30 minutes and chemically cleaned in diluted NaOH. Studying of samples' structure was carried out by Atomic Force Microscopy in tapping mode on Scanning Probe Microscope "Solver-Next" NT-MDT. To obtain images, both standard (NSG01) and high-resolution diamond-like cantilevers (NSG10 DLC) were used.

We implemented two-step anodizing technique. For anodizing we used water solution of oxalic acid as an electrolyte at the 1st stage; and a special multicomponent (mixture of oxalic, citric, and boric acid as well as isopropyl alcohol) electrolyte for the 2nd stage to prepare flexible films.

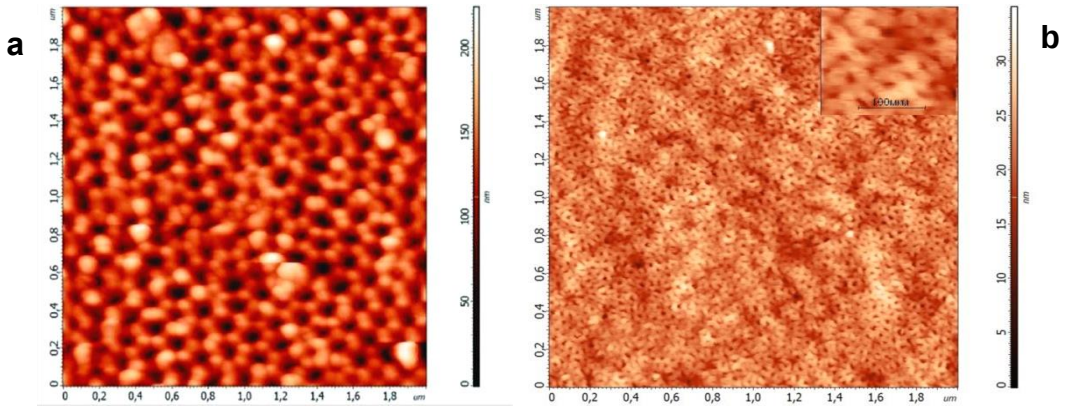

Figure 1. AFM images of: (a) porous layer surface of porous anodic alumina films, (b) barrier layer after their thinning.

From AFM images we got an approximate size of cells (250 nm) and pores (80 nm). It is found that the resulting anodic oxide film had increased elasticity and ability to withstand bending angle of 120°. For removal of films' barrier layer we used a method of barrier layer thinning "from above". For that, sequential decrease in voltage was carried out, which led to stepwise reduction of the current. Reaching the zero (or close to zero) value meant appearing of barrier layer permeability.

The next stage in fabrication of nanomembrane was removal of metal in a solution based on $CuCl_2$. After that we got partly permeable membranes, as it is shown in Figure 1a,b. It is seen that this procedure leads to generation of holes of about 20 nm from the side of the barrier layer.

Thus it has been shown that the developed two-step anodizing technique using special multicomponent electrolyte at the 2nd stage allows forming nanoporous alumina films of high flexibility. We found that a method of barrier layer thinning "from above" in combination with chemical removal of metal enables permeable alumina membranes fabrication.

P-40

Fabrication of probes for scanning near-field optical microscopy using focused ion beam

A.S. Kolomiytsev, N.A. Shandyba, I.V. Panchenko, S.A. Lisitsyn

Southern Federal University, 344006, Taganrog, Russia
e-mail: askolomiytsev@sfedu.ru

At the present stage of nanotechnology development one of the most promising methods of surface diagnostics is scanning probe microscopy (SPM). The use of SPM methods makes it possible to study the local geometric, electrical and mechanical properties of the substrate surface, as well as to form nanoscale structures on the surface of solids [1]. The perspective direction of SPM is scanning near-field optical microscopy (SNOM), which significantly allows to increase the optical microscopy resulution and provide reliable control of the distance between the tip and the sample. SNOM is a microscopy technique for nanostructure investigation that breaks the far field resolution limit by exploiting the properties of evanescent waves. In SNOM, the excitation laser light is focused through an aperture with a diameter smaller than the excitation wavelength, resulting in an evanescent field (or near-field) on the far side of the aperture [2]. When the sample is scanned at a small distance below the aperture, the optical resolution of transmitted or reflected light is limited only by the diameter of the aperture. One of the main problems in SNOM technology is the creation of probes with a controlled aperture size. The use of traditional technological processes does not allow to vary the aperture diameter and create probes for SNOM of the required shape. The application of new methods of local nanostructuring makes it possible to form probes of various geometric shapes for specialized methods of SPM and SNOM. One of the most promising methods for the formation of nanoscale structures with high accuracy and resolving power is the method of focused ion beams (FIB) [3,4]. The FIB method allows to perform technological operations of local ion beam etching and ion-induced deposition of materials from the gas phase without the needs of resists, masks and chemical etchants. A wide range of materials deposited by this method allows the use of FIB in the formation of nanoscale structures probes for nanodiagnostics. The aim of this work is to create probes for scanning near-field optical microscopy using the FIB method and their experimental study [5].

Traditionally, FIB technology is used to etch the tip of the probe through and thus forming an aperture probe. However, this approach has several disadvantages: the small diameter of the aperture inlet, the complexity of aligning the aperture with the axis of the probe tip, the negative effect of the redeposited material. To eliminate these drawbacks, it is proposed to use the ion-induced deposition method to form a hollow tip of a probe with a controlled aperture diameter.

Experimental studies were carried out using a Dual beam (FIB-SEM) system Nova NanoLab 600 (FEI Company) and the Ntegra Vita scanning probe microscope (NT-MDT, Russia). The standard AFM cantilevers NSG-10 (NT-MDT, Russia) with broken probes due to operation were used as a substrate. At the initial stage of the formation of a new probe tip by ion-beam etching removed part of the beam containing silicon tip. The ion-beam etching current was 20 nA.

At the next stage of the research, a through hole was formed in the cantilever beam using focused ion beam milling on Nova NanoLab 600 system. The resulting hole of 5 μm in diameter is the input for optical radiation in the SNOM method (Fig 1a).

After forming the hole through the beam, gas C6H14 was supplied to the area of the formed hole through the gas injector, which, when interacting with the gallium ion beam with an energy of 30 keV, decomposed into volatile components (which were immediately removed by the vacuum system of the microscope) and solid carbon, which was deposited on the surface. The trajectory of the ion beam was determined by digital patterns so that the deposition of carbon occurred in an orderly manner from the base of the cone (about 5.5 μm in diameter) to its tip. The result was a conical tip formed by the edge height of about 5-6 microns (Fig 1b).

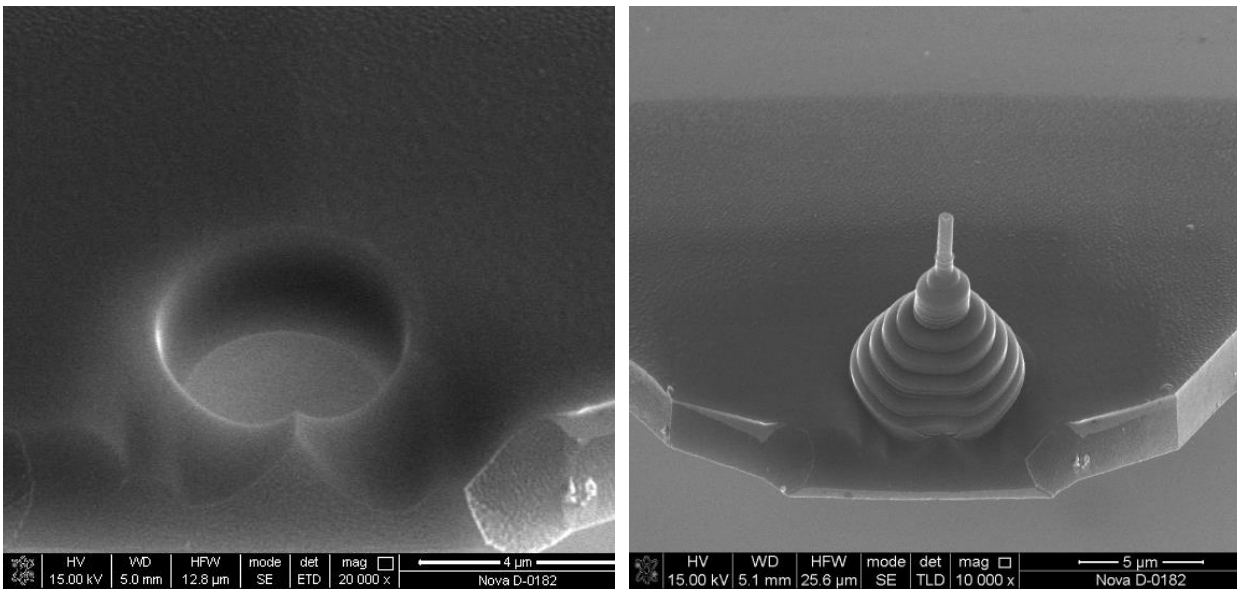

(a) (b)

Figure 1. (a) SEM images of the 5 μm hole in the cantilever and conical aperture probe, (b) fabricated by FIB-induced deposition.

After that, at the end of the cone by ion-beam etching at low ion beam currents, an outlet for optical radiation with a diameter of 50-200 nm was formed. The main advantage of the proposed technology is the ability to form probe tips of different shapes and sizes. The probe shown in Figure 1b has a tip radius of about 200 nm, which also allows it to be used to obtain AFM images.

The fabricated probes have been tested, and it has been found that the probes created by this method have a longer service life as an AFM measurement tool. In addition, the ability to vary the diameter of the aperture makes it possible to form optimized probes for the desired wavelengths. The ability to form aperture SNOM probes based on broken cantilevers makes it possible to significantly improve the economic efficiency of the proposed technology.

The results obtained in the study can be used in the development of technological processes for the fabrication and modification of special aperture probes for scanning near-field optical microscopy, and in the development of procedures for the express monitoring of parameters of the technological process for manufacturing elements for micro- and nanoelectronics and micro- and nanosystems engineering.

The results were obtained using the infrastructure of the Center for Shared Use “Nanotechnology” of the Southern Federal University.

1. M. Soliman et al, *J. Phys.: Condens. Matter* **29**, 173001 (2017).
2. Wu Xiao-Yu et al, *Chinese Phys. B* **24**, 054204 (2015).
3. B.G. Konoplev, O.A. Ageev, V.A. Smirnov, et al., *Russ. Microelectron* **41** (2012).
4. O.A. Ageev, Al.V. Bykov, A.S. Kolomiitsev, et al., *Semiconductors* **49**, 13 (2015).
5. O.A. Ageev, A.S. Kolomiytsev, A.V. Bykov, et al., *Microelectron. Reliab*. **55**, 2131 (2015).

P-41

Investigation of geometric characteristics of the titanium alloy surface subjected to magnetic-impulse processing by means of SPM

A.S. Pomel'nikova, A.V. Komshina, A.S. Komshin, A.B. Syritskii

MSTU Bauman, 105005, Moscow, Russia
e-mail: komshin_as@mail.ru

With the development of nanotechnology, obtaining surface properties by coating and improving the properties of the surface layer becomes essential. However, it is important to move from property research to the measurement of the geometric parameters of the surface, taking into account the traceability of measurements of linear dimensions in the nanometer range [1].

In addition, when switching to submicron and nanometer ranges, special attention should be paid to both environmental parameters and measurement techniques. One example is the measurement of roughness parameters of the surfaces using scanning probe atomic force microscope. The paper presents the study of the surface properties of titanium alloy products after magnetic-pulse processing (m & e).

It is established that the use of m & e provides smoothing of the surface of small micronutrients of parts. The detected effect of roughness reduction is associated with the melting of micro-steps and facilitation of micro-deformation of the surface layer, as well as due to the impact on the metal of the main and reflected shock waves, which leads to microplastic deformation on the surface. [2]. The reduced surface roughness RA was reduced from 0.125 μm (reference sample) to 0.032 μm (reference sample after MIO) [3].

It is also essential that, from the metrological point of view, the area of measurement of the obtained surface characteristics is at the level of 12-14 purity class, which in turn meets the requirements of measuring the effective surface roughness height in the submicron range using SPM. The results of the analysis of the profiles obtained by scanning probe microscope Solver P - 47 show that the measured altitude values of the roughness correspond to the size of the scanning area 256x256 points (3x3 microns) reduced roughness values at 0.03-0.05 microns.

Figure 1 shows an example of the surface obtained with the Solver p-47 SPM.

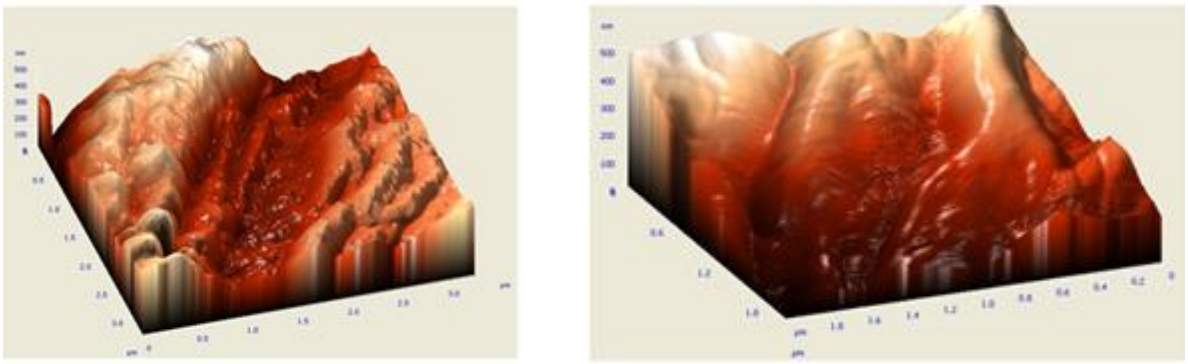

(a) (b)

Figure 1. (a) Initial sample; (b) Sample after MIO.

The paper deals with the practical application of the method of magnetic-impulse processing in order to improve the surface properties of titanium alloys on the example of VT23, the methods of evaluation and elimination of measurement errors in order to implement measures of metrological support in production conditions in the interests of industry on the example of practical application of scanning probe microscopy [4].

1. K. Gogolinsky et al., *Nanoindustry* **1**, 48 (2012).
2. V. Konshin, A.S. Pomelnikova et al., *Technology of metals* **1**, 22 (2013).
3. A.V. Komshin, A.S. Pomelnikova, N. Nochovnaya, *Metallography and heat treatment of metals* **6**, 50 (2015).
4. A.S. Komshin, A.B. Siritzky, *Nanoengineering* **4**, 14 (2014).

P-42

Control of operational properties of the structural materials using AFM and SEM methods

A.S. Komshin, E.V. Maslennikova, S.R. Orlova

MSTU Bauman, 105005, Moscow, Russia
e-mail: komshin_as@mail.ru

In technology find widespread practical the use of string and string elements. In the field of measuring technology, there are many devices in which the sensitive elements are elements in the form of strings: strain gauges, accelerometers, crack meters, etc. String sensors are widely used due to its simplicity and low cost.

It is no secret that during the testing and operation of structural materials subject to various loads and stresses, structural materials "slowly" change their properties. A significant role is played by the measurement of degradation of the properties of structural materials in time during operation, metrological support of measurements, etc. [1]

The concept of the proposed study is based on the hypothesis that the rate of degradation can be significantly influenced by factors such as the topography of the surface, especially in the elemental and chemical compositions, which also need to be taken into account. The use of phase-chronometric method with the theory of reduction of measurements opens up new opportunities to study the behavior and degradation properties of structural materials, including elastic and rheological [2].

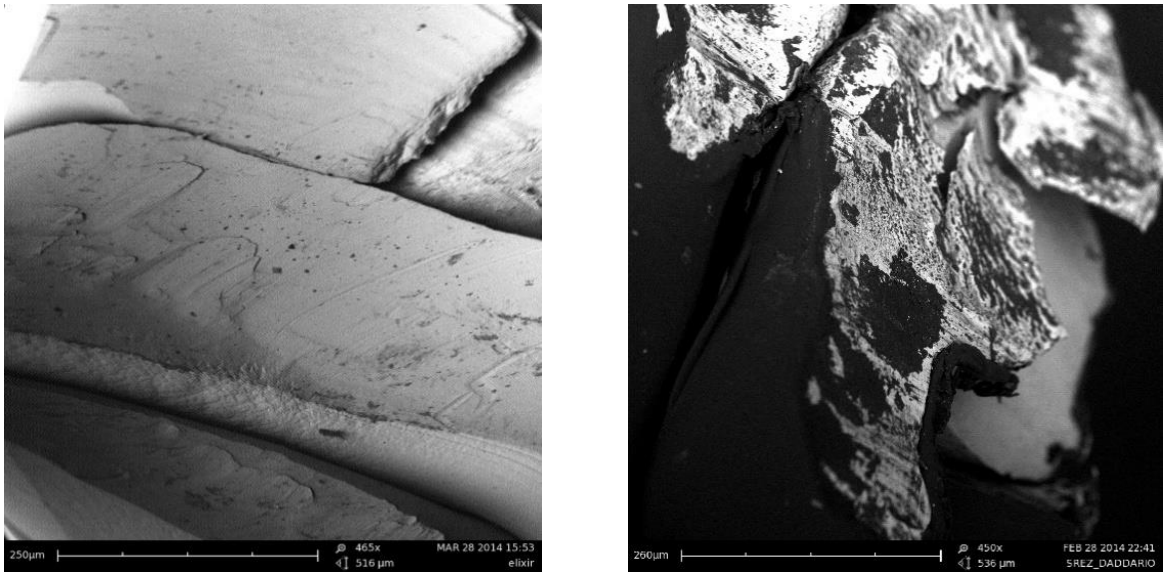

(a) (b)

Figure 1. The surface of (a) the string Elixir PolyWeb and (b) the string D'addario EXP26 obtained by REM.

The paper presents the results of studies of the surface of the strings of various manufacturers by atomic force microscopy (AFM) and scanning electron microscopy (SEM), which provide the study of topography and surface structure. The results of elemental and chemical analysis by cattle, Auger spectroscopy, and IR spectroscopy are presented.

1. A.S. Komshin, S.R. Orlova, *Measurement Techniques* **59**, 589 (2016).
2. A.S. Komshin, *Measurement Techniques* **53**, 976 (2010).

P-43

Application of atomic force microscopy to studying of aluminum nanopowder

E.K. Kosareva[1], N.V. Muravyev[1], R.V. Gainutdinov[2], A.N. Pivkina[1]

[1]*Semenov Institute of Chemical Physics RAS, 119991, Moscow, Russia*
e-mail: catherine.kos@yandex.ru

[2]*Shubnikov Institute of Crystallography of FSRC "Crystallography and Photonics" RAS, 119333, Moscow, Russia*

Present study reports a detailed investigation of aluminum nanopowder ALEX (ALuminum Electro-eXploded) using various atomic force microscopy methods, *i.e.*, Kelvin probe force microscopy, force modulation methods, AFM spectroscopy, and capacitance contrast method. Nowadays aluminum nanopowder is considered as highly promising component of energetic formulations due to its higher reactivity towards oxidation, incremented burning rate and combustion efficiency, shortened ignition delays and agglomerate burning time with respect to compositions containing micron-sized metal.

However, drawbacks of Al nanopowders include the lowered active metal content and high electrostatic discharge (ESD) sensitivity. Thermal analysis experiments revealed the active metal content to be 84 wt.% with the rest of material appeared to be an aluminum oxide cover.

Application of the above AFM methods enabled to not only build the particle size distribution, but also to map local properties such as hardness, surface potential, and volume distribution of capacity. The last two parameters are of the paramount importance to study the ESD-sensitivity for Al nanopowders and its compositions. The particle size distribution data were confirmed by laser diffractometry, and AFM-obtained microscopic properties were compared with existing macroscopic characteristics of ALEX powder.

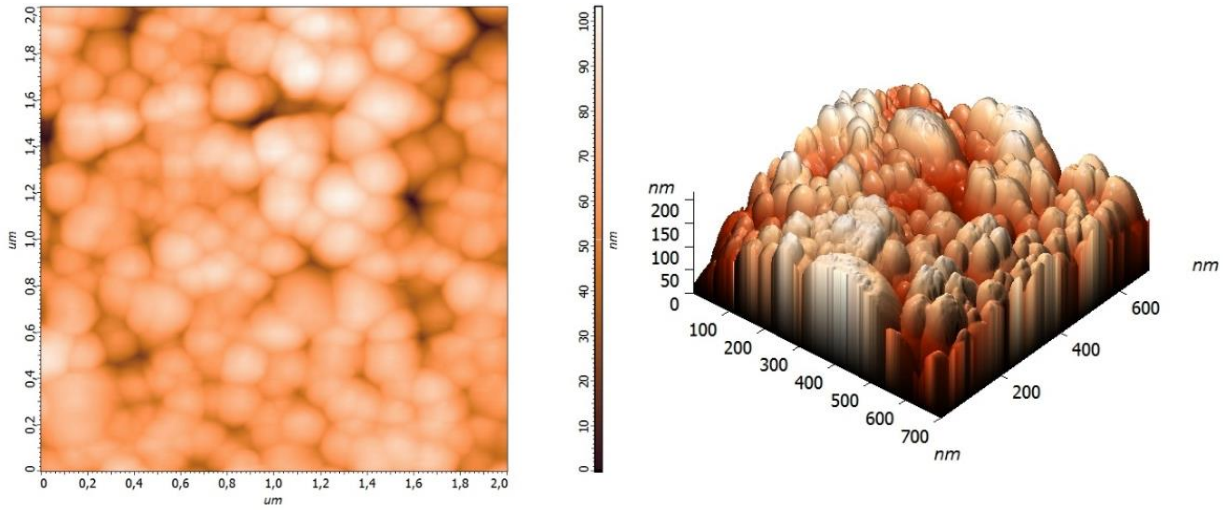

Figure 1. Contact (2D) and semicontact (3D) topography images of ALEX.

P-44

Masking layer formation on silicon substrate by the focused ion beams method for plasma-chemical treatment

I.N. Kots[1], V.S. Klimin[1,2], A.A. Rezvan[1], V.V. Polyakova[1], O.A. Ageev[2]

[1]*Institute of Nanotechnologies, Electronics, and Electronic Equipment Engineering, Southern Federal University, 347928, Taganrog, Russia*
e-mail: inkots@sfedu.ru

[2]*Scientific and educational center "Nanotechnologies", Southern Federal University, 347928, Taganrog, Russia*

At present, the question arises of mastering new methods of nanoscale profiling. Optical lithography today is the simplest and most technologically advanced method of forming structures with tens of nanometers in size. However, this method has reached its limit in the field of hard ultraviolet. The method of focused ion beams (FIB) is based on the interaction of accelerated ions with the surface of the substrate, which allows it to be modified with gallium ions and subsequently used for plasma-chemical etching (PCE). The PCE method, firstly, is based on the chemical interaction of the ionized working gas with the substrate, and secondly, on the ions physical interaction of the working gas with the sample surface [1-4].

The studies were performed using a scanning electron microscope (SEM) Nova NanoLab 600 (FEI company, Netherlands), a plasma etching device in an inductively-coupled plasma STE ICP E68 (NTO, Russia) and a scanning probe microscope Ntegra Vita (NT-MDT, Russia).

At the initial stage of experimental studies using the FIB method, the silicon surface was modified by a template with dimensions of 5x5 μm, with parameters with a minimum diameter of the ion beam, but with different number of its passes at each point (Fig. 1).

After that, the samples were subjected to plasma-chemical etching in a fluorine-containing plasma at powers of W_{ICP} = 200 W, W_{RIE} = 10 W, etching time of 30 and 120 seconds.

At the next stage, the samples were studied by atomic force microscopy (AFM) (Fig. 2). Scanning was carried out by a semi-contact method.

When the ion beam is applied to the silicon substrate surface, the material is modified. Further, the modified regions exhibit a masking effect. So, with the number of passes 10 and the etching time in the plasma of 30 seconds, the height of the obtained structures was 10 nm, and with an increase in the number of passes to 100 and the etching time to 120 seconds, the height of the resulting structures reached 250 nm. This is explained by the number of gallium ions implanted in silicon, which react with the working gas much less than silicon.

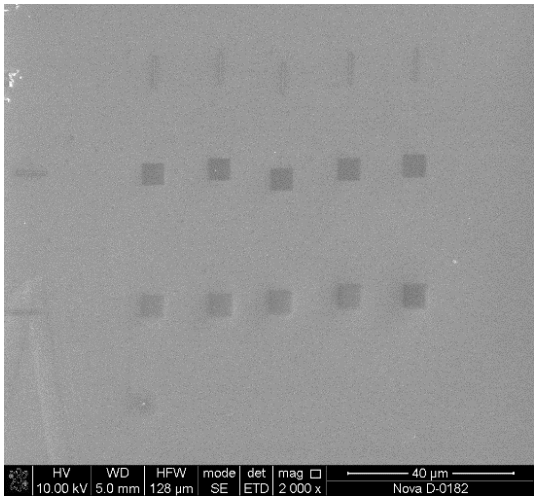

Figure 1. SEM image of an obtained structures array.

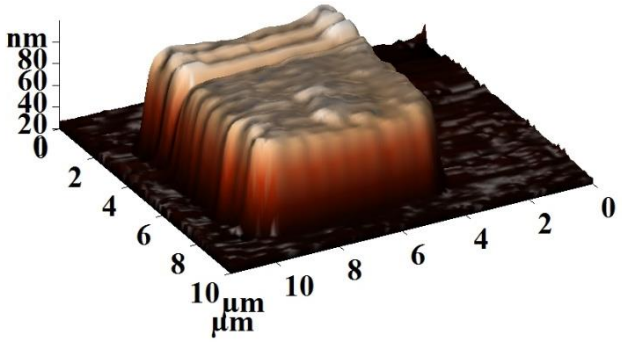

Figure 2. AFM the formed structure image after PCE.

This work was carried out using the equipment of the scientific educational center and the center of collective use "Nanotechnology".

1. I.N. Kots, V.S. Klimin, A.S. Kolomiitsev, et al., *Physics and Mechanics of New Materials and their Applications (PHENMA 2017)*, 123 (2017).
2. I.N. Kots, V.S. Klimin, A.S. Kolomiitsev et al., *Physics and Mechanics of New Materials and their Applications (PHENMA 2017)*, 122 (2017).
3. O.A. Ageev, A.S. Kolomiytsev, A.V. Bykov, et al., *Microelectronics Reliability* **55**, 2131 (2015).
4. O.A. Ageev, A.S. Kolomiytsev, B.G. Konoplev, *Semiconductors* **45**, 89 (2011).
5. E. Salvati, L.R. Brandt, C. Papadaki, et al., *Mater. Lett.* **213**, 346 (2018).

P-45

Improved ferroelectric performance of La:$Hf_{0.5}Zr_{0.5}O_2$ thin films

M.G. Kozodaev[1], A.G. Chernikova[1], R.R. Khakimov[1], C.S. Hwang[1,2], A.M. Markeev[1]

[1]*Moscow Institute of physics and technology, 141700, Dolgoprudny, Moscow region, Russia*
e-mail: kozodaev.mg@mipt.ru

[2]*Department of Materials Science and Engineering and Inter-University Semiconductor Research Center, Seoul National University, Seoul 08826, Republic of Korea*

Ferroelectricity (FE) in doped HfO_2 thin films firstly reported in 2011 [1] is now a quite relevant topic due to the possibility of its implementation into ferroelectric memory (FeRAM) since it provides many advantages over perovskites, including CMOS and BEOL compatibility. Moreover, HfO_2-based films may be successfully grown by ALD, which allows the possibility of 3D FeRAM realization and, therefore, solves its scaling challenge.

According to the general point of view, FE effect in HfO_2 is usually associated with the stabilization of the non-centrosymmetric polar o-phase *($Pca2_1$)*, confirmed both theoretically and experimentally [2,3]. Moreover, it has been already found that many dopants can provoke FE in HfO_2. However, different fundamental and technological tasks are upcoming. The most prominent $Hf_xZr_{1-x}O_y$ system demonstrates the clear FE response in wide stoichiometry range after annealing at relatively low T (≈400°C) [4]. However, its properties are usually much deteriorated by presence of parasitic non-FE m-phase. The most effective way to suppress m-phase stabilization was doping by La, Y and Gd [5-7]. However, its FE performance strongly depends on dopant concentration; moreover, a high-T annealing (≈550°C), exceeding the BEOL limit (400-450°C), was required.

Secondly, HfO_2-based FE films are characterized by high coercive field (1.0-1.5 MV/cm) compared to PZT (0.1-0.2 MV/cm) [8], which requires 2.5-3.0 V of operating voltage to achieve the saturated polarization value. Such field is very close to the breakdown one, which usually results in early hard breakdown. Practical switching endurance of such films is limited by value ~10^9, significantly smaller than for PZT (~10^{12}). So, coercive field decrease is highly desirable.

The most recent work [9] described the possibility to combine advantages of low-level La doping with low crystallization temperature of HZO, which resulted in several interesting results. A significant decrease of the coercive field (by ~30%) was observed, which allowed applying lover voltage for ferroelectric switching and resulted in a great endurance improvement (up to 4×10^{10} cycles) while maintaining rather high $2P_r$ value. However, an unexpected transition from AFE-like material after 400°C annealing to clear FE after 450°C annealing was also observed.

Thus, the aim of the present work was a deeper insights into phase transitions in ternary La:$Hf_{0.5}Zr_{0.5}O_2$ system. For such task four different La concentrations in the range 0.7-2.1 mol. % were utilized. It was shown that the crystallization temperature of these films did not exceed 400°C. The detailed structural and electrical measurements were carried out to investigate such films. XRD data analysis allowed to expect t→o phase transition during La concentration variation, which was confirmed by small-signal CV measurements and DC-IV measurements which revealed a significant change in *k* value and leakage current density, respectively. In addition AFE-like to FE-like transition occurred during field cycling for two intermediate La concentrations. As a result of such detailed analysis rather promising ferroelectric response and long endurance following 5×10^{10} cycles with no breakdown was obtained.

This work was supported by Russian Science Foundation (Project. No 18-19-00527).

1. T.S. Boescke et. al., *Applied Physics Letters* **99**, 102903 (2011).
2. R. Materlik et. al., *Journal of Applied Physics* **117**, 134109 (2015).
3. M. H. Park et. al., *Advanced Materials* **27**, 1811 (2015).
4. J. Mueller et. al., *Nano Letters* **124318** (2012).
5. A.G. Chernikova et. al., *Applied Physics Letters* **108**, 242905 (2016).
6. J. Mueller et. al., *Journal of Applied Physics* **110**, 114113 (2011).
7. M. Hoffmann et. al., *Journal of Applied Physics* **118**, 072006 (2015).
8. G. Perez de la Cruz, et. al., *Applied Physics Letters* **108**, 114106 (2010).
9. A.G. Chernikova et. al., *ACS Applied Materials&Interfaces* **10**, 2701 (2018).

P-46

The use of atomic force microscopy for human mesenchymal stem cells study

L.V. Kukharenko[1], Th. Schimmel[2], H. Fuchs[3], M. Barczewski[2], T.V. Shman[4], A.V.Tarasova[4]

[1]*Belarusian State Medical University, 220116, Minsk, Belarus*
e-mail: KukharenkoLV@bsmu.by

[2]*Institute of Nanotechnology, Karlsruhe Institute of Technology, 76344, Karlsruhe, Germany*

[3]*Center for Nanotechnology and Institute of Physics, University of Münster, 48149, Münster, Germany*

[4]*Belarusian Center for Pediatric Oncology and Hematology, 223040, Pos.Lesnoe, Belarus*

The AFM use opens up exciting new possibilities for investigation of mechanical properties (stiffness, elasticity, and hardness) of a wide variety of biological cells in relation with dynamic processes and cellular functions [1]. In this work the actin cytoskeleton and mechanical properties of human mesenchymal stem cells (hMSC) were studied using fluorescence microscopy and AFM. Study in details of hMSC mechanical properties such as elasticity, adhesion and stiffness, cytoskeleton organization and cell shape is required to realize their promising potential for development of new therapies for regenerative medicine and stem-cell-based tissue engineering.

For AFM investigations the hMSCs were fixed with 2% glutaraldehyde for 30 min. All data were obtained on Nanoscope (R) IIIa MultiMode AFM. Force modulation mode was used to study mechanical properties (local stiffness and adhesion) of the hMSCs. The images were acquired by using silicon nitride cantilevers (NSC12/50) with a nominal force constant of 0.65 N/m (NT-MDT, Russia). The measurements were performed in air at RT. AFM investigations of hMSCs exhibited a considerable range of morphologies as well as spreading and the lengthened shape of the cells. Cells possess irregularly shaped flat lamellipods. For the spindle shaped cell the nuclear region height varies from 400 nm to1 μm, whereas lamellipodia thickness varies from 150 to 340 nm. For the star shaped cell nuclear region height is about 400-800 nm with the lamellipodia thickness 180-300 nm. Lamellipodia contain orthogonally arranged actin networks at the hMSC peripheries. The nucleus zoomed area of star shaped cell is shown in Figure 1. The area around nucleus looks like a smooth fiber mesh. Zooming in on the nucleus the granular structure of elongated bundles of actin filament with 20-70 nm granule size is visualized. AFM images demonstrate many parallel actin bundles extending throughout the nuclear region. Darker parts in adhesion image correspond to low adhesion value. The nucleus appears to be distinctly softer than the flat lamellipodia.

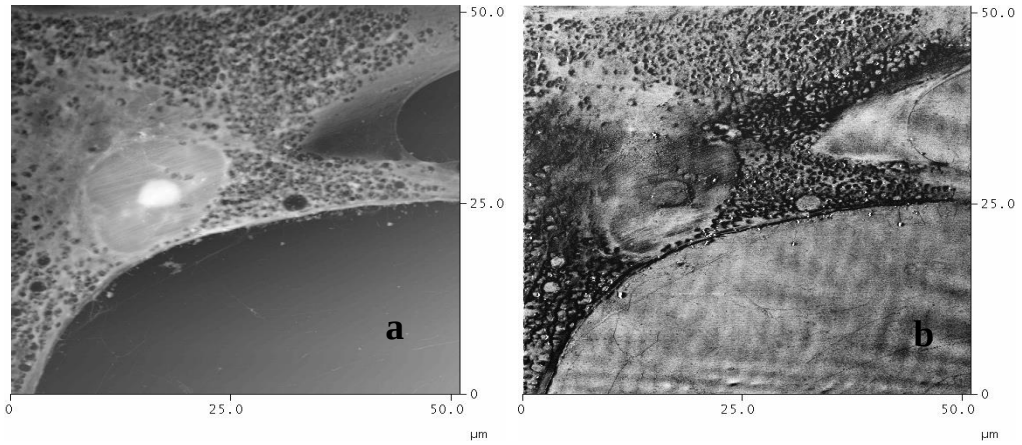

Figure 1. AFM images of human mesenchymal stem cell: (a) contact mode topography and (b) force modulation image (adhesion).

According to the hMSC fluorescent images the microfilaments are linear in form and mostly is localized over the nucleus. The microtubules more often appear curved in form and span large regions of the hMSCs. Mechanical properties of hMSC most likely are regulated by the actin cytoskeleton, its structure and dynamics. This study demonstrates that the pulsed force mode for atomic force microscope combined with fluorescence microscopy opens up possibilities for investigation of the mechanical properties of hMSCs in relation with cytoskeleton organization.

1. N.I. Nikolaev, T. Müller, D.J. Williams, et al., *J. Biomech.* **47**, 625 (2014).

P-47

Study of charge state of polarization domain walls in organic ferroelectric 2-methylbenzimidazole crystals

T.S. Kunkel[1,2], A.V. Ankudinov[2], E.V. Balashova[2], B.B. Krichevtsov[2]

[1]*SPbPU, 195251, Saint-Petersburg, Russia*

[2]*Ioffe Institute 194021, Saint-Petersburg, Russia*

e-mail: tatyana_kunkel@mail.ru

Nowadays, there is an active search [1] of organic and semi-organic, environmentally safe and biocompatible ferroelectric materials that do not contain lead and heavy metals.

2-methylbenzimidazole (MBI) can be considered as a promising chemically inert organic ferroelectric [2]. The crystal structure of MBI has pseudosymmetry and is described by the tetragonal space group $P4_2/n$ (real group Pn [3]). Dielectric hysteresis loops were observed for electric fields perpendicular to the pseudotetragonal axis in MBI crystals. The spontaneous polarization and coercive field at room temperature were $P_s \sim 5$ μC/cm^2 and $E_c \sim 3$ V/μm at a frequency of $\nu = 30$ Hz [2].

Domain structures were observed at the surface of MBI crystal using piezoresponse force microscopy (PFM) [3]. The observed PFM contrast interpretation given by the authors implied the continuity of the normal polarization at a domain wall. This is equivalent to uncharged domain walls.

We applied atomic force microscopy (AFM) to investigate MBI crystalline samples. We found out that the samples were rather soft, Young module was less than 1 GPa. This complicated the contact probing the sample's polarization domain structures. Therefore we used non-contact AFM modes: Kelvin-probe force microscopy (KPFM) and electrostatic force microscopy (EFM). This permitted us to observe cross-hatched patterns of the surface potential relief that may be related to the polarization distribution.

We studied two types of MBI samples: single crystals, Figure 1, and microcrystalline films, Figure 2. The single crystals were fabricated from a solution of MBI powder in ethanol by evaporation and slow cooling method. The films were formed by the deposition of MBI from the ethanol solution onto Pt coated Si substrates [2].

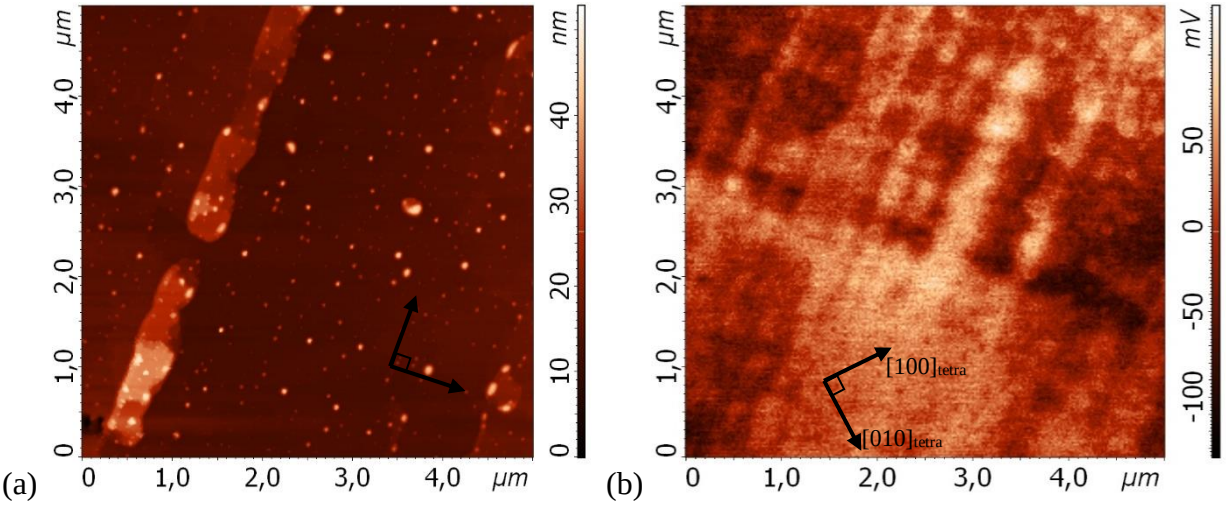

Figure 1. Taping mode AFM topography image (a) and simultaneously obtained surface potential map (b) of the MBI single crystal surface. Parameters of visualization: soft CSG10 probe with a resonant frequency of 29,9 kHz and free / set point oscillation amplitude of about 9 nm / 5 nm; probe-sample distance at KPFM mode is about 13 nm. The crystallographic directions are shown by arrows; pseudotetragonal axis is perpendicular to the figure plane.

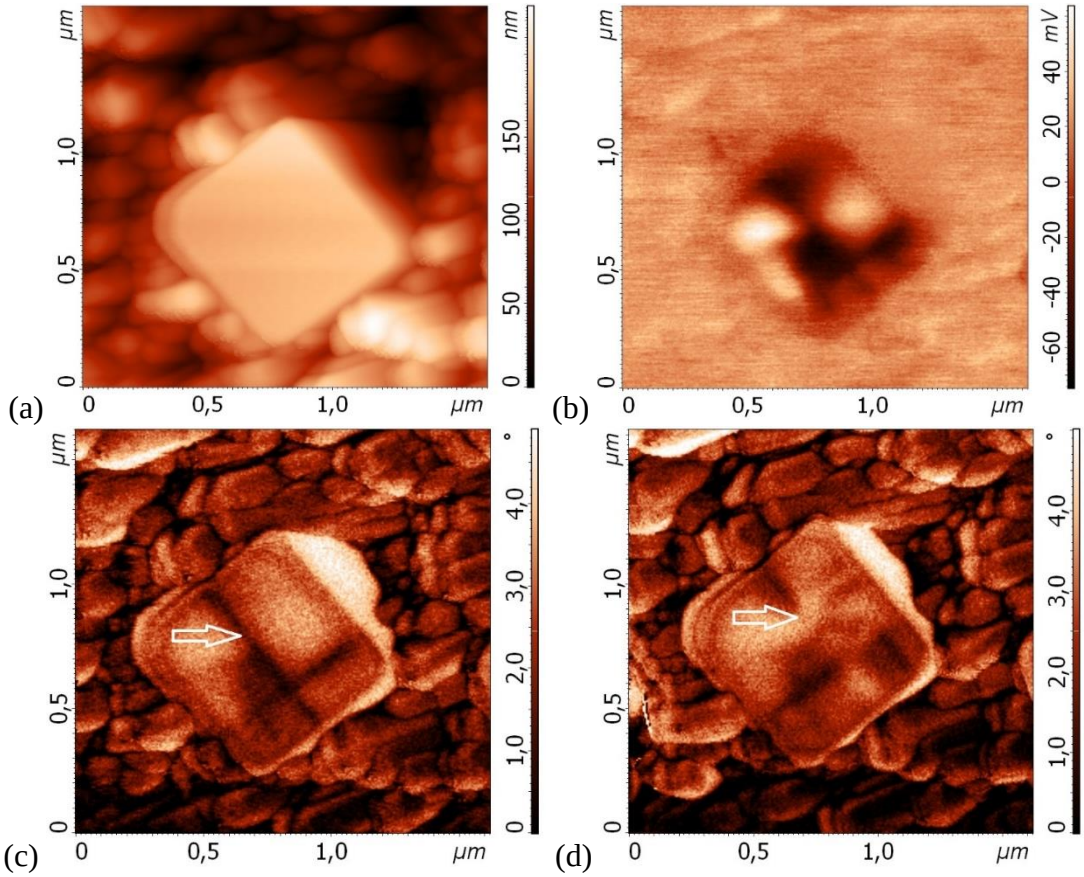

Figure 2. Taping mode AFM topography image (a) and simultaneously obtained surface potential map(b) of the MBI film on Pt coated substrate; EFM images before (c) and after (d) square voltage pulse application (τ = 6 s, U = 3 V). Parameters of visualization: fnp01Pt with a resonant frequency of 123 kHz and free / set point oscillation amplitude of about 9 nm / 8 nm; average probe-sample distances both at KPFM and EFM mode are about 8 nm, free amplitude oscillations at EFM mode is 4,5 nm. Arrows indicate the place the pulse was applied.

The amplitude of surface potential variations for the single crystal in Figure 1b is of order of 100 mV, while the spatial scale of these variations is about 100 nm. Hence, the characteristic in-plane electric field is 10 KV/cm and, accordingly, the charge density at the domain wall is about 1 nC/cm^2. Rectangular flat flakes were found on the film (Fig. 2a). The surface potential morphology at the flake (Fig. 2b) is similar to the pattern observed for the single crystal (Fig. 1b). It was possible to modify the spontaneous domain structure of the flake (Fig. 2c,d).

Our study is still in progress. It is planned to carry out combined KPFM, EFM and PFM investigations of both samples.

The work is supported by the RFBR grant № 16-02-00399.

1. S. Horiuchi, Y. Tokura, *Nature Materials* **7**, 357 (2008).
2. E.V. Balashova, B.B. Krichevtsov, F.B. Svinarev, et al., *Scientific and Technical Journal of Information Technologies, Mechanics and Optics* **16**, 801 (2016).
3. S. Horiuchi, F. Kagawa, K. Hatahara et al., *Nature Communications* **3**, 2322 (2012).

P-48

The changes in morphology of the wear-resistant ZrN coatings surfaces under the influence of the third elements additives

T.A. Kuznetsova[1], V.A. Lapitskaja[1], S.A. Chizhik[1], B. Warcholinski[2], A. Gilewicz[2]

[1]*A.V. Luikov institute of Heat and Mass Transfer of National Academy of Science of Belarus, 220072, Minsk, Belarus*
e-mail: kuzn06@mail.ru

[2]*Koszalin University of Technology, Faculty of Technology and Education, Koszalin, Poland*

The transition metal nitrides coatings are widely applied for cutting tools and tribological surfaces. ZrN coatings occupy a special place among them [1,2]. They have a favorable combination of mechanical properties under conditions requiring high thermal stability. The coatings on the base ZrN are known as a decorative thin films with color dependent on their chemical composition.

ZrN, Zr-O-N and Zr-Si-N coatings were synthesized using cathodic arc evaporation on HS6-5-2 steel substrates. Tribological properties of coatings are largely determined by the properties and morphology of their surface. The purpose of this work was to determine the effect of additives of Si and O on the morphology of the surface of wear-resistant ZrN coatings. The studies were carried out on an atomic force microscope (AFM) of the model NT-206 (Belarus).

ZrN, Zr-O-N and Zr-Si-N coatings show classical surface microstructure characteristic for coatings deposited using PVD methods, especially cathodic arc evaporation. On the coating surface the numerous craters and a macroparticles are apparent. The surface microstructure is one of the most important parameter of the coatings. The surface obtained by AFM as 3D images is interpreted for ZrN coatings as a consisted from grains with diameter less than 50 nm structure, for Zr-Si-N coatings as a multi-cell structure in which lowered bottom of the cells and elevated vertical grain boundaries are visible, for Zr-O-N coatings as a consisted from the rounded "large" crystallites with diameter about 300 nm (Fig.1).

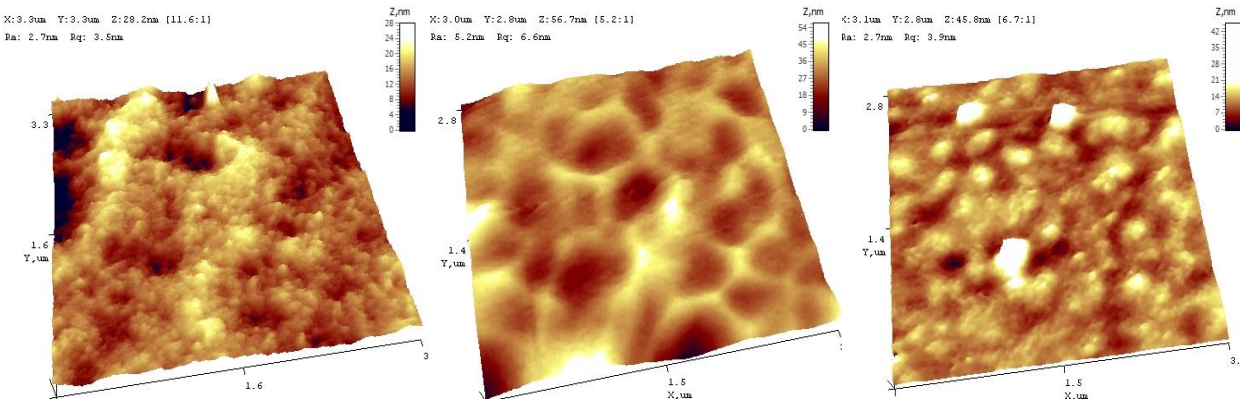

(a) (b) (c)

Figure 1. Three-dimentional images, scanned area 3x3 μm^2: (a) ZrN, (b) Zr-Si-N (2,2 % Si), (c) Zr-O-N (10 % O).

1. T.A. Kuznetsova, M.A. Andreev, L.V. Markova, *Friction and Wear* **26**, 521 (2005).
2. T.A. Kuznetsova, *Friction and Wear* **27**, 69 (2006).

P-49

Morphology of multilayer AlN/SiN coatings

T.A. Kuznetsova[1], V.A. Lapitskaja[1], S.A. Chizhik[1], V.V. Uglov[2], V.I. Shymanski[2], N.T. Kvasov[2]

[1]*A.V. Luikov institute of Heat and Mass Transfer of National Academy of Science of Belarus, 220072, Minsk, Belarus*
e-mail: kuzn06@mail.ru

[2]*Belarusian State University, 220030 Minsk, Belarus*

Coatings based on aluminum nitrides are optimal for operation in conditions of high temperature and mechanical stress. To increase their mechanical properties, slowing the cracks propogation, coatings are formed as multilayer structures with a period of layers from several to a dozen nanometers. Such a composition can be a sequence of layers AlN/SiN. The nanostructured state of the films, on the one hand, leads to a significant increase in their mechanical and functional properties; on the other hand, excess surface energy at the interphase boundaries leads the nanostructure to a nonequilibrium state, which in turn can lead to mechanical degradation of the films, especially at elevated temperatures under conditions open air atmosphere. AlN and AlN/SiN coatings were formed on monocrystalline silicon substrates with the (100) orientation by reactive magnetron sputtering with consecutive use of aluminum and silicon targets in Ar + N_2 plasma. The coatings thickness was about 300 nm. Multilayer coatings AlN/SiN were obtained with two thicknesses of single layer of 5 and 10 nm. The purpose of this work was to determine the effect of single layer thickness on the morphology of AlN and AlN/SiN coatings surfaces. AFM NT-206 (Belarus) was used in this work for the coatings surfaces characterization.

It was established that AlN coating surface consists of rounded crystals with diameter 50-100 nm (Fig. 1a). In this case, it has the lowest roughness of 4.8 nm at 1x1 μm^2 of scanned area. Despite the fact that this coating has the thickest layer of the same composition of 300 nm, the size of the crystals there is minimal. The surface of the AlN/SiN coating with layers of 5 nm consists of triangular crystallites with diameter of 100-150 nm. Its roughness at 1x1 μm^2 of scanned area is 14.9 nm (Fig. 1b). The surface of the AlN/SiN coating with layers of 10 nm consists of triangular crystallites with diameter of 150-250 nm. Its roughness at 1x1 μm^2 of scanned area is 41.1 nm (Fig. 1c). Thus, in spite of the small individual layers excluding the columnar growth of crystallites, the largest layer of AlN/SiN with 10 nm layers has the largest crystallite size, which on the one hand can reduce its mechanical properties, but on the other, increase the thermal stability due to the reduced area of intergranular boundaries compared with coatings with nanoscale crystallite size.

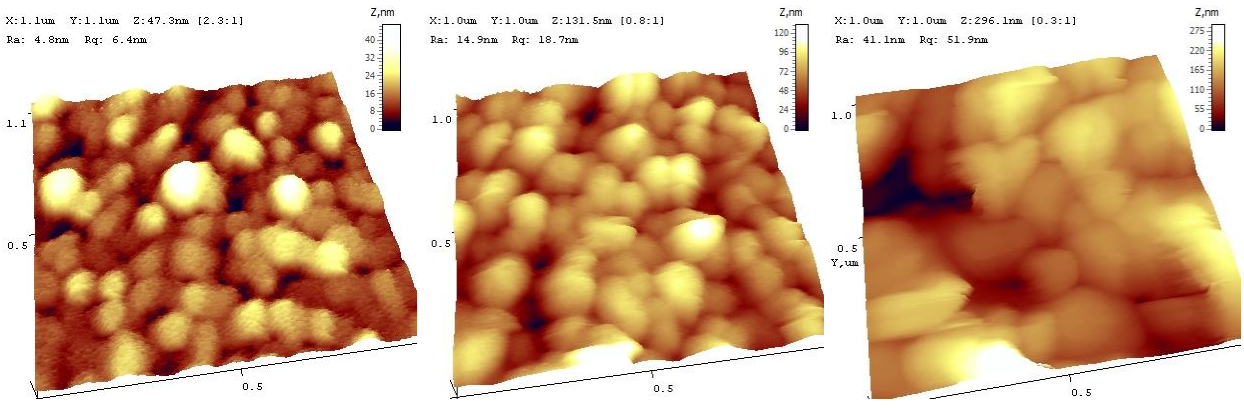

(a) (b) (c)

Figure 1. Three-dimentional images, scanned area 1x1 μm^2: (a) AlN, (b) AlN/SiN (5 nm), (c) AlN/SiN (10 nm).

1. V.M. Anishchik, V.V. Uglov, A.K. Kuleshov, et al., *Thin Solid Films* **482**, 248 (2005).

P-50

Friction coefficient obtained using AFM as a criterion of changes in the surface properties after low-temperature plasma treatment

V.A. Lapitskaya[1], T.A. Kuznetsova[1], K.A. Sudzilouskaya[1], T.I. Zubar[1], S.A. Chizhik[1], D.A. Kotov[2], S.A. Nikitiuk[2]

[1]*A.V. Luikov institute of Heat and Mass Transfer of National Academy of Science of Belarus, 220072, Minsk, Belarus*
e-mail: vasilinka.92@mail.ru

[2]*Belarusian State University of Informatics and Radioelectronics, 220013, Minsk, Belarus*

Technologies for materials joining require an increase in the contact and adhesion properties of their surfaces. There are different methods of these properties operation. The low-temperature plasma treatment is a perspective and ecological method. It allows you to change the properties of the surface layer to several nm without changing the volume characteristics of the material [1]. Frequently such a modification does not even lead to a change of the surface topography, determined by the high-resolution method of atomic force microscopy (AFM).

In this case the method of friction coefficient (Cfr) measurement using AFM in process of time is an effective way of the quantitative surface control. AFM NT-206 (Belarus) was used in this work. The method of Cfr measurement using AFM is based on the determination of angle of the probe arm twisting around its axis under the action of frictional forces between the surface and the probe [2].

The surface adhesion is exerted substantial influence on the value of Cfr. Adhesion increases after the exposure to plasma and according to it the console twisting and Cfr increases too. A two-layer polymer film PMF-351 was investigated. Cfr was measured within 70 minutes after exposure to plasma. It was found that during the first 35 minutes after the film treatment Cfr (Fig. 1) varies in the range from 0.015 to 0.025 and during the next 35 minutes it decreases according to a logarithmic dependence. The film surface in process of time loses its properties and returns to its original level. The determination of the time range at which the surface processed in the plasma retains its modified properties is an actual problem.

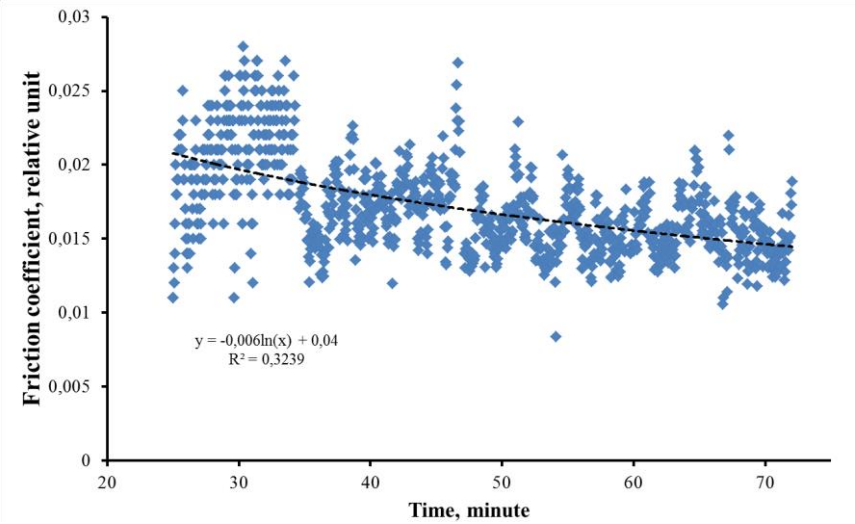

Figure 1. The change of friction coefficient a two-layer polymer film of PMF-351.

This research was supported by the grant of Belarussian Republican Foundation for Fundamental Research BRFFR No.F17-118.

1. A.B. Gilman, M.S. Piskarev, A.A. Kuznetsov, et al., *High Energy Chemistry*. **51**, 147 (2017).
2. T.A. Kuznetsova, T.I. Zubar, V.A. Lapitskaya, et al., *IOP Conf. Series: Materials Science and Engineering* **256**, 012022 (2017).

P-51

The influence of multilayer metal-carbon coatings composition with different arrangement of functional layers on their surface morphology

V.A. Lapitskaya[1], T.A. Kuznetsova[1], T.I. Zubar[1], S.A. Chizhik[1], A.A. Rogachev[2]

[1]*A.V. Luikov institute of Heat and Mass Transfer of National Academy of Science of Belarus, 220072, Minsk, Belarus*
e-mail: *vasilinka.92@mail.ru*

[2]*Francisk Skorina Gomel State University, 246019, Gomel, Belarus*

Recently, metal-containing diamond-like coatings deposited by various methods have become widespread in materials science. But the practical application of such coatings in pure form is limited by the peculiarities of their structure. There are various ways to control their structure and one of which is the inclusion of metal and nitride layers into such coatings [1].

The purpose of this work was to determine the influence of the composition of multilayer coatings (Ti-(Ti+DLC); Ti-(Ti+DLC)-DLC; Ti-(Ti+N+DLC)-DLC; Ti-(Ti+N+DLC); TiN-(Ti+DLC)) on the surface morphology. The investigations were carried out with an atomic force microscope (AFM) Dimension FastScan (Bruker, USA). The carbon component of the coating was deposited using a pulsed cathode-arc method with the following parameters: pulse repetition frequency of 15 Hz, discharge voltage of 350 V. Doping with nitrogen was due to sputtering at the nitrogen partial pressure in the chamber of 5×10^{-2} Pa. The metal component was formed using a DC arc discharge at the arc current of 70 A. VT-100 titanium alloy as a cathode was used. The thickness of the layered coating depended on its architecture and was in the range from 300 to 500 nm.

Surface morphology, roughness, distribution of coarse grains in the coating and the structure of the carbon matrix largely depend on the sequence (architecture) and the type of layers deposited.

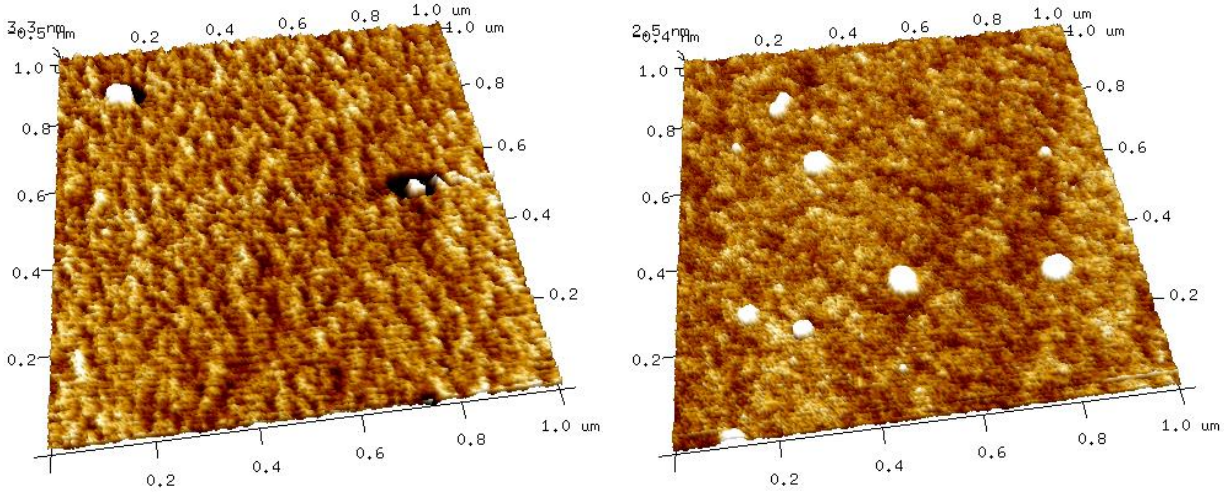

(a) (b)

Figure 1. Three-dimentional images, scanned area 1x1 μm^2:
(a) Ti-(Ti+DLC)-DLC; (b) Ti-(Ti+N+DLC)-DLC.

This research was supported by the grants of Belarussian Republican Foundation for Fundamental Research BRFFR № T17KIG-009.

1. H.A. Castillo, *Applied Surface Science* **257**, 2665 (2011).

P-52

Scanning capacitance microscopy of TGS − TGS + Cr ferroelectric crystals

R.V. Gainutdinov[1], N.V. Belugina[1], A.K. Lashkova[1], K.L. Sorokina[1], V.N. Shut[2], I.F. Kashevich[3], S.E. Mozzharov[2], A.L. Tolstikhina[1]

[1]*Shubnikov Institute of Crystallography of Federal Scientific Research Centre "Crystallography and Photonics" of Russian Academy of Sciences, 119333, Leninsky pr. 59, Moscow, Russia*

e-mail: aklashkova@yandex.ru

[2]*Institute of Technical Acoustic NASB, 210027, Vitebsk, Belarus*

[3]*Vitebsk State University, 210032, Vitebsk, Belarus*

Scanning capacitance microscopy (SCM) is known as a method for measuring spatial variations in capacitance with high resolution. It is mainly used for high-precision analysis of the dopant concentration in semiconductor structures, for the quantitative evaluation of the dielectric films thickness or for the dielectric constant [1]. To the ferroelectrics so far this method has been applied little, as one can see from the limited number of research papers [2,3].

The main objects of study were TGS–TGS + Cr crystals with a profile impurity distribution of chromium ions grown at the Institute of Technical Acoustics NASB [4]. The banded crystals TGS-TGS + Cr were studied in the work by SCM, PFM, KPFM methods. A periodic change in the composition was achieved by growing the seed in solutions of a different composition (nominally pure and containing an admixture of Cr^{3+} (5-6% by weight)). Difference in concentration of Cr^{3+} between nominally pure and containing an impurity stripes turns out ~0.08% by weight.

Combining a large number of consecutive images into one allows to imagine the general situation of the domain structure in different stripes. Figure 1 shows the panoramic image composed of 16 PFM images. The domain structure of nominally pure and containing an impurity stripes is markedly different. Fine-dispersed domain structure corresponds to the impurity areas.

On PFM image, the contrast is formed only on the positive and negative domains (Fig. 2a). The presence of the fine-dispersed domains on one side of the boundary and in the stripe itself indicates an impurity area. The same situation is repetitive in the SCM image (Fig. 2b). This can be evidence of the existence of a capacitive contrast associated with the domain structure. In this case three contrasts are observed: light (corresponding to domain boundaries), dark (corresponding to the stripe of pure TGS) and medium (corresponding to the stripe with impurity). Medium contrast in our case is due to the presence of an impurity.

Figure 1. Panoramic PFM image of the domain structure of TGS–TGS + Cr crystals.

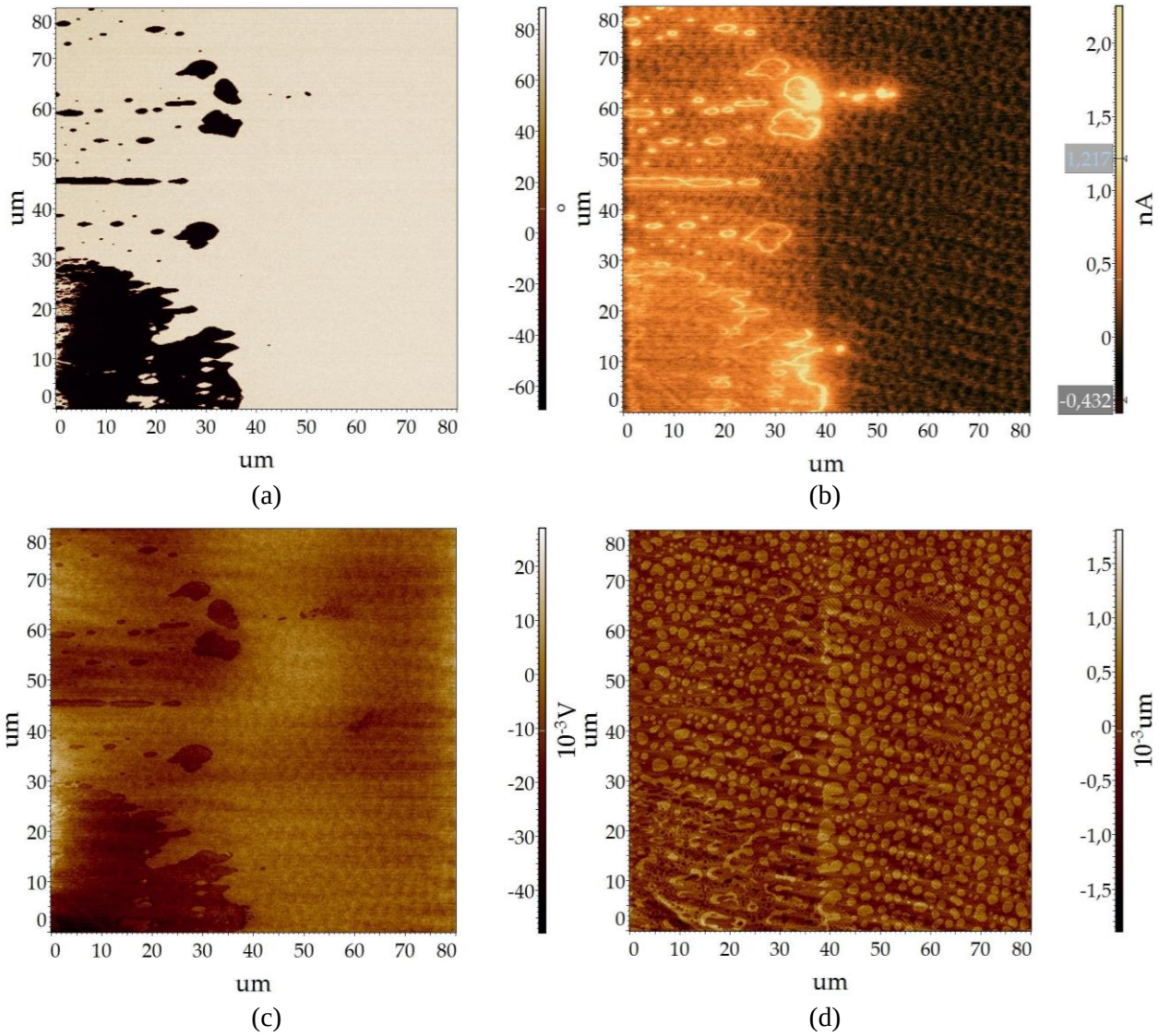

Figure 2. Image of the same surface area of TGS – TGS + Cr with containing an impurity of Cr3+ stripe (left) and nominally pure TGS (right): (a) PFM, (b) SCM, (c) KPFM, (d) corresponding surface relief. Size 80×80 μm.

This shows that the SCM method is more informative than PFM and KPFM, because they do not have sensitivity to the presence of impurities in the crystal. If there is no characteristic fine-dispersed domain structure on the researching surface, these methods will not show the boundary of the impurity stripe.

It is demonstrated that SCM is an effective method for controlling the spatial variation of the local permittivity and studying the relationship between the features of the domain structure and the impurity composition of local regions of ferroelectric crystals with a profile impurity distribution. Measurements with the help of the B2987A petaohmmeter at the Cascade Microtech Tesla probe station do indeed show 1.5-2 times larger current value for the impurity regions of the surface at ohmic regions of volt-ampere characteristics in comparison with the pure ones.

1. B. Bhunshan, H. Fuchs, M. Tomitori, *Applied Scanning Probe Methods YIII: Scanning Probe Microscopy Techniques* (Springer-Verlag), (2008).
2. C.-C. Leu et al. *Electrochem. Solid-State Lett* **7**, A327 (2004).
3. Y. Naitou, H. Ogiso. *Jap. J. Appl. Phys.* **45**, 1922 (2006).
4. V.N. Shut, I.F. Kashevich, B.E. Votts, *Crystallogr.Rep*. **49**, 206 (2004).

P-53

Work function tuning of the individual polyaniline/carbon nanotube nanostructures

I.A. Lobov, N.A. Davletkildeev, D.V. Sokolov

OSC SB RAS, 644024, Omsk, Russia
e-mail: LI__87@mail.ru

The creation of electronic components on single nanostructures is an important direction in the development of science. Polyaniline (PANI) composites with carbon nanotubes (CNTs) are a promising material for achieving this goal. This is primarily due to the unique properties of the polymer, as well as their improvement when introducing CNTs into its matrix [1]. It is possible to extract single nanotubes coated with a PANI layer, which should have better electrical properties than the bulk PANI/CNT composite. The aim of this work is to study the electronic properties of individual PANI/CNT nanostructures.

Composite PANI with nitrogen-doped CNT (N-CNT) was obtained via in-situ chemical oxidative polymerization of aniline in the presence of nanotubes. Individual nanostructures of PANI/N-CNTs were separate from the volume of the composite by sonication. The suspension was deposited on a $Si0_2$/Si substrate for study by AFM. Electrostatic force microscopy (EFM) was used to calculate the work function. For comparison, the values of the work function of N-CNT and PANI/N-CNT composite film (thickness 40 nm) were used.

Figure 1 shows an example of the PANI/N-CNT nanostructure morphology, EFM signal, and EFM profile along the line at a tip potential equal to 5V. N-CNTs are coated with a polymer layer, as indicated by a comparison of the average diameter of N-CNTs before and after synthesis.

Based on the results of the contact potential difference, the work function of the electron was calculated (Table 1) [2]. It is shown that the work function of the nanostructure is larger than the work function of the CNTs. Furthermore, the work function of the PANI/N-CNT film is higher than that of the nanostructure.

Table 1. Work function, eV

N-CNT, [2]	PANI/N-CNT nanostructure	PANI/N-CNT film
4.5±0.12	4.67±0.26	4.79±0.18

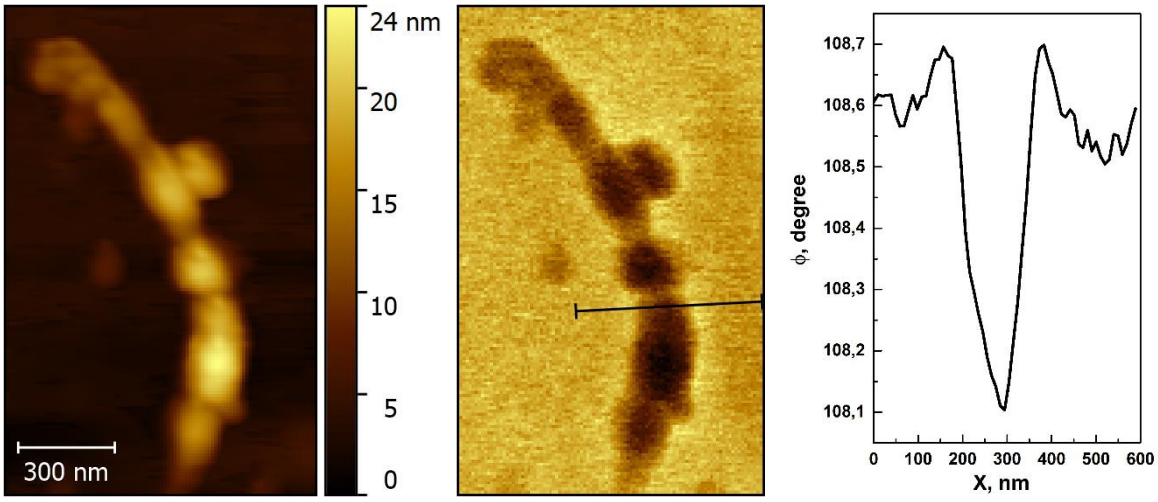

(a) (b) (c)

Figure 1. (a) AFM and (b) EFM images of PANI/N-CNT nanostructure and (c) cross section line.

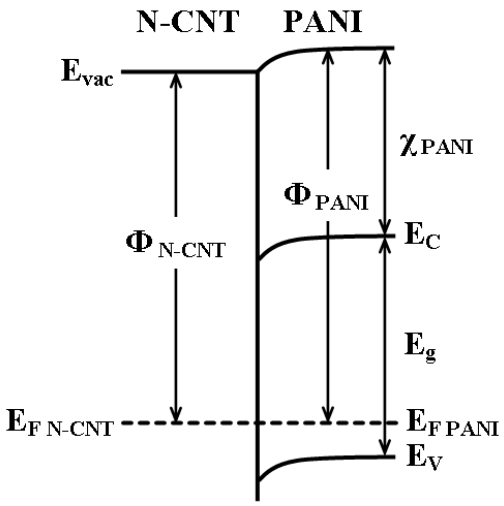

Figure 2. Energy diagram of PANI/N-CNT structure.

Figure 2 shows the energy diagram of the PANI/N-CNT structure. At the junction of the polymer/CNT, a space-charge region enriched in electrons arises in the polymer. PANI band bending down leads to a decrease in the work function. Therefore, with decreasing thickness of the polymer layer on CNT decreases the work function of PANI/N-CNT nanostructure. The work function of the bulk layer of PANI/N-CNT considerably exceeds the work function of nanostructure. This is due to the fact that the main contribution in the work function is provided by thick polymer layers on the CNTs, or unrelated polymer particles. Thus, the variation of both work function in the nanotubes and the thickness of the PANI layer on the CNTs make it possible to tuning the work function in the individual nanostructures of PANI/N-CNTs.

1. M. Eising, C.E. Cava, R.V. Salvatierra, et al., *Sensors and Actuators B: Chemical* **245**, 25 (2017).
2. N.A. Davletkildeev, D.V. Stetsko, V.V. Bolotov, et al., *Materials Letters* **161**, 534 (2015).

P-54

Fabrication process for producing silicon nanowire field effect transistors

A.V. Lukyanenko[1,2], A.S. Tarasov[1,2], I.A. Yakovlev[1], F.V. Zelenov[2], T.E. Smolyarova[1,2], I.A. Bondarev[1,2], S.G. Ovchinnikov[1,2], N.V. Volkov[1]

[1]*Kirensky Institute of Physics, Federal Research Center KSC SB RAS, 660036, Krasnoyarsk, Russia*

[2]*Institute of Engineering Physics and Radio Electronics, Siberian Federal University, 660041, Krasnoyarsk, Russia*

e-mail: lav@iph.krasn.ru

An important task to date is the development of new hybrid semiconductor/ferromagnet devices [1] that could become promising devices and play a role, both logic and memory, and could be produced within the same technology. Earlier, we already made similar structures using Deep Pen Nanolithography method [2], but due to a number of technical difficulties, we decided to abandon this technology and use a different approach.

In this work, we would like to show a simple technology for manufacturing Silicon Nanowire Field Effect Transistors and focus on the prospect of using such transistors not only as elements of microelectronics [3], but also as high-precision sensors for medical applications. A simple approach to manufacturing makes these devices advantageous candidates for use as test devices for studying the fundamental properties of materials. The technology described by us allows us to abandon the complex stage of silicon doping with impurities. And we also demonstrate a single exposure for electronic lithography, and the subsequent stage of liquid chemical etching.

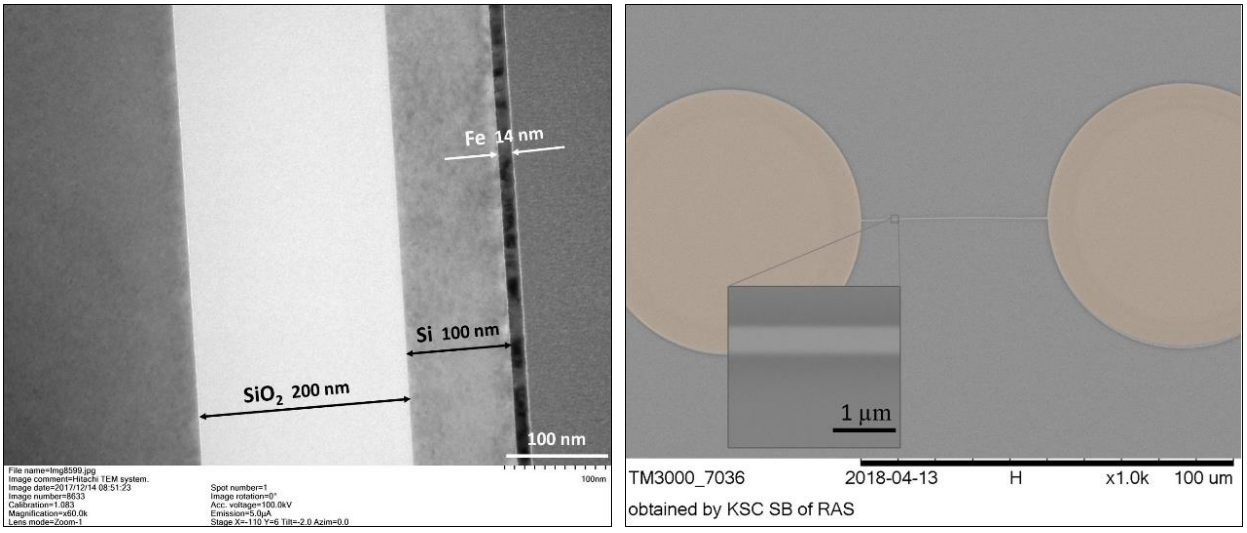

Figure 1. TEM image of Fe film deposed on SOI wafer (a).

The work was supported by the Russian Foundation for Basic Research, Government of Krasnoyarsk Territory, Krasnoyarsk Region Science and Technology Support Fund project no. 18-42-243022. This work is partially supported by the Ministry of Education and Science of the Russian Federation and by Siberian Branch of the Russian Academy of Sciences (Project II.8.70) and Fundamental research program of the Presidium of the RAS no. 32 «Nanostructures: physics, chemistry, biology, basics of technologies». This work was supported by and carried out on the equipment of the Center for Common Use of the Krasnoyarsk Scientific Center, Siberian Branch, Russian Academy of Sciences.

1. I.A. Yakovlev, S.N. Varnakov, B.A. Belyaev, et al., *JETP Letters* **99**, 527 (2014).
2. A.V. Lukyanenko, T.E. Smolyarova, *Semiconductors* **52**, 636 (2018).
3. Y. Cui, C.M. Lieber, *Science* **291**, 851 (2001).

P-55

Structural, electronic and optical properties of heterointerfaces based on antiferromagnet $LaMnO_3$ and ferroelectrics isostructural to $BaTiO_3$

Yu.V. Lysogorskii[1,2], I.I. Piyanzina[1,2], A.V. Leontyev[1], A.S. Elshin[1,3], D.A. Tayurskii[2], P.F. Mamin[1]

[1]*Zavoisky Physical-Technical Institute, FRC KazanSC of RAS, 420029, Kazan, Russia*

[2]*Kazan Federal University, 420008, Kazan, Russia*
e-mail: i.piyanzina@gmail.com

[3]*Moscow Technological University, 191454, Moscow, Russia*

The astounding phenomenon was found at the interface between two nonmagnetic wide-band-gap insulative oxides $LaAlO_3$ (LAO) and $SrTiO_3$ (STO) in 2004 [1]. A two dimensional electronic system (2DES) is formed in the STO layers next to the interface which becomes superconducting below a temperature of 300 mK [1,2]. Remarkably, this superconducting state coexists with a magnetic state being stable up to the room temperature. It was concluded, that the primary mechanism responsible for the 2DES formation is the electronic reconstruction followed by structural reconstruction.

Since then 2DES has been later found in other non-magnetic dielectrics. And all of them have in common is that the creation of 2DES is due to either the polar nature of one of components or due to defects of dopants. Latter, it has been shown that 2DES can be created at the interface of nonpolar oxides one of which is ferroelectric [3,4]. The main advantage of using ferroelectrics is a possibility to switch on and off the polarization and thus to control properties of the electron system.

One of the most important feature related to the 2DEG formation is the local polarity of layers inside the LAO slab. In the present work we have chosen the $BaTiO_3/LaMnO_3$ (BTO/LMO) heterostructure, where all layers in the simple electronic limit are neutral, but there is a ferroelectric polarization due to the Ti atoms displacements out of octahedron center in the BTO. The direction of such a polarization might be switched by an external electric field. Based on first-principles band structure calculations, we demonstrate the possibility of q-2DES (quasi-two-dimensoinal electron system) formation at the interface composed of perovskite ferroelectric BTO and antiferromagnet manganite LMO. We present the results of structural, electronic and optical properties calculations of BTO/LMO heterostructure composed of varying number of layers. We analyze an impact of ferroelectric polarization onto the q-2DES conducting properties by layer-resolved density of states calculations. Experimental results of optical investigation of $Ba_{0.8}Sr_{0.2}TiO_3/LaMnO_3$ heterostructure are also presented.

The reported study was funded by Russian Scientific Foundation according to the research project No. 18-12-00260.

1. A. Ohtomo, and H. Hwang, *Nature* **427**, 6973 (2004).
2. N. Reyren, S. Thiel, A. Caviglia et al., *Science* **317**, 5842 (2007).
3. M.K. Niranjan, Y. Wang, S.S. Jaswal, et al., *Phys.Rev.L.* **103**, 016804 (2009).
4. K.D. Fredrickson, A. Demkov, *Phys.Rev.B.* **91**, 115126 (2015).

P-56

Optical stimulated transfer from glass state to polar phase in relaxors

S.A. Migachev, R.F. Mamin

Zavoisky Physical-Technical Institute, FRC KazanSC of RAS, 420029, Kazan, Russia
e-mail: rf_mamin@yahoo.com

Relaxors have been subject to intensive research. Interest in these compounds is determined by a combination of ferroelectric, piezoelectric and optical properties and the ability to use these materials in optoelectronics and data storage systems. The distinguishing features of relaxors are a strongly diffuse maximum in the temperature behavior of permittivity, the shift of this maximum toward higher temperatures with rising measuring field frequency, and a strong frequency dependence of permittivity at very low frequencies. Numerous experimental data show that the properties of the low-temperature phase depend on the history of samples, so nonergodic behavior is observed in the low-temperature phase [1]. In an applied electric field, the transition to a uniform state of polarization is observed in the low-temperature phase after zero-field cooling. Such a phase transition was observed in [1] after a sufficiently long delay time had passed from the beginning of field application. The dependences of delay time t_0 of the phase transition on temperature T and external electric field E were established.

The observed regularities have been discussed using an approach [2] developing on the basis of the model of diffuse phase transition in the system with defects [3]. It is shown that in the frame of that approach the delay phase transition in polar phase in relaxor could be explain if the dynamic of electron system would be take in consideration [2]. For examine that model we investigate the effect of illumination on the delay time t_0 of the phase transition in $PbMg_{1/3}Nb_{2/3}O_3$ in [110] orientation. The delay time t_0 of the phase transition have been measured for different temperatures and applied electric field. The photoconductivity has been investigated and the correlation of observed results with developed model is discussed.

The reported study was funded by RFBR according to the research project № 18-02-00675a.

1. E.V. Colla, E.Yu. Koroleva, N.M. Okuneva et al., *PRL* **74**, 1681 (1995).
2. R.F. Mamin, R. Blinc, *Physics of the Solid State* **45**, 942 (2003).
3. R.F. Mamin, *Physics of the Solid State* **43**, 13141319 (2001).

P-57

Domain formation by ion beam in lithium niobate crystal with suppression of surface charging by electron and UV-flood guns

K.V. Maslyanaya, D.S. Chezganov, E.O. Vlasov, D.K. Kuznetsov,
E.D. Greshnyakov, V.Ya. Shur

School of Natural Sciences and Mathematics, Ural Federal University, 620002, Ekaterinbur, Russia
e-mail: christina.maslyanayay@gmail.com

The lithium niobate ($LiNbO_3$, LN) is one of the most popular ferroelectric crystals for domain engineering due to its outstanding piezoelectric, nonlinear-optical and electro-optical properties. The charged particles beams are utilized for studying and modification of various properties of such crystals. However, the accumulation of injected charge leading to the surface charging limits the using of these techniques.

In this study, we have used the methods of a surface charge control upon focused ion beam (i-beam) irradiation and investigated its influence on ferroelectric domain formation by i-beam in LN crystals [1].

The samples were represented by 0.5-mm-thick Z-cut LN wafers. The irradiated Z^+ polar surfaces were prepared by two different methods: (1) spin coating of 500-nm-thick layer of positive photoresist AZ nLOF 1505 (MicroChemicals GmbH) and (2) careful cleaning in acetone and isopropanol using ultrasonic bath. The opposite Z^- polar surface was covered by solid 100-nm-thick copper electrode. The irradiations by electrons and Ga^+ ions were performed by dual-beam workstation Auriga Crossbeam (Carl Zeiss) attached with i-beam lithography system Elphy Multibeam (Raith). The created domain structures were visualized at the polar surfaces by optical and scanning electron microscopies after selective chemical etching in pure HF and by confocal Raman microscopy in the crystal bulk.

The method for charging control using simultaneous i-beam irradiation and defocused electron (e-beam) proposed in Ref. [2] has been used for domain patterning. The optimal ratio of the e- and i-beam currents for domain patterning has been obtained. It was demonstrated that irradiation by e-beam changed the domain shape due to partial backswitching.

We have used also the method of surface charge control during i-beam irradiation by simultaneous UV illumination (wavelengths 275 and 310 nm) by means of light-emitting diodes (LED) [3]. It was shown that the method allowed to improve the period and uniformity of created periodical 1D and 2D structures. The method efficiency can be adaptively controlled by the change of the UV LED intensity. It was shown that method efficiency depends on LED wavelength. UV LED illumination decreases the domain depth and changes of the shape of isolated domains. The UV LED illumination during 1D periodical poling resulted in uniform nucleation of domains within the irradiated area and increase of the switched area. The role of photo-domain effect due to effective bulk screening induced by photoconductivity has been discussed [4, 5].

The equipment of the Ural Center for Shared Use “Modern nanotechnology” Ural Federal University was used. The research was made possible by the Russian Science Foundation (grant № 17-72-10152).

1. D.S. Chezganov, V.Ya. Shur, E.O. Vlasov, L.V. Gimadeeva, D.O. Alikin, A.R. Akhmathanov, M.A. Chuvakova, V.Y. Mikhailovskii, *Appl. Phys. Lett.* **110**, 082903 (2017)
2. D.J. Stokes, T. Vystavel, F. Morrissey, *J. Phys. D.* **40**, 874 (2007).
3. G. Gervinskas, G. Seniutinas, S. Juodkazis, *Laser Photonics Rev.* **7**, 1049 (2013).
4. V.M. Fridkin, A.A. Grekov, N.A. Kosonogov, T.R. Volk, *Ferroelectrics*, **4**, 169 (1972).
5. M.P. Michailov, *C. R. Acad. Bulg. Sci.* **21**, 1029 (1968).

P-58

The influence silicon dioxide nanoparticles on mechanical properties of erythrocyte and platelet membranes estimated by atomic force microscopy method

G.B Melnikova[1], E.E Konstantinova[1], T.N. Tolstaya[1], A.S. Petrovskaya[1], S.A. Chizhik[1], O.N. Shyshko[2]

[1]*A.V. Luikov Heat and Mass Transfer Institute of National Academy of Science of Belarus, 220072, Minsk, Belarus*
e-mail: galachkax@gmail.com

[2]*Belarusian State Medical University, Minsk, Belarus*

Silicon dioxide is widely used as excellent adsorbent, for production of different drugs, drugs carrier, and also has other applications. The research of interaction nanoparticles with biological cells is important, because not only the drug itself affects cell membrane, but also excipients do. The using of modern methods for nanoscale objects research allows to giving detailed information about changes after different action.

In our research the group of patients with average years 55 (50; 59) and type 2 diabetes mellitus (DM 2) were formed. These did not achieve compensation for HbA1c 9.1 (8.30, 10.4). Men and women were in same age, and they have DM 2 during last of 5–10 years.

Silicon dioxide nanoparticles (NP, Sigma – Aldrich, d = 10–20 nm) in physiological solution (C = 0.2 and 1 mg/ml) were used to affect on RBCs and platelets suspensions. Cells were incubated at room temperature during 40 and 60 minutes. After that suspensions of cells were fixed with glutaraldehyde on the mica plates. The influence of silicon dioxide nanoparticles on structure and mechanical properties of membranes blood cells by AFM method have been studied. We used standard silicon cantilevers (Mikromash, K= 3 N/m, R= 30 nm) for researching by atomic force microscope (NT-206, Belarus). Elastic modulus was calculated by Jonson-Kendall-Robertz model [1].

In early research we showed, that gold and polyacrylic acid nanoparticles do not influence on elastic modulus of RBCs membranes, results were based on AFM method data [2]. In this we found that cells membranes structure didn't change after incubation with NP. We supposed this associated with interaction NP to membranes structural element and shaping uniform structure with the cell. It was confirmed that in some cases aggregation stability of RBCs was decreased in NP presence. It is connected with adsorbance NP by cells and the result charge changing on erythrocytes surface and their aggregation.

The average elasticity modulus of initial RBCs membranes is 128.5 ± 10.0 % MPa and for platelets is 151.6 ± 10.0 % MPa, adhesion force is 23.0± 10.0 % and 26.0± 10.0 % nN, respectively. After cells incubation with silicon dioxide the elastic modulus changed for two types cells within experimental error. Changes of adhesion force are minor, however insignificant variations were found in the case of incubation RBCs with NP (c= 0.1 mg/ml) during 40 minutes and reached 22.0 % of initial values.

So, the obtained results can be used to develop methods for determining the properties of blood cells under various affects and pathologies.

The investigation performed within the Programs of State Research "Energy systems, process and technologies", project 2.2.

1. K.L. Johnson, K. Kendall, A.D. Roberts, *Proc. R. Soc. Lond.* **324**, 301 (1971).
2. G.B. Melnikova et al., *Series on Biomechanics* **29**, 12 (2015).

P-59

The characterization soft and heterogeneous surfaces with map of elasticity properties obtained by atomic force microscopy method

G.B. Melnikova, A.S. Petrovskaya, A.A. Makhanek, S.A. Chizhik

A.V. Luikov Heat and Mass Transfer Institute of National Academy of Science of Belarus, 220072, Minsk, Belarus
e-mail: galachkax@gmail.com

One of the important problems is to determine local mechanical properties heterogeneous surfaces by atomic force microscopy method [1]. The first task is to select a model for calculating the modulus of elasticity. We used the Tabor parameter to achieve that. For example, if we calculate using Jhonson – Kendall – Robertz model we can take into consideration adhesion force between cantilever and sample surfaces [2]. This model is more suitable for the polymeric materials, fixed and living biological cells [3].

As usual, objects are characterized by convexities and concavities. Characteristics are may also vary in different point of studied objects. At present researches did not take into consideration different types of influences on calculation of elasticity modulus. It is important to make an amendment for shape of the probe that is well described in F. Borodich's article [4]. Other corrections to make are angle under which the presser on the convexity is applied and interacting of the probe with the concavity. Consideration of all these corrections, as well as studying by constructing elasticity maps, allows us to minimize variance of elasticity for the surface being researched.

In our research we used two types of material – fixed biological cells (heterogeneous surface) and polydymethylsiloxane (PDMS, homogeneous surface). The distribution data of elasticity modulus PDMS surface 1x1 μm presented on Figure 1.

After addition these corrections elasticity modulus is decreased on 10 % in second case, and modulus decreased on 20 % for biological cell membranes and variance of values is minimized.

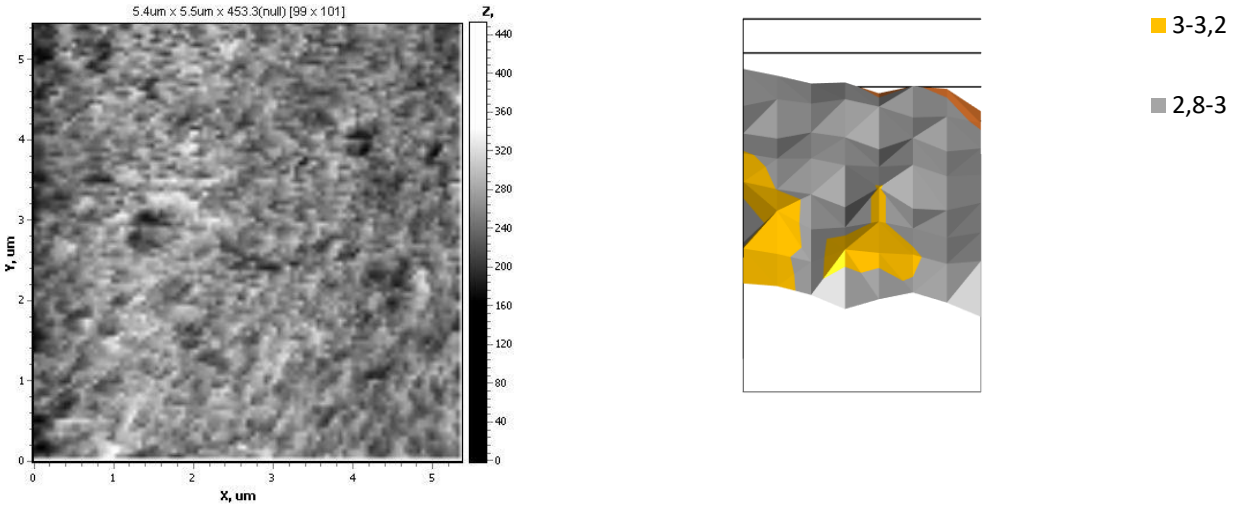

Figure 1. Structure in (a) Torsion and (b) elasticity modulus (MPa) of PDMS surface 1x1 μm.

1. E. Gorshkova et al., *Nanoindustry. Nanotechnology for medicine* **4**, 50 (2012). (In Russian)
2. S.A. Chizhik et al., *Langmuir* **14**, 2606 (1998).
3. G.B. Melnikova et al., *5th Eurosummer school on biorheology and symposium on micro and nanomechanics and mechanobiology of cells, tissues and systems*. **33** (2015).
4. F. Borodich, *Advances in Applied Mechanics* **47**, 225 (2014).

P-60

Giant strain and induced ferroelectricity in smorphous $BaTiO_3$ films and multiferroic heterostructure under poling

P. Mirzadeh Vaghefi[1], A. Baghizadeh[2], A.A.C.S. Lourenço[1], V.S. Amaral[1], A.L. Kholkin[1,3]

[1]*Department of Physics & CICECO-Aveiro Institute of Materials, University of Aveiro, 3810-193 Aveiro, Portugal*
e-mail: kholkin@ua.pt

[2]*Department of Materials and Ceramics Engineering & CICECO - Aveiro Institute of Materials, University of Aveiro, 3810-193 Aveiro, Portugal*

[3]*School of Natural Sciences and Mathematics, Ural Federal University, 620000 Ekaterinburg, Russia*

Amongst the benefits of nanotechnology in science and industrial applications, it offers novel high resolution nanopatterning techniques that are useful to overcome the restrictions of conventional lithography [1,2]. With that purpose, several lithographic methods have been developed in past decades, including those based on scanning probe microscopy (SPM) [3]. These methods offer important advantages, such as a few nanometers resolution and high versatility. In the recent years, much attention has been paid to the ferroelectric lithography that relies on the polarization reversal by the tip of piezoresponse force microscope (PFM) exposing to polarization sensitive media [4]. These methods use local polarization reversal accompanied by the reversible strain that very often does not exceed 1% even under applying of a very high electric field [5,6]. Morphological changes due to the application of an external electrical bias, i.e. electric poling treatment have been previously observed and attributed to the interaction between conductive probe and the trapped charges injected into the film during poling process in polymers [5] and PZT/LSMO [6] thin films. In oxide ferroelectrics, these effects have not been seen so far.

In this work, we report the giant surface modification of a 5.6 nm thick $BaTiO_3$ film grown on Si (100) substrate under poling by conductive tip of a scanning probe microscope. The surface is locally elevated by about 9 nm under -20 V applied voltage during scanning, resulting in the maximum strain of 160%. The threshold voltage for the surface modification is about 12 V. The modified topography is stable enough with time and slowly decays after poling with the rate ~0.02 nm/min. Also, strong vertical piezoresponse after poling is observed.

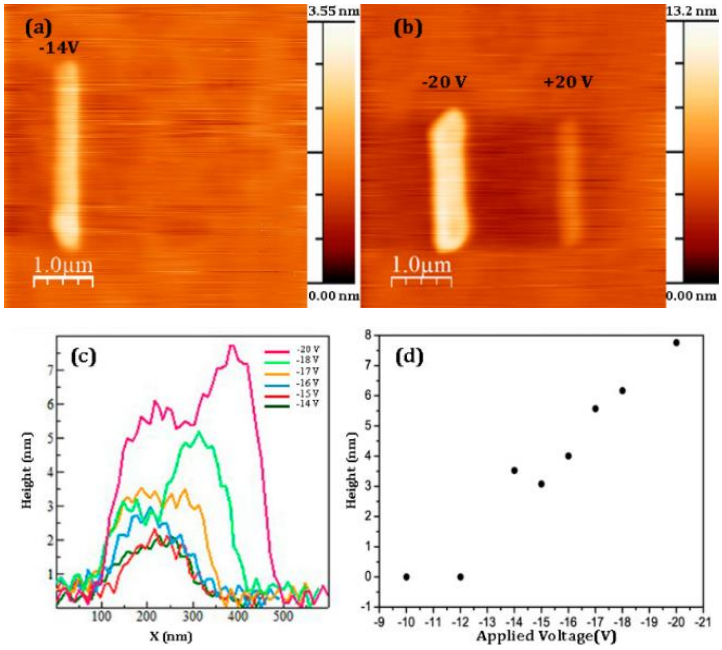

Figure 1. Topography of $BaTiO_3$ thin film after application of (a) ±14 V and (b) ±20 V during scanning of the area 0.2x2 μm^2. (c) Comparison of the topography cross-sections of the areas poled with different voltages. (d) Average height of the poled areas vs. applied negative voltage.

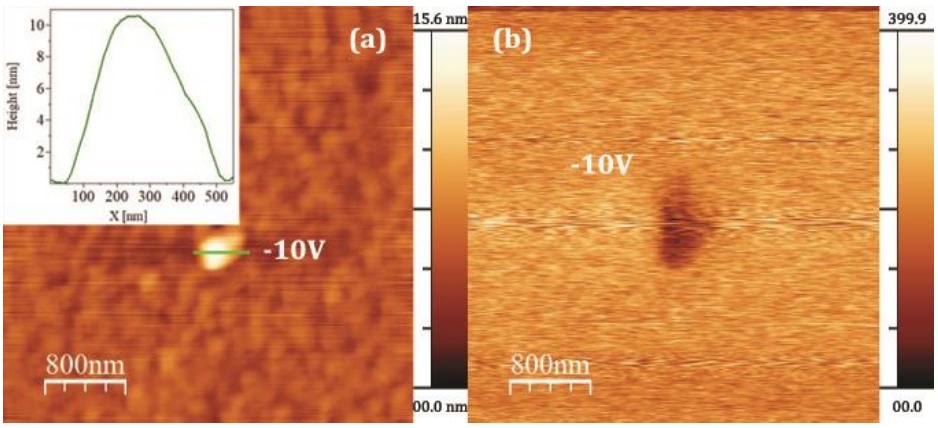

Figure 2. (a) Topographic AFM change of the LBMBT surface after poling of -10V and (b) piezoresponse of the poled area.

Combined measurements by SPM and piezoresponse force microscopy (PFM) prove that the poled material develops high ferroelectric polarization that cannot be switched back even under oppositely oriented electric field. The topography modification is hypothesized to be due to a strong Joule heating and concomitant interface reaction between underlying Si and $BaTiO_3$. Top layer is supposed to become ferroelectric as a result of local crystallization of amorphous $BaTiO_3$.

Later, we extended the patterning method to a multiferroic heterostructure of magnetic layers ($La_{0.9}Ba_{0.1}MnO_3$) covering 30 nm $BaTiO_3$ layer [7]. Coupling of polarization, in-plane strain and magnetic properties in a heterostructures can be used to engineer the symmetry of thin films and heterostructures and be applied in ferromagnetic shape memory alloys [8-10]. The surface of heterostructure is locally elevated by 10.5 nm under -10 V applied voltage during scanning, resulting in 135% strain. Asymmetrical polarization was observed regarding the sign of applied voltage. This work illustrates a novel approach of nanopatterning of ferroelectric films and creation of ferroelectric nanodomains by means of PFM technique and opens up new ways to create nanoscale ferroelectric structures to be used in ferroelectric memory devices.

1. B.D. Gates, Q.B. Xu, J.C. Love, et al., *Annual Review of Materials Research* **34**, 339 (2004).
2. B.D. Gates, Q.B. Xu, M. Stewart, et al., *Chemical Reviews* **105**, 1171 (2005).
3. M. Cavallini, F. Biscarini, S. Leon, et al., *Science* **299**, 531 (2003).
4. S.V. Kalinin, D.A. Bonnell, T. Alvarez, et al., *Advanced Materials* **16**, 795 (2004).
5. G. Zhu, J. Xu, Z. Zeng, et al., *Applied Surface Science* **253**, 2498 (2006).
6. S.V. Kalinin, S. Jesse, A. Tselev, et al., *ACS Nano* **5**, 5683 (2011).
7. P. Mirzadeh Vaghefi, A. Baghizadeh, M. Wllinger, et al., *Superlattices and Microstructures* (2017).
8. S. Datta, M. Rioult, D. Stanescu, et al., *Thin Solid Films* **607**, 7 (2016).
9. H. Lu, C. W. Bark, D. E. de los Ojos, et al., *Science* **336**, 59 (2012).
10. Y. Tokunaga, N. Furukawa, H. Sakai, et al., *Nature Materials* **8**, 558 (2009).

P-61

Microstructural approach in addressing the issue of repeated use of TFE-fluorocarbon additives and its influence on car engines

V.E. Rogov[1], L.A. Bokhoeva[2], U.L. Mishigdorzhiyn[3]

[1]*Baikal Institute of Natural Management, Siberian Branch of Russian Academy of Sciences, 670047, Ulan-Ude, Russia*

[2]*Department of Strength of Materials, East Siberia State University of Technology and Management, 670013, Ulan-Ude, Russia*

[3]*Department of Metals Science and Materials Processing Technology, East Siberia State University of Technology and Management, 670013, Ulan-Ude, Russia*
e-mail: druh@mail.ru

The paper considers some aspects of TFE-fluorocarbon additives application in lubrication systems of internal combustion engines (ICE), their influence on processes of friction and wear during multiple uses. Working surfaces of different parts of ICE were observed by means of scanning electron microscope (SEM) at high resolution. Polymeric protective coating are formed on the metal and non-metal surfaces. TFE-fluorocarbon additives' particles severely deform are severely deformed during operating, changing their initial spherical shape to elongated and needle-like shapes. The overabundance of these deformed polymer particles leads to a state when they become a major source of wear products formation instead of protecting engine friction units and reducing wear. The results indicate that repeated use of FORUM additive in the lubrication system of internal combustion engines may cause gumming of the piston rings.

P-62

Borided steel topography and phase contrast in tapping mode

U.L. Mishigdorzhiyn

Department of Metals Science and Materials Processing Technology, East Siberia State University of Technology and Management, 670013, Ulan-Ude, Russia
e-mail: druh@mail.ru

It is known, that atomic force microscopy (AFM) analysis is powerful instrument of surface characterization, such as phase-contrast imaging and topography. However, fewer literature sources devoted to AFM application in thermochemical surface treatment investigations, for instance in boriding. One of the problems that researchers face while observing hardened layers, such as boronized ones, is uneven surface topography, which prevents the adequate phase contrast, based on elastic modulus data. The paper presents results of AFM analysis of carbon and alloyed steel after boriding in boron carbide containing pastes. Aluminum powder was added to boriding media for layer's brittleness reducing and microstructure transformation. Topography and phase map of borided layer's cross sections were investigated by means of AFM in tapping mode. Empirically the research area of 25x25 μm was defined. Etching positive effect upon topography data was revealed due to surface oxidation after etching. In addition to cross sections, the treated surface topography and phase map were analyzed as well. Based on these data, morphology and crystal orientation of iron borides were established. Elongated crystals topography and phase map is different from cross section one, where elongated crystals were observed.

P-63

Influence of quantity of amino-acid residues in the oligopeptides based on glycine on their self-organization in films

A.S. Morozova[1], C.A. Ziganshina[2], M.A. Ziganshin[1], A.A. Bukharaev[1,2]

[1]*Kazan Federal University, 420008, Kazan, Russia*
e-mail: morozova_anna_s@mail.ru

[2]*Zavoisky Physical-Technical Institute, Federal Research Center «Kazan Scientific Center of Russian Academy of Sciences», 420029, Kazan, Russia*

At last time the considerable interest of researchers is attracted to shortchain peptides (oligopeptide). Materials on their basis are biocompatible, they have the increased thermal stability and biological activity. A key feature of oligopeptides is their ability to self-organization with formation of various structures: nanoparticles, nanofibres, nanorods, nanowires, nanotubes, nanospheres, nanobubbles etc [1,2]. Glycine is a part of many proteins and the biologically active compounds. In a human body glycine used as an energy source and participates in glucose synthesis, plays an important role in functioning of a brain [3]. Di- and tripeptides based on glycine are also biologically active compounds, represents the glycine source in a human body. The studies of properties of oligopeptides based on glycine (glycyl-glycin and glycyl-glycyl-glycin) are of great interest due to the possibility of its use for production of the biologically active compounds and drugs.

At present work using the atomic-force microscopy (AFM) the self-organization di- and tripeptide based on glycine in a film on various substrates under the influence of vapors of organic compounds (alcohols, nitrogen compound and chlorderivatives) and water was studied.

Dipeptide glycyl-glycine (GG) and a tripeptide glycyl-glycyl-glycin (GGG) were used as objects. Three smooth substrates with differing properties were used: hydrophobic highly oriented pyrolytic graphite (HOPG), hydrophilic mica and monocrystal silicon. Monocrystal silicon have the hydrophilic surface, however, unlike a fresh surface of mica, does not carry on itself the negative charge.

AFM images of films of GG and GGG on mica, HOPG and silicon were obtained. It was established that the substrate has a significant influence on morphology of initial film of di- and a tripeptide. Moreover, depending on a way of film preparation the morphology of its surface is various. So, on a surface of HOPG and mica di- and a tripeptide form amorphous films. While dropping the GG solution on silicon surface with the spontaneous solvent evaporation leads to the formation of layered nanocrystals. According to a powder x-ray diffractometry these crystals represent an alpha phase of dipeptide. The investigation of the influence of vapors of organic compounds and water requires the formation of amorphous films on all substrates. For this purpose the special techniques of the formation of oligopeptides amorphous films on HOPG, mica and silicon were developed.

Depending on the nature of the interacted vaporous compounds the layered nanocrystals, nanocrystals collected from fibers and nanospheres are formed on a surface of diglycine and triglycine films. After the saturation of the GGG film deposited on silicon with ethanol vapors (Fig. 1d) rectangular crystals (from 800 nm to 4 μm length, from 750 nm to 3 μm width) were received and the ways of the masstransfer of tripeptide to crystal are visible. The ethanol vapors occurs the significant effect on the dipeptide film deposited on silicon substrate. After influence of these vapors on a film of GG the flat crystalline structures of a triangular and trapezoidal shape with clear boundaries are received. Nanostructures form the beams dispersing from the center of a circle. Width and length of crystals in the center are 150 – 400 nm and 200 – 900 nm respectively. During moving away from the center of the circle the shape of crystals becomes triangular, length increases to 0,9 – 8 μm, width is 0,3 – 1 μm and 1,5 – 2,5 μm in narrow and wide sides of a trapeze.

The received results show that the type of substrate and the nature of vapors of organic compounds have a significant effect on a shape of the nanostructures formed during the self-organization of oligopeptides.

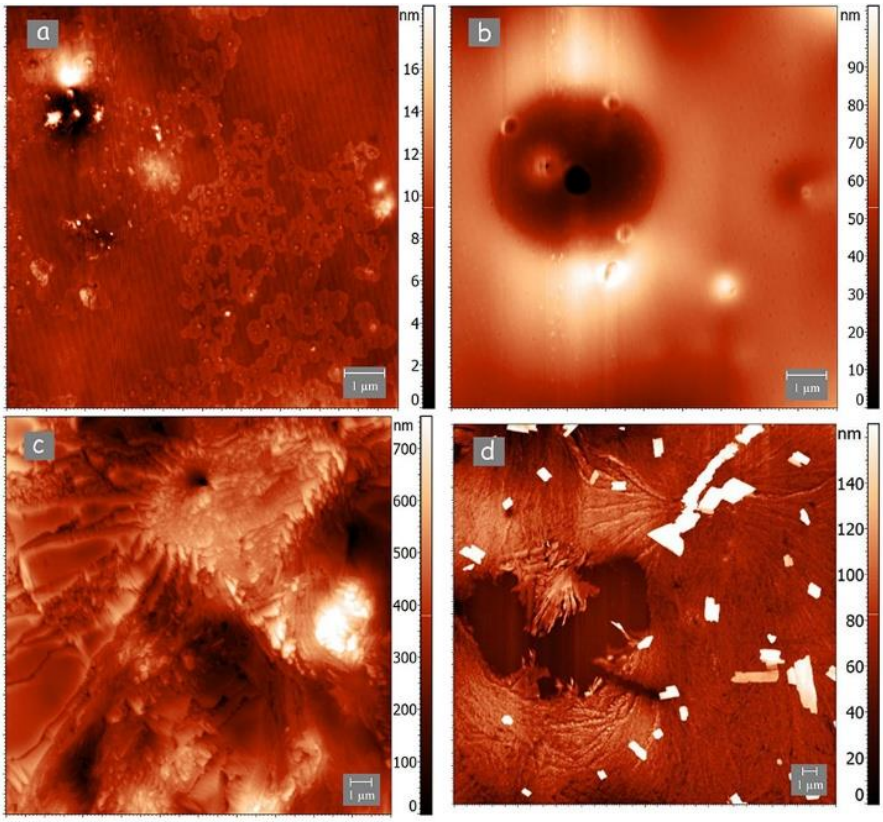

Figure 1. AFM images of (a, c) GG and (b, d) GGG films formed on silicon (a, b) before and (c, d) after the interaction with ethanol vapors.

1. C. Guo, Y. Luo, R. Zhou, et al., *Nanoscale* **6**, 2800 (2014).
2. A.M. Smith, E.F. Banwell, W.R. Edwards, et al., *Adv. Funct. Mater*. **16**, 1022 (2006).
3. N. Habibi, N. Kamaly, A. Memic, et al., *Nano Today* **11**, 41 (2016).

P-64

Structural phase transitions during annealing of proton-exchanged layers on X-cut and Z-cut lithium niobate

S.S. Mushinsky, I.V. Petukhov, M.A. Permyakova, V.I. Kichigin, L.N. Malinina, A.B. Volyntsev

PSU, Perm Research and Production Instrument Making Company (PNPPK), Perm, Russia
e-mail: sergey.mushinsky@gmail.com

Isothermal phase transitions during annealing of proton-exchanged (PE) layers on X-cut and Z-cut lithium niobate (LN) crystals were studied. Congruent lithium niobate crystals (Crystal Technology, Sipat) were used. Proton exchange was carried out in the molten benzoic acid at temperatures ranging from 175°C to 190°C during 2-6 hours. Samples were annealed consequently with a step of 1 hour at 330°C. Samples were investigated by means of polarized light optical microscopy, mode spectroscopy, IR-spectroscopy and XRD.

The following sequence of phase transitions during annealing of PE-layers on X-cut was proposed and successfully confirmed: β1, β2-phases→κ2-phase→κ1-phase→α-phase. Main feature of κ2-phase→κ1-phase transition in X-cut LN is the formation of particles of κ1-phase (which create a modulated structure) but not a layer.

Since κ2-phase formed on X-cut LN is characterized by high strain perpendicular to the substrate surface while strain of κ_1-phase formed on X-cut LN are one order of magnitude lower, a relaxation through incoherent boundaries formation between κ_2-phase and κ_1-phase takes place during annealing. New interphase boundary leads to the formation of additional structural defects. After interphase boundary vanishing during subsequent annealing, some part of aforementioned defects may persist. These structural defects may attract charges (e.g. during temperature changes) which can adversely affect the operation of integrated optical devices.

Phase transitions during annealing of PE-layers on Z-cut are significantly different. The sequence of phase transitions during annealing is the same: β_1, β_2-phases→κ_2-phase→κ_1-phase→α-phase. However, in this case PE-waveguide consists of coherent layers until their full transformation into α-phase. Particles of κ_1-phase are not formed because of lower strains of κ_2-phase and κ_1-phase in Z-cut crystal and smaller difference in their values compared to X-cut.

Increasing temperature and duration of proton exchange does not change characteristic features of structural phase transitions during waveguide annealing. However thicker waveguides need greater annealing time to complete phase transition.

This work was supported by Russian Foundation For Basic Research (project № 17-43-590309 p_a).

P-65

Comparative analysis of spherical focusing transducers from dense and porous piezoceramic materials

N.L. Korepanova, A.V. Nasedkin

Institute of Mathematics, Mechanics and Computer Science, Southern Federal University, 344090, Rostov-on-Don, Russia
e-mail: nasedkin@math.sfedu.ru

This paper considers a finite element investigation of ultrasonic spherical transducers made of dense or porous piezoceramic materials polarized in the thickness. By virtue of the axial symmetry of piezoelectric transducers we examined the axisymmetric problems in the plane of the meridian section. Considered transducer includes spherical segment, radial surface of which was covered by the electrodes. For effectiveness of acoustic wave excitation, due to the large difference between impedance of piezoelectric ceramics and impedance of surrounding acoustic medium, one or two elastic matching layers with successively decreasing impedances were added to the active element of transducer.

In the case of porous piezoceramics in order to determine its effective moduli, a comprehensive approach was used, which includes the effective moduli method, the modeling of special porous structures of representative volumes, and the finite element method. This technology has been realized in the finite element packages ANSYS and ACELAN-COMPOS.

For considered transducers in the finite element package ANSYS the regular grid of quadrilateral bilinear elements were built, where each piezoelectric element had its elemental coordinate system with the axis of ordinates is directed along the radial direction. Irregular grid of acoustic finite elements with impedance conditions on the external boundary of acoustic region has been formed in the area, surrounding transducer.

In the first stage, modal and harmonic analyses for piezoelectric transducers without acoustic medium were carried out. Further for the considered transducers the coupled harmonic problem of electroelasticity and acoustics has been solved in ANSYS for the main resonance frequency of thickness mode and the characteristics of the focal spot in the acoustic medium have been identified.

The operating modes of the transducers near the electric resonance frequencies were investigated, when the oscillations were excited by voltage, as well as the operating modes of the transducers near the electric antiresonance frequencies were investigated, when thevibrations were excited by an electric current applied to electrodes.

Finite element calculations showed that the porous piezoelectric ceramics has a greater effectiveness of wave excitation in the acoustic medium in comparison with dense piezoceramics. Furthermore, in the case of porous piezoceramic the transducer may be composed from only one layer, while for dense ceramic the best results are obtained in the presence of additional matching elastic layers.

The second author is grateful for the support of the Ministry of Education and Science of the Russian Federation, project 9.1001.2017/4.6.

P-66

Domain kinetics during polarization reversal in 36º Y-cut CLN

E.A. Neradovskaia[1,2], M.M. Neradovskiy[1,2], A.S. Esin[2,3], M.A. Chuvakova[2,3], P. Baldi[1], M.P. De Micheli[1], A.R. Akhmatkhanov[2,3], V.Ya. Shur[2,3]

[1] *Institut de Physique de Nice, 06108, Nice, France*
neradovskaia.elizaveta@ya.ru

[2]*School of Natural Sciences and Mathematics, Ural Federal University, 620000, Ekaterinburg, Russia*

[3]*Labfer Ltd., 620014, Ekaterinburg, Russia*

Modern market of technologies formed demand on low price middle-infrared (mid-IR) lasers [1]. The mid-IR is defined as 2-20 μm spectral range with a number of so-called "water windows", representing wavelength of light which can propagate through Earth's atmosphere without absorption by water vapor [2]. Moreover, most molecules have distinct absorption lines in the mid-IR, providing a fingerprint that makes it possible to identify them by optical spectroscopy [3].

To realize the optical frequency mixers adapted to the ultra-short pulses sources (<100 fs) and high average power (above 10 W) in mid-IR it is necessary to have non-linear components offering large aperture (about 1 cm^2). The periodically poled non-linear optical crystals lithium niobate (LN) and lithium tantalate are well suited to the optical parametric amplification in the mid-IR due to wide transparency range and high non-linearity, but the usual poling technique is not suitable for producing the components with required large aperture.

In order to overcome this technological barrier, the "slanted poling" (or axis-slant QPM) have been demonstrated [4]. The essence of the method is to produce periodical grating in plate with slanted polar axis, specifically in 25º X-cut MgO-doped LN (MgO:LN). In our work we investigated 36º Y-cut congruent LN (CLN) crystals, which are used for surface acoustic wave devices. The main advantages of these crystals are low price and great offer on the market.

The studied samples represent the 0.5-mm-thick double polished plates with 36º angle between Y-axis and normal to surface of the sample. The polarization reversal under application of pulses with increasing field and varied field rate was realized using liquid electrodes (aqueous solution of LiCl). The poling was performed in SF_6 to exclude electric arc discharge. The switching current and the set of instantaneous domain images visualized by optical microscopy have been recorded simultaneously.

It was demonstrated that the shape of micro-domains correlates with the crystal symmetry C_{3v} [5]. The static domain structure in the bulk was visualized by Cherenkov-type second harmonic generation [7]. Forward and sideways domain wall motions have been measured.

The dependence of threshold field on field rate (dE/dt) has been measured. The threshold fields E_{th} at constant field were estimated E_{th} = *32.8±0.3 kV/mm* along normal to the sample surface and E_{th} = *19.3±0.3 kV/mm* along Z-axis. Last value is close to the threshold field in Z-cut CLN, $E_{th} = 21$ kV/mm [6].

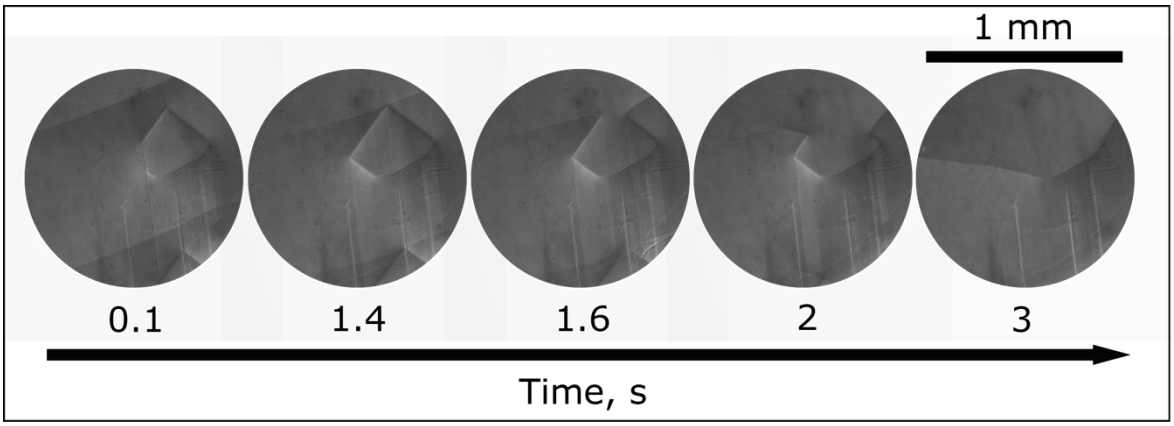

Figure 1. Time resolved coalescence of domains in 36º Y-cut CLN *in situ* visualized by optical microscopy during polarization reversal with liquid electrodes. E_{max} = 33 kV/mm.

The field dependence of domain wall velocity was studied by application of pulses with variation of $\Delta E_{ex} = E_s - E_{th}$ (excess of switching field above the threshold value). Complete switching by wall motion occurred for $\Delta E_{ex} > 2.4$ kV/mm.

Local polarization reversal has been studied by application *dc* voltage ranged from 100 to 250 V and duration from 0.1 s to 100 s to conductive tip of scanning probe microscope. Resulting static domain structure was visualized by piezoresponse force microscopy. Each pulse ended before withdrawing of the tip.

The dependences of domain diameter on pulse duration and amplitude have been measured. The obtained partial backswitching effect becomes more pronounced with pulse duration. Almost complete backswitching was obtained for U = 100 V and t_p = 100 s.

Self-organized nanodomain arrays were formed when grounded conductive tip was moved in vicinity of the freshly switched domains. The acceleration of backswitching effect has been observed when grounded tip was moved through freshly switched domain.

The equipment of the Ural Center for Shared Use “Modern nanotechnology” Ural Federal University was used.

1. R. Szweda, *III-Vs Rev.* **15**, 38 (2002).
2. D. Lubin, *J. Clim.* **7**, 121 (1994).
3. J.E. Bertie, Z. Lan, *Appl. Spectrosc.* **50**, 1047 (1996).
4. H. Ishizuki, T. Taira, *Opt. Mater. Express* **1**, 1376 (2011).
5. V.Y. Shur, A.R. Akhmatkhanov, I.S. Baturin, *Appl. Phys. Rev.* **2**, 040604 (2015).
6. V. Shur, E. Rumyantsev, R. Batchko, G. Miller, M. Fejer, R. Byer, *Ferroelectrics* **221**, 157 (1999).
7. Y. Sheng, A. Best, H.-J. Butt, W. Krolikowski, A. Arie, K. Koynov, *Opt. Express* **18**, 16539 (2010).

P-67

Visualization of mechanical stress of near-surface layer by analyze of MFM images of planar permalloy microparticles formed on surface

N.I Nurgazizov, D.A. Biziyaev, A.A. Bukharaev, I.V. Russkikh, Yu.V. Sadchikov

Zavoisky Physical-Technical Institute, FRC Kazan Scientific Center of RAS, 420029 Kazan, Russia
e-mail: niazn@mail.ru

The possibility of using the Villari effect (or the magnetoelastic effect, in which the magnetic properties of a solid change under mechanical action) has been intensively studied by scientists for application with changing of magnetization of micro- and nanostructures [1,2]. Moreover a change in the magnetization of particles can be used for detection of mechanical stresses that arise in the particle. By detecting the changes of a magnetization of planar particles located on a solid surface one can register the mechanical stresses in the near-surface layer of the substrate. In this case, the lateral resolution of this technique will be comparable with the lateral sizes of the particle.

The studies were carried out on samples representing an array of the planar Py (Ni79%, Fe16%, Mo4%) particles (with the size of 25×25 μm^2) located on a glass substrate. Heights of particles were varied for different samples in range 10−50 nm. Particles were fabricated by electron beam evaporation under ultrahigh vacuum conditions by using a "Multiprobe P" device (Omicron). An array of identical particles was formed by sputtering through a metal grid placed on the surface of the substrate.

To create stressed particles, the substrate was elastically bent. For this purpose the flat holder was used. The thin metal wire was placed under the center of a sample and the edges of a sample were clamped. Different tension of substrate and particles on it was carried out by changing of diameter of the wire. At the same time it was possible to investigate the same particle always by using of the system of optical positioning of a SPM tip.

A scanning probe microscope (SPM) Solver P47 (NT-MDT) and a magnetic cantilever of the model "N18 Co-Cr" (MikroSience) were used to perform MFM studies. MFM was used for visualization of particles domain structure. The obtained MFM images were compared with results of computer modeling of a particle magnetic structure. Its calculations were carried out by the OOMMF [3] and "Virtual MFM" [4] software. The size and the form of particles obtained by MFM were used for modeling. A modeling of distribution of a tension tensor in a substrate surface depending on its bend was carried out.

It has been shown that uncompressed particles have classical four-domain structure, with domains equal by the sizes. At one axe tension of particles is resulted to an increasing of the sizes of domains with direction of magnetization perpendicular to a tension. Increase of the size of domains with direction perpendicular to the tension caused by a negative sign of a magnetostriction constant of the used permalloy. Increasing of a domain size leads to form a characteristic bridge between them, which is clear observed on the MFM images.

Based on the experimental MFM results and the executed calculations for an each characteristic length of the observed bridge were got of a value of the tension tensor of a near-surface layer calculated for a curved substrate. It has been shown the direction of a bridge observed on the MFM image of Py particle is give possibility to find of a direction of the particle stretch. Thus, the planar ferromagnetic particles may be used for visualizing of mechanical stress in the substrate.

The work was support by RFBR 17-08-00915.

1. G. Dai, Q. Zhan, H. Yang et al., *J. Appl. Phys*. **114**, 173913 (2013).
2. S. Finizio, M. Foerster, M. Buzzi et al., *Phys. Rev. Applied* **1**, 021001 (2014).
3. M.J. Donahue, D.G. Porter: (http://math.nist.gov/oommf/).
4. D.V. Ovchinnikov, A.A. Bukharaev, *Technical Physics* **46,** 1014 (2001).

P-68

Repolarization of ferroelectric superlattices $BaZrO_3/BaTiO_3$

A.S. Sidorkin[1], L.P. Nesterenko[1], Y. Gagou[2], P. Saint-Gregoire[3,4], E.V. Vorotnikov[1], A.Yu. Pakhomov[1]

[1]*Voronezh State University, Voronezh, Russia*
e-mail: alexeypakhomovvv@gmail.com

[2]*Universite de Picardie Jules Verne, 80039 Amiens Cedex, France*

[3]*ICGM, C2M, 34095 Montpellier Cedex, France*

[4]*University of Nimes, 30021 NIMES Cedex 01, France*

Using the modified Sawyer-Tower scheme and the Mertz technique the repolarization properties of ferroelectric barium zirconate/barium titanate superlattices $BaZrO_3/BaTiO_3$ on a single-crystal magnesium oxide MgO substrate were investigated.

Experimental studies of switching currents have shown that switching processes in synthesized superlattices are carried out in two stages - activation motion ("creep" mode) and nonactivation (slip mode). The presence of an activation switching stage means that with high probability switching processes in the investigated superlattice are realized by the motion of domain walls. The threshold field separating creep and slip stages decreases with increasing temperature when approaching the Curie point of the superlattice similar to the coercive field. The activation mode of motion revealed in the work that does not obeying the strictly exponential dependence on the field strength was modeled by the dependence with a critical exponent for the applied electric field. The angle of slope in the field dependence of the switching current in the linear region decreases with increasing of the temperature, which may be due to a decrease in the polarization as the phase transition temperature approaches the nonpolar state in the lattice. Both used methods show that the investigated superlattices have a small internal bias field directed from the superlattice to the substrate. To explain the direction of the internal biasing field obtained in the researched structures, one can use the representations of the flexoelectric effect.

To use superlattices in dynamic memory devices, it is necessary to know the characteristics of switching in strong fields, which is determined by the velocity or mobility of the domain walls. For the region of strong fields, the mobility of the domain walls at various temperatures was calculated on the basis of the switching time. As the temperature increases, the switching time grows, which means a decrease in the mobility of the domain walls associated with a critical deceleration of the polarization relaxation near the Curie point.

The study was supported by Russian Science Foundation, project No. № 17-72-20105.

P-69

Development of multi-legged walking robot using piezoelectric benders

S.K. Cheon[1], T.G. Park[1], M.H. Kim[2] T.K. Song[2]

[1]*Dep. Electrical Engineering, 51140, Changwon, Republic of Korea*
e-mail: tgpark@changwon.ac.kr

[2]*Dep. Convergence Materials Science and Engineering, 51140, Changwon, Republic of Korea*

Biomimetic robots still have many problems to overcome in order to realize the diverse and efficient movement of life. To solve these problems, various attempts have been made. Many researchers are trying to make robots that are similar to the movement of living things and efficient and applying them to biomimetic robots through a new manufacturing process and materials, for example, such as soft mechanisms, piezoelectric, SMA and artificial muscle actuators. To solve this problem, a small robot using a piezoelectric bender was proposed.

In this study, a driving source of the biomimetic robot was investigated and a piezoelectric actuator as the most competitive driving source was found. The bimorph structure using piezoelectric ceramics had simple structure and easy to fabricate, and it had an excellent potential in terms of efficiency, as speed and energy density when comparing with other actuators for small robots. A piezoelectric small robot as shown in Fig. 1, using the piezoelectric benders as the small scale ambulatory robots was proposed.

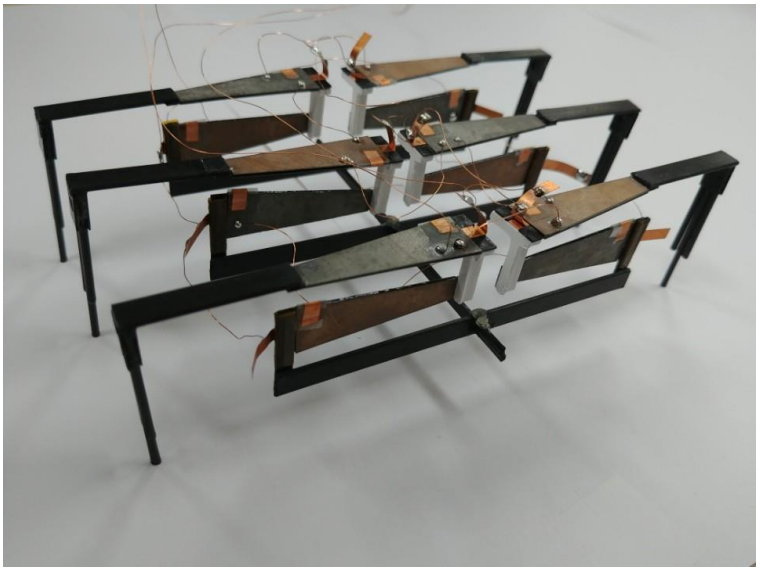

Figure 1. Manufactured multi-legged walking robot.

In order to make the motion of the biomimetic robot legs similar to the movements of the cockroaches or similar insects, two pairs of legs in the diagonal direction in the four leg structures are required to make the same movement. And the elliptical displacement is realized by considering the horizontal and vertical displacements of the multimodal vibration with intersecting perpendicular fields and by driving them by means of electrical signals with a phased difference of 90°. The piezoelectric small robot showed very competitive driving characteristics as a small scale robot actuator with simple structure.

1. R.J. Wood, S. Avadhanula, R. Sahai, et al., *Journal of Mechanical Design* **130**, (2008).
2. M. Goldfarb, M. Gogola, G. Fischer et al., *Journal of Micromechatronics* **1**, 205 (2001).
3. A. Yumaryanto, J. An and S. Lee, *IEEE Conf. on Robotics, Automation, and Mechatronics*, 1 (2006).
4. J. Morrey, B. Lambrecht, A. Horchler et al., *IEEE Conf. on Intelligent Robots and Systems*, 82 (2003).
5. P. Birkmeyer, R. Fearing, *IEEE/RSJ International Conf. on Intelligent Robots and Systems*, 418 (2009).

P-70

Electrical properties of heterointerfaces composed of complex ferroelectric oxides: an experimental investigation

D.P. Pavlov[1], R.R. Zagidullin[1], I.I. Piyanzina[1,2], A.A. Kamashev[1], D.A. Tayurskii[2], R.F. Mamin[1]

[1]*Zavoisky Physical-Technical Institute, FRC KazanSC of RAS, 420029, Kazan, Russia*
e-mail: dmitry.p.pavlov@gmail.com

[2]*Kazan Federal University, 420008, Kazan, Russia*

For the paradigmatic oxide heterostructure with $LaAlO_3$ (LAO) thin films grown on $SrTiO_3$ (STO) substrates, distinct electronic phases have been extensively characterized at the LAO/STO interface: for LAO films with more than three layers and LaO termination towards the TiO_2 interface, a two dimensional electronic gas (2DEG) is formed in the STO layers next to the interface [1]. It was concluded, that the primary mechanism responsible for the 2DEG formation is electronic reconstruction.

Since then 2DEG has been later found in other non-magnetic dielectrics. But the common feature for all systems is that the creation of the 2DEG can be due to either the polar nature of one of components or due to defects or dopants. It has been shown that analogous to the ionic polar discontinuity, 2DEG may be created at an interface due to electric polarization discontinuity [2,3]. Attractive materials for such a purpose are ferroelectrics. They have a wide range of different distinctive properties, among them: spontaneous polarization switching, high dielectric permeability, dielectric nonlinearity, piezo- and pyro- activity, linear and quadratic electro-optical effects. That can expand the scope of application in nanoelectronics.

Recently, it has been theoretically predicted that q2DEG can be created at the interface of nonpolar oxides one of which is ferroelectric [2,3]. And In the present work we experimentally test the possibility of such a switchable q2DEG realization. The thin film of epitaxial $Ba_{0.8}Sr_{0.2}TiO_3$ (BSTO) was sputtered on the top of single crystalline $SrTiO_3$ (STO) substrate using the magnetron sputtering technique. We also are investigating bilayer structure $Ba_{0.8}Sr_{0.2}TiO_3/Ba_{0.2}Sr_{0.8}TiO_3$ on MgO. Conductivity measurements were performed by a four-point probe method. In our investigation we present electrical resistivity versus temperature measurements and results are still under consideration.

The reported study was funded by RFBR according to the research project № 18-32-00595.

1. A. Ohtomo, H. Hwang, *Nature* **427**, 6973 (2004).
2. M.K. Niranjan, Y. Wang, S.S. Jaswal, et al., *Phys.Rev.L.* **103**, 016804 (2009).
3. K.D. Fredrickson, A. Demkov, *Phys.Rev.B.* **91**, 115126 (2015).

P-71

Quasi-two-dimensional electron system at the interface between antiferromagnet $LaMnO_3$ and ferroelectric $Ba_{0.8}Sr_{0.2}TiO_3$

D.P. Pavlov, N.N. Garig'yanov, A.V. Leontyev, D.K. Zharkov, V.V. Kabanov, R.F. Mamin

Zavoisky Physical-Technical Institute, FRC KazanSC of RAS, 420029, Kazan, Russia
e-mail: dmitry.p.pavlov@gmail.com

It has been shown that analogous to the ionic polar discontinuity, the quasi two dimensional electron gas (q2DEG [1]) may be created at an interface due to electric polarization discontinuity [2,3]. A two dimensional electronic gas (2DEG) is formed in the STO layers next to the interface which becomes superconducting below a temperature of 300 mK [1,4]. Remarkably, the superconducting state coexists with a magnetic state being stable up to the room temperature. Ferroelectrics are attractive materials for such purpose. They have a wide range of different distinctive properties, among them: spontaneous polarization switching, high dielectric permeability, dielectric nonlinearity, piezo- and pyro- activity, linear and quadratic electro-optical effects. That can expand the scope of application in nanoelectronics. The direction of such polarization in the ferroelectric film might be switched by an external electric field.

Antiferromagnetic $LaMnO_3$ might be transferred to ferromagnetic state by increasing the concentration of free carriers by injection. This means that increasing the free change carriers might lead to the local ferromagnetic state and magneto-resistivity in a system with 2DEG. Therefore, there is an opportunity to switch both conductivity by an electric field (trigger effect), and the magnetic order (magnetoelectric effect) in the heterostructures similar to BTO/LMO.

In the present work the thin film of epitaxial $Ba_{0.8}Sr_{0.2}TiO_3$ (BSTO) was sputtered on the top of single crystalline $LaMnO_3$ samples using the magnetron sputtering technique. Conductivity measurements were performed by a four-point probe method. Measurements were performed for three types of samples: (1) sample N_1 is a heterostructure based on single crystalline LMO with a BSTO film on top of it (*c* axis of LMO is parallel to the deposition plane); (2) sample N_2 is a heterostructure based on single crystalline LMO with a BSTO film on top of it (*c* axis is perpendicular to the deposition plane); (3) samples N_{01} and N_{02} are single crystals LMO without films with polarization axis as in the cases of N_1 and N_2, respectively.

Our measurements demonstrated that the resistivity of samples with deposited film of BSTO decreases strongly, and below the temperature of 160 K passes to a metallic-like behavior. The results of optical investigations of BSTO/LMO heterostructure are presented. In the case of the *c* axis perpendicular to the film surface the substrate has a compressive effect on the film.

The reported study was funded by Russian Scientific Foundation according to the research project No. 18-12-00260.

1. A. Ohtomo, H. Hwang, *Nature* **427**, 6973 (2004).
2. M.K. Niranjan, Y. Wang, S.S. Jaswal, et al., *Phys.Rev.L.* **103**, 016804 (2009).
3. K.D. Fredrickson, A. Demkov, *Phys.Rev.B.* **91**, 115126 (2015).
4. N. Reyren, S. Thiel, A. Caviglia et al., *Science* **317**, 5842 (2007).

Local polarization reversal in KTP single crystals

E.V. Pelegova, E.V. Shishkina, A.R. Akhmatkhanov, M.S. Kosobokov, V.Ya. Shur

School of Natural Sciences and Mathematics, Ural Federal University, 620000 Ekaterinburg, Russia
e-mail: elena.pelegova@urfu.ru

Single crystals of potassium titanyl phosphate ($KTiOPO_4$, KTP) with periodical ferroelectric domain structure are widely used for nonlinear optical applications including forward and backward second harmonic generation and optical parametric oscillation [1-3]. The domain structure evolution in KTP can be considered as a model process for investigation of the kinetics of the first order phase transitions in the crystals with C_{2v} symmetry. Previously, domain kinetics was studied *in situ* by optical methods [4,5], but, to our knowledge, local polarization reversal in crystals of KTP family was not investigated systematically [6]. Usage of the scanning probe microscopy methods gives the opportunity to study the domain kinetics with nanoscale resolution, which is very important for understanding the mechanisms of domain evolution.

We have studied KTP single crystals (Crystals of Siberia Ltd., Russia) grown by top-seeded solution method. The sample cut perpendicular to the polar axis was stuck to the ceramic plate on the UF-glue and polished down to 10 μm. The bottom electrical contact was provided by the indium tin oxide (ITO) electrodes deposited on the bottom side of the sample and the ceramic surface. The bottom electrode was grounded during switching and domain visualization.

Investigation of the local polarization reversal was performed by the scanning probe microscope NTEGRA Aura (NT-MDT). All experiments were performed at RT. The controlled relative humidity in the microscope camera ranged from 4% to 30%. The constant electric field pulse was applied to the top z+ polar surface by the conductive tip NSC14-Pt (MikroMasch®) with typical resonance frequency 160 kHz and force constant 5 N/m. Domain size dependences on pulse duration and amplitude were measured in the wide range: amplitude from 30 to 200 V (Fig. 1), duration from 10 ms to 200 s (Fig. 2).

The field was switched off only after the tip withdrew the surface to eliminate the backswitching effect. Domains have been written in arrays at the distance of 3 μm to each other in order to avoid their interaction. The switched domains were visualized just after polarization reversal by the same tip in piezoresponse force microscopy (PFM) mode by applying at 20 kHz modulation voltage of 3 V rms.

The switched domains were of hexagonal shape elongated in Y direction determined by the crystal symmetry. The obtained linear dependence of the domain length on the applied voltage (Fig. 1c) is typical for switching in uniaxial ferroelectrics [7,8].

We propose the following scenario of domain growth for elongated domains formed in the inhomogeneous field of the conductive tip: (1) domain nucleation under the tip, (2) domain growth in width due to step generation at the side walls, (3) domains growth in length due to step generation at the vertices and kink motion.

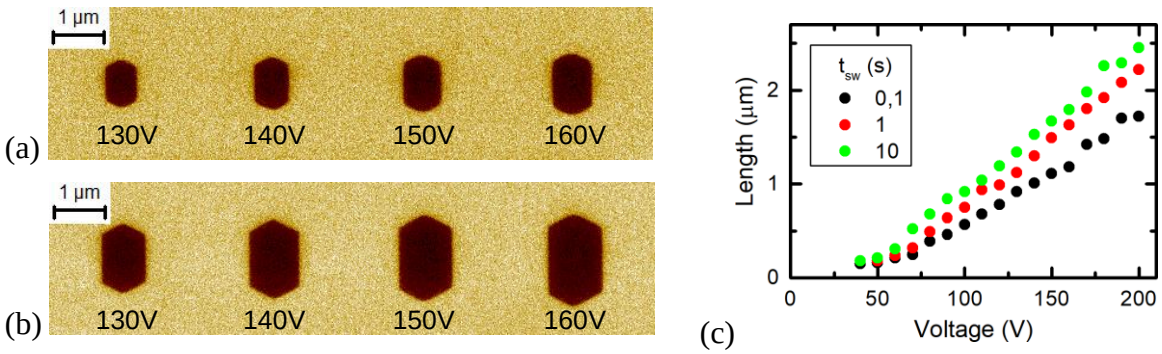

Figure 1. (a), (b) PFM images of domains obtained by local switching in KTP. Switching time: (a) 100 ms, (b) 10 s. Switching voltage: 130, 140, 150, and 160 V. (c) Domain length dependence on the pulse amplitude (switching voltage).

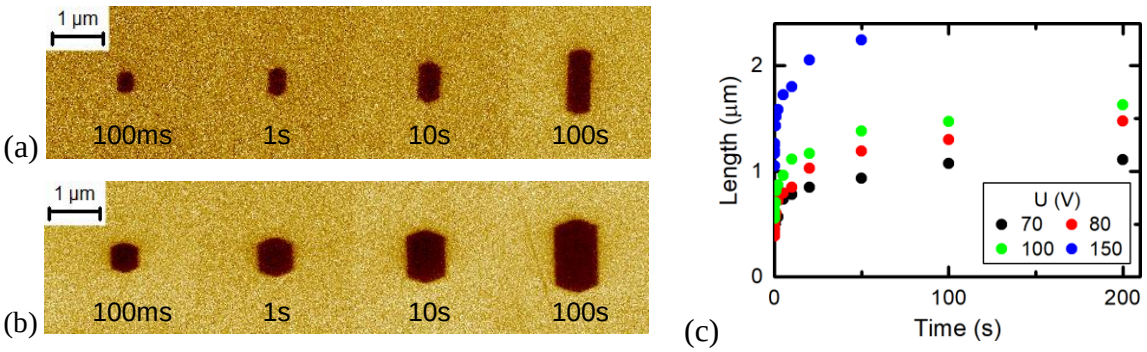

Figure 2. (a), (b) PFM images of domains obtained by local switching in KTP. Switching voltage: (a) 80 V, (b) 100 V. Switching time: 100 ms, 1 s, 10 s, 100 s. (c) Domain length dependence on the pulse duration (switching time).

The independence of the domain width on switching time for fields below 70 V has been attributed to the applied field value below the threshold for step generation at the domain walls. Domain length and width for pulse durations 100 ms and 1 s practically coincide in wide field range for low humidity (RH = 4%). It means that the domain rather fast reaches the size limited by the spatial distribution of the switching field. In the case of low humidity, the surface is free of water resulting in absence of external screening.

The obtained experimental data have been discussed in terms of the universal kinetic approach taking into account the influence of the screening retardation effect [9,10]. The spatial distribution of the residual depolarization field and switching field at the domain wall was calculated by COMSOL. The effect of step generation at the polygon vertices has been confirmed.

The research was made possible in part by RFBR (grant 16-02-00724) and by President of Russian Federation grant for young scientists (Contract 14.Y30.17.2837-MK). The equipment of the Ural Center for Shared Use “Modern nanotechnology” Ural Federal University was used.

1. C. Canalias, V. Pasiskevicius, F. Laurell, *Ferroelectrics* **340**, 27 (2006).
2. A. Arie, G. Rosenman, V. Mahal, A. Skliar, M. Oron, M. Katz, D. Eger, *Opt. Commun.* **142**, 265 (1997).
3. J. Hellström, V. Pasiskevicius, H. Karlsson, F. Laurell, *Opt. Lett.* **25**, 174 (2000).
4. V.Ya. Shur, E.M. Vaskina, E.V. Pelegova, M.A. Chuvakova, A.R. Akhmatkhanov, O.V. Kizko, M. Ivanov, A.L. Kholkin, *Appl. Phys. Lett.*, **109**, 132901 (2016).
5. V.Ya. Shur, A.A. Esin, M.A. Alam, A.R. Akhmatkhanov, *Appl. Phys. Lett.* **111**, 152907 (2017).
6. G. Rosenman, P. Urenski, A. Agronin, A. Arie, Y. Rosenwaks, *Appl. Phys. Lett.* **82**, 3934 (2003).
7. B.J. Rodriguez, R.J. Nemanich, A. Kingon, A. Gruverman, S.V. Kalinin, K. Terabe, X.Y. Liu, K. Kitamura, *Appl. Phys. Lett.* **86**, 012906 (2005).
8. V.Ya. Shur, A.V. Ievlev, E.V. Nikolaeva, E.I. Shishkin, M.M. Neradovskiy, *J. Appl. Phys.* **110**, 052017 (2011).
9. E.A. Eliseev, A.N. Morozovska, G.S. Svechnikov, E.L. Rumyantsev, E.I. Shishkin, V.Ya. Shur, S.V. Kalinin, *Phys. Rev. B* **78**, 245409 (2008).
10. V.Ya. Shur, *J. Mater. Sci*. **41**, 199 (2006).

P-73

Study of the surface profiling of silicon based on the method of local anodic oxidation using scanning probe microscopy

V.V. Polyakova[1], I.N. Kots[1], V.A. Smirnov[1], O.A. Ageev[2]

[1]*Southern Federal University, Institute of Nanotechnologies, Electronics, and Electronic Equipment Engineering, Taganrog, Russia*
e-mail: vpolyakova@sfedu.ru, ageev@sfedu.ru

[2]*Southern Federal University, Scientific and Educational Center "Nanotechnology", Taganrog, Russia*

The paper presents the results of studying the methods of nanoscale profiling of the surface of a silicon substrate by the method of local anodic oxidation and liquid chemical etching.

The development of the elemental base of nanoelectronics places high demands on the resolution and accuracy of the technological operations. At the same time, the improvement of the design of the elements leads to a reduction in the minimum dimensions in the formation of elements of micro- and nanoelectronics. Among the methods of lithography, one of the promising is local anodic oxidation (LAO), which provides high spatial resolution, the possibility of profiling the substrate surface without additional photolithography operations, high reproducibility [1]. The method of LAO is implemented using an atomic force microscope (AFM) and allows the formation of oxide nanoscale structures (ONS) on the surface of various materials that can be used in developing and creating elements of micro- and nanoelectronics, resistive memory elements based on memristor structures, lithographic masks, nanowires [2,3]. However, despite the rather large amount of publication on this problem, the regularities of the influence of technological regimes of local anodic oxidation on geometric pairs. The dimensions of the profiled nanosized structures on the silicon surface remain insufficiently studied.

Two methods were developed for profiling the silicon surface. For each of them, at the first stage, on the surface of a silicon substrate, KEF-0.1, the LAO matrix was formed using the Ntegra probe nanoscale laboratory (NT-MDT, Russia) in AFM contact mode using NSG11 cantilevers. According to the first procedure, ONS was removed by liquid etching in aqueous HF (1:3) solution at ambient temperature. As a result, matrices of profiled nanosized structures (PNS) were formed on the silicon surface. Then, the statistical processing of AFM images was carried out using the Image Analysis 2.0 software package, which resulted in the dependence of the geometric parameters of the ONS and PNS of silicon on the relative humidity at different values of the amplitude of the LAO voltage pulses shown in Figure 1.

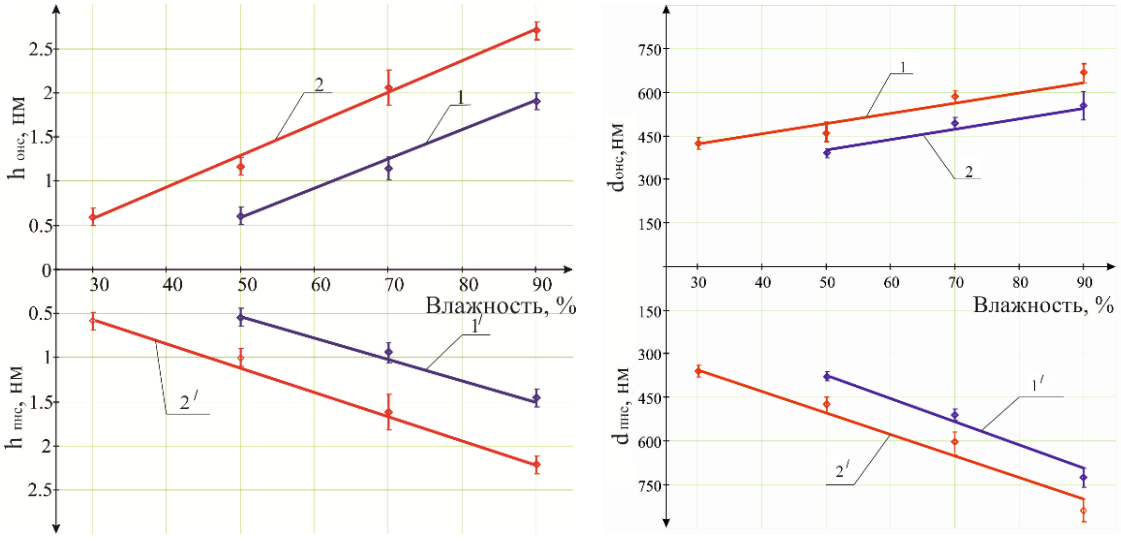

(а) (б)

Figure 1. Dependence of geometric parameters of nanostructures on relative humidity for different amplitude of voltage pulses (1 - 10V; 2 - 15V): (a) height of ONS and depth of PNS; (b) diameters of ONS and PNS.

According to the second method, silicon ONS obtained by the LAO method at a humidity of 70 ± 1% was used as a mask in liquid etching in a solution of KOH (60%) + IPA (5:1) at 70°C. As a result, a PNS 70 ± 10 nm in height was formed on the silicon surface.

Thus, it is shown that local anodic oxidation is a promising method of probe nanolithography, the use of which allows for surface profiling at the nanometer scale, and can be used to create nanowires, as well as elements of nanoelectronics and nanosystems.

The results of the work were obtained using the infrastructure of the Scientific and Educational Center and the Center for Collective Use "Nanotechnology" of the Southern Federal University.

1. Yu.A. Chaplygin, *Nanotechnology in electronics 3.1* ("TECHNOSPHERE", Moscow), 216 (2016).
2. V.I. Avilov, O.A. Ageev, V.A. Smirnov et al., *Nanotechnologies in Russia* **10**, 214 (2015).
3. M. Baker, A.J. Maguy, K. Vikas, et al., *Nanotechnol Rev*. **3**, 301 (2015).

P-74

As-grown domain structure in lithium tantalate with inhomogeneous distribution of stoichiometry deviation

V.I. Pryakhina, E.D. Greshnyakov, B.I. Lisjikh, M.S. Nebogatikov, P.S. Zelenovskiy, V.Ya. Shur

School of Natural Sciences and Mathematics, Ural Federal University, 620000 Ekaterinburg, Russia
e-mail: viktoria.pryahina@urfu.ru

We investigated the dependence of as-grown domain structure in $LiTaO_3$ (LT) on spatial distribution of Li concentration. Vapor transport equilibration process (VTE) was used for Li concentration increase from congruent (48.8 mol.%) to stoichiometric (50 mol.%) composition. Spatially inhomogeneous distribution was obtained by variation of VTE process time.

The Li concentration spatial distribution was measured by confocal Raman spectroscopy (Alpha AR300, Witech, Germany). Domain structure was visualized at the surface using optical (BX61, Olympus, Japan) and scanning electron (Merlin, Carl Zeiss, Germany) microscopies after selective etching and in the bulk using second harmonic generation microscopy (Ntegra Spectra, NT-MDT, Russia).

The inhomogeneous distribution was defined as the difference between surface and bulk Li concentrations (Δc). Three types of the distribution were defined: (a) near congruent composition with inhomogeneity near surfaces, (b) inhomogeneous distribution – stoichiometric composition at surfaces with decrease of Li concentration in the bulk, and (c) near stoichiometric composition.

The as-grown domain structure formed due to cooling below Curie temperature after VTE process. The formation of wide domain boundary due to phase transition depends on LT composition distribution. Congruent composition of LT led to formation of wide domain boundary consisted with maze domain structure. The narrow domain boundary was formed in LT with the inhomogeneous distribution due to toward moving of phase boundaries from surfaces to bulk. Domain structure in LT with near stoichiometric composition was represented by the interlaced layers of smooth head-to-head and zig-zag tail-to-tail charged domain walls.

The subsequent cooling to room temperature resulted in formation of isolated domains in the volume between surfaces and narrow domain boundary due to pyroelectric field. The isolated domains represented by both through and non-through domains with diameter up to 2 μm. The domain shape changed depending on local stoichiometry deviation from hexagonal for stoichiometric composition to trigonal for congruent one.

The different type of charged domain walls in ferroelectrics attracts interest due to possibilities of its applications.

The equipment of Ural Center for Shared Use “Modern Nanotechnology” Ural Federal University was used.

1. V.I. Pryakhina, E.D. Greshnyakov, B.I. Lisjikh, A.R. Akhmatkhanov, D.O. Alikin, V.Ya. Shur, A. Bartasyte, *Ferroelectrics* **525**, 47 (2018).

P-75

The effect of mechanical activation on the relaxor properties of $PbMg_{1/3}Nb_{2/3}O_3$ - $PbFe_{1/2}Nb_{1/2}O_3$ solid solution ceramics

S.I. Raevskaya[1], A.A. Gusev[2], V.P. Isupov[2], I.P. Raevski[1], A.G. Razumnaya[1], V.V. Titov[1], M.A. Malitskaya[1], G.R. Li[3], C.-C. Chou[4], S.P. Kubrin[1], E.I. Sitalo[1]

[1]*Research Institute of Physics and Faculty of Physics, Southern Federal University, 344090, Rostov-on-Don, Russia*
e-mail: sveta.raevskaya@mail.ru

[2]*Institute of Solid State Chemistry and Mechanochemistry SB RAS, 630128, Novosibirsk, Russia*

[3]*Shanghai Institute of Ceramics, Chinese Academy of Sciences, 200050, Shanghai, China*

[4]*National Taiwan University of Science and Technology, 10672, Taipei, Taiwan, China*

Recently we have found out that the high-energy mechanical activation of the starting oxides reduces dramatically the frequency shift ΔT and increases by about 20 K the temperature T_m of the dielectric permittivity maximum for ceramics of a classical ferroelectric-relaxor $PbMg_{1/3}Nb_{2/3}O_3$ (PMN) sintered from the mixture of these oxides [1]. Similar changes of ΔT and T_m were predicted previously, basing on the first-principle calculations, for PMN with an increased degree of a short-range ordering of Mg^{2+} and Nb^{5+} cations [2]. However, as we used for mechanical activation a high-energy planetary-centrifugal mill AGO-2 with both jars and balls made of the stainless steel, one could expect that a small amount of iron from a milling media incorporates into the processed powder and the $(1-x)PbMg_{1/3}Nb_{2/3}O_3$ - $xPbFe_{1/2}Nb_{1/2}O_3$ (PMN-xPFN) solid solution is formed during sintering. The formation of such solid solution, in principle, could explain the observed increase of T_m as well as a smaller unit cell parameter value (4.037 Å instead of ≈4.05 Å for a usual PMN ceramics) observed for PMN ceramics studied in [1]. The scope of the present work was to obtain several PMN-PFN solid solution compositions by both the usual solid-state synthesis and by high-energy mechanochemical synthesis and compare their relaxor properties and the values of the unit cell parameters.

Energy dispersive X-ray analysis (EDXA) has shown that the PMN samples obtained using high-energy mechanochemical synthesis contain about 1 wt.% of iron. Raman studies revealed that an additional band appears in the spectrum of such ceramics at 700 cm-1. Similar band is present in the Raman spectrum of PFN and it corresponds to the Fe-O stretching mode [3]. Thus at least a part of iron incorporates into the lattice of PMN. If one assumes that all this iron incorporates into the crystal lattice of PMN, the 0.8PMN-0.2PFN solid solution composition would be formed, which contains some MgO excess. Our studies have shown that for the PMN-PFN compositions from the $0 \le x \le 0.2$ range both the unit cell parameter and the ΔT values are smaller when ceramics is obtained using high-energy mechanochemical synthesis. On the other hand Tm values were very similar for the ceramics of the same composition obtained by both methods. Thus, one may conclude that the increase of Tm in the PMN ceramics obtained using high-energy mechanochemical synthesis may be ascribed, at least partially, to the formation of the PMN-PFN solid solution. However the main origin of the unit cell parameter and ΔT changes observed for such ceramics seems to be not the incorporation of iron from the milling media into the lattice, but rather the effect of high-energy mechanical activation.

This study was supported by RFBR (project 17-03-01293_a) and by the Ministry of Education and Science of the Russian Federation (project 3.1649.2017/4.6).

1. S.I. Raevskaya, A.A. Gusev, V.P. Isupov, et al., *Ferroelectrics* **525**, 37 (2018).
2. S. Prosandeev, L. Bellaiche, *Phys. Rev. B* **94**, 180102 (2016).
3. Yu.I. Yuzyuk, I.P. Raevski, S.I. Raevskaya, et al., *J. Alloys Compnds* **695**, 182 (2017).

P-76

The effect of the bias electric field on the dielectric and pyroelectric properties of single crystals and ceramics of Pb_2ScNbO_6 relaxor ferroelectric

S.I. Raevskaya[1], A.G. Lutokhin[1], Y.N. Zakharov[1], I.P. Raevski[1], A.A. Gusev[2], V.P. Isupov[2], V.V. Titov[1], M.A. Malitskaya[1], G.R. Li[3]

[1]*Research Institute of Physics and Faculty of Physics, Southern Federal University, 344090, Rostov-on-Don, Russia*
e-mail: igorraevsky@gmail.com
[2]*Institute of Solid State Chemistry and Mechanochemistry SB RAS, 630128 , Novosibirsk, Russia*
[3]*Shanghai Institute of Ceramics, Chinese Academy of Sciences, 200050, Shanghai, China*

Relaxor ferroelectrics are now in the focus of both material science, and physics of the inhomogeneous media as they exhibit giant dielectric, electrostrictive, pyroelectric, and piezoelectric responses, while the origin of these remarkable properties is not fully understood yet. Of special interest are 1:1 ternary perovskites of the $Pb_2B^{3+}B^{5+}O_6$ type (B^{3+} - Sc, In, Yb and B^{5+} - Nb, Ta) because one can change their properties from a usual ferroelectric or antiferroelectric with a sharp phase transition to a relaxor ferroelectric, characterized by a diffuse and frequency-dependent maximum of the dielectric permittivity ε, by varying the ordering degree S of B^{3+} and B^{5+} cations. As the S values depend on the preparation conditions there is a large scattering of the data concerning the properties of $Pb_2B^{3+}B^{5+}O_6$ perovskites. In the present work we studied the effect of the bias electric field on the dielectric and pyroelectric properties of both single crystals and ceramics of the canonic relaxor Pb_2ScNbO_6 (PSN) obtained by different methods. Single crystals were grown by the spontaneous crystallization from the flux at different cooling rates. Ceramics was fabricated using a one-step sintering either of the mixture of the starting oxides with 2 wt.% of Li_2CO_3 addition, or of the PSN powder obtained by mechanochemical synthesis using a high-energy planetary-centrifugal mill AGO-2.

Dielectric measurements have shown that all the samples studied exhibit a diffused ε(T) maximum. Both the temperature $T_{m\varepsilon}$ of this maximum (360-370 K) and a substantial relaxor-like frequency shift of $T_{m\varepsilon}$ are typical of disordered PSN. However a sharp and frequency-independent step is observed in the ε(T) curves at 340-350 K, which seems to be due to the presence of highly-ordered regions in the samples. Similar to a 1:2 textbook relaxor $Pb_3MgNb_2O_9$ (PMN) and its solid solutions with $PbTiO_3$ (PT) [1] $T_{m\varepsilon}$ depends on the bias field strength E only above some threshold E value. At zero field the maximum of the dynamic pyroelectric coefficient γ dependence on T is observed in the vicinity of the Vogel-Fulcher temperature. At rather small bias fields, this maximum shifts to the position of the supposed critical point (which is in the vicinity of $T_{m\varepsilon}$) and grows in magnitude. The γ(T) maximum increases up to the field corresponding to the critical point in the E-T phase diagram (it can be roughly estimated from the inflexion in the $T_{m\varepsilon}$(E) dependence) and decreases at higher fields. These data are similar to those obtained for PMN-PT crystals with a small PT content [1] as well as for single crystals of the uniaxial relaxor $Sr_{0.75}Ba_{0.25}Nb_2O_6$ [2] and support the presence of a critical point and a quasicritical behavior of pyroelectric coefficient in PSN ceramics. Dielectric, pyroelectric and piezoelectric properties near critical points are compared and discussed for 1:1 and 1:2 relaxor ferroelectrics.

This study was supported by RFBR (project 17-03-01293_a), by the Ministry of Education and Science of the Russian Federation (project 3.1649.2017/4.6) and by the Chinese Academy of Sciences President's International Fellowship Initiative (project 2018VEA0011).

1. S.I. Raevskaya, Yu.N. Zakharov, A.G. Lutokhin, et al., *Appl. Phys. Lett*. **93**, 042903 (2008).
2. S.I. Raevskaya, A.G. Lutokhin, A.M. Pugachev, et al., *Ferroelectrics* **440**, 59 (2012).

P-77

Local anodic oxidation by the probe method as a surface modification method for nanoscale profiling

A.A. Rezvan, V.S. Klimin

Southern federal university, 347922, Taganrog, Russia
e-mail: arezvam@sfedu.ru

In connection with the miniaturization of electronic devices, as well as an increase in the density of base elements location on the crystal, it is quite natural that today there is a serious need for the development of new nanolithography methods. That would allow for precise profiling and surface treatment of structures whose linear dimensions are approximately tens nanometers [1-3].

Lithography with using of probe nanotechnology by the method of local anodic oxidation is a promising technology for formation of various kinds of electronic and mechanical nanoelectronics elements, starting form quantum dots and ending with one-electron transistors. This fact is confirmed by the main feature of this method is ability to control in real time electrical and topographic characteristics of the formed nanoscale structures Thus, it is relevant to study the application of local anodic oxidation with subsequent plasma chemical etching for nanoelectronic devices [4-6].

Plates of GaAs were used as the main material of the substrate. These plates were subjected to standard liquid polishing to improve the corresponding geometric parameters of structures surfaces. Using a probe of an atomic force microscope, a local anodic oxidation of GaAs structures surfaces was carried out in a noncontact mode. Oxide nanostructures of GaAs were formed in moist oxygen, the relative humidity of working medium of the microscope was 90%, with a probe displacement rate of 1.5-5 μm/sec. As the result, structures in subsequent plasma chemical etching processes will be used as masking layers [7-8].

For formation of nanoscale structures based on GaAs, selective parameters of plasma chemical etching processes were used for each mask. The samples were subjected to plasma chemical etching in high frequency inductively coupled plasma. As the chlorine containing gas, BCl3 was used, which has its own peculiarities in the etching of structures based on A3B5. The etching was carried out with the following parameters: the gases atmosphere pressure in the working chamber was 2 Pa; the power of the source of the capacitive plasma was W_{RIE} - 35 W, with a bias voltage U_{bias} - 10^2 V. In addition, the power of the inductively coupled plasma source was W_{ICP} - 400 W; the flow velocity of the intermediate carrier gas N_{Ar} - 100 cm^3/min and the chlorine-containing gas N_{BCl3} - 10 cm^3/min. The total etching time with these parameters ranged from 0.5 to 2 minutes.

The subsequent investigations of surfaces topology of structures obtained were carried out by scanning electron microscopy.

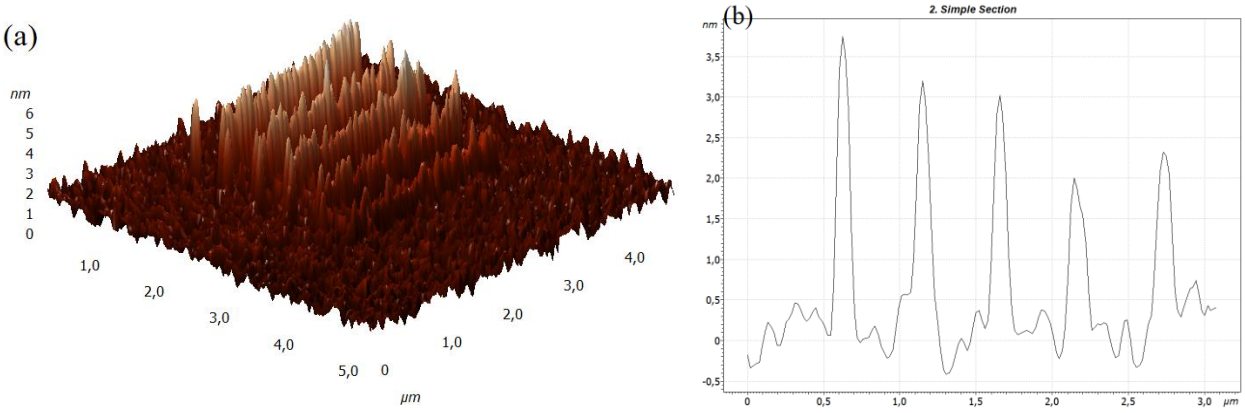

Figure 1. (a) The structures obtained by plasma chemical etching process and (b) profilogram across the structures.

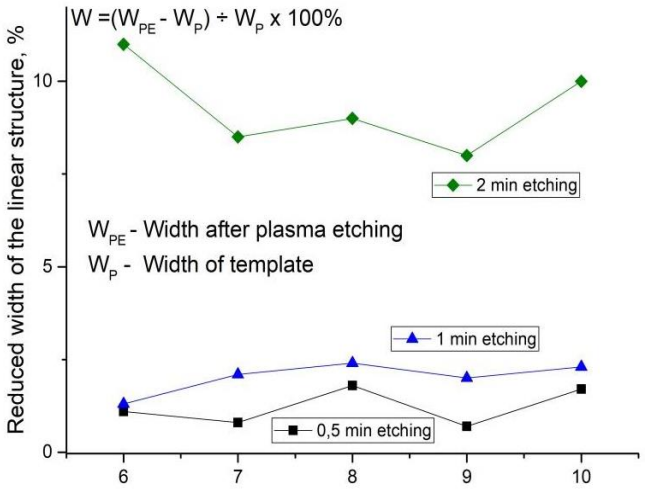

Figure 2. Dependence of the formation stress and etching time on the reduced width of the obtained nanostructures.

According to the experimental data, the geometrical parameters of formed structures were evaluated, at different stresses of LAO formation and etching time.

The obtained experimental dependences show that a combination of selective parameters of the local anodic oxidation method and plasma chemical etching makes it possible to modify the surface layer of GaAs structures with a specified degree of accuracy and roughness.

During the implementation of experimental studies, a technique for nanosized profiling of GaAs structures by a combination of local anodic oxidation and plasma chemical etching was developed and implemented. This work was carried out with support of the Southern Federal University (grant VnGr-07/2017-02). The results were obtained using the equipment of the Research and Education Center and Center for Collective Use "Nanotechnologies" of Southern Federal University.

1. V.S. Klimin et al., *J. Phys.: Conf. Ser.* **917**, 092005 (2017).
2. R.V. Tominov et al., *IOP Conf. Ser.: Mater. Sci. Eng.* **256**, 012023 (2017).
3. V.S. Klimin et al., *J. Phys.: Conf. Ser.* **741**, 012178 (2016).
4. N.N. Rudyk et al., *J. Phys.: Conf. Ser.* **917**, 082008 (2017).
5. R.V. Tominov et al., *J. Phys.: Conf. Ser.* **917**, 032023 (2017).
6. V.S. Klimin et al., *Proc. of SPIE* **10224**, 102241Z (2016).
7. M.V. Ilina et al., *Proc. of SPIE* **10224**, 102240U (2016).
8. V.S. Klimin et al., *J. Phys.: Conf. Ser.* **917**, 092023 (2017).

P-78

Study of formation of high aspect GaAs structures based on the method of focused ion beams

A.A. Rezvan, V.S. Klimin, M.S. Solodovnik

Southern federal university, 347922, Taganrog, Russia
e-mail: arezvam@sfedu.ru

The possibilities of nanolithography technologies aren't able to match modern requirements for processing and forming a surface of a predetermined type of relief with high resolution. At the current moment, there are a number of technologies with a combination of photo- or electron beam lithography and liquid etching, which don't allow obtaining the required result. This fact is supported by the dependence of size of structures formed by the methods of photo- or electron beam lithography, on the wavelength of exposure. In this connection, traditional methods of lithography aren't able to overcome the barrier of topological size in 50 nm [1-4].

One of the solutions to this problem is the application of method of focused ion beams with subsequent plasma chemical etching. Thanks to this methods combination, it is possible to select such selective parameters, which allow for precise formation of structures and profiling of the surfaces of these structures in accordance with specified characteristics over a wide range.

The experiment method. Experimental studies were performed on plates of intrinsic GaAs with a chemically purified and polished surface. After improving the geometric characteristics, the plates were subjected to processing by the method of focused ion beams. Built-in functions of Nova NanoLab 600 software, the surface layer was modified according to a pre-prepared template. The main parameters of the formation were the ion beam current I = 1 pA, the accelerating voltage U = 30 keV. The number of passes varied from 50 to 120. During this treatment, Ga+ ions were implanted into the surface of the GaAs plate, which resulted in the formation of a near-surface layer of the amorphous state, which was later used as a masking one[5-8].

Plasma chemical etching was carried out in a chlorine-containing medium. The chlorine-containing gas was BCl3 with varied flow rate of N_{BCl3} from 5 to 15 cm^3/min, the Ar gas was used as the transport gas with flow velocity N_{Ar} - 100 cm^3/min. The values of using powers of resistively and inductively coupled plasma are, respectively, W_{RIE} = 10 V and W_{ICP} = 200 V. The etching time ranged from 1 to 3 minutes.

Subsequent investigations of surfaces topology of obtained structures were carried out by scanning electron microscopy.

As a result of the experimental session, dependencies of the flow rate of the chlorine-containing gas on the deviation angle from the vertical for different crystallographic axes was obtained.

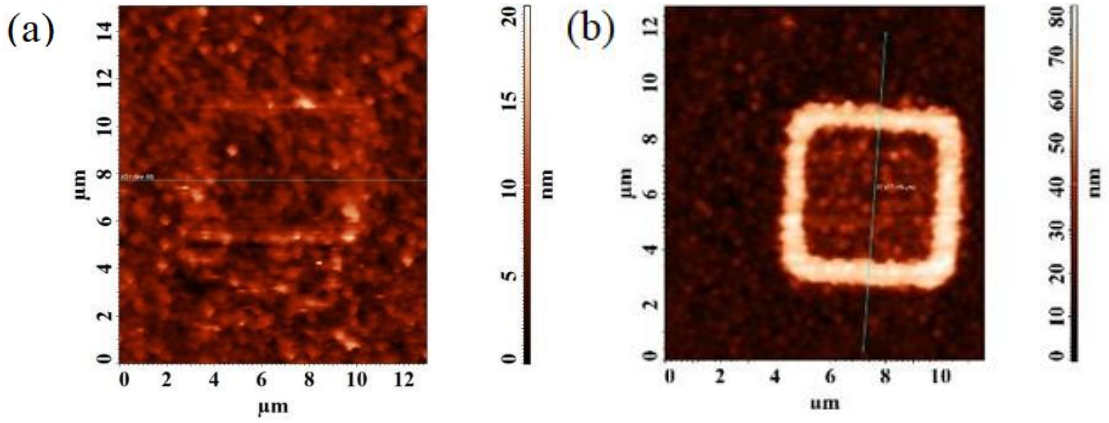

Figure 1. The structures etched by plasma chemical etching after electronic processing at 100 passes, 30 seconds of exposure in plasma (a) before plasma chemical etching, (b) after plasma chemical etching

According to these dependencies, it was concluded that when the flow of chlorine-containing gas is reduced, an increase in the verticality of walls is observed, regardless of the direction of crystallographic axes. Obtained parameters of the etching process can be integrated into different technologies of obtaining structures with nanoscale lateral characteristics. With the increase of flow, a flat wall is formed, which allows, in the presence of various layers in the structure, to bring electrical contact to different layers of the given structure

During the implementation of experimental studies, a technique for nanosized profiling of GaAs structures by a combination of local anodic oxidation and plasma chemical etching was developed and implemented.

This work was supported by the Russian Science Foundation Grant No. 15-19-10006. The results were obtained using the equipment of the Research and Education Center and Center for Collective Use "Nanotechnologies" of Southern Federal University.

1. V.S. Klimin et al., *J. Phys.: Conf. Ser.* **917**, 092005 (2017).
2. R.V. Tominov et al., *IOP Conf. Ser.: Mater. Sci. Eng.* **256,** 012023 (2017).
3. V.S. Klimin et al., *J. Phys.: Conf. Ser.* **741,** 012178 (2016).
4. N.N. Rudyk et al., *J. Phys.: Conf. Ser.* **917,** 082008 (2017).
5. R.V. Tominov et al., *J. Phys.: Conf. Ser.* **917,** 032023 (2017).
6. V.S. Klimin et al., *Proc. of SPIE* **10224**, 102241Z-1 (2016).
7. M.V. Ilina et al., *Proc. of SPIE* **10224,** 102240U-1 (2016).
8. V.S. Klimin et al., *J. Phys.: Conf. Ser.* **917,** 092023 (2017).

P-79

Light diffraction on periodically poled domain structures in lithium niobate crystal in an sunusoidal voltage

E.N. Savchenkov[1], S.M. Shandarov[1], A.E.Mandel[1], A.R. Akhmatkhanov[2], V.Ya. Shur[2]

[1]*Tomsk State University of Control Systems and Radioelectronics, 634050, Tomsk, Russia*
e-mail: rossler@mail.ru

[2]*School of Natural Sciences and Mathematics, Ural Federal University, 620000, Ekaterinburg, Russia*

Periodical domain structures (PDS) in lithium niobate are attractive for electro-optic (EO) applications like Bragg deflectors, optical switches and wide-band optical amplitude modulators with the small values of control voltage [1-3]. We report on the experimental investigations of Bragg diffraction in the presence of an external sinusoidal electric field, which has been implemented for extraordinary light waves with the wavelength $\lambda = 655$ nm on PDS produced by electric field poling in a $LiNbO_3$: 5 % MgO crystal in Labfer Ltd, Russia. To account for obtained results in the frame of known model of Bragg diffraction [4] the dielectric permittivity perturbations caused by electrically-induced in PDS phase grating [1-3] as well as by alternating 180-degree domain walls [5,6] are considered.

The examined PDS with the Y-walls and the spatial period $\Lambda = 8.79$ μm was fabricated in the single crystal sample having sizes 40×2×1 mm^3 along the X, Y, and Z axis, respectively. The lateral dimensions of domain walls agree with associated sizes of the crystal. A sinusoidal voltage with the frequency $f = 1$ kHz and amplitudes U_m from 0 to 136 V was applied to the sample along Z axis by the use of the pressed metallic electrodes. The focused to the central part of sample by cylindrical lens Z-polarized light beam with $\lambda = 655$ nm and power of 25 mW was propagated in XY plane at Bragg angle θ_B to the Y axis and experienced transformation to the diffracted beam on an interaction length $d = 2$ mm. The time dependences of diffracted beam were recorded by using the photodiode and digital oscilloscope Tektronix TDS 2012C.

It was established that experimental time evolution of diffraction efficiency can be represented as the following Fourier decomposition:

$$\eta(t,U_m) = \eta^{(0)}(U_m) + \eta^{(1)}(U_m)\sin\left[\frac{2\pi}{T}(t+t_0)\right] + \eta^{(2)}(U_m)\cos\left[\frac{4\pi}{T}(t+t_0)\right], \qquad (1)$$

where $T = 1/f$ and the parameter t_0 is determined by initial phase of applied voltage. The amplitudes of Fourier harmonics, which were found from the fitting the dependence (1) to the experimental data for $\eta_{ex}(t)$ at different amplitudes U_m are shown by points in Figure 1.

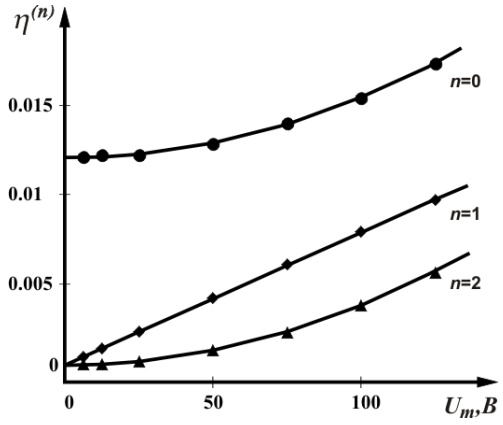

Figure 1. Amplitudes of Fourier harmonics $\eta^{(n)}$ in decomposition of time evolution for efficiency of Bragg diffraction on PDS vs amplitude of applied sinusoidal voltage. The curves are least-square fit to the Eqs. (4)–(6).

The description of observed Bragg diffraction with weak efficiency the approximate expression derived from [3, 4] can be used:

$$\eta_e \approx \left(\frac{\pi d}{\lambda \cos\theta_B} \right)^2 \left| \Delta \dot{n}_e \right|^2 . \qquad (2)$$

The amplitude of the 1-st spatial harmonic for perturbation of extraordinary refractive index n_e with tacking into account the sinusoidal in time EO contribution of PDS as well as the stationary one from electric and elastic fields of domain walls [5, 6] we derive as

$$\Delta \dot{n}_e(t) = -\frac{1}{2} n_e^3 \left[r_{33} \dot{F}_{eo}^{(1)} \frac{U_m}{h} \sin\left(\frac{2\pi}{T} t \right) - \left(R_{33} + p_{31} \frac{d_{31}^S}{C_{11}^P} \right) P_S^2 \dot{F}_{dw}^{(1)} \right], \qquad (3)$$

where h is the crystal thickness, $\dot{F}_{eo}^{(1)}$ and $\dot{F}_{dw}^{(1)}$ is the amplitudes of the first spatial harmonic generated by the external electric field (*eo*) and domain walls (*dw*), r_{33} is the linear EO coefficient, R_{33} is the EO constant of the quadratic effect, p_{31} is the elasto-optic constant, d_{31}^S is the electrostriction coefficient of the mechanically clamped crystal, C_{11}^P is the modulus of elasticity for the constant electric polarization, and P_S is the modulus of the spontaneous polarization. Use of Eqs. (2) and (3) yields

$$\eta_e^{(0)}(U_m) = \left(\frac{\pi d n_e^3}{2\lambda \cos\theta_B} \right)^2 \left[\left(R_{33} + p_{31} \frac{d_{31}^S}{C_{11}^P} \right)^2 P_S^4 \left(F_{dw}^{(1)} \right)^2 + \frac{\left(r_{33} F_{eo}^{(1)} \right)^2}{2h^2} U_m^2 \right], \qquad (4)$$

$$\eta_e^{(1)}(U_m) = -2 \left(\frac{\pi d n_e^3}{2\lambda \cos\theta_B} \right)^2 r_{33} \left(R_{33} + p_{31} \frac{d_{31}^S}{C_{11}^P} \right) P_S^2 \frac{F_{eo}^{(1)} F_{dw}^{(1)}}{h} \cos\Delta\varphi U_m , \qquad (5)$$

$$\eta_e^{(2)}(U_m) = -\left(\frac{\pi d n_e^3}{2\lambda \cos\theta_B} \right)^2 \frac{\left(r_{33} F_{eo}^{(1)} \right)^2}{2h^2} U_m^2 , \qquad (6)$$

where $\dot{F}_{eo}^{(1)} = F_{eo}^{(1)} \exp(i\varphi_{eo})$, $\dot{F}_{dw}^{(1)} = F_{dw}^{(1)} \exp(i\varphi_{dw})$, and $\Delta\varphi = \varphi_{eo} - \varphi_{dw}$.

The results of our fit procedure based on Eqs. (4)–(6) and on the uses of the material parameters of lithium niobate (see, for example, [3, 5, 6]), namely, r_{33}=30.8 pm/V, R_{33}=0.091 m^4/C^2, p_{31}=0.17, d_{31}^S=0.216·10^9 m^{2}N/C^2, C_{11}^P=2.03·10^{11} N/m^2, P_S=0,75 C/m^2, and n_e=2.187, as well as the values F_{eo} = 0.538, F_{dw}=42.9·10^{-6} and $\Delta\varphi$ = 65°, are shown in Fig. 1 by the solid lines.

The distinction between F_{eo} = 0.538 and $2/\pi$ = 0.637 inherent for ideal PDS [7] can be due to the availability of air gaps between the pressed electrodes and the $LiNbO_3$: 5 % MgO sample.

This study was carried out with the financial support of Ministry of Education and Science of Russia (within the task No. 3.1110.2017/4.6 of the project part) and RFBR (Grant 16-29-14046-ofi_m). The equipment of the Ural Center for Shared Use “Modern Nanotechnology” UrFU has been used.

1. M. Yamada, *Rev. Sci. Instrum*. **71**, 4010 (2000).
2. J.A. Abernethey, C.B.E. Gawith, R.W. Eason et al., *Appl. Phys. Lett.* **81**, 2514 (2002).
3. I. Mhaouech, V. Coda, G. Montemezzani, et al., *Opt.Lett*. **41**, 4174 (2016).
4. H. Kogelnik, *Bell Syst. Tech. J*. **48**, 2909 (1969).
5. S.M. Shandarov, A.E. Mandel, S.V. Smirnov, et al., *Ferroelectrics* **461**, 134 (2016).
6. S.M. Shandarov, A.E. Mandel, A.V. Andrianova, et al., *Ferroelectrics* **508**, 49 (2017).
7. S.T. Lin, S.Y. Hsu, Y.Yin. et al., *IEEE Photonics J.* **5**, 1501507 (2013).

P-80

Microstructure and piezoelectric response of AlN/SiC heterostructures grown on silicon substrates of different orientation

S.V. Senkevich[1], S.S. Sharofidinov[1], D.A. Kiselev[2], I.P. Pronin[1], S.A. Kukushkin[3]

[1]*Ioffe Institute, 194021, St. Petersburg, Russia*
e-mail: SenkevichSV@mail.ioffe.ru

[2]*National University of Science and Technology «MISiS», 119049, Moscow, Russia*

[3]*Institute of Problems of Mechanical Engineering RAS, 199178, St. Petersburg, Russia*

Thin aluminum nitride (AlN) films are promissing materials as for optoelectronics and microelectromechanics [1-2]. Of special interest are AlN epitaxial films that can be grown on silicon substrates (Si) with a thin buffer layer of silicon carbide (SiC). Due to a small mismatch between the lattice parameters of AlN and SiC (on the order of 1%), epitaxial AlN films were successfully grown on these substrates by molecular beam epitaxy and chloride-hydride epitaxy (CHE) [3].

In the work, we studied the topography of the surface and the piezoelectric response of AlN/SiC heterostructures grown on Si substrates of different orientations - (100), (110) and (111). For these purposes, an atomic force microscope AFM-PFM Ntegra (NT-MDT) was used. Buffer layers of SiC 50-80 nm thick were formed by atoms substitution method [4]. To grow thin layers of AlN (thickness from fractions to several microns), the CHE method was used. The experiments revealed a strong difference in the growth pattern of the films. In particular, the normal growth of the hexagonal (polar) axis on the SiC/Si(111) substrate was replaced by a growth texture oriented at an angle of 50-53 degrees to the SiC/Si(100) substrate plane. Accordingly, the block size and the surface morphology were substantially changed (Fig. 1), as well as the magnitude of the piezoelectric response. The obtained results are discussed.

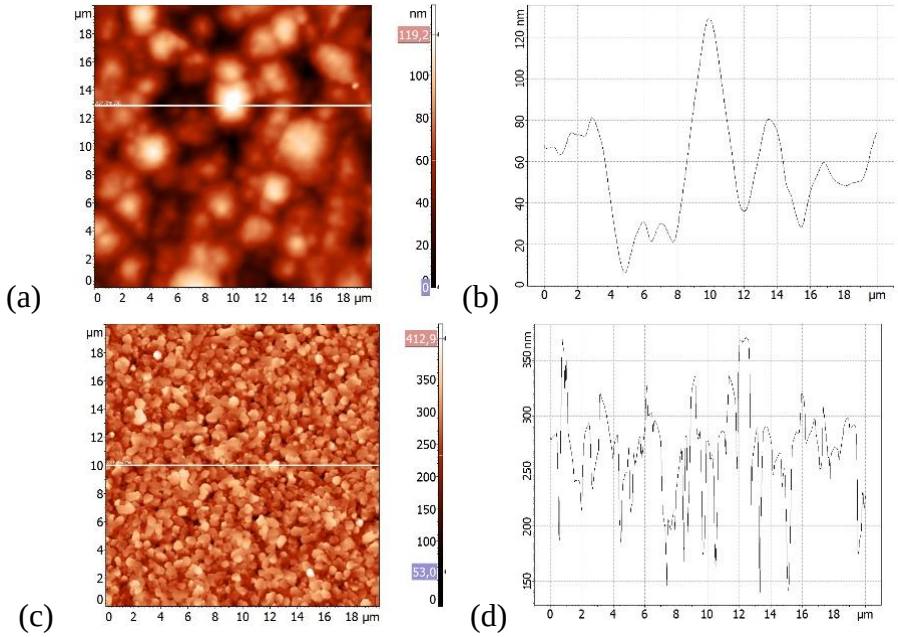

Figure 1. AFM images of thin AlN layers grown on (a, b) SiC/Si (111) and (c, d) SiC/Si (100) substrates.

The work was partly supported by the Ministry for Education and Science (Russian Federation) (Grant No 16.2811.2017/4.6).

1. Fissel, *Physical Reports* **379**, 149 (2003).
2. P. Muralt, *Journal of the American Ceramic Society* **91**, 1385 (2008).
3. V.N. Bessolov, Yu.V. Zhilyaev, E.V. Konenkova et al., *Technical Physics Lett.* **36**, 496 (2010).
4. S.A. Kukushkin, A.V. Osipov, I.P. Soshnikov, *Reviews on Advanced Materials Science* **52**, 29 (2017).

P-81

Microstructure and electrical properties of thin SiC films on Si substrates of *p*- and *n*-types

O.N. Sergeeva[1], A.V. Solnyshkin[1], G.M. Nekrasova[2], S.V. Senkevich[3], I.P. Pronin[3], S.A. Kukushkin[4]

[1]*Tver State University,170100, Tver, Russia*
e-mail: o_n_sergeeva@mail.ru

[2]*Tver State Agricultural Academy,170904, Tver, Russia*

[3]*Ioffe Institute, 194021, St. Petersburg, Russia*

[4]*Institute of Problems of Mechanical Engineering RAS, 199178, St. Petersburg, Russia*

Silicon carbide (SiC) is one of the key semiconductor materials for power electronics and photoelectric transducers and sensors. In optoelectronics, nanometer silicon carbide layers grown on silicon substrates (SiC/Si) are used as a buffer layer for the formation of epitaxial layers of gallium and aluminum nitrides [1]. Moreover, hexagonal modifications of SiC are polar ones possessed the macroscopic spontaneous polarization [2].

In this work, surface morphology, dielectric properties and the photovoltaic activity induced by optical irradiation are studied for SiC/Si heterostructures subject to the donor or acceptor character of the silicon substrate doping. The thin SiC layers with 60-80 nm thickness were grown on the Si substrates by atoms substitution method [3]. The substrates with (111) orientation were doped with boron or phosphorus atoms. To study SiC layers topology, the atomic force microscope AFM Ntegra (NT-MDT) was used. Spectral distribution of the photovoltaic response was studied in the optical range of 400-1000 nm.

C-V dependences of SiC/Si structure revealed sharp changes in capacitance when the positive and negative voltage was applied (Fig. 1). It is evidenced the presence of a heterojunction barrier, in which the internal field direction depended on the type of the dopant.

The optical radiation effect on the SiC/Si structure induced the stationary photovoltaic response, whose sign also depended on the type of the dopant (Fig. 2).

The nature of the observed effects is discussed.

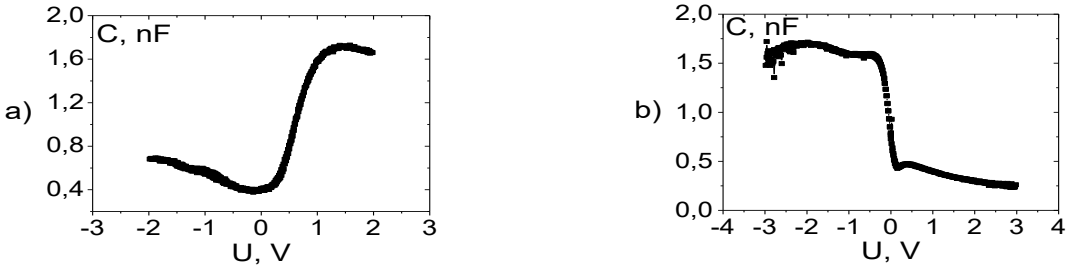

Figure 1. C-V dependences of SiC/Si structures doped with (a) boron or (b) phosphorus atoms.

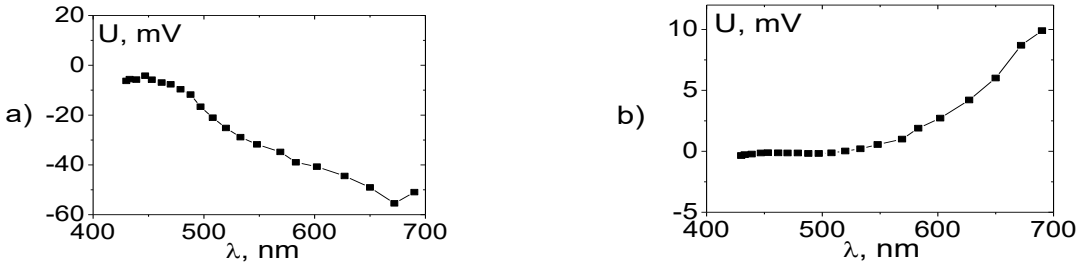

Figure 2. Spectral dependences of photovoltaic signal of SiC/Si structures doped with (a) boron or (b) phosphorus atoms.

1. V.N. Bessolov, Yu.V. Zhilyaev, E.V. Konenkova et al., *Technical Physics Lett.* **36**, 496 (2010).
2. S.Yu. Davydov, A.V. Troshin, *Physics of the Solid State*, **49**, 759 (2007).
3. S.A. Kukushkin, A.V. Osipov, I.P. Soshnikov, *Reviews on Adv. Mat. Sci.* **52**, 29 (2017).

P-82

Probe microscopy in the study of the process of template synthesis

A.S. Shatalov[1], D.L. Zagorsky[2], I.M. Doludenko[1,2]

[1]*National Research University Higher School of Economics, 101000, Moscow, Russia*
e-mail: Shura_shatalov@inbox.ru

[2]*FSRC "Crystallography and Photonics" RAS, 119333, Moscow, Russia*

Template synthesis. The method of template synthesis is one of the promising methods for obtaining one-dimensional nanostructures [1]. The idea of the method is to fill the pores of a specially manufactured matrix with the required material. In this case, the manufacture of the matrix, its preparation and actual filling, represent separate processes, well-studied, controlled and reproducible. The method provides a unique opportunity to obtain identical nanosized structures with variable dimensional parameters from different materials. The cheapness and simplicity of the processes are also advantages of the method. There are several different variations of the method-as for the used templates (porous alumina, track membranes, etc.), and by the methods of filling them (galvanic, chemical, mechanical). In this work, polymer track membranes were used as templates (matrices), the pores in which were filled with various metals by an electrochemical (galvanic) method [2,3]. The result of the process was the production of an array of metallic filaments (nanowires, NWs) located within the polymer matrix. The purpose of this work is to assess the capabilities of probe microscopy and other microscopy methods when analyzing the various stages of obtaining NWs for the validation of the original matrices, NWs arrays within matrices, and isolated NW arrays.

Optical microscopy was used for express analysis and for selecting areas for subsequent study at all stages of obtaining NW arrays. The wide range of problems was solved with the help of electron microscopy (SEM). The advantages of the latter include a large depth of field, the possibility of a more precise identification of pores (except for cases of diameters less than 50-70 nm), the possibility of changing the viewing angle. A great value in the study of multicomponent structures has the ability to conduct elemental analysis. The disadvantage of this approach include the relative complexity and duration of sample preparation; impossibility of subsequent use of the sample.

Probe microscopy from all of these methods gives the greatest resolution. When studying the matrix, this is the only way to see pores with dimensions less than 50-70 nm. In addition, it becomes possible to study the surface roughness of the matrix, which is important in evaluating the adhesion properties and pores, and the flat surface of the polymer matrix. The method is of greatest interest in the study of a polymer matrix filled with an NWs (a kind of "metal-polymer composite"). In this case, the SPM modes (spreading currents) and magnetic-force microscopy are used, the first one allows one to determine the electrical conductivity of individual NW. The image of the topography and a corresponding picture of the spreading current pattern for a membrane with pores 0.1 μm, some of which is filled with copper are given in Figure 1.

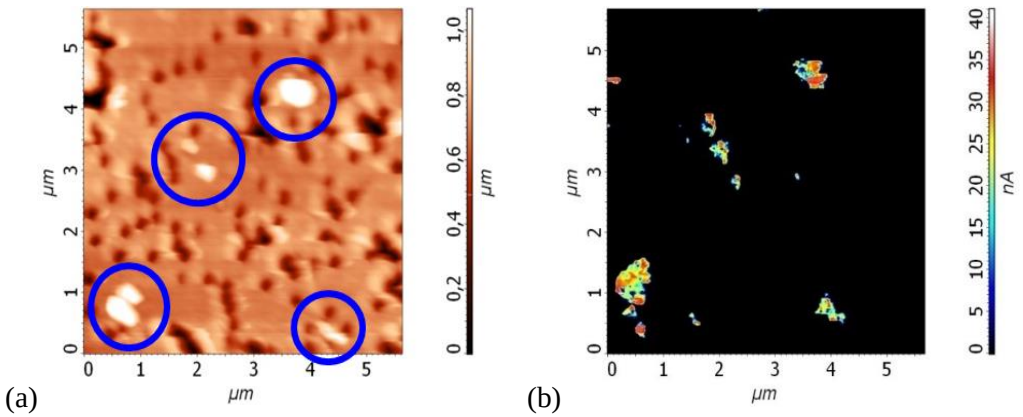

(a) (b)

Figure 1. SPM image of the TM surface with pores partially filled with copper: (a) surface topography, (b) the picture of the flow currents.

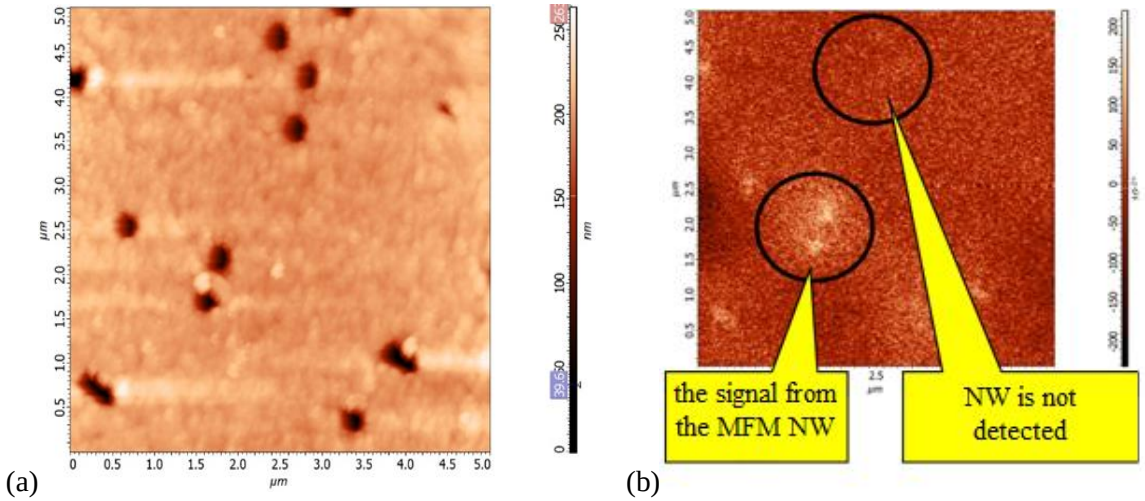

(a) (b)

Figure 2. SPM image of the TM surface with pores partially filled with cobalt: (a) surface topography, (b) the corresponding MFM image.

The results obtained make it possible to clearly distinguish the filled pores, and for the NPs themselves to estimate the electrical conductivity, it turned out to be much less than the corresponding values for bulk copper. Successful use of the method of magnetic force microscopy (MFM) for detecting NP from magnetic material (cobalt) growing into the pores of TM is demonstrated. Figure 2 shows the images of topography obtained in two-pass mode and the corresponding magnetic force picture.

The above results indicate the high sensitivity of the methods (detecting those that have not yet appeared on the surface of the NW) and the uneven growth of the NW (magnetic signal is observed only for a part of the pores). (Previously, the method has already been used to solve similar problems [4]).

Finally, the method was successfully used to study the topography of the surface of an NWs with a length (height) up to 1 μm (here the scale of determining the height was limited by the magnitude of the vertical displacement of the cantilever).

This work was supported by the Federal Agency of Scientific Organizations (Agreement No 007-ГЗ/Ч3363/26). The authors thank O.Rybalko (MIEM) and V.Lavrentiev (INP, Rezh, Czech Republic) for their assistance in conducting the experiments.

1. V.M. Anishchik, *Nanomaterials and nanotechnology*, (Minsk, *BSU)*, 372 (2008).
2. C.R. Martin, *Science* **266**, 1961 (1994).
3. A.D. Davydov, V.M. Volgin, *Electrochemistry* **52**, 905 (2016).
4. T.G. Sorop, C. Untiedt, F. Luis, et al., *Phys. Rev. B* **67**, 014402 (2003).

Nanoindentation of human donor cornea for detecting the effectiveness of laser-induced collagen crosslinking

B.S. Shavkuta[1,2], N.V. Minaev[1], S.L. Kotova[1,3], P.S. Timashev[1,2]

[1]*Institute of Photonic Technologies, Research Center "Crystallography and Photonics" RAS, 108840, Moscow, Troitsk, Russia*

[2]*Institute for Regenerative Medicine, Sechenov First Moscow State Medical University, 119991, Moscow, Russia*

e-mail: b.shavkuta@gmail.com

[3]*N.N. Semenov Institute of Chemical Physics RAS, 119991, Moscow, Russia*

One of the most important characteristics of a material is its mechanical properties. Methods to determine the micromechanical properties of biological samples are highly varied. At the moment, to measure the local mechanical characteristics of samples, the nanoindentation method has been gaining popularity. The method is based on indenting a sample with a spherical tip attached to a flexible cantilever and detecting the cantilever's deflection interferometrically, which results in a load-indentation curve. This curve is used to calculate the Young's modulus *E*. This method allows one to work with various biological materials, as well as to measure the local *E* of the sample surface. In our research, we use a PIUMA nanoindenter (Optics11) to estimate the effectiveness of a method developed for hardening the human cornea.

One of the most common diseases of the cornea is keratoconus, a pathological process leading to thinning of the cornea and, as a result, loss or deterioration of vision. The traditional approach to the treatment of keratoconus involves UV-photocrosslinking of the corneal collagen with riboflavin as a photoinitiator. However, such a method has disadvantages, such as difficulty of a precise regulation of cornea irradiation and, as a consequence, damage to the healthy regions and impossibility of crosslinking fibers through the whole thickness. Therefore, for the effective treatment of keratoconus without negative consequences, a two-photon laser femtosecond crosslinking (2P-CXL) method at the wavelength of 525 nm was developed. The most important advantage of 2P-CXL is its extremely local effect: 0.5 - 5 μm along the X and Y axes (the width of the laser radiation caustic), 2 - 20 μm along the Z axis (the caustic length) which allows collagen to be crosslinked without damaging the endothelial and epithelial corneal layers.

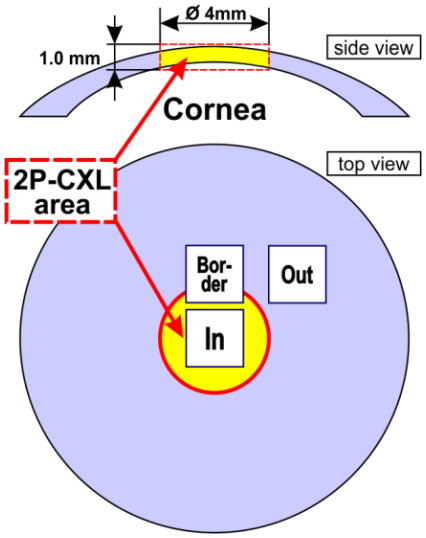

Figure 1. Schematic image of the cornea with the designated areas in which the femtosecond treatment and measuring the effective Young's modulus by nanoindentation took place. Yellow (IN) is the region where the cornea was treated with 2P-CXL. Blue (OUT) is the intact cornea region. Nanoindentation was performed inside both the regions and also at the border (BORDER) between the regions.

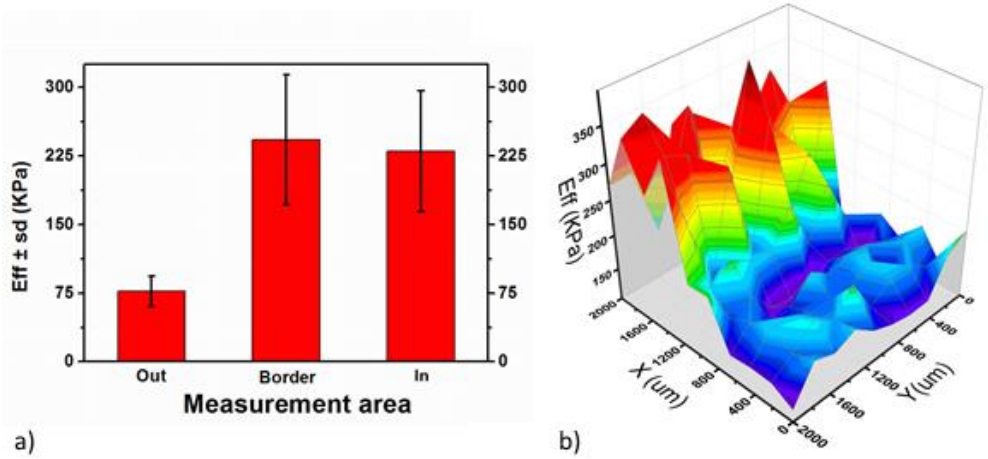

Figure 2. (a) The surface effective Young's moduli Eff for the three corneal areas, in accordance with Figure 1; (b) E_{ff} distribution over the corneal surface at the border of the treatment zone.

The sample without epithelium was treated with 0.1% riboflavin solution for 30 minutes prior to the laser irradiation, and in the course of the experiment the treatment was repeated every 2 minutes using a pipette. The treatment of the human donor cornea with 2P-CXL was performed layer by layer in the central area with a diameter of 4 mm and a thickness of 1mm (Fig. 1). The local mechanical characteristics of the cornea were determined with a PIUMA nanoindenter using the Hertzian contact mechanics model for a spherical body indenting a flat surface.

The *E* measurements were carried out in a solution for the cornea storage heated to 34°C, which is a normal temperature for the human cornea. For indentation we used a cantilever with a spring constant of 2.94 N/m and a tip with the 45 μm radius of curvature. The samples were immobilized at the bottom of a Petri dish using a weight. The area of the *E* mapping was 2000×2000 μm with the step of 200 μm by the X- and Y-axes.

In Figure 2a, a histogram of the effective Young's moduli E_{ff} of the corneal surface is displayed for the three regions of measurements according to Figure 1. It demonstrates that the E_{ff} value at the border of the treatment and within the area of the femtosecond treatment grows by about three times (Fig. 2a), from 77±16 kPa to 230±66 kPa. In Figure 2b, a typical E_{ff} 3D plot is depicted, located in the region of the border between the treated and intact zones.

The increase of the Young's modulus of the human donor cornea, which was determined by nanoindentation, allows us to make a conclusion about a good potential of a femtosecond laser with a wavelength of 525 nm for the clinical use, to increase the stiffness of the cornea by 2P-CXL.

1. P.R. Moshtagh, B. Pouran, N.M. Korthagen, et al., *J. Biomech.* **49**, 3602 (2016).
2. M. Naderan, S. Shoar, M.A. Kamaleddin, et al., *Cornea* **34**, 1005 (2015).
3. M. Farjadnia, M. Naderan, *Oman J. Ophthalmol*. **8**, 86 (2015).
4. E. Spoerl, M. Mrochen, D. Sliney, et al., *Cornea* **26**, 385 (2007).
5. G. Mattei, G. Gruca, N. Rijnveld, et al., *J. Mech. Behav. Biomed. Mater* **50**, 150 (2015).
6. B.S. Shavkuta, M.Y. Gerasimov, N.V. Minaev, et al., *Laser Phys. Lett.* **15**, 015602 (2018).

Probe microscopy in the study of the surface of aluminum alloys

O.O. Shcherbakova[1], T.I. Muravyeva[1], Yu.A. Bobrov[2], D.L. Zagorskiy[1,3], I.V. Shkaley[1]

[1]*Institute for Problems in Mechanics of RAS, 119526, Moscow, Russia*
e-mail: shcherbakovaoo@mail.ru

[2] *NT-MDT, Zelenograd, Russia*

[3]*Institute of Crystallography of RAS, 119333, Moscow, Russia*

The work is devoted to the study of the surface of antifriction aluminum alloys. The effect of heat treatment on topography and electrical properties of the surface was investigated. The studies were carried out using a set of different methods of microscopy: topography, spreading currents and Kelvin-mode.

Aluminum alloys have the widest range of applications. One of the fields of their application is the use as bearing materials in mechanical engineering - they are cheap and have high operational properties [1]. One of the stages of their fabrication is heat treatment (HT). The most important control parameter of such samples is their surface properties: topography and elemental composition, as well as electrical properties. In the present work, alloys of the composition Al-5% Si-4% Cu-4% Sn, with additives (0.5% each) Bi, Pb and Cd were studied. It was shown that the optimal mode of treatment for such alloys is heating up to 500°C, followed by cooling in water.

How does such HT affect the alloy surface? To answer this question, a complex of microscopic studies was carried out. SEM studies were performed on a Quanta-650 microscope with an X-ray spectral microanalyzer EDAX (accelerating voltage 25 kV). For SPM studies, Smart SPM-TM (AIST-NT) and Ntegra Prima (NT-MDT) instruments (tapping regime, cantilevers of the fpN10 series, NSC18/Pt) were used. The results of microscopic studies of the surface are shown in Figure 1.

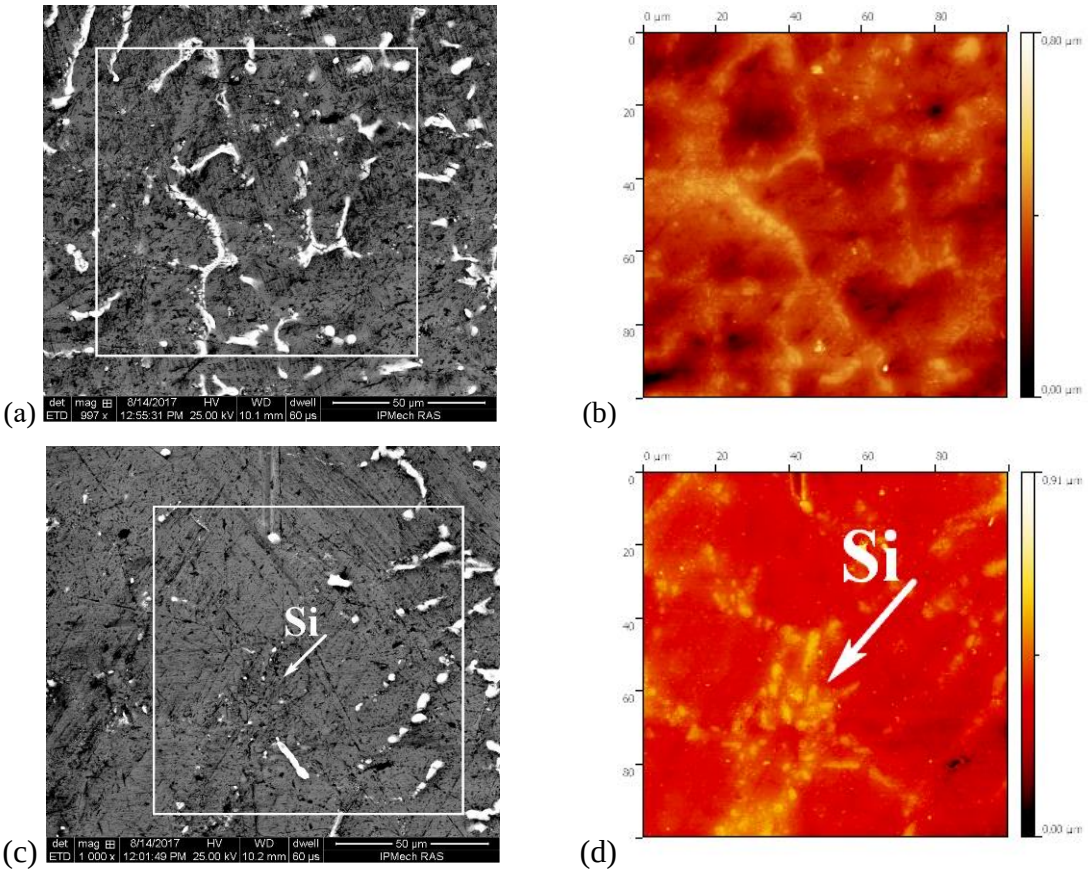

Figure 1. The image of the surface of the alloy: (a, b) cast sample, (c, d) heat-treated sample. (a, c) SEM (squares indicate the areas of SPM research), (b, d) SPM.

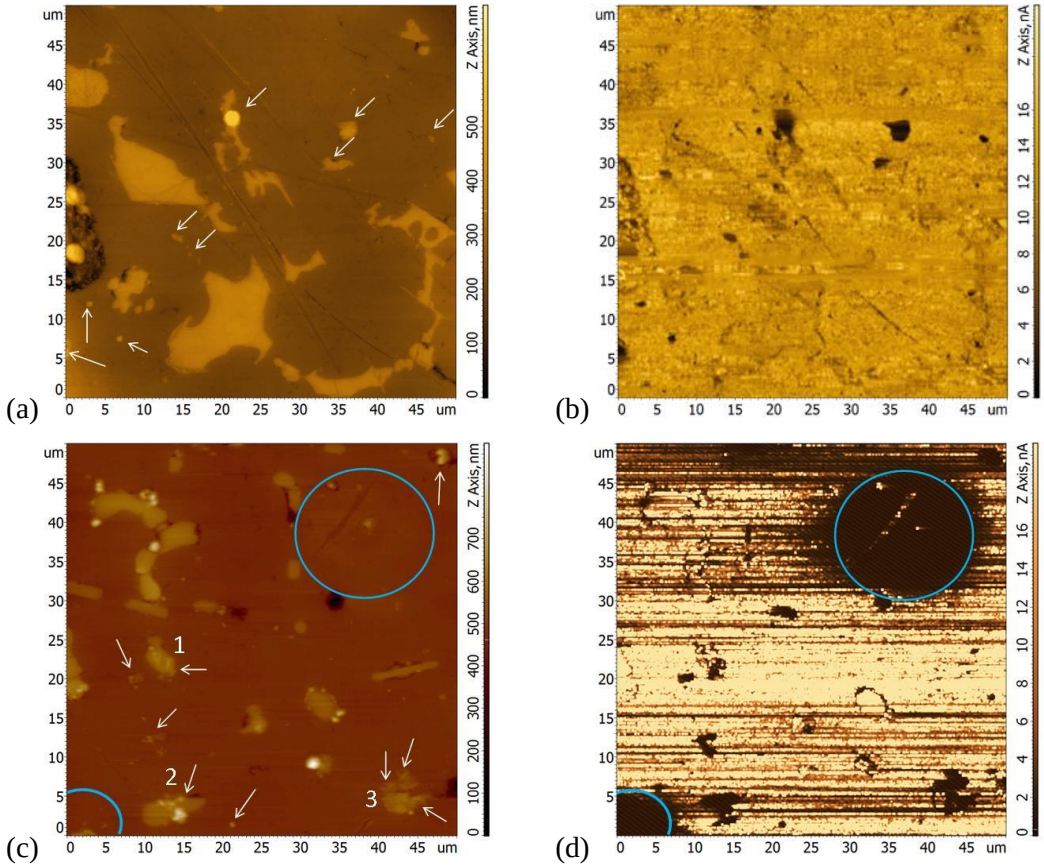

Figure 2. The image of the surface of the alloy: (a, b) cast sample, (c, d) heat-treated sample. (a, c) SPM image and (b, d) flow currents.

It can be seen that HT leads to spheroidization of the particles (the phase constituents of the alloy). The methods used complemented each other: SPM allowed to visualize elements that are difficult to distinguish on SEM images (due to the proximity of atomic numbers). It also allows to estimate the spatial geometry of individual phase components [2]. For example, silicon, which is actually indistinguishable in the aluminum matrix (according to SEM), is clearly visible in the SPM image.

The electrical properties of the surface were also measured: it is known that the electrical conductivity directly correlates with the thermal conductivity. The latter is the most important operational parameter, but it is difficult to measure it directly. The obtained results are shown in Figure 2.

It can be seen that after the HT the picture of the spreading currents has changed: big areas with a significantly lower electrical conductivity appeared, although in general the electrical conductivity has changed insignificantly. At the same time, it can be assumed that if, according to the SEM and SPM (topography), the HT leads to homogenization and homogeneity of the alloy. The flow current pattern, on the contrary, indicates the differentiation of different regions.

The picture of the surface potential correlates with the measured flow currents (measurements in the Kelvin mode). All these results indicate the prospectivity of the application of electrical methods for studying the surface properties of alloys.

The work was supported by the Grant of the RNF 14-19-01033-P (study of topography and elemental composition of the surface) and the State Task (№ State registration AAAA-A17-117021310379-5 - study of electrical properties of the surface). The authors are grateful to N.A. Belov (MISiS) for providing samples.

1. B.N. Arzamasov, T.V. Solov'eva, S.A. Gerasimov et al., *Handbook of structural materials*, (Moscow: Bauman MSTU), 640 (2005).
2. O.O. Stolyarova, T.I. Muraveva, D.L. Zagorsky et al., *Physical mesomechanics* **19**, 104 (2016).

P-85

Influence of the domain structure on piezoelectric, dielectrics properties of relaxor SBN single crystals

V.A. Shikhova[1], V.V. Fedorovyh[1], A.D. Ushakov[1], A.A. Esin[1], V.A. Anikin[1], D.O. Alikin[1,2], D.S. Chezganov[1], V.Ya. Shur[1], A.L. Kholkin[1,2], L.I. Ivleva[3]

[1]*School of Natural Sciences and Mathematics, Ural Federal University, 620000 Ekaterinburg, Russia Corresponding author e-mail: vera@urfu.ru*

[2]*Department of Physics and CICECO – Aveiro Institute of Materials, University of Aveiro, 3810-193 Aveiro, Portugal*

[3]*Prokhorov General Physics Institute, Russian Academy of Sciences, 119991 Moscow, Russia*

We have studied influence of the initial domain structure on piezoelectric, dielectrics properties of $Sr_xBa_{1-x}Nb_2O_6$ (SBNx) single crystals. SBN61 undoped, Ce and Ni doped single crystals were grown in Prokhorov General Physics Institute of RAS. The studied samples were cut normally to the polar axis and carefully polished.

The local polarization reversal, piezoelectric and dielectrics properties were studied in samples with initial domain structure created by: (1) zero-field cooling, (2) in-field cooling, (3) scanning by biased tip, (4) scanning by electron beam, (5) partial polarization reversal.

The domain structure after zero-field cooling represented a mixture of the nanoscale fractal-type maze domains. The geometry of the as-grown domain structure was characterized by fractal dimension and average correlation length.

The local switching in SBN crystals with various initial domain states using conductive tip of scanning probe microscope (SPM) was studied. The dependences of effective domain radius on the voltage and pulse duration were derived. The domain "shape factor", wall mobility, and threshold voltage were obtained. We proposed application of the "shape factor" of the domains formed by local switching for quantitative characterization of the domain state. The obtained results allowed to reveal the most effective method for the creation of a single domain state.

The temporal relaxation of the polarized state created by conductive SPM tip was investigated at various temperatures. It has been shown that the radius of created domains decreasing with temperature. The difference between piezoelectric responses in the polarized areas produced by application of the field of opposite sign (contrast) has been obtained. The average value of the induced contrast decreases during heating for all investigated crystals. Below the freezing temperature the induced state remains stable after an initial relaxation. Above the freezing temperature the induced state is unstable and gradually decays with time. The state stability is affected by the measuring conditions, notably continuous scanning results in a faster decay. It was shown that increasing of the field amplitude and pulse duration leads to higher stability. The polarized state created in the single domain state was remarkably more stable than in the multi-domain one. The obtained effects are attributed to decrease of the induced polarization and backswitching of the polarized area under the action of the depolarization field.

The peculiarities of integral piezoelectric effect and dielectric permittivity were studied. The frequency dependences of piezoelectric coefficient were obtained. The temperature and frequency dependences of dielectric permittivity were measured. The chemical composition of the surface was studied by X-ray photoelectron spectroscopy.

The equipment of the Ural Center for Shared Use "Modern nanotechnology" Ural Federal University was used. The research was made possible by Russian Foundation of Basic Research (Grant16-02-00821-a).

1. V.A. Shikhova, V.V. Fedorovyh, A.P. Turygin, L.V. Gimadeeva, D.S. Chezganov, E.O. Vlasov, D.O. Alikin, L.I. Ivleva, A.L. Kholkin, V.Ya. Shur, *Ferroelectrics* **525**, 100 (2018).
2. V.Ya. Shur, V.A. Shikhova, D.O. Alikin, V.A. Lebedev, L.I. Ivleva, J. Dec, D.C. Lupascu, V.V. Shvartsman, *Scientific Reports* **7**, 125 (2017).

P-86

Methods of probe microscopy in the study of topography and elastic properties of cold-resistant elastomers

O.O. Shcherbakova[1], T.I. Muravyeva[1], R.V. Gainutdinov[2], I.V. Shkalei[1], D.L. Zagorskiy[1,2], N.N. Petrova[3], E.N. Timofeeva[3]

[1]*Ishlinsky Institute for Problems in Mechanics RAS, Moscow, 119526, Russia*
e-mail: ioann_shiva@list.ru

[2]*FSRC "Crystallography and Photonics" RAS, Moscow, 119333, Russia*

[3]*Ammosov North Eastern Federal University, Yakutsk, 677000, Russia*

Expansion of the range of manufactured elastomers is an important task for the national economy. These materials must correspond to different operating conditions. In particular, the actual problem remains the modernization of rubber, operated in the conditions of the North Territories. One way to improve the properties is to add various modifiers to the base composition of the elastomers. In the present work, composites based on ER (epichlorohydrin rubber), which are intended to be used as seals in machine units operating at low temperatures, have been studied. The modifiers of rubber were carbon nanotubes (CNTs), added to the base composition in a different percentage.

The operation mode was modeled by tribological tests carried out on a UMT-2 friction machine under the following conditions: contact pressure varied from 0.1 to 0.3 MPa, the slip velocity varied from 1 to 100 mm/s, the bulk temperature of the test samples ranged from -25 to 22ºC

The most important estimate is the change in the surface of rubbers during operation. In this paper, we propose complex methods for studying the surface, including not only studies of topography, but also evaluation of surface properties.

The surface of the samples before and after friction tests was examined on a scanning electron microscope (SEM) - a FEI Quanta 650 device was used, operating in a low vacuum mode, using secondary and back-reflected electron detectors. Images obtained for the sample with 2 mass parts of CNTs are presented in Figure 1.

It can be seen that the topography of the sample after friction-tests has changed, areas have appeared that differ in color. However, the X-ray spectral analysis did not show any significant changes in the composition after the tests. The areas on the sample after friction-tests, differing in color, also have a close elemental composition. (It is possible that the difference in color is due to the difference in the emission parameters of the regions caused by uneven friction).

(a) 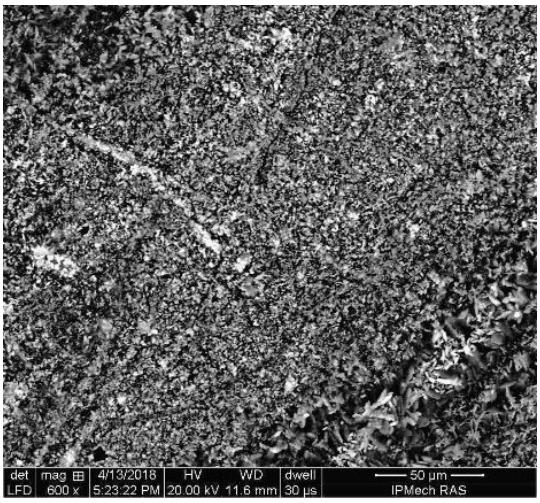

(b) 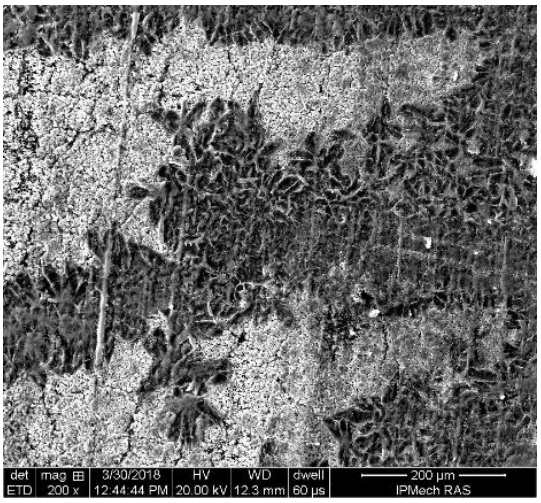

Figure 1. SEM images (secondary electrons) of the sample surface with 2 m.p. CNT: (a) original sample, (b) sample after tribo test.

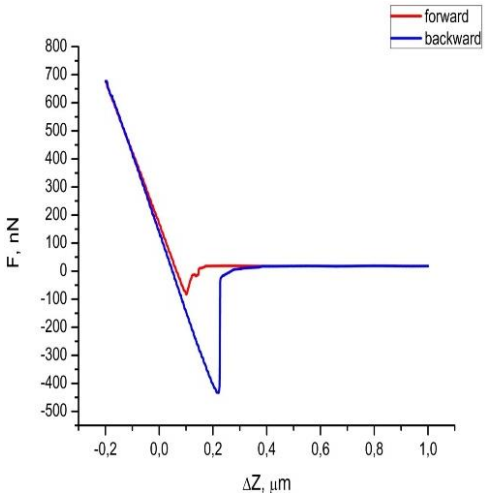

Figure 2. Force-distance curves (samp-2mp CNTs).

Table 1. Visco-elastic properties of Samples with different parts of CNTs before and after friction tests

№	ER+ CNTs	F_{ADH}, nN		E, MPa		A, nA	
		before	after	before	after	before	after
1	0 mp	158,1	37,8	111,9	76,5	2,9	4,4
2	0 mp	71,8	41	92,8	82,4	2,3	4,2
3	0,1 mp	194,1	206,3	57,2	44,4	2,6	3,5
4	0,3 mp	324,2	203,6	584,4	123,6	2,4	3,8
5	1,0 mp	139	322	309,7	144	3,0	3,9
6	2,0 mp	89,7	136	354,8	197,4	3,2	4,2
7	10 mp	238,3	99,8	2511,9	197,1	2,6	3,3

The main method of investigation was probe microscopy. Surface topography was studied at the device "Smart SPM-TM" AIST-NT (in the tipping mode, probes of the fpN10 series). The surface properties were examined on a NTEGRA Prima NT-MDT instrument (HA-NC ScanSens probe). To evaluate the adhesion, the methods of obtaining force curves (force-distance) were used; Young's modulus was estimated from the slope of the graph. Visco - elastic characteristics were studied by the method of "Power modulation". The results of the surface investigation by the SPM method are presented in Fig. 2 (for a sample with 2 mass parts of CNT, before friction-tests) and in Table. 1 (data are given for all samples before and after the tests).

The analysis of the obtained results allows making a number of conclusions:

Adhesion forces: the addition of CNTs leads to an increase in adhesion: in samples without CNTs, adhesion is small enough, adding even 0.1 parts of CNTs leads to a sharp increase in adhesion strength. However, a clear dependence of adhesion on the quantity of CNTs could not be identified. The same pattern is observed for samples after friction tests. We note that it was not possible to reveal a general pattern for the effect of friction on adhesion.

Elastic characteristics:

Young's modulus, measured from the slope of the curve: for samples without CNTs and for samples with a small value of CNTs (up to 0.1 m.p.) Young's modulus is relatively small, but with an increase in the CNTs content (starting from 0.3 m.p.) there is a sharp increase in the Young's modulus. For this concentration range, (as for the case of adhesion forces), the dependence on the number of CNTs was not revealed. After friction tests, the Young's modulus decreases for all samples.

Method of Power Modulation: The results of studying the elasticity by the modulation of force indicate that the elasticity measured by this method differs little for different samples. However, it can be seen that, after friction tests, in all cases a noticeable increase in the rigidity of the sample is observed.

In general, this investigation showed that modification of the basic composition of rubber by nanotubes significantly changes the properties of rubber. At the same time, it should be noted that the conclusions obtained do not make it possible to establish an unambiguous correlation between the elastic properties expressed in terms of the Young's modulus and the elastic parameters determined by the modulation method of force. Obviously, additional experiments are required here.

The work was carried out under the financial support of the Russian Science Fund, grant 14-29-00198-П(sample preparation and scanning electron microscopy) and the Federal Agency of Scientific Organizations - Agreement No 007-ГЗ/Ч3363/26 (scanning probe microscopy).

P-87

The limit of mass determination with an AFM cantilever-based system

I.D. Shumov[1], S.L. Kanashenko[1], V.S. Ziborov[2], Yu.D. Ivanov[1], A.I. Archakov[1], T.O. Pleshakova[1]

[1]*Institute of Biomedical Chemistry, 119121, Moscow, Russia*
e-mail: shum230988@mail.ru

[2]*Joint Institute for High temperatures RAS, 125412, Moscow, Russia*

Nowadays, modern nanotechnology-based analytical systems employing molecular detectors - such as atomic force microscope (AFM) - are being developed. Among nanotechnology-based systems, one can distinguish nanomechanical cantilever-based ones, which allow one to operate with condensed matter at the nanoscale, thus enabling determination of various characteristics (mass [1], elasticity [2] etc.) at the level of single macromolecules or nanoparticles. In these systems, the target objects are adsorbed from the volume of analyzed sample onto the cantilever, and the resonance frequency of the AFM cantilever (which decreases in a linear proportion to the added mass) is measured [3]. The adsorption of target objects increases the mass of the cantilever; this causes shift in the resonance frequency of the cantilever, which is measured by AFM electronics. As target objects, nanoparticle-labeled single molecules of protein markers of diseases can be used [3].

In our present study, the sensitivity of a microcantilever system employing standard AFM microcantilevers for measurements in vacuum, has been estimated. We have demonstrated that such a system allows one to register ~100 gold nanoparticles (AuNPs), what corresponds to 17 μL of 10^{-17} M solution of protein labeled with these nanoparticles. The convenience of this approach consists in that no additional equipment (such as atomic weights [1,4]), is required to measure the mass of the adsorbed protein.

To measure the resonance frequency shift caused by adsorption of nanoparticles onto the cantilever, the following technique was employed. AFM cantilever (PPP-CONTR-50, Nanosensors Inc., USA; resonance frequency 6 to 21 kHz; height 450±10 μm; width 50±7.5 μm; thickness 2±1 μm; force constant 0.02 to 0.77 N/m), whose resonance frequency was measured prior to the experiment, was incubated in a drop of solution containing 20-nm-diameter AuNPs during 10 min. After the incubation, the cantilever was dried and placed in the vacuum chamber of an NTEGRA Aura AFM (NT-MDT, Zelenograd, Russia), and its resonance frequency was measured and compared with that before the incubation. All measurements have been performed in vacuum at 0.1 Torr. The mass of the AuNPs adsorbed onto the cantilever was estimated from the resonance frequency shift according to Kosaka et al [3]:

$$\Delta m = \frac{2m(f_1 - f)}{f},$$

where f and f_1 are the resonance frequencies of the cantilever before and after the incubation, respectively; m is the mass of the cantilever; and Δm is the mass of the adsorbed AuNPs.

Therefore, given the mass of a single AuNP, the total number of the AuNPs adsorbed onto the cantilever can be determined. The size of AuNPs and the number of AuNPs adsorbed onto the cantilever were estimated by scanning electron microscopy (SEM) visualization of the cantilever with adsorbed AuNPs employing a Hitachi S5500 electron microscope (Hitachi, Japan).

Since the resonance frequency shift for a 20-kHz cantilever, registerable with the system employed in our study, is 20 Hz (what amounts to 0.1% from 20 kHz), the mass of the adsorbed AuNP causing this shift must be 1000 times smaller than that of the cantilever itself. Let us estimate the mass of the silicon (of 2.33 g/cm^3 density) cantilever:

$$m=\rho V=2.33\ \text{g/cm}^3(450\times50\times1\times10^{-12})\ \text{cm}^3=5.24\times10^{-8}\ \text{g}.$$

For such a cantilever, 0.1% mass increase ($\Delta m/m$=0.001) corresponds to Δm of the order of 10^{-10} g. Since the masses of 20-nm and 100-nm AuNPs make up $6\text{x}10^{-16}$ g and $6\text{x}10^{-14}$ g, respectively, the number of these AuNPs causing $\Delta m=10^{-10}$ g corresponds to ~10^6 (for 20-nm

AuNPs) and ~10^4 (for 100-nm AuNPs). Fig. 1 displays the data obtained in our experiments. These data have indicated that adsorption of 10^6 of 20-nm AuNPs caused 20-Hz shift in the cantilever's resonance frequency (what is in a good agreement with the theoretical estimations) - in contrast to the case with 10^4 of 20-nm AuNPs, when no shift in the resonance frequency was registered.

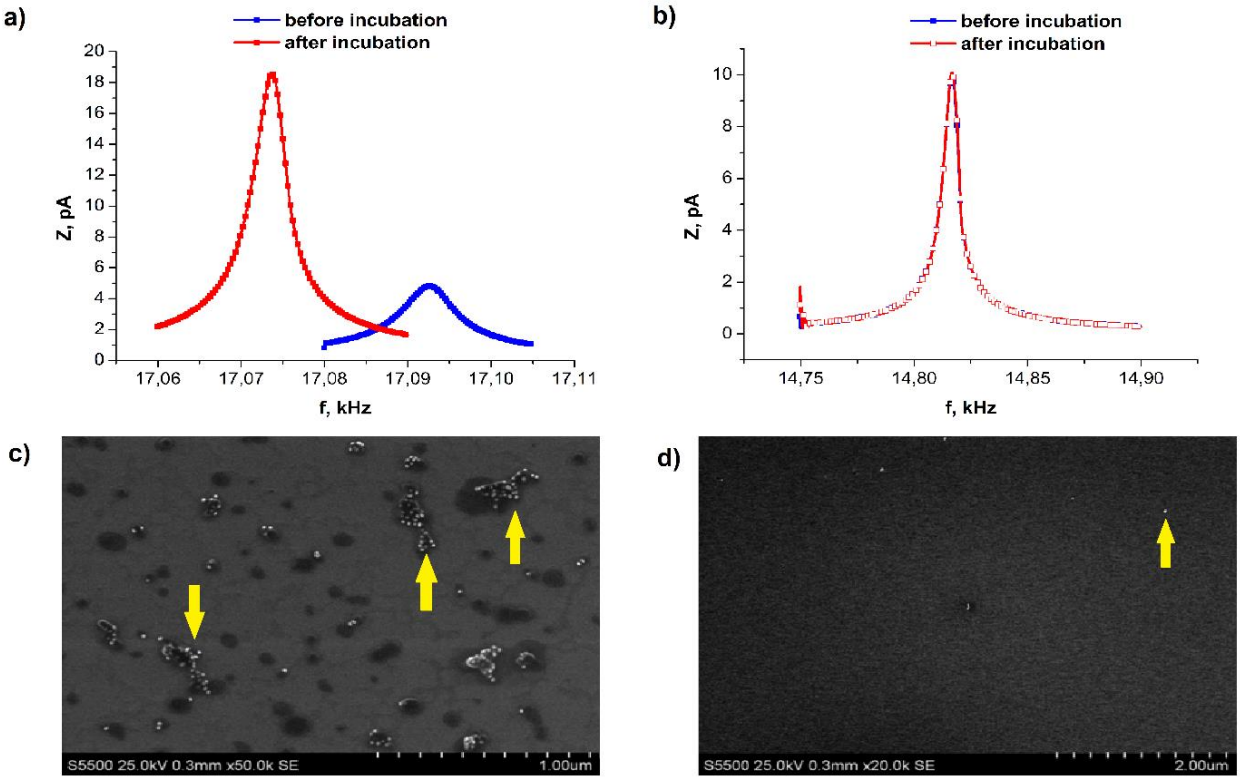

Figure 1. The resonance frequency curves of the AFM cantilever obtained before (red curves) and after (blue curves) their incubation in AuNP-containing solution, and corresponding SEM images of single AuNPs adsorbed onto the cantilever surface, in the case of adsorption of 10^6 (a, c) and 10^4 (b, d) 20-nm AuNPs.

Due to high sensitivity of mass determination, the use of cantilever-based method for protein detection in biomedical applications is promising. To date, modern techniques allow labeling of protein molecules with AuNPs in 1:1 ratio [5]. This fact gives an oportunity for the detection of so-labeled protein molecules with high sensitivity. In this way, using 20-nm AuNPs for this purpose, the 10^{-15} M protein detection limit can be attained upon analysis of 1 mL of sample. Moreover, if 100-nm AuNPs will be used instead of 20-nm ones, the detection limit of labeled protein molecules can be shifted down to 10^{-17} M.

This study was performed in the framework of the Program for Basic Research of State Academies of Sciences for 2013-2020. Shumov I.D. is a recipient of Russian Federation President scholarship for young scientists for 2016-2018 (project identificator SP-4280.2016.4).

1. G.A. Kiselev, I.V. Yaminsky, *Nanotechnologies in Russia* **2**, 112 (2007).
2. Yu.D. Ivanov, N.S. Bukharina, T.O. Pleshakova, et al., *Biophysics* **56**, 892 (2011).
3. P.M. Kosaka, V. Pini, J.J. Ruz, et al., *Nature Nanotechnol.* **9**, 1047 (2014).
4. E.V. Ukraintsev, G.A. Kiselev, D.V. Bagrov, et al., *Sensors and Systems* **1**, 18 (2007).
5. D.M. Rissin, C.W. Kan, T.G. Campbell, et al., *Nature Biotech.* **28**, 595 (2010).

P-88

Local study of lithiation and degradation paths in $LiMn_2O_4$ battery cathodes via scanning probe microscopy and confocal raman microscopy

B.N. Slautin[1], D.O. Alikin[1,2], K.N. Romanyuk[2], D. Rosato[3],
D.V. Pelegov[1], V.Ya. Shur[1], A.L. Kholkin[1,2]

[1] *School of Natural Sciences and Mathematics, Ural Federal University, 620002, Ekaterinburg, Russia boris.slautin@urfu.ru*

[2] *Physics Department & CICECO – Aveiro Institute of Materials, University of Aveiro, 3810-193, Aveiro, Portugal*

[3] *Robert Bosch GmbH, 70839 Gerlingen-Schillerhoehe, Germany*

Lithium manganese-based cathodes ($LiMn_2O_4$, LMO) are widely used in rechargeable batteries due to their low cost, safety, and ecological stability. Enhancement of the LMO properties is impossible to be realized without understanding of nature of the processes occurring inside the cathodes at the nanoscale. In this contribution we studied comprehensively structural and functional transformations of the LMO electrode occurring with its lithiation and degradation via Scanning probe microscopy (SPM) and confocal Raman microscopy.

SPM makes possible studying of the ionic mobility at the nanoscale via local excitation by the biased scanning probe tip, so-called electrochemical strain microscopy (ESM) [1]. We developed novel quantitative ESM approach based on analyzing of frequently dependent electro-mechanical response [2]. ESM measurements showed that Li ions are distributed non-uniformly inside the LMO particles. The average diffusion coefficient in individual particles ~2×10-10 cm^2s^{-1} had a value close to the expected one for fully charged LMO. Enhancement of the concentration in the vicinity of particle boundaries can be attributed to the limited diffusion path of lithium forming an apparent core–shell structure. We registered also about 50% decrease of the diffusion coefficient at thin interface layer of the individuals LMO particles (from a few to tens nanometers).

Structural study of LMO electrodes by spatially resolved Raman spectroscopy showed that cycling leads to: (1) formation of Mn_3O_4 phase with its further dissolution in the electrolyte; (2) qualitative change of the lithiation process in cycled LMO cathodes with formation of the significant inhomogeneous lithiation state. Spatial distribution of Mn_3O_4 phase was spatially correlated with the cracks on the particles surface revealed by optics, which means that appearance of Mn_3O_4 phase can be responsible for the mechanical stresses in the material. The segregation of Mn_3O_4 phase was found as well in vicinity of the particle boundaries and thereby determine diminished electrochemical activity. On contrary, Mn_3O_4 phase was not revealed in aged cathodes, which prove that the dissolution of this phase occurs mostly at the beginning of cycling while further mechanism of capacitance fade is due to inhomogeneity of the delithiation process [3].

Thereby the final model of the material could be following: structural transformation with formation of the weak electrochemically active phase near the particle interface lead to the impeding of lithiation process and formation of inhomogeneous distribution of the ‘state of charge’. This inhomogeneity increases self-consistently during lithiation process regardless dissolution of the additional phases possibly due to impact of chemically induced stresses. The inhomogeneous lithiation is than believed to be responsible for the capacity fade in the battery.

The work was financially supported by Russian Science Foundation (Grant 17-72-10144). The equipment of Ural Center for Shared Use “Modern Nanotechnology” Ural Federal University was used.

1. J. Li, J.-F. Li, Q. Yu, Q. N. Chen, S. Xie, *J. Mater.* **1**, 3 (2015).
2. D.O. Alikin, K.N. Romanyuk, B.N. Slautin, D. Rosato, V.Ya. Shur, A.L. Kholkin, *Nanoscale* **10**, 2503 (2018).
3. B. Slautin, D. Alikin, D. Rosato, D. Pelegov, V. Shur, A. Kholkin, *Batteries* **4**, 21 (2018).

P-89

Characterization of Au-Fe nanocrystals obtained by MBE

T.E. Smolyarova[1,2], I.A. Tarasov[2], A.V. Lukyanenko[1,2]

[1]*Siberian federal university, 660041, Krasnoyarsk, Russia*

[2]*Kirensky Institute of Physics, 660036, Krasnoyarsk, Russia*
e-mail: smol.nano@yandex.ru

Bimetallic magnetic nanomaterials are under extensive investigations now due to their possible application in nanotechnology and nanomedicine. The distinctive characteristic of such materials is their superparamagnetic behavior, which is important for biomedical, diagnostic and therapeutic applications. At present, the Au-Fe based nanomaterials attract much attention due to higher saturation magnetization in comparison with the Au-Fe oxide core-shell structures, which synthesis has heavily been investigated over the last decade [1]. So far, several scientific reports about the synthesis of the Au-Fe core-shell nanostructures have been made. It is clear that this question has not been illuminated enough yet in the literature. That variety of different possible forms of nanostructures, that The Au-Fe system potentially encloses, give us a hope to understand and establish the relationship between technological procedures of their synthesis and resultant properties desirable for practical application.

Hybrid crystalline Au-Fe nanoparticles have been successfully synthesized using the epitaxial growth process. The first step in fine particle characterization was to observe the particles using atomic force microscopy (Fig. 1).

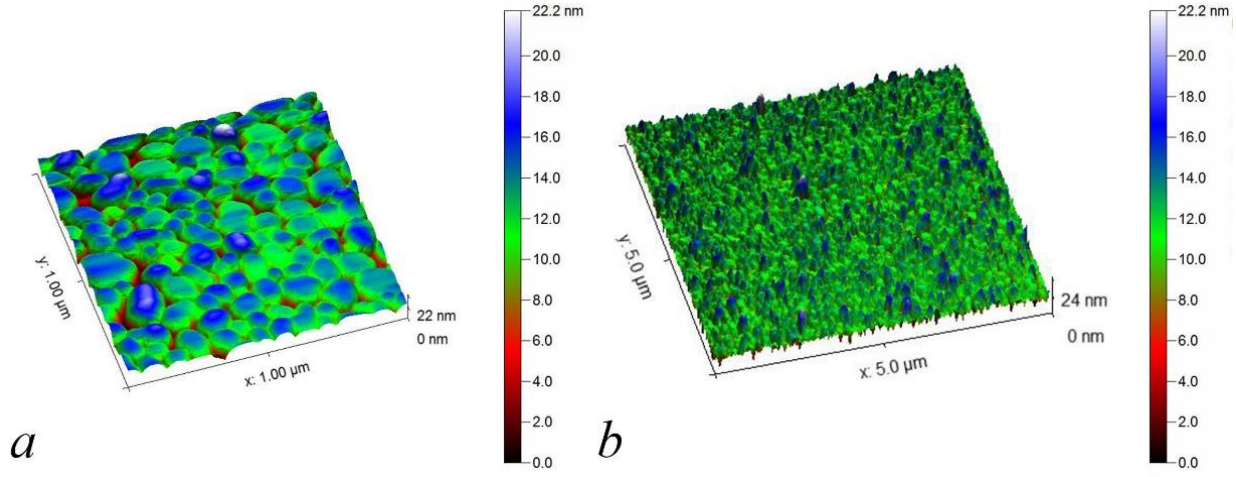

Figure 1. 3D AFM images of hybrid crystalline Au-Fe nanoparticles (a) 1×1 µm^2, (b) 5×5 µm^2.

AFM measurements have better resolution than traditional instruments and can be applied for measurements of bare and untreated surfaces without complicated sample preparations. Precise information about the height of nanocrystalls could be extracted (Fig. 2).

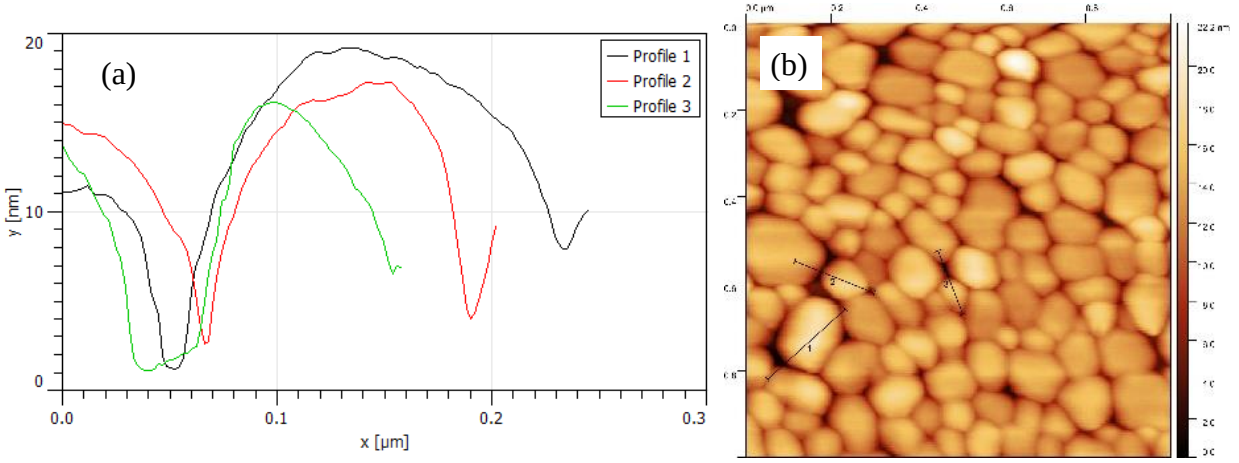

Figure 2. (a) 1D profile and (b) surface map of AFM measurements of Au-Fe nanocrystalls.

The next step was to get most common measurements that are related to the width and shape of the particle distribution. Firstly, it is possible to process the measurements based on the level of assumptions and the degree to which the results are calculated. For instance, the first measurement is the projected two-dimensional area, which is calculated as the sum of the areas of each individual pixel (Fig. 3a). So, most of the nanocrystals have area near 100 nm^2. Using various equations we can calculate the aspect ratio. Modern literature defines aspect ratio as the ratio of the Feret's minimum length to the Feret's maximum length [2]. The maximum Feret's diameter, also called the maximum distance in some references, is defined as the furthest distance between any two parallel tangents on the particle. Likewise, the minimum Feret's diameter, also called the minimum distance in some references, is defined as the shortest distance between any two parallel tangents on the particle. Thus, as the width and length of the shape approach the same value, the aspect ratio approaches one. This does not necessarily mean the shape is circular, though a perfect circle does have an aspect ratio of 1.0. Often very symmetric shapes also have a very high aspect ratio (Fig.3b). In our work most of hybrid crystalline Au-Fe nanoparticles have aspect ratio close to 0.5.

Furthermore, circularity was defined as the degree to which the particle is similar to a circle, taking into consideration the smoothness of the perimeter. This means circularity is a measurement of both the particle form and roughness. Thus, the further away from a perfectly round and smooth circle that a particle becomes, the lower the circularity value. Circularity is a function of the area divided by the square of the perimeter. Conversely, as a shape becomes less round or as the shape becomes less smooth, the circularity should approach zero. Most of synthesized crystalline Au-Fe nanoparticles have circularity close to 0.9. This analysis shows that the most of particles have shape closed to spherical (Fig. 3c).

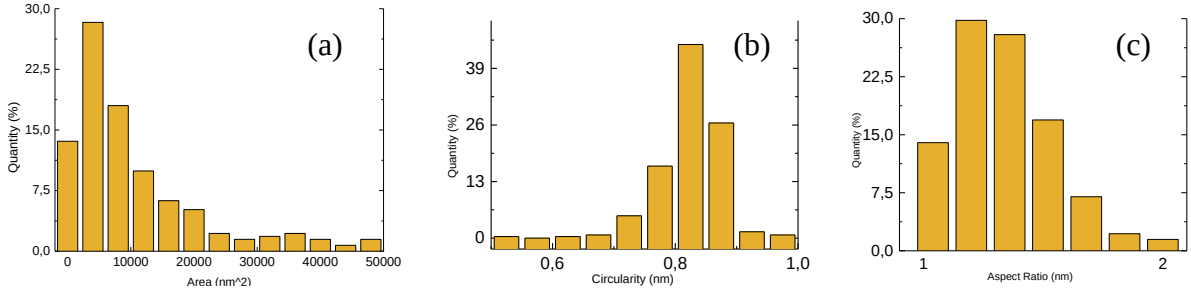

Figure 3. Histogram distributions of area (a), circularity (b) and aspect ratio (c) measurements of Au-Fe nanocrystalls.

Using these measurements may not be adequate to describe a typical non-spherical particle with some degree of surface roughness. There are various definitions and several standardized shape factors available that can provide additional descriptors to a particle population of interest. These valuable shape descriptors can be measured using image analysis. There are numerous examples of how the shape of the particle may influence its behavior or correlate to a response of interest. Because of this importance, shape factors may be necessary to consider in validated characterization methods.

Hybrid crystalline Au-Fe nanoparticles are perspective candidates for solving the problem of increasing the density of information recording on non-volatile media. Despite the high cost of gold, its insolubility in iron in bulk materials makes it possible to form thin shells on the faces of iron nanocrystals due to phase segregation at high temperatures [3], which allows using the least amount of the expensive metal. Besides, having strong spin-orbital coupling and resistance to oxidation, gold provides opportunities for improving the magnetic characteristics of hybrid nanocrystals based on Au-Fe.

1. Z.D. Pozun, S.E. Rodenbusch, E. Keller, et al., *J. Phys. Chem*. **117**, 7598 (2013).
2. E.G. Michel, *Appl. Surf. Sci*. **117**, 294 (1997).
3. M. Benoit, N. Tarrat, *J. Morillo, Phys. Chem*. **18**, 9112 (2016).

P-90

Biofunctionalized magnetic microdiscs applied in medicine

T.E. Smolyarova[1,2], A.V. Lukyanenko[1,2], A.S. Tarasov[1,2], D.A. Smolyakov[2]

[1]*Siberian federal university, 660041, Krasnoyarsk, Russia*

[2]*Kirensky Institute of Physics, 660036, city, Krasnoyarsk, Russia*
e-mail: smol.nano@yandex.ru

Biocompatible magnetic microdiscs can be used in medicine for the treatment of malignant tumors [1]. These microdiscs are coated with gold (Au) and do not have a negative effect on the human body. Without the influence of the magnetic field, magnetic vortex is located in the center of the disc, when magnetic field is applied magnetic vortex shifts toward the increasing magnetization, creating an oscillation, which transmits mechanical force to the cell. Then this mechanical force is efficiently transduced to the membrane and after that to the subcellular components. We used a new approach to fabricate biocompatible microdiscs with a spin-vortex ground state. Dip-Pen Nanolithography (DPN) method is easy-to-use and it is flexible technique for fabrication of magnetic nanostructures. We used Au/Fe_3Si structure grown on Si(111) substrate [2] by molecular beam epitaxy (MBE) in extra-high vacuum on an atomically clean surface. In the experiment, by DPN method the ink (MHA-Acetonitrile) is deposited along the tracing path and diffuses away from the tip. This way we can form desired pattern, on a Fe_3Si/Si(111) substrate coated with Au. SiN probe, coated with ink was used in the experiment. By varying the dwell time, it is possible to create dots of various radii. We used 10 seconds for dwell time. Thus, this way structured array of 0.9-μm-diameter magnetic microdiscs (dots) was fabricated (Fig. 1a).

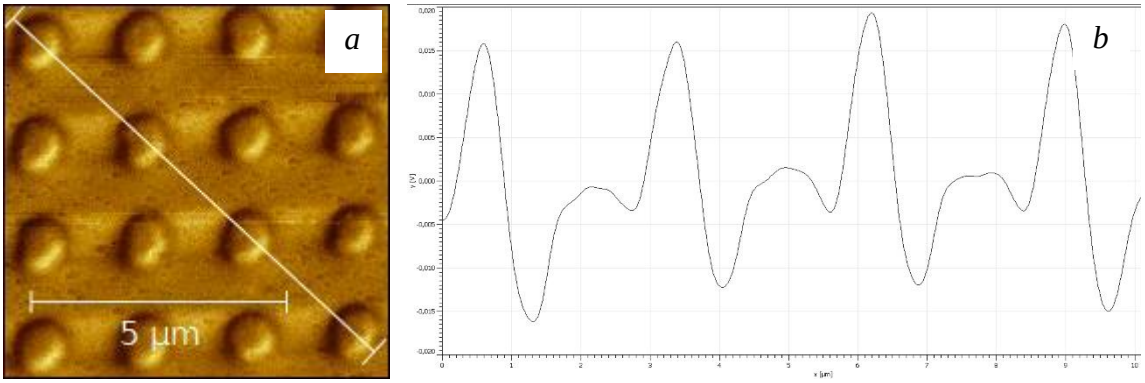

Figure 1. (a) MFM image and (b) the cross-section of MFM signal of Au/Fe_3Si microdiscs.

Fabricated nanostructured array of ferromagnetic microdiscs was studied by MFM mode to display the magnetic signal. The MFM probe used for the measurement was oriented perpendicular to the sample ($\alpha = 90°$) and the cantilever was tilted at an angle $\beta c = 4°$ with respect to the sample plane. With this probe configuration, the magnetic transitions appear as either dark or bright spots, corresponding to attractive or repulsive force derivatives, respectively. This response is shown explicitly by the constant force derivative contour in Figure 1b. Experimental MFM image microdiscs have the ground state of the homogenous magnetization, oriented along the direction of the external magnetic field. This image shows that all nanodiscs demonstrate the dipole distribution of MFM contrast typical for homogenous magnetized state.

The work was supported by the Russian Foundation for Basic Research, Government of Krasnoyarsk Territory, Krasnoyarsk Region Science and Technology Support Fund to the research project № 18-32-00035\18.

1. D.H. Kim, E.A. Rozhkova, I.V. Ulasov, et al., *J. Nature Materials* **9**, 165 (2014).
2. S.W. Chung, A. Mirkin, H. Zhang, *J. Nano Lett.* **3,** 43 (2010).

P-91

Study of ferroelectric and elastic properties of ferroelectric capacitors based on hafnium oxide films by Band Excitation techniques

M. Spiridonov, S. Zakharchenko, A. Chouprik, A. Chernikova, R. Kirtaev, D. Negrov

[1]*Moscow Institute of Physics and Technology, Dolgoprudny, 141700, Russia*
e-mail: spiridonob@yandex.ru

The Band Excitation (BE) approach [1,2] in piezoresponse force microscopy (PFM) provides an alternative to standard single frequency PFM technique by exciting and detecting response at all frequencies within a specified frequency range simultaneously. BE introduces a synthesized digital signal that spans a continuous band of frequencies, and monitors the response within the same frequency band. This approach allows to obtain full piezo- and mecanical response spectra and process them considering the specific conditions like atomic force microscopy (AFM) background. Resonance-enhanced combined band-excitation (BE) PFM and atomic force acoustic microscopy (BE AFAM) techniques was home-implemented [3] in commercially available AFM Ntegra (NT-MDT) using digital signal processor (Nanoscan Technologies) to study domain structure of ferroelectric (FE) thin $Hf_{0.5}Zr_{0.5}O_2$ films which are considered as the main functional material for nonvolatile FE random access memory (FeRAM) [4]. Analysis of the local FE and elastic properties of $Hf_{0.5}Zr_{0.5}O_2$ films allows to understand the nature of structural transformations during first stages of FE capacitor operation and paves way to engineering of hafnium oxide memory cells to improve their performance.

For fitting of acquired spectral response, we used the model of harmonic oscillator with additional shift linearly dependent on frequency. The last contribution is intended to compensate a possible AFM background and finally allows to obtain most correct values of piezoresponse amplitude and phase. For fitting, we applied the vector technique [5]. Both piezo- and mechanical contact response was fitted with the rational function approximation $H(s) = \frac{c_0}{s - a_0} - \frac{c_0}{s - \bar{a}_0} + d + sh$, where s is complex frequency parameter, a_0 and $\bar{a}_0$ are two complex conjugate poles, c_0 is residue, d is shift parameter, h is slope parameter. First two factors in transfer function $H(s)$ represent resonant system formed by cantilever in contact with sample surface, while the expression $d + sh$ describes AFM background in AFM Ntegra. Both in BE PFM and BE AFAM, in each point of scan the optimal parameters of the fit yield resonance amplitude A, phase φ, contact resonance frequency f_c, d and h parameters in each point of scan. In addition, we calculate parameter Q, typically characterizes quality factor. Therefore, 12 parameters are mapped during scanning in PFM and AFAM: A, φ, f_c, Q, d h. Obtained data contains a diversity of information about the FE and elastic properties of structure under investigation. In addition to domain structure, the local elastic properties (including Young's modulus, parameter of dissipation, mechanical stress) can be acquired and analyzed. In addition, the information about mechanical response allows to eliminate the topographical crosstalk in PFM data.

In conclusion, the combined band-excitation BE PFM and BE AFAM technique allows to reveal the domain structure of novel FE thin $Hf_{0.5}Zr_{0.5}O_2$ films and obtain the additional information about evolution of elastic properties during the operation of memory cell.

1. S. Jesse, S. Kalinin. *J. Phys. D: Appl. Phys.* **44**, 464006 (2011).
2. S. Jesse et al. *Nanotechnology* **18**, 435503 (2007).
3. A. Chouprik et al. *ACS Appl. Mater. Interfaces* **10**, 8818 (2018).
4. M.H. Park et al., *Appl. Phys. Lett.* **102**, 242905 (2013).
5. Gustavsen, A. Semlyen, *IEEE Transactions on Power Delivery* **14**, (1999).

P-92

Restricted geometry effect on Phase Transitions in Rb_2ZnCl_4

L.S. Stekleneva[1], E. Rysiakiewicz-Pasek[2], V.S. Bondarev[3], I.N. Flerov[3], M.S. Molokeev[3], L.N. Korotkov[1]

[1] *Voronezh State Technical University, Moskovsky pr. 14, 394026, Voronezh, Russia*
[2]*Faculty of Fundamental Problems of Technology, Wroclaw University of Science and Technology, 50-370, Wroclaw, Poland*
[3]*Kirensky Institute of Physics, Federal Research Center KSC SB RAS, 660036, Krasnoyarsk, Russia*
e-mail: lubov_stekleneva@mail.ru

The physical effects in conventional nanosized ferroelectrics have been studied to some extent at present. At the same time, the problems associated with the appearance of an incommensurate phase, its temperature evolution, and the transition to a commensurate polar phase under conditions of restricted geometry have not been practically investigated.

Suitable objects for such studies are nanocomposites based on Rb_2ZnCl_4, which in the bulk state undergoes transition from paraelectric to incommensurate phase near $T_i \approx 303K$ and transition from incommensurate to ferroelectric phase in the vicinity of $T_C \approx 192K$. These transitions are accompanied by distinct anomalies of dielectric permittivity ε.

The purpose of the present work is calorimetric, dielectric and X-ray investigation of Rb_2ZnCl_4 - SiO_2 nanocomposites.

The matrix nanocomposites of Rb_2ZnCl_4 - SiO_2 system were prepared by embedding of Rb_2ZnCl_4 into porous glasses with average diameter of through pores near 320, 160, 46 and 23 nm from saturated aqueous solution (Abbreviations of the samples are RS-23, RS-46, RS-160 and RS-320). X-ray analysis (Cu-Kα radiation) showed that the crystallized in porous material and bulk Rb_2ZnCl_4 possess identical crystalline structure.

Analysis of powder patterns revealed that (2/3 2 0) peak appeared at 300K and its intensity increases under cooling. There were not found any other superstructure peaks under cooling.

Results of dielectric and calorimetric measurements are presented in Figures 1 and 2.

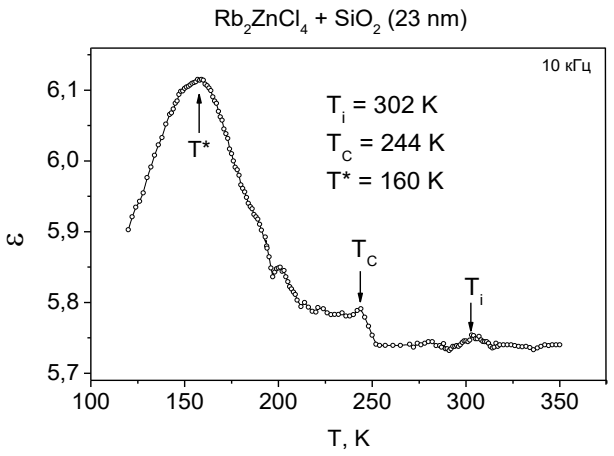

Figure 1. Temperature dependence of the dielectric permittivity for RS-23 sample

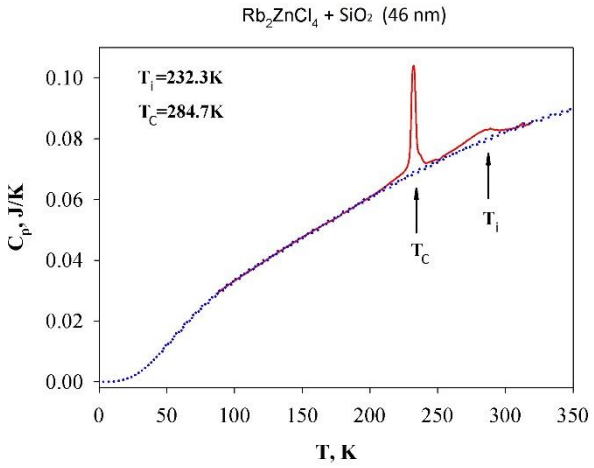

Figure 2. Temperature dependence of the heat capacity for RS-46 sample

Three anomalies of dielectric permittivity (ε) at temperatures of about 160, 246 and 302 K for RS-23, RS-160 and RS-320 samples were found (Fig. 1). The weak maximum of ε at T_{i2}=302K coincides with the diffused maximum of heat capacity C_p (Fig. 2). The distinct peak of C_P near 232K is accompanied by the step-like anomaly of ε (≈ 244K). These anomalies are associated with the ferroelectric phase transition that in the single crystal of Rb_2ZnCl_4 is observed at $T_C \approx 192K$.

The diffused maximum of ε near T* = 160K is not accompanied by any peculiarities in the $C_P(T)$ dependence. The origination of this maximum of ε is discussed.

P-93

Scanning probe microscopy application in a research of opal nanostructures

A.B. Syritskii, E.V. Panfilova

[1]*MSTU Bauman, 105005, Moscow, Russia*
e-mail: syritsky@yandex.ru

The paper presents the results of a study of the formation of multilayer structures based on opal films on a scanning probe microscope Solver P-47 using atomic force and tunneling microscopy and current spectroscopy. It has been revealed that tunneling microscopy methods are suitable for studying chromium-opal-gold-carbon layered structures.

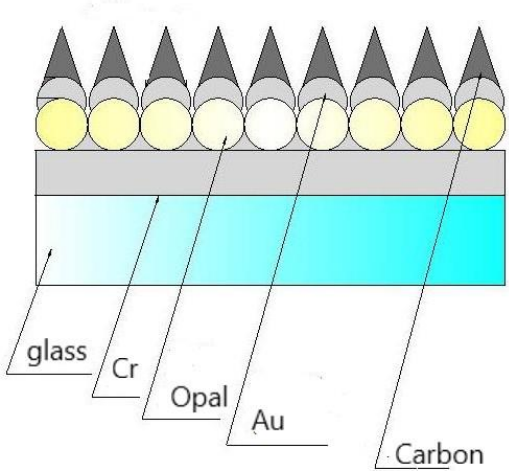

Figure 1. Chrome - opal - gold - carbon structure.

Surface images and current-voltage characteristics obtained as the structures are formed along the layers are shown. It is shown that the formation of film structures on the surface of opal matrices begins with the formation of "islands" on tops of silica spheres. It was found that the deposition of carbon films on the surface of the chrome-opal-gold structure leads to an increase in tunnel currents in the tip-sample gap. The presented results can be used in the development of technology for the formation of a variety of layered structures on the surface of opal matrices, in particular, in the production of photonics, various sensor systems and emission devices.

A comparison of the profiles of the surfaces of opal films and the gold layer formed on it once again confirmed the mechanism of growth of metal films detected earlier on [1,2] and the above mentioned mechanism on the surface of the opal matrix. The study of images and profiles of the surface deposited on the gold layer of carbon showed that carbon structures were formed mainly on the areas located above the vertices of the silica spheres on the "islets" of gold, which led to an increase in the relief height of these sections. The carbon layer has a "pimply" surface, this is noticeable both in the surface image, and in the relief profiles. At the same time, the relief of the peaks became more developed. Moreover, the deposition of carbon not from the gas phase, but by the magnetron method, performed for comparison on some samples, led to the formation of a surface with a similar relief character.

1. E.V. Panfilova et al., *Nanoengineering* **1**, 12 (2016).
2. E.V. Panfilova, A.B. Syritskii, E.V. Vagulina, *Nanoengineering* **1**, 1 (2015).

P-94

SPM investigations of domain walls in Barium titanate PTC thermistors

S.A.M. Tofail[1,2], M. Karimi-Jafari[1,2], A. Stapleton[1,2], Y. Guo[2], K. Kowal[1,2], D. Chovan[1,2], L. Kailas[2], A. Gandhi[1,2], K. O'Sullivan[3], A. Maher[3], E.U. Haq[1,2]

[1]*Department of Physics, University of Limerick, Limerick, V94 T9PX, Ireland*
e-mail: Tofail.Syed@ul.ie; Ehtsham.U.Haq@ul.ie

[2]*Bernal Institute, University of Limerick, Limerick, V94 T9PX, Ireland*

[3]*BorgWarner Beru Systems, Monavalley Industrial Estate, Tralee, Co. Kerry, Ireland*

Barium titanate ($BaTiO_3$) has been a very attractive material for electroceramics and microelectronics industry due to its high dielectric constant and low loss characteristics. These characteristics make it a material of choice in multilayer capacitors and energy storage devices.

Barium titanate is a ferroelectric insulator at room temperature; however, by suitable doping with ions like La^{+3}, Sm^{+3}, Ho^{+3} or Nb^{+5} the material can be tailored to become ferroelectric semiconductor at room temperature. The semiconducting property in ferroelectric $BaTiO_3$ gives rise to a huge resistivity change at the ferroelectric-paraelectric transition temperature with a positive temperature coefficient of the resistivity (PTCR) [1,2]. The PTCR effect has found numerous industrial applications like over-voltage protection, automobiles, hair-dryers and self-regulating heaters. In this study, two surface analysis tools, electron backscatter diffraction (EBSD) and piezoresponse force microscopy (PFM) were combined to investigate the crystallographic orientation, topography and intergranular polarization in polycrystalline PTC $BaTiO_3$ ceramic that leads to PTC effect.

EBSD of $BaTiO_3$ reveals individual grains of $BaTiO_3$ possess a preferred orientation. Ferroelectric domains and twinning is evident in both electron back scattered images and PFM images. In individual grains, the domains mostly appear in a single twin pair set rather than random pairs of all available phase variants. While the EBSD on these thermally etched samples showed 90° domains it could not discern the type between a-a and a-c domains. PFM, on the other hand, clearly distinguishes a-a and a-c type domains using vertical and lateral piezoresponse (Fig. 1). The work reported here will contribute to grain boundary control of PTC effect in semiconducting ferroelectric barium titanate ceramics.

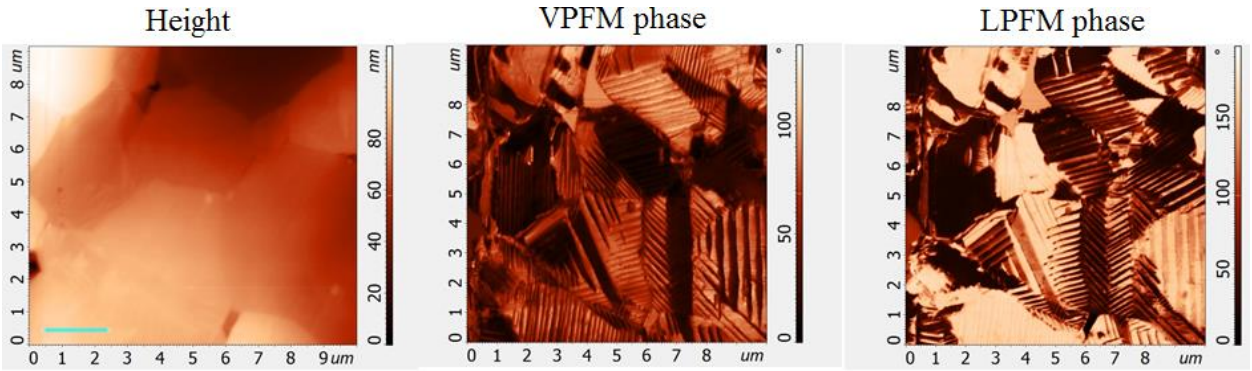

(a) (b) (c)

Figure 1. (a) Atomic force microscopy topography, (b) vertical and (c) lateral piezoresponse force microscopy (phase) of barium titanate PTC thermistors.

1. J. Daniels, K. Härdtl, R. Wernicke, *Philips Technical Review* **38**, 73 (1979).
2. B. Huybrechts, K. Ishizaki, M. Takata, *Journal of Materials Science* **30**, 2463 (1995).

Phase transition in triglycine sulfate by piezoelectric response force microscopy and dielectric spectroscopy

A.L. Tolstikhina[1], R.V. Gainutdinov[1], N.V. Belugina[1], E.S. Ivanova[1], G.I. Ovchinnikova[2]

[1]*Shubnikov Institute of Crystallography, Federal Scientific Research Centre "Crystallography and Photonics", Russian Academy of Science, 119333, Moscow, Russia*
e-mail: alla@ns.crys.ras.ru

[2]*Faculty of Physics, Lomonosov Moscow State University, 119991, Moscow, Russia*

Many studies were performed for a better understanding of the phase transition in triglycine sulfate (TGS) well known as ferroelectric organic compound. The material undergoes second – order phase transition at about 49.5°C. From the three glycine molecules (G1, GII, GIII) forming the unit cell the non – planar GI molecule is responsible for the polarization and shows a complex dynamics much faster than that performed by the other glycine molecules [1]. Despite a large number of works on the investigation of phase transition in TGS, the mechanism by which a spontaneous dipole moment is created, is still not fully understood, the processes of the appearance of polar state at cooling and destruction of ferroelectric domains upon heating remain unstudied at the nanoscopic level. The narrowest region near Tc remained the least studied [2,3].

The phase transition in TGS has been studied in this work by means of dielectric spectroscopy and piezoelectric force microscopy (PFM). The TGS dielectric spectra were measured in a wide frequency range. The total dielectric spectra of TGS crystal measured near phase transition temperature is presented in the Figure 1. At least two characteristic times can be clearly revealed from this spectra; 300 kHz and 40 GHz. An attempt was made to combine the molecular dynamics data [1] in TGS near phase transition temperature with dielectric dispersion and observed in PFM structure transformation features.

The images obtained by PFM *in situ* reflected the evolution of TGS surface structure during the phase transition (Fig. 2). The formation of surface polarized structure in the form of elongated thin lamellas was recorded at T ≈ 49.5°C under conditions of slow cooling the sample. The width of lamellas is $w_1 \approx 50 \pm 10$ nm (light contrast), $w_2 \approx 74 \pm 10$ nm (dark contrast) (Fig. 2a). When the temperature drops to 49.2°C, the lamellas become enlarged, their width and its dispersion increase to $w_1 \approx 105$-291 nm, $w_2 \approx 137 - 342$ nm (Fig.2b). The regions with a light contrast occupy ~ 50% of the total image area at T ≈ 49.5°C and ~ 62% at 49.2°C. The domains coalesce upon further cooling to 48.7°C and below, gradually increasing in size, while a slight predominance of one sign over the other remains.

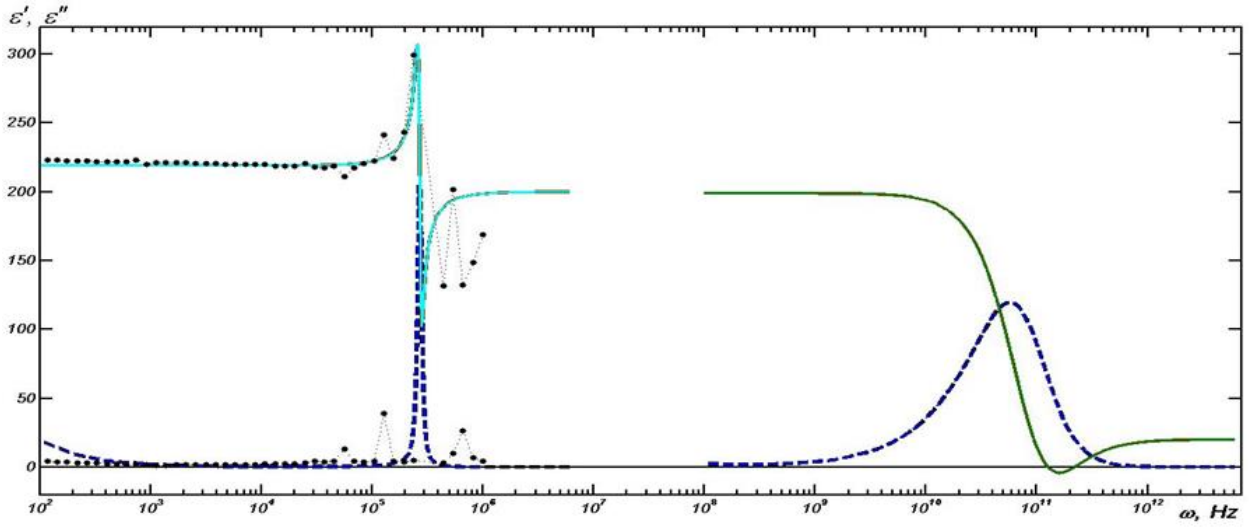

Figure 1. Dielectric spectra of TGS in the hole investigated frequency region.

To the right of the images of domain structures, their two-dimensional amplitude Fourier spectra are shown. The Fourier transformation of the phase images showed that a quasiperiodic one-dimensional domain structure is formed in the immediate vicinity of phase transition point $Tc-1°C < T < Tc$, which is characterized by the repetition of bands of the same width with a small random dispersion around the mean value. Notably, obvious features of the quasi-periodicity of domain structure disappear at a distance from the phase transition point by a degree or more, the width of the domains and the dispersion of width values from the mean value increase significantly.

The calculation of two-dimensional correlation functions made it possible to determine the period of the structure and analyze the temperature dynamics of the TGS crystal in this region. The quasi-periodicity of structure is become apparent most clearly at $T \approx Tc - 0.2°C$.

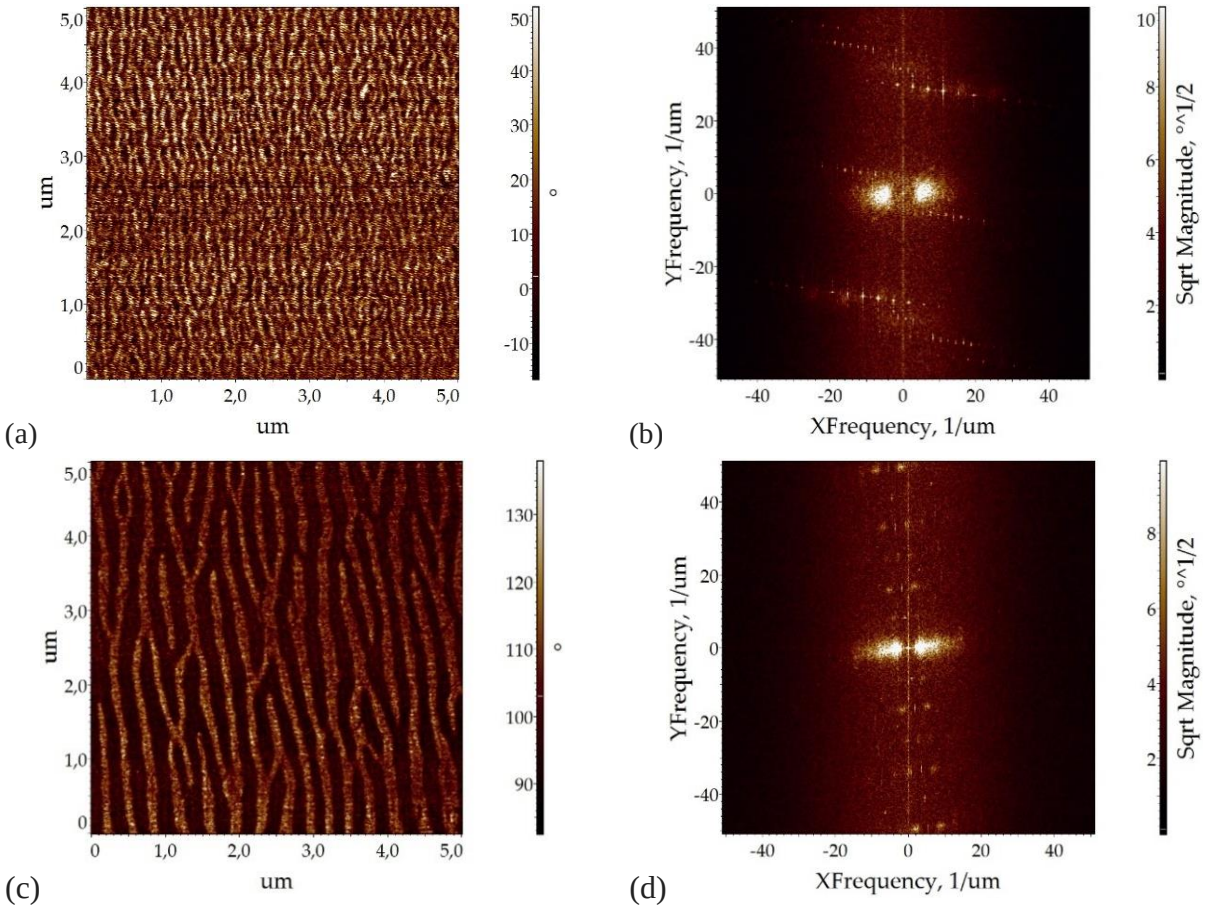

Figure 2. (a, b) PFM image of quasiperiodic structure of TGS crystal: (a) 49.5, (b) 49.2. (c, d) Corresponding two-dimensional amplitude Fourier spectra.

According to X-ray and neutron studies of TGS single crystals near Tc, diffuse scattering of Bragg reflections *0kl* is observed in the inverse space, which indicates correlation interactions at the local structure level: from one-dimensional zigzag chains of N^+H_3 groups aligned along *b* to three-dimensional ordering in network [4]. It is obvious that the processes observed here at the microscopic level are directly related to structural rearrangements occurring at the atomic level.

The correlation between the features of wide-band dielectric spectra and quasiperiodic structure of TGS crystal in the immediate vicinity of phase transition is discussed.

1. V. Tripadus, A. Radulescu, J. Piepe, at all., *Chemical Physics* **322**, 323 (2006).
2. E.Z. Luo, Z. Xie, J.B. Xu, et al., *Phys.Rev.B.* **61**, 203 (2000).
3. X.K. Orlik, V. Likodimos, L. Pardi, at al., *Appl. Phys. Lett*. **76**, 1321 (2000).
4. J.M. Hudspeth, D.J. Goossens, T.R. Welberry, et al., *J Mater Sci*. **48**, 6605 (2013).

Formation of memristor structures based on ZnO thin films by scratching probe nanolithography

R.V. Tominov, V.I. Avilov, V.S. Klimin, V.A. Smirnov, N.E. Chernenko

[1] *Southern Federal University, Research and Education Center "Nanotechnology", Institute of Nanotechnologies, Electronics and Equipment Engineering, 347928, Taganrog, Russia*
e-mail: roman.tominov@gmail.com

Development of the next generation computer memory is the promising direction of electronics. One of the promising types of memory is metal oxide memristor structures-based non-volatile resistive memory (RRAM), which has high-density integration, low-power consumption, and fast write/read operations. Zinc oxide (ZnO) is the one of the promising oxides, which widely used in electronic element developments, sensors and microsystem technology. Also ZnO demonstrates memristor effect and is compatible with semiconductor technology [1,2]. To fabricate ZnO based RRAM it is necessary to carry out prototyping and investigations of ZnO memristor structures. Thus, it becomes necessary to develop new nanolithography techniques, which allow fabricating the structure of elements of RRAM at lower expenses and within shorter periods than conventional methods of photo- and electron-beam lithography.

One of the promising methods for the formation of nanoscale structures is scratching probe nanolithography (SPN) of atomic force microscope (AFM) [3,4]. The SPN method involves the modification of thin polymer films by the formation of profiled nanosized structures using the tip of the AFM probe. Through the profiled nanosized structures various technological operations (deposition, etching) could be performed. The advantages of SPN include high resolution and the absence of physical templates. Various structures of the elements of nanoelectronics and microsystem engineering were formed using SPM.

The aim of this work is fabrication of ZnO thin film-based memristor structures using scratching probe nanolithography, and also investigation memristor effect on them.

ZnO thin film was grown using pulsed laser deposition technique. Al_2O_3/ZnO:In as a wafer was used. Deposition performed under the following conditions: wafer temperature: 400°C, target–wafer distance: 50 mm, O_2 pressure: 1 mTorr, pulse energy: 300 mJ.

The solution of photoresist/thinner (FP-383/RPF383F) at volume ratios of 1: 10 was transferred onto ZnO using the centrifugal method at the rotation speed of a Laurell WS-400B-6NPP centrifuge 5000 rpm. After the deposition of the film, the photoresist/thinner film was dried at the temperature of 90°C for 25 min. Thickness of the photoresist/thinner film was equal to 75.1±3.3 nm.

Scratching probe nanolithography (SPN) on the photoresist/thinner film was performed using a Solver P47 Pro scanning probe microscope (NT-MDT, Russia). Thus, array of the 9 squared nanostructure-grooves was formed. Then thin Ti film was deposited using BOC Edwards Auto 500 system. After that lift-off process was applied using dimethylformamide.

Electric measurements of the Al_2O_3/ZnO:In/ZnO/Ti structure was carried out using Solver P47 Pro oscilloscope. ZnO:In film was grounded during measurements. W_2C AFM probe was used as a top electrode. Current-voltage curves were obtained at –3 to +3 voltage sweep.

Figure 1 shows experimental investigation of ZnO and Ti films morphology. It is shown that ZnO film surface has a granular structure with 0.12±0.26 μm^2 grain size (Fig. 1a). Thickness of Ti structures was equaled 2.5±0.4 nm (Fig. 1b). The ZnO film thickness was investigated using AFM by scanning bottom electrode/ZnO film boundary, and was equaled 10.2±3.4 nm.

Figure 2 shows electric measurements of Al_2O_3/ZnO:In/ZnO/Ti/W_2C structure. Resistive switching from high resistance state (HRS) to low resistance state (LRS) was occurred at 2.1±0.3V, and from LRS to HRS at -1.5±0.3 V (Fig. 2a).

Endurance test shown that HRS was 5.5±0.4 GΩ, LRS was 2.3±0.3 GΩ (Fig. 2b). The HRS/LRS coefficient was equaled 21±3 at –3 to +3 voltage sweep. Read voltage was 1.5 V.

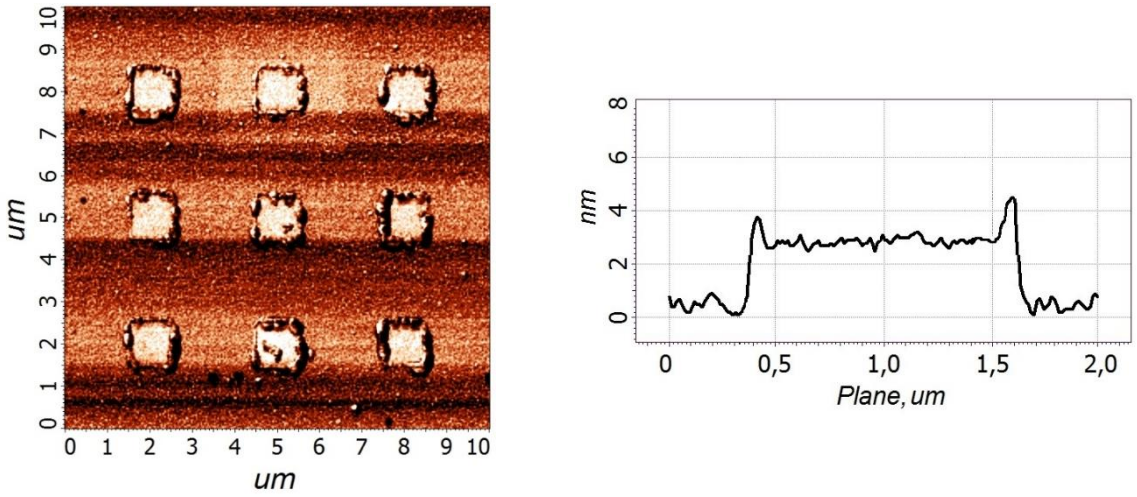

(a) (b)

Figure 1. 3×3 array of Ti structures: (a) AFM-image; (b) average profilogram of Ti structures.

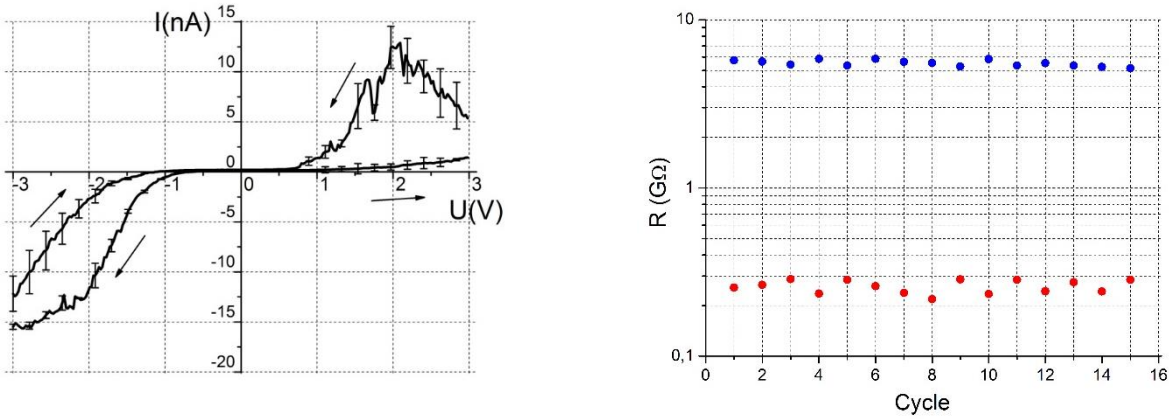

(a) (b)

Figure 2. Electric measurements of Al_2O_3/ZnO:In/ZnO/Ti/W_2C structure:
(a) current-voltage characteristic at –3 to +3 voltage sweep; (b) endurance test.

The results can be useful for micro- and nanoelectronics elements manufacturing, as well as micro- and nanosystem engineering using probe nanotechnologies and for ZnO- based RRAM fabrication.

This work was supported by Grant of the President of the Russian Federation No. MK-2721.2018.8. and by RFBR according to the research project № 18-37-00299

1. D.A. Khakhulin, Z. E. Vakulov, V.A. Smirnov, et al., *Journal of Physics Conference Series* **9**, 917 (2017).
2. V.I. Avilov, N.V. Polupanov, R.V. Tominov, et al., *IOP Conference Series: Materials Science and Engineering* **256,** 012001 (2017).
3. D.A. Bizyaev, A.A. Bukharaev, D.V. Lebedev, et al., *Technical Physics Letters* **7**, 645 (2012).
4. V.A. Smirnov, R.V. Tominov, N.E. Chernenko et al., *Nanotechnologies in Russia* **12**, 11 (2017).

P-97

Local electromechanical properties of barium strontium titanate based glass-ceramics

A.P. Turygin[1], A.S. Abramov[1], D.O. Alikin[1], D.S. Chezganov[1], I.S. Baturin[1], X. Song[2], T. Zhang[2], Y. Zhang[2], K. Hu[2], Z. Zhao[2], V.Ya. Shur[1]

[1] *School of Natural Sciences and Mathematics, Ural Federal University, Ekaterinburg, Russia anton.turygin@urfu.ru*

[2]*Beijing Key Laboratory of Fine Ceramics, State Key Laboratory of New Ceramics and Fine Processing, Institute of Nuclear and New Energy Technology, Tsinghua University, Beijing 100084, PR China*

Glass-ceramics comprising of ferroelectric grains surrounded by glass matrix are of significant interest for power electronics applications due to enhanced energy storage capabilities [1]. Barium strontium titanate (BST) ferroelectric glass-ceramics is one of the most promising candidates due to dielectric constants and high breakdown strengths [2,3]. In spite of macroscopic properties of BST ceramics are known, there is still lack of studies on local distribution of ferroelectric phase and its evolution during ceramics cycling.

We have studied microstructure, surface morphology and local piezoelectric activity of $(Ba_{0.25},Sr_{0.75})TiO_3$ based glass-ceramics with different amount of Mn additive (from 0 to 0.5%) prepared from melted and quenched mixed powders. The as-quenched was annealed and subjected to a controlled crystallization in air for 2h in temperature range from 850 to 950°C.

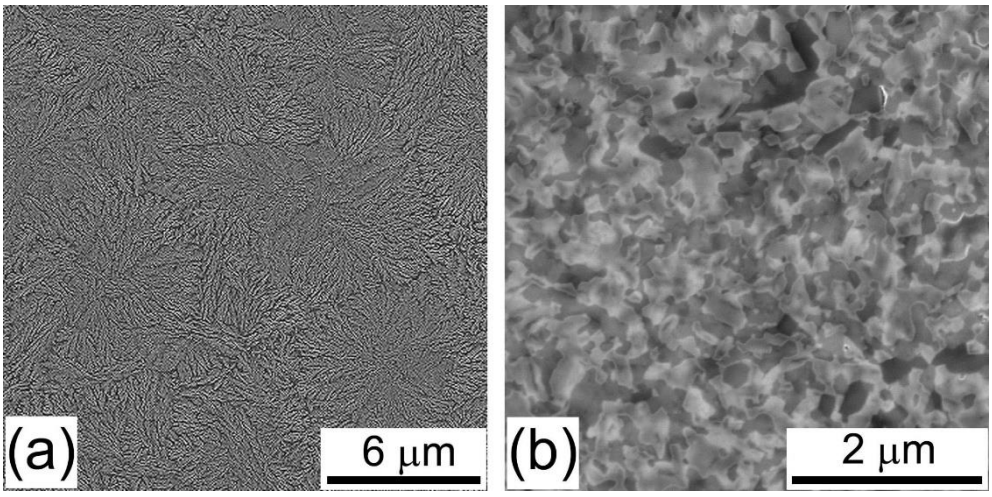

Figure 1. Microstructure of BST ceramics, annealed at: (a) 850°C, (b) 950°C.

Scanning electron microscopy studies of microstructure demonstrated the formation of the dendrite-like aggregates with sizes about 3-6 μm in ceramics annealed at 850°C and conventional faceted-shape grains with about 50-200 nm typical size in ceramics annealed at 950°C. Angle-resolved piezoresponse force microscopy measurements revealed absence of piezoresponse in dendrite-like aggregates, while faceted-shape randomly oriented grains were piezoelectrically active. The calculated fraction of piezoelectrically active phase was about 0.5. The individual piezoelectrically active grains mainly are in single-domain state and we couldn't realize tip-induced domain switching with applied voltage up to 200 V, which can be attributed to effective bulk screening. The observed effects emphasize the key role of microstructure in polarization reversal and dielectric properties of glass-ceramics.

The equipment of the Ural Center for Shared Use "Modern Nanotechnology" Ural Federal University was used. The research was made possible by Russian Foundation for Basic Research (Grant 18-52-53032).

1. Q. Tan, P. Irwin, Y. Cao, *IEEJ Trans. FM* **126**, 1153 (2006).
2. Y. Zhang, J.J. Huang, T. Ma, X.R. Wang, C. Deng, X. Dai, *J. Am. Ceram. Soc*. **94**, 1805 (2011).
3. X. Wang, Y. Zhang, I. Baturin, T. Liang, *Mat. Res. Bull*. **48**, 3817 (2013).

P-98

Domain kinetics in [001] -poled PMN-39PT single crystal during polarization reversal

A.D. Ushakov[1], A.A. Esin[1], A.R. Akmatkhanov[1], Q. Hu[2], X. Liu[1,2], Y. Zhao[1,2], X. Wei[2], V.Ya. Shur[1]

[1] *School of Natural Sciences and Mathematics, Ural Federal University, Ekaterinburg 620000, Russia bddah@ya.ru*

[2] *Electronic Materials Research Laboratory, Key Laboratory of the Ministry of Education & International Center for Dielectric Research, Xi'an Jiaotong University, 710049 Xi'an, China*

Relaxor-based ferroelectric lead magnesium niobate-lead titanate (PMN-PT) is of high scientific interest due to their outstanding piezoelectric properties. However, there is an information vacuum surrounding the domain kinetics and domain structure evolution. These aspects of investigation are of great importance for development of domain engineering in such crystals.

Here we present the results of domain kinetics study during polarization switching in tetragonal PMN-PT single crystals in clamped area by direct optical observation accompanied by analysis of the switching current. Complementary analysis of current and obtained optical images allowed to reveal the main parameters of switching. We found three types of processes through which the switching took place: a) formation and growth of macroscopic *a*-domains; b) formation of charged domain structures due to intersections of macroscopic *a*-domains; c) formation and growth of *c*-domains. The estimation of optical current showed that the main switching current peak is related to growth of *c*-domains, while the charged domain walls on the intersections of *a*-domains are the reason of the additional small current peak. The two orders of magnitude enhancement of dielectric permittivity was attributed to appearance of such charged domain walls.

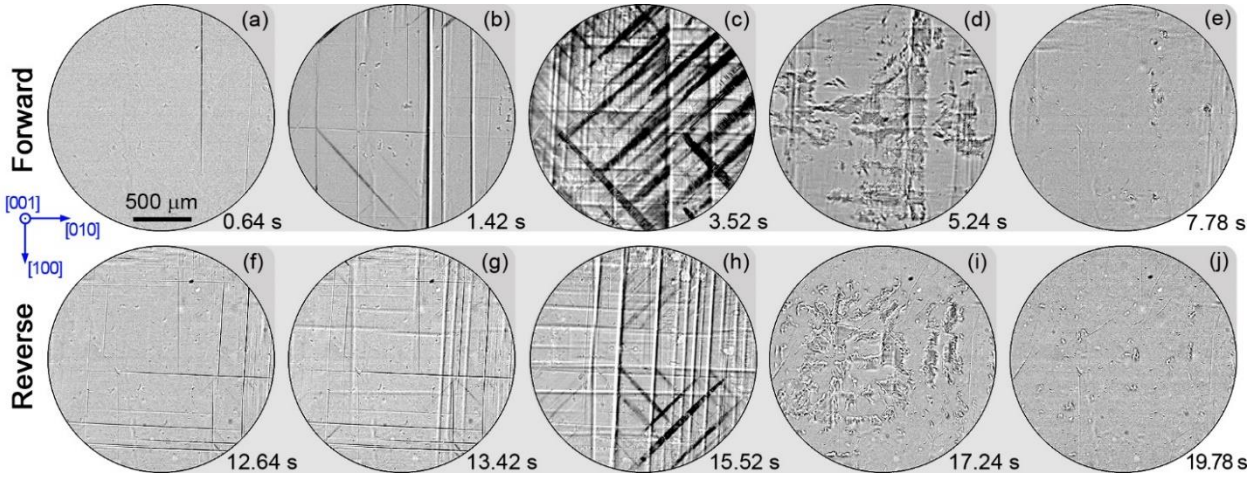

Figure 1. Instantaneous images of domain structure patterns during polarization reversal.

The equipment of the Ural Center for Shared Use "Modern Nanotechnology" Ural Federal University has been used. The research was made possible in part by Government of the Russian Federation (Act 211, Agreement 02.180 A03.21.0006) and RFBR (grant 17-52-80116-BRICS_a). V.S. and A.A. acknowledge financial support within the State Task from the Ministry of Education and Science of the Russian Federation (Project No. 1366.2014/236 and contract No. 3.4973.2017/7.8).

1. E. Sun, W. Cao, *Prog. Mater. Sci.* **65**, 124 (2014).
2. V.Ya. Shur E.V. Nikolaeva, E.I. Shishkin, V.L. Kozhevnikov, A.P. Chernykh, K. Terabe, K. Kitamura, *Appl. Phys. Lett.* **79**, 3146 (2001).

P-99

Investigation of polarization switching processes in PMN single crystal in a temperature range from 4 K to 300 K

A.F. Vakulenko[1], S.B. Vakhrushev[1,2]

[1]*Peter the Great Saint-Petersburg Polytechnic University, 195251, St. Petersburg, Russia*
e-mail: Vakulenko705@gmail.com

[2]*Ioffe Institute, 194021, St. Petersburg, Russia*

Relaxor ferroelectric materials have been widely studied with different techniques because of its great piezoelectric, dielectric and electromechanical properties. Where are many studies about domain structure and polarization switching processes in relaxor ferroelectric materials such as PMN, PMN-PT [1-4] but most of them were performed above the room temperature. In this work we study polarization switching processes in PMN single crystal via switching spectroscopy piezoresponse force microscopy (SS-PFM) in wide temperature range from 4 K to 300 K.

For a detailed study of polarization switching processes we simultaneously apply two different methods: switching spectroscopy piezoresponce force microscopy and modified Sawyer-Tower circuit «double wave method» [5]. We used a special electrode system consisting of two electrodes on the surface of the sample and one common electrode on bottom. Two surface electrodes have thickness 15 nm and area 400x400 μm^2. Distance between electrodes is about 20 μm. Bottom electrode covers all the sample area and its thickness is 80 nm. This scheme allows to provid measurements with Sawyer-Tower circuit, PFM through electrode and classic PFM without surface electrode. Two electrodes placed close to each other on the sample surface allows to create in-plane electrical field inside the sample. Also, presence of surface electrodes allows us to provide in-field cooling.

To test and establish PFM method with electrodes on sample surface the series of experiments have been done on $BaTiO_3$ single crystal. Thickness of BTO crystal was about 50 μm. Using switching spectroscopy PFM we have obtained piezoresponse hysteresis loops in BTO single crystal at room temperature and it was found that PFM works well with 15 nm thick of surface electrodes.

The experiment was carried out using a cryogenic atomic force microscope Attocube Systems AttoAFM I equipped with an external lock-in amplifier SR844 (Stanford Research Systems) and a functional generator Yokogawa FC120. AttoAFM I allows to perform «out of-plane» PFM measurements in temperature range from 4 to 300 K. Switching spectroscopy PFM method was created in the LabView 13, external devices were connected to PC with GPIB-USB interface. We employed the commercial platinum-iridium coated silicon cantilevers CSG30/Pt (NT-MDT). Golden electrodes was created on the sample surfaces by e-beam evaporation using a Moorfield Minilab 80 e-beam evaporator under high vacuum.

1. Q. Li, Y. Liu et al., *Journal of Applied Physics* **112**, 052006 (2012).
2. D. Liu, Chuanguo Ma et al., *Journal of Alloys and Compounds* **696**, 166 (2017).
3. Y. Zhang, X. Li et al., *Journal of Crystal Growth* **318**, 890 (2011).
4. V.V. Shvartsman, A.L. Kholkin, *Journal of Advanced Dielectrics* **2**, 1241003 (2012).
5. M. Fukunaga, Y. Noda, *Journal of the Physical Society of Japan* **77**, 064706 (2008).

P-100

Effect of thickness on the piezoelectric properties of $LiNbO_3$ films

Z.E. Vakulov[1], Y.N. Varzarev[1], A.V. Skrylev [1], A.E. Panich[1], D.A. Golosov[2], S.M. Zavadskiy[2], A.P. Dostanko[2], O.A. Ageev[1]

[1]*Southern Federal University, 347922, Taganrog, Russian Federation*
e-mail: zvakulov@sfedu.ru

[2]*Belarusian State University of Informatics and Radioelectronics, 220013, Minsk, Belarus*

Currently, lithium niobate ($LiNbO_3$) is widely used with the development and manufacture of acousto-optical devices, optical phase modulators, waveguides, elements of non-volatile memory due to unique combination of its physical and optical properties [1]. Moreover, $LiNbO_3$ films are multicomponent oxides and their properties (crystallographic orientation, surface roughness, resistivity, concentration and mobility of charge carriers, optical and piezoelectric properties) depends on the stoichiometric composition and structure, which in turn depends on the method and formation conditions.

The formation of nanostructured $LiNbO_3$ films was carried out in multifunctional nanotechnology complex NANOFAB NTK-9 (NT-MDT, Moscow) comprising Pioneer 180 pulsed laser deposition module (Neocera Co., USA). The evaporation of $LiNbO_3$ target was carried out with KrF excimer laser (Coherent Inc., USA) (λ = 248 nm). The number of pulses varied from 50 000 to 200 000 at a repetition rate of 10 Hz. The oxygen pressure in the growth chamber was 10^{-2} Torr.

Figure 1 shows the dependences of the polarization on the magnitude of electric field strength for $LiNbO_3$ films with different thicknesses.

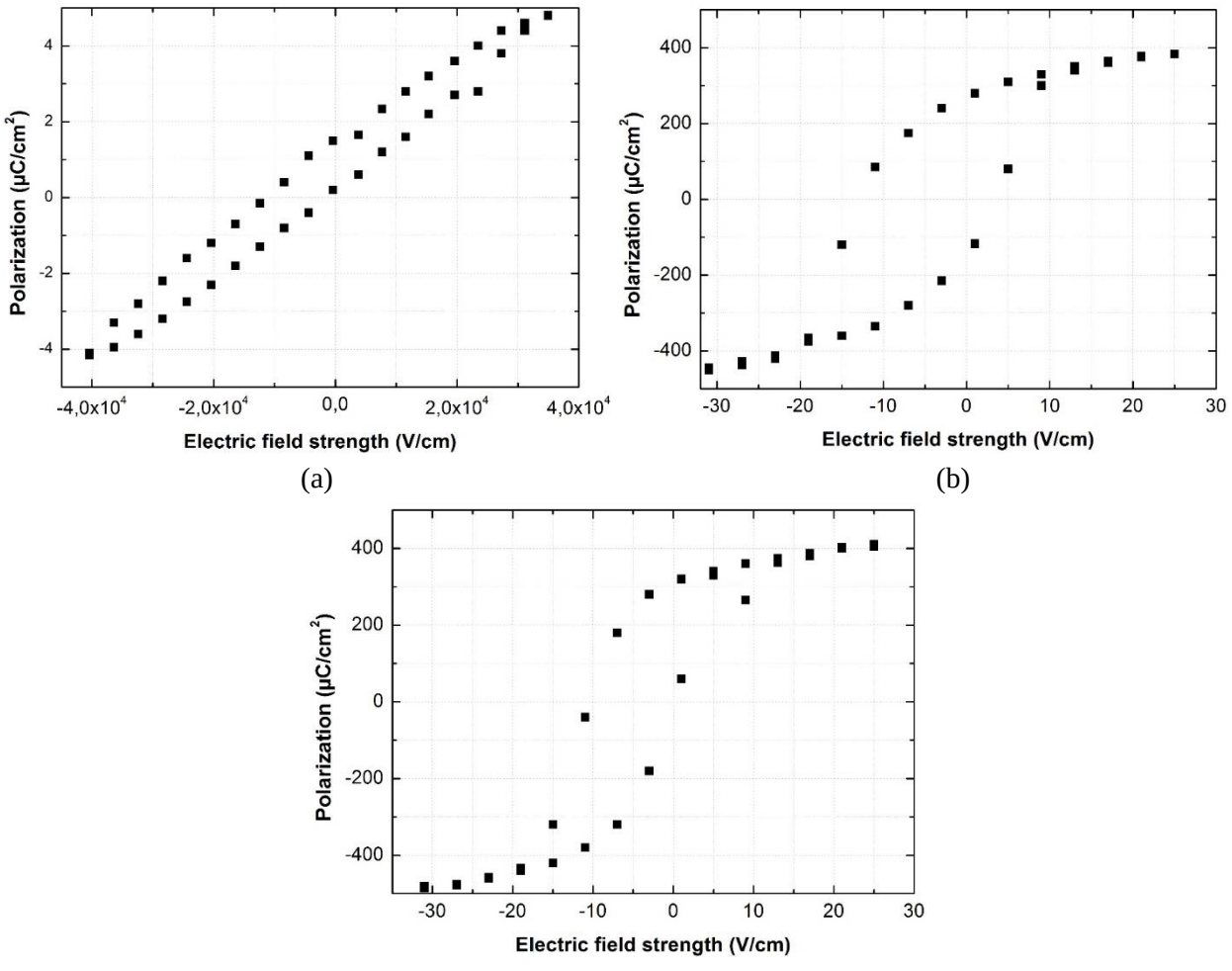

(a) (b)

(c)

Figure 1. Dependence of the polarization on the field strength for samples with different thicknesses: (a) 47.5 nm, (b) 110.1 nm, (c) 143.8 nm.

With increasing of film thickness from 110.1 to 143.8 nm, the dependences of polarization on the field strength were hysteresis (Fig. 1a,b). This fact characterizes the films as ferroelectric. An analogous dependence for the sample with 47.5 nm film thickness has the shape of an ellipse (Fig. 1c). The obtained dependences characterize the samples, with a thickness of 110.1 - 143.8 nm, as films with spontaneous polarization, whereas the sample with thickness of 47.5 nm has relaxation character of polarization. Moreover, it is established that increasing charge carriers mobility from 75.553 to 131.033 $cm^2/V \cdot s$ results in decreasing in the value of the residual polarization from 322 to 243 $\mu C/cm^2$. Changing in the charge carriers concentration from $7.325 \cdot 10^{17}$ to $3.24 \cdot 10^{19}$ cm^{-3}, leads to the value of the dielectric loss tangent increases from 0.35 to 70. With the further increasing in the concentration to $7.918 \cdot 10^{19}$ cm^{-3}, the dielectric loss tangent decreases to 5.6. Obtained results could be used in the developing and manufacturing of integrated acousto-optical devices and sensors based on surface acoustic waves.

The results were obtained using the equipment of Research and Education Center and the Center of collective use "Nanotechnology" of Southern Federal University.

1. J. Piprek, *Handbook of Optoelectronic Device Modeling and Simulation: Fundamentals, Materials, Nanostructures, LEDs, and Amplifiers* (CRC Press), 814 (2017).

P-101

β-glycine piezoelectric and ferroelectric properties behavior at elevated temperatures

S.G. Vasilev[1], D.S. Vasileva[1], P.S. Zelenovskiy[1], V.Ya. Shur[1], A.L. Kholkin[1,2]

[1] *School of Natural Sciences and Mathematics, Ural Federal University, 620000 Ekaterinburg, Russia vasilev.semen@gmail.com*

[2]*Physics Department & CICECO – Aveiro Institute of Materials, University of Aveiro, 3810-193, Aveiro, Portugal*

Investigation of the ferroelectric properties of organic molecular crystals is one of the fundamental problems. Interest in this class of crystals is associated with the possibility of their use in biocompatible electro-optical and electromechanical devices since many of them have pronounced piezoelectric and nonlinear optical properties.

Recent studies of the simplest amino acid glycine (NH_2CH_2COOH) single crystals revealed that among three polymorphic phases α, β and γ formed at ambient conditions, only β-phase possesses both piezoelectric and ferroelectric properties [1]. The faceted crystals with in-plane polar axis were grown from aqueous solution via drop drying on Pt/SiO/Si substrate in air with controlled relative humidity.

The detail experimental study of as-grown domain structure evolution in wide temperature range, domain switching by pyroelectric field and temperature induced polymorphic phase transition in β-glycine microcrystals using atomic force (AFM) and piezoresponse force microscopy (PFM) was realized by scanning probe microscope Asylum MFP 3D SA (Asylum Research, USA).

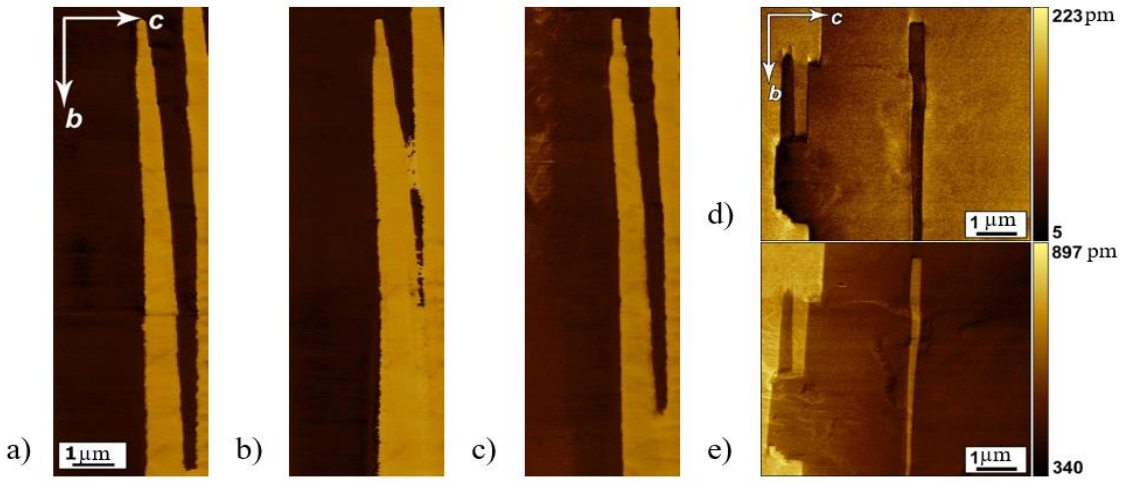

Figure 1. PFM images of the domain structure: (a) as-grown, (b) after heating from 10 to 35°C, (c) after cooling from 35 to 10°C; (d) as-grown and switching before and (e) after phase transition, caused by heating to 50°C.

Switching of the as-grown domain structure by pyroelectric field appeared during heating and cooling and frozen-in domain structure after β→γ phase transition induced by heating up to 50ºC have been obtained (Fig. 1).

The research was carried out using equipment of Ural Center for Shared Use "Modern Nanotechnologies" Ural Federal University. The reported study was funded by RFBR according to the research project № 18-32-00390.

1. A. Heredia, V. Meunier, et al., *Adv. Funct. Mater.* **22**, 2996 (2012).

P-102

Micro-relief and roughness of the surface of the profiled sulfocation-exchange membrane after its contact with phenylalanine solution

V.I. Vasil'eva, E.A. Goleva, M.A. Smagin, E.O. Abramova, D.V. Kostylev

Voronezh State University, 394018,Voronezh, Russia
e-mail: viv155@mail.ru

Using atomic force microscopy the surface of the profiled cation-exchange membrane MK-40pr was investigated before and after its contact with amino acid solutions. Micro-profiles and average statistical parameters of the surface roughness for the original conditioned membrane and the sample were determined after their contact with phenylalanine solution. The problem of this work is to find out the influence of alkylaromatic amino acid – phenylalanine – on the micro-relief and surface roughness of the profiled sulfocation-exchange membrane.

Heterogeneous sulfocation-exchange membrane MK-40pr with geometrically inhomogeneous (profiled) surface was employed as an object of investigations. Conditioned samples and membranes were studied after their contact with phenylalanine solution with the concentration of 0,15 M for 100 hours. Investigations of the surface micro-relief of the membrane were performed by atomic force microscopy (AFM) with the use of scanning probe microscope produced by NT-MDT Corporation (model Solver P47 Pro) (Zelenograd, Russia) performed in semi-contact mode applied to the air-dry samples. Results were estimated by the representation of relief in the form of topographic map as two-dimensional and three-dimensional digital images of the surface. Analysis of the obtained AFM images was performed with the use of software package AFM Solver P47 Pro Nova RC1 and it was concerned with the analysis of the amplitude average statistical parameters of the surface roughness in accordance with the international standards ISO 4287/1 and ANSI B. 46.1: R_y – is the height spread (maximum heights drop between the highest and lowest points of the surface profile) R_a – is the arithmetical mean roughness, R_q – is round mean square roughness, R_z – is the surface roughness over ten selected maximum heights and hollows.

AFM-images and microprofiles of the surface for the profiled membrane MK-40pr were obtained with a scanned area of 10×10 μm before and after the contact with phenylalanine solution. Image of the surface for the conditioned sample of sulfocation-exchange membrane MK-40pr appears as a developed chaotic structure with micrometer-scaled roughness: arithmetical mean roughness R_a fits with 186,4 nm at R_z=953,1 nm.

The effect of phenylalanine on the properties of the surface for the original sulfocation-exchange membrane MK-40pr is in the decrease of all the amplitude roughness parameters. Surface of the membrane after itscontact with phenylalanine became more uniform:surface roughness R_z fitted with 745,0 nm, while ariythmetical mean scale of roughness R_a – 172,8 nm.

Histograms comparing the heights density distributions on the surface of conditioned sample of MK-40pr membrane before and after its contact with phenylalanine solution are studied. As for the conditioned sample of MK-40pr membrane the maximum density corresponds to the mean value of the surface roughness equal to 1 μm, while for the sample of membrane after its contact with phenylalanine histogram is characterized by a spread maximum and a decrease of the mean roughness value up to 0,6 – 0,8 μm, as well.

Thus, the difefrences in the properties of the surface for the samples of profiles heterogeneous sulfocation-exchange membrane before and after its contact with phenylalanine solution have been visualized. An increase of uniformity for the membrane surface was found after its contact with the amino acid.

The work was conducted under financial support of RFBR (project N 18-08-01260).

P-103

Domain creation by electron and ion beams in lithium tantalate crystals

E.O. Vlasov, D.S. Chezganov, L.V. Gimadeeva, M.A. Chuvakova,
P.S. Zelenovskiy, V.Ya. Shur

School of Natural Sciences and Mathematics, Ural Federal University, 620000 Ekaterinburg, Russia
Corresponding author e-mail: evgeny.vlasov@urfu.ru

We have studied the domain formation induced by electron (e-beam) and ion beam (i-beam) irradiation in congruent lithium tantalate ($LiTaO_3$, CLT) crystals. The obtained results have been explained in terms of kinetic approach based on analogy with a first order phase transition [1].

The studied samples represented the 0.5-mm-thick Z-cut wafers of CLT single crystals produced by Oxide Corporation. The irradiated polar surface was covered by artificial dielectric layer. The copper solid electrode was deposited on the opposite surface and grounded during irradiation. The irradiation experiments were performed using dual-beam Auriga Crossbeam Workstation (Carl Zeiss). The control of irradiation parameters and beam positioning was carried out by the electron-ion beam lithography system Elphy Multibeam (Raith GmbH). The domain structures were visualized by piezoresponse force microscopy and scanning electron microscopy after selective chemical etching in pure HF during 20 min at the room temperature.

The formation of arrays of circular domains and domain wall shape instability (appearance of domain fingers) [2] as a result of dot irradiation have been revealed (Fig. 1). The dependence of domain radius on dose was measured. The isotropic domain growth was attributed to stochastic nucleation due to prevailed isotropic screening mechanism. The domain wall shape instability was caused by screening retardation in highly non-equilibrium switching conditions due to presence of the artificial surface dielectric layer.

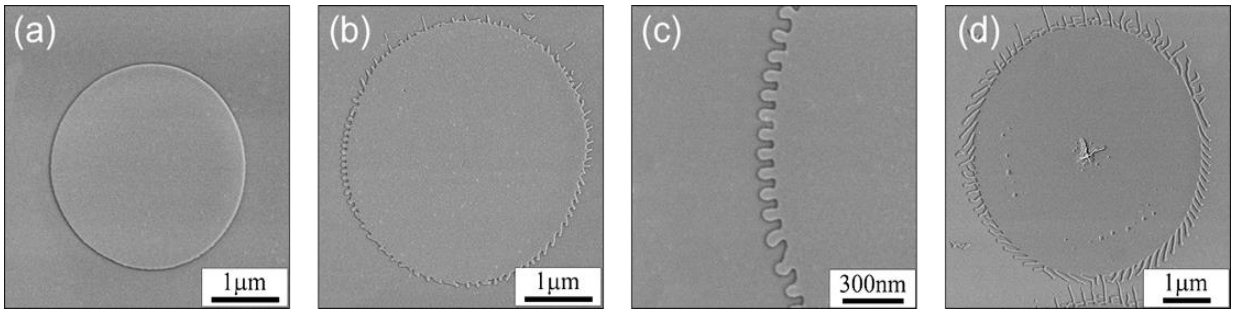

Figure 1. Scanning electron microscopy images of the etched surface topography corresponded to domains created by ion beam irradiation at the doses (pC): (a) 10, (b), (c) 60, (d) 110.

We have studied the domain formation after stripe irradiation by e-beam and i-beam. The dose dependencies of geometrical parameters of such domain structures were obtained. The main stages of domain formation such as: (1) discrete nucleation, (2) nuclei merging, and (3) continuous stripe domain formation were revealed. The appearance of domain wall instability after continuous stripe formation was found as well.

The obtained knowledge was used for optimization of periodical poling process in CLT. The periodically poled CLT with a period down to 2 μm has been created by using i-beam irradiation technique.

The equipment of the Ural Center for Shared Use “Modern nanotechnology” Ural Federal University was used. The research was made possible by the Russian Science Foundation (grant № 17-72-10152).

1. V.Ya. Shur, *J. Mater. Sci.* **41**, 199 (2006).
2. D.S. Chezganov, L.V. Gimadeeva, E.O. Vlasov, E.M. Vaskina, V.Ya. Shur, *Ferroelectrics* **525**, 28 (2018).

P-104

Investigation of the properties of quantum-dimensional semiconductor particles A^3B^5 by scanning probe microscopy, obtained by liquid chemical etching

N.Yu. Yashina[1,2], M.V. Gavrikov[1], A.J. Al-Alwani[1],
O.Yu. Tsvetkova[2], V.P. Sevostyanov[3], V.F. Kabanov[1], E G Glukhovskoy[1,2]

[1]*Department of Nano- and Biomedical Technologies, Saratov State University, Saratov 410012, Russia*

[2]*Education and Research Institute of Nanostructures and Biosystems, Saratov State University, Saratov 410012, Russia*

[3]*Scientific Research Institute of Technology of Organic, Inorganic Chemistry and Biotechnology, Saratov, 410012, Russia*
e-mail: manshev7@gmail.com

Nanoparticles of semiconductor monocrystals A^3B^5 (GaAs) were ground mechanically submicron dispersion in a planetary ball mill by liquid chemical etching in a peroxide-ammonia solution were obtained. Dimensions of nanoparticles were in the range from 1 to 5 nm with a predominant size of 2-3 nm. Particle sizes were determined by Z-saizer-nano granulometric analysis and atomic force microscopy (AFM). Current-volt characteristics (CVC) were studied by the method of scanning tunneling microscopy (STM). The results correspond to the theory of field emission in the range of electric field strengths roughly of 1 V/nm. The obtained particles of gallium arsenide can be used for the production of semiconductor colloidal quantum dots, promising in optical sensors.

Gallium arsenide has a rather narrow width of the forbidden band, high mobility of electrons and holes. These properties are of interest for the wide use of this substance in optoelectronics.

The GaAs single crystal was milled on a planetary ball mill of the PULVERISETTE type (Fritsch - Germany). The particle size resulting from milling is 250-1300 nm. Liquid chemical etching of the nanopowder was carried out by a peroxide-ammonia mixture, which is "classical" for polishing the surface of gallium arsenide semiconductor films and its analogs in industry by adjusting the concentration of etchants [1].

The obtained GaAs samples were placed on a glass substrate with a layer of indium-tin oxide. The investigations were carried out using atomic force microscopy (AFM) and scanning tunneling microscopy (STM) using the NANOEDUCATOR-2 microscope.

The tunneled CV characteristics of the investigated objects were obtained by the STM method. In the course of the studies, tunneling CVCs with a negative bias potential on the substrate relative to the probe were examined and analyzed (Fig. 1). In this case, electrons tunnel from the ITO electrode through the discrete levels of the quantum-dimensional object to the probe of the tunneling microscope. The experimental results show their correspondence to the theory of field emission in the range of electric field strengths roughly of 1 V/nm.

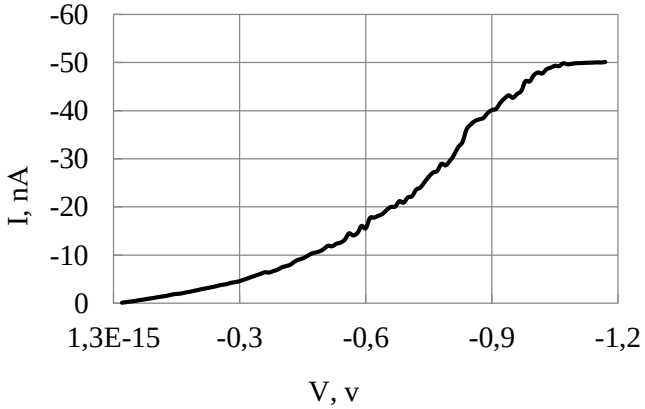

Figure 1. CVC of the GaAs quantum dots.

In the course of the experiment, the optimal conditions for chemical etching of the nanopowder (GaAs) with a peroxide-ammonia mixture for obtaining the desired nanoparticles were chosen. The results of the investigation of the surface morphology and I-V characteristics of the obtained particles by scanning probe microscopy method are obtained. The synthesized material can be used as a basis. This approach can be used to obtain semiconductor colloidal quantum dots (using an additional coating by their cladding), promising in optical sensors [2,3].

The study was carried out with the financial support of the Russian Foundation for Basic Research in the framework of scientific projects 17-07-00407-a and 17-07-00139.

1. N.J. Kadhim, S.H. Laurie, D. Mukherjee, *J. Chem. Educ.* **75**, 840 (1998).
2. P. Reiss, M. Protiere, L. Li, *Small* **5**, 154 (2009).
3. E.S. Speranskaya, V.V. Goftman, I.Yu. Goryacheva, *Nanotechnologies in Russia* **8**, 129 (2013).

P-105

Structural and electronic properties of heterointerfaces composed of complex ferroelectric oxides

R.R. Zagidullin[1], I.I. Piyanzina[1,2], D.P. Pavlov[1], D.A. Tayurskii[2], P.F. Mamin[1,2]

[1]*Zavoisky Physical-Technical Institute, FRC KazanSC of RAS, 420029, Kazan, Russia*
e-mail: i.piyanzina@gmail.com

[2]*Kazan Federal University, 420008, Kazan, Russia*

In 2004 the astounding phenomenon was found at the interface between two nonmagnetic wide-band-gap insulative oxides $LaAlO_3$ (LAO) and $SrTiO_3$ (STO) [1]. A two-dimensional electronic system (2DES) is formed in the STO layers next to the interface which becomes superconducting below a temperature of 300 mK [1,2]. Remarkably, this superconducting state coexists with a magnetic state being stable up to the room temperature. It was concluded, that the primary mechanism responsible for the 2DES formation is the electronic reconstruction followed by structural reconstruction.

Since then 2DES has been later found in other non-magnetic dielectrics. And all of them have in common is that the creation of 2DES is due to either the polar nature of one of components or due to defects of dopants. Latter, it has been shown that 2DES can be created at the interface of nonpolar oxides one of which is ferroelectric [3,4]. The main advantage of using ferroelectrics is a possibility to switch on and off the polarization and thus to control properties of the electron system.

In the present work based on first-principles band structure calculations, we theoretically investigate the interface between a ferroelectric film ($KNbO_3$, $BaTiO_3$, $LiNbO_3$, $PbTiO_3$) and a nonpolar insulating $SrTiO_3$ (and MgO) substrate. We demonstrate the possibility of a 2DES formation at the interface. We analyze an impact of ferroelectric polarization onto the 2DES conducting properties, as well as a possibility of switchable and controllable metal-insulator transition in considered types of heterostructures. We present comparative study of different combinations of components containing varying number of ferroelectric overlayers, as well as layer-resolved density of states.

The reported study was funded by RFBR according to the research project № 18-32-00595.

1. A. Ohtomo, H. Hwang, *Nature* **427**, 6973 (2004).
2. N. Reyren, S. Thiel, A. Caviglia et al., *Science* **317**, 5842 (2007).
3. M.K. Niranjan, Y. Wang, S.S. Jaswal, et al., *Phys.Rev.L.* **103**, 016804 (2009).
4. K.D. Fredrickson, A. Demkov, *Phys.Rev.B.* **91**, 115126 (2015).

P-106

Mathematical model and optimization of solder microstructure in a three-layer beam

S.P. Pavlov, K.S. Bodyagina, N.V. Bekrenev, I.V. Zlobina

Yuri Gagarin State Technical University of Saratov, 410054, Saratov, Russia
e-mail: irinka_7_@mail.ru

Thermal stresses that occur during soldering, vary within wide limits depending on the nature of the temperature fields, the geometric configuration and material properties. Substantial levels of stress can lead to cracking, plastic deformation and other undesirable phenomena which reduce the strength of the solder joint. Optimization of the solder layer topology can solve the problem of excessive stresses within the specified design and technological limitations. The report presents a mathematical formulation and method of solving a wide class of optimization problems that arise in connection with the heating of multilayer plates.

Consider the element of the unit length of the solder joint of the beam (Fig. 1) made of two layers with different materials, which are soldered together by a thin layer of solder. Assume the width of the beam *2l*, *l=2,5cm*. The table shows the thickness, Young modules, Poisson coefficients and coefficients of thermal expansion of layers h_i, E_i, ν_i, α_i, respectively, (*i=1* – the upper layer of iron-Nickel alloy (5Ni), *i=2* – a layer of solder tin, *i=3* – the lower layer of quartz glass). In the initial state the beam is at a melting point of solder ($\theta_{solder}=232\ ^\circ C$) without stress.

	h_i, *cm*	E_i, *N/cm*^{2}	ν_i	α_i,*1/ grad*
i=1	*1*	$20.58\cdot10^6$	*0.3*	$6.7\cdot10^{-6}$
i=2	*0.1*	$5.39\cdot10^6$	*0.3*	$15\cdot10^{-6}$
i=3	*1*	$6.86\cdot10^6$	*0.3*	$2\cdot10^{-7}$

When the beam is cooled down after soldering to the operating temperature θ_{exp}, displacements u_i, deformations ε_{ij} and stresses σ_{ij} occur in the elastic field. The behavior of the linear thermoelastic body is determined by the defining relations for the stress tensor σ, of strain tensor ε and deviation θ of the operating temperature $\theta_{exp}=25\ ^\circ C$ from the soldering temperature θ_{solder}.

$$\sigma_{ij} = 2G\left\{\varepsilon_{ij} + \frac{1}{1-2\nu}\left[\nu\varepsilon_{kk} - \alpha(1+\nu)\theta\right]\delta_{ij}\right\}. \quad (1)$$

The thermoelasticity problem is described by a system of differential equations:

$$\sigma_{ij,j} + \rho F_i = 0, \quad (2)$$

where ρ - density, G - shear modulus, E - modulus of elasticity, ν - Poisson's ratio, α - coefficient of linear thermal expansion. Equation (2) must be solved under the following boundary conditions: $\sigma n=0$.

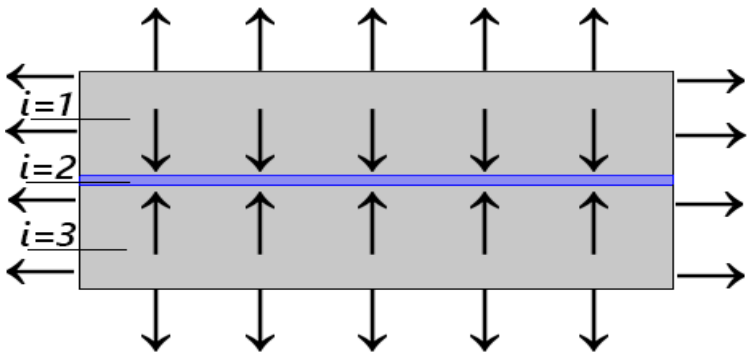

Figure 1. The element solder joint of beam.

Topology optimization the shape of the solder layer is in search of a better distribution of the greatest amount of solder on the layer 2 with a constraint on the magnitude of shear stress σ_{12}. In the topological optimization method [1-3], the Young modulus in the optimizable domain Ω, in our case it is a solder layer 2, is a function of artificially introduced material density $\rho(x)$. The stress tensor is considered to be a function of the Young module E_2 – of the solder material and $\rho(x)$ is a control variable in the optimization problem:

$$E(\mathbf{x}) = \rho(\mathbf{x})^p E_2, \quad \mathbf{x} \in \Omega.$$

With $\rho(x)=1$, the entire area is completely filled with material. Thus, you must find $\max_{\rho(\mathbf{x})} \int_\Omega \rho(\mathbf{x}) d\Omega$, with the constraint $\int_\Omega \sigma_{12} d\Omega \le \int_\Omega \sigma_{12}^{\max} d\Omega$, where $\sigma_{12}^{\max}$ - the set limit on the level of shear stresses. Problem (2) is solved by finite element method. As a result, optimal distributions of solder material for two constraints (Fig. 2) were obtained.

(a)

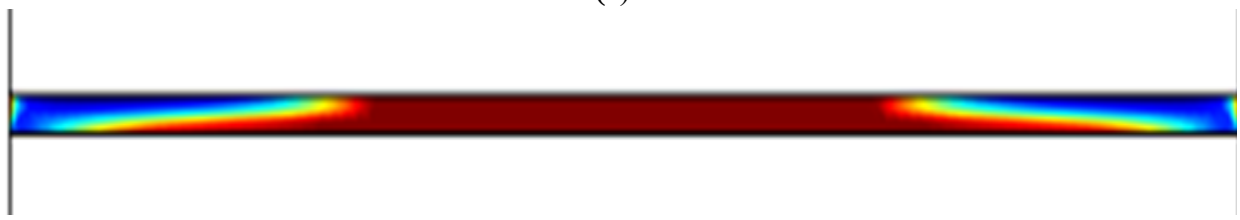

(b)

Figure 2. Optimal distribution of the solder material.

When restricted to a shear stress of 1000 N (Fig. 2a) the amount of solder material amounted to 0.87, while limiting in 1145 N (Fig. 2b) the amount of material was 0.92. For the same amount of material with homogeneous distribution, the stresses were 1168.4 N and 1194.4 N respectively.

The studies were carried out with the support of RFBR grant No. 17-03-00720 "Methodology of optimizing micro construction of composite materials for objects of complex shape with enhanced dynamic strength layered by electrotechnological methods".

1. M.P. Bendsoe, O. Sigmund, *Topology optimization: theory, methods and applications*. (Springer Science & Business Media), (2003).
2. M. Bruggi, *Struct. Multidiscip. Optim.* **36**, 125 (2008).
3. G. Cheng, Z. Jiang, *Eng. Optim.* **20**, 129 (1992).
4. J. Awrejcewicz, S.P. Pavlov, K.S. Bodyagina, et al., *Composite Structures* **174**, 19 (2017).

P-107

In-situ nanoindentation of titania microspheres with different crystallinity

V.A. Lebedev[1], A.S. Poluboiarinov[2], R.M. Sakaev[3], V.I. Chelpanov[4], D.A. Kozlov[2], K.A. Khazova[2], Ya.Yu. Philippov[1,2,5], A.V. Khokhlov[5], A.V. Garshev[1,2,4]

[1]*Faculty of Chemistry, Lomonosov Moscow State University, Moscow, Russia*
vasya_lebedev@mail.ru

[2]*Faculty of Materials Science, Lomonosov Moscow State University, Moscow, Russia*

[3]*Department of Mechanics and Mathematics, Lomonosov Moscow State University, Moscow, Russia*

[4]*Baikov Institute of Metallurgy and Material Science RAS, Moscow, Russia*

[5]*Institute of Mechanics, Lomonosov Moscow State University, Moscow, Russia*

Titania microspheres are the perspective object for the fabrication of high performance liquid chromatography (HPLC) columns. The usual material for this application are silica microspheres of ⌀1-10 μm. The proposed method of $Ti(^nBuO)_4$ controlled hydrolysis allows one to obtain titania microspheres with high specific surface area (up to 300 m^2/g), predefined size (from 0.3 to 1.5 μm) and narrow size distribution (σ ranging from 10 to 15 %, Fig. 1a). Initially amorphous particles present an opportunity to obtain materials with dissimilar crystallinity by choosing the appropriate treatments. Following treatments were used for partial crystallization of particles: annealing at 400°C, annealing at 700°C, hydrothermal treatment (HT), hydrothermal treatment with subsequent annealing at 400°C. Mechanical properties of the individual particles from the untreated and treated samples were measured *in-situ* with the use of the MEMS-based Hysitron PI-95 at Zeiss Libra 200MC TEM (Fig. 1b). Particles were sedimented on the silicon wedge (1 μm flat-top) by dry coating. Compression tests at constant rates under displacement and load control as well as cyclic loading with partial unloading were performed. Observation of the indentation processes were performed in HAADF-STEM mode, corresponding video data were acquired.

In order to perform graphical data treatment a Python-based software was developed. For the indenter tip tracking the Digital Image Correlation (DIC) method was used. Obtained data allows us to estimate the drift function with the use of theoretical and calculated displacements, and to quantify the shape evolution of the particles.

The reduced Young's module was evaluated implying axially symmetric deformation. It was demonstrated, that partially amorphous HT-processed TiO_2 particles have a lesser strength limit in comparison with both the initial amorphous and annealed crystalline particles. This effect is presumably caused by the heterogeneous spatial distribution of the amorphous and crystalline phases in the HT-processed sample.

(a) 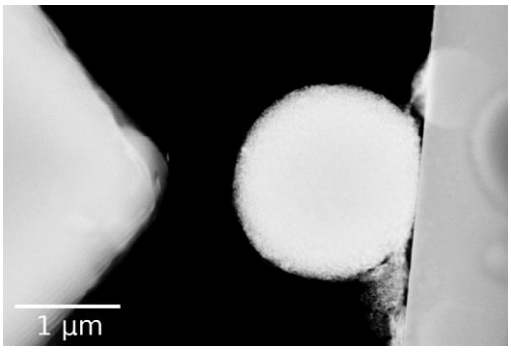

(b) 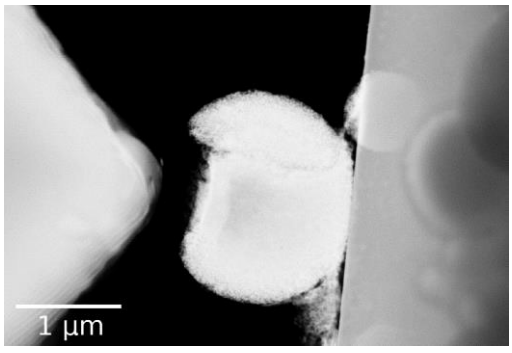

Figure 1. Titania microspheres, STEM: (a) before the indentation, (b) after the indentation.

This work was supported by the Lomonosov MSU Program of Development.

P-108

Juxtaposition of in vivo vs. in vitro assessments of nanoparticles combined toxicity

I. Minigalieva[1], T. Bushueva[1], E. Fröhlich[2], V. Panov[3], E. Shishkina[4], B. Katsnelson[1]

[1]*Medical Research Center for Prophylaxis and Health Protection in Industrial Workers, Ekaterinburg, Russia*

[2]*Center for Medical Research of the Medical University of Graz, Graz, Austria*

[3]*Institute of Industrial Ecology, the Urals Branch of the Russian Academy of Sciences*

[4]*School of Natural Sciences and Mathematics, the Ural Federal University, Ekaterinburg, Russia*

The overwhelming majority of the experimental studies in the field of metal nanotoxicology have been performed on cultures of established cell lines, with very few researchers focusing on animal experiments, while a juxtaposition of conclusions inferred from these two types of research is blatantly lacking. The least studied aspect of this problem relates to characterizing and predicting the combined toxicity of metallic nanoparticles,

Comparative and combined toxic effects of purposefully prepared spherical NiO and Mn_3O_4 nanoparticles (mean diameters 16.7±8.2 nm and 18.4±5.4 nm respectively) was estimated on cultures of human cell lines: MRC-5 fibroblasts, THP-1 monocytes, SY-SY5Y neuroblastoma cells, as well as on the latter two lines differentiated to macrophages and neurons, respectively. The combined cytotoxicity was mathematically modeled using the Response Surface Methodology.

The comparative assessment of the studied NPs unspecific toxicity obtained *in vivo* was satisfactotily reproduced by the *in vivo* tests. However, with respect to manganese-specific brain damage which had been demonstrated by us in animal experiment with the same NPs, the testing on on neuronall cell crlture showed only a certain enhancing effect of Mn_3O_4-NPs on the toxic action of NiO-NPs, while the role of the latter prevailed.

From the point of view of the preventive toxicology, the experimental modeling of metallic NPs combined toxicity on cell cultures may give non-reliable predictions of actual health risks.